ISSN: 2408-2384 (Online)
ISSN: 1686-5456 (Print)

Environment and Natural Resources Journal

Volume 20, Number 6, November - December 2022

Environment and Natural Resources Journal (EnNRJ)

Volume 20, Number 6, November - December 2022 ISSN: 1686-5456 (Print)
ISSN: 2408-2384 (Online)

AIMS AND SCOPE

The Environment and Natural Resources Journal is a peer-reviewed journal, which provides insight scientific knowledge into the diverse dimensions of integrated environmental and natural resource management. The journal aims to provide a platform for exchange and distribution of the knowledge and cutting-edge research in the fields of environmental science and natural resource management to academicians, scientists and researchers. The journal accepts a varied array of manuscripts on all aspects of environmental science and natural resource management. The journal scope covers the integration of multidisciplinary sciences for prevention, control, treatment, environmental clean-up and restoration. The study of the existing or emerging problems of environment and natural resources in the region of Southeast Asia and the creation of novel knowledge and/or recommendations of mitigation measures for sustainable development policies are emphasized.

The subject areas are diverse, but specific topics of interest include:

- Biodiversity
- Climate change
- Detection and monitoring of polluted sources e.g., industry, mining
- Disaster e.g., forest fire, flooding, earthquake, tsunami, or tidal wave
- Ecological/Environmental modelling
- Emerging contaminants/hazardous wastes investigation and remediation
- Environmental dynamics e.g., coastal erosion, sea level rise
- Environmental assessment tools, policy and management e.g., GIS, remote sensing, Environmental Management System (EMS)
- Environmental pollution and other novel solutions to pollution
- Remediation technology of contaminated environments
- Transboundary pollution
- Waste and wastewater treatments and disposal technology

Schedule

Environment and Natural Resources Journal (EnNRJ) is published 6 issues per year in January-February, March-April, May-June, July-August, September-October, and November-December.

Publication Fees

There is no cost of the article-processing and publication.

Ethics in publishing

EnNRJ follows closely a set of guidelines and recommendations published by Committee on Publication Ethics (COPE).

Environment and Natural Resources Journal (EnNRJ)

Volume 20, Number 6, November - December 2022 ISSN: 1686-5456 (Print)
ISSN: 2408-2384 (Online)

Editorial Office Address
Research Management and Administration Section,
Faculty of Environment and Resource Studies, Mahidol University
999, Phutthamonthon Sai 4 Road, Salaya, Phutthamonthon, Nakhon Pathom, Thailand, 73170
Phone +662 441 5000 ext. 2108 Fax. +662 441 9509-10
Website: https://ph02.tci-thaijo.org/index.php/ennrj/index
E-mail: ennrjournal@gmail.com

Environment and Natural Resources Journal (EnNRJ)

Volume 20, Number 6, November - December 2022 ISSN: 1686-5456 (Print)
ISSN: 2408-2384 (Online)

CONTENT

REVIEW ARTICLE

Interactive Governance for the Sustainability of Marine and Coastal Resources in Thailand#

Suvaluck Satumantpan[1*] and Ratana Chuenpagdee[2]

[1]Faculty of Environment and Natural Resource Studies, Mahidol University, Nakhon Pathom 73170, Thailand
[2]Department of Geography, Memorial University of Newfoundland, St. John's, Newfoundland and Labrador, Canada

ARTICLE INFO

Received: 25 May 2022
Received in revised: 18 Jul 2022
Accepted: 22 Jul 2022
Published online: 25 Aug 2022
DOI: 10.32526/ennrj/20/202200115

Keywords:
Wicked problems/ Resources governance/ Governing interaction/ Governability/ Coastal zones/ Thailand

*** Corresponding author:**
E-mail:
suvaluck.nat@mahidol.ac.th

 # This review article was invited by the Editor-in-Chief.

ABSTRACT

Coastal zones are biodiverse, with complex and dynamic interconnectivity between terrestrial and marine areas, and with multiple interactions between ecological and social systems. Despite on-going efforts to conserve and protect these ecosystems, destructive extraction and unsustainable resource utilization are persistent, posing challenges for governance. Issues and concerns in coastal zones are cross-sectoral and cross-boundary, often with overlapping jurisdictions. They are considered 'wicked' governance problems, requiring nuanced approaches to address, rather than technical quick fixes. Interactive governance is one such approach that examines relationships within and between the ecological and social systems, as well as with the governing system. Theoretically, the governability of coastal zones depends on the inherent quality of these systems and their interactions, and improving governability needs to take place in all three orders of governance. At the 'first order', a better understanding of the diversity, complexity and dynamics of coastal zones, and related scale issues is required. Improving governability at the 'second order' involves evaluating and adjusting the existing legal and institutional frameworks to improve the performance and the correspondence with the systems they aim to govern. Finally, discussion about coastal governance needs to be elevated to 'meta-order' where principles are set and values derived so that hard choices can be made, for instance, between conservation and utilization of coastal resources. Guided by the interactive governance framework, the paper presents an overview of coastal governance in Thailand, summarizing key features of the natural, social and governing systems associated with coastal zones, and discussing what can be done to improve coastal governability.

1. INTRODUCTION

Coastal zones and the adjacent seas are biodiverse, with complex and dynamic terrestrial/marine inter-relationships and with multiple interactions between ecological and social systems. Coastal areas around the world face rapid and unplanned development, population growth and demographic change, which contribute to loss of habitats, increased erosion and ecological degradation, among others issues. Despite on-going efforts to conserve and protect aquatic resources and coastal ecosystems, destructive extraction practices, and unsustainable resource utilization remain.

Multiple uses and activities in coastal systems, which are often cross-sectoral, cross-boundary and with overlapping jurisdiction, create 'wicked' governance problems that are difficult to define and solve. As posited by Rittel and Webber (1973) and Jentoft and Chuenpagdee (2009), they require nuanced approahes to address, rather than technical fixes. Conceptually, integrated coastal management (ICM) recognizes the wicked nature of coastal issues and is considered a better alternative to the traditional sectoral management (Cicin-Sain and Knecht, 1988; GESAMP, 1996; Satumanatpan, 2018). ICM is a dynamic process designed as an intersectoral,

Citation: Satumantpan S, Chuenpagdee R. Interactive governance for the sustainability of marine and coastal resources in Thailand. Environ. Nat. Resour. J. 2022;20(6):543-552. (https://doi.org/10.32526/ennrj/20/202200115)

intergovernmental, land-sea and science-based management, which has been employed globally in promoting sustainable coastal development since the early 1980s. The goal of which is to maintain or restore ecological integrity and enhance the quality of life, while focusing also on developing the economies (Burbridge, 2004; Cicin-Sain and Belfiore, 2005; United Nations, 1982; Celliers et al., 2021).

Despite long experiences of ICM practices around the world, coastal ecosystem health continues to decline, making sustainability a lofty goal. Olson (2000) posits that ICM challenges are linked to governance processes, which, according to Christies et al. (2005), require integration and coordination support, participative management, relevant policies, legislation and institutional arrangements and long-term commitment. It has been argued that continuing evaluative and adaptive processes are imperative, using a system of indicators, but the application of this is not without a challenge due to the multi-faceted nature of coastal ecosystem. Eger et al. (2021), for instance, suggest that governance characteristics, including formal governance structure, engagement with diverse actors, and innovative mechanisms for coordination and cooperation among multi-actor groups, are key elements that need to be examined for successful ICM, measured by numerous input, process and output indicators (Ehler, 2003).

A shift from traditional, single sector-based management approaches to cross-sectoral coastal governance is considered a critical pathway towards coastal sustainability. While there are several models that promote holistic and integrated perspectives in coastal zones, this paper follows the interactive governance theory (Kooiman et al., 2005) in examining the relationships and interactions within and between the natural and social coastal systems that are being governed, and the governing system, as key areas for improving coastal governance, as well as governability over time. The latter is a related concept that refers to the overall quality of the governance system, which includes the inherent characteristics of the systems themselves, as well as the capacity of the governing system to perform its tasks. In the first instance, a coastal system can be more or less governable depending on the diversity, complexity, dynamics and scale of the natural and social systems (Jentoft and Chuenpagdee, 2009). Generally speaking, a system that is diverse, complex, dynamic, and has scale and boundary issues is likely to be less governable, unless the governing system is adaptive and highly capable of dealing with the challenges posed by these characteristics. The diversity, complexity, dynamics and scale of the governing system also contribute to governability, which additionally depends on how well it aligns and corresponds to the nature of the coastal systems that it aims to govern.

The interactive governance theory further posits that sources of governability (and opportunities to enhance it) can be found in all three orders of governance. The meta order is concerned with values, images and principles guiding governing institutions at the second order and governing interactions at the first order. When meta-order elements are well articulated and appreciated by all involved coastal stakeholders, and that laws and regulations are formulated accordingly (second order), which make it easy for the implementation on the ground (first order), coastal governability is likely to be high. Adjustment and transformation may be needed to better align the three orders of governance, which would then lead to improving governability (Chuenpagdee and Jentoft, 2009).

The article extends from the work by Satumanatpan et al. (2014), Satumanatpan and Chuenpagdee (2015), and Satumanatpan et al. (2018) in looking at how interactive governance and three governance orders provide the needed foundation to help achieve coastal sustainability in Thailand. With a maritime territory of more than 320,000 km^2, or about 60 percent of the land area, and with 23 provinces adjacent to coastal seas, Thailand's coastal and aquatic resources generate a high economic value of about 24 trillion baht annually. The Thai government has been supportive of ICM and dedicated the responsibility of coastal management to the Department of Coastal and Marine Resources (DMCR) in 2015. Like other coastal regions elsewhere, Thailand faces several governance challenges related to inter-governmental and inter-sectoral coordination, communication and dissemination of information, stakeholder participation, long-term financial support, and consistent monitoring and evaluation, among others (see e.g., Christie et al., 2005; White et al., 2006; Satumanatpan et al., 2017; Eger et al., 2021). Thailand is a signatory to Sustainable Development Goals (SDGs) (NESDC, 2021), supporting the ocean sustainable development agenda, including the most recent Blue Growth and Blue Economy initiatives.

Coastal areas are among the most complex and challenging systems to govern. On that premise alone,

the application of a theoretical framework like interactive governance to unpack the wicked problems embedded in the coastal system offers valuable lessons. Thailand coastal system is presented in the paper to illustrate such an application. Yet, how coastal areas in Thailand are governed presents additional challenges, as well as opportunities for improving governance, given the new laws and regulations governing coastal and fisheries resources. It serves as a good case study for resource governance reform, which many countries are either implementing or contemplating.

In this paper, we first undertook a desk review of the policy and legal basis for governing marine and coastal resources in Thailand. The review included the following key documents: the 20 years National Strategy and the Master plan, the National Economic and Social Development Plans, the Five Year Environmental Management Plan, and other relevant national laws. After completing the reviews, we employed the interactive governance in guiding the discourse analysis by exploring the overall coastal system, including the systems that are being governed, the governing system and the governing interaction. Additionally, we examined these systems in three orders of governance, in the understanding of coastal governability, using the following questions. For the Meta-order governance: What are the goals and principles underlying the coastal governance system? Do governing actors recognize or ignore them? For the second-order governance: What institutional characteristics do the governance system have? Are existing regulations conducive for effective coastal management? Are there instruments to support the goals? And finally, for first-order governance: What are the day-to-day operations? Are patterns of interaction among stakeholders supporting coastal management? Where appropriate, we also put relevant examples, which clearly explain where and how to address the coastal challenges and improve governance.

The article is organized as follows. We begin with the theoretical framework of interactive governance and the description of the natural and social coastal systems, the governing system, and the interaction between the two. Key legislations that took place since the Rio's conference in 1992 are highlighted to illustrate the diversity, complexity and dynamic of the governing system. This is followed by discussion about issues and challenges in coastal governance following the three orders analysis. We conclude with suggestions about how to improve coastal governability in Thailand, as part of the possible pathways towards sustainable coastal development.

2. INTERACTIVE GOVERNANCE AND GOVERNABILLITY

Governance is a concept that has several meanings and definitions (Graham et al., 2003; Lockwood et al., 2010; Moore et al., 2011). For instance, Graham et al. (2003) define governance as the interactions among structures, processes and traditions that determine how power and responsibilities are exercised, how decisions are taken, and how citizens or other stakeholders have their say. Moore et al. (2011) state that governance involves the exercise of power, decision making, and implementation of decisions. They also point to laws or rules, institutions and processes among the key governance components. In another instance, governance is referred to as the structural, institutional, and procedural umbrella under which development programs and management practices operate (Bennett and Dearden, 2014). Singh (2014), on the other hand, defines governance as the ability of a state to govern its resources as prescribed in the form of legal instruments, supplemented by policy, programs and institutional interventions, all operating in a holistic manner with effective synergies among and within the various entities.

Interactive governance, as defined by Kooiman (2003), is similar to the above but has its emphasis on interactions. Specifically, interactive governance refers to "the whole of public as well as private interaction taken to solve societal problems and create societal opportunities" (Kooiman et al., 2005). It includes the formulation and application of principles guiding those interactions and care for institutions that enable them. The emphasis on interactions, posited in interactive governance theory, encourages a whole-system analysis of all aspects of governance, in identifying challenges and obstacles, and in exploring new opportunities and perspectives to address them. These interactions occur in all levels and all orders of governance, and these interactions are part of what make the system more or less governable (Chuenpagdee and Jentoft, 2009).

In accord with the interactive governance concept, coastal systems are characterized by the diversity, complexity and dynamics of the system components, which operate at various scales. These characteristics can be found in the natural and the

social systems-to-be-governed (SG), the governing system (GS) and the governing interaction (GI) within and between the SG and GS. They are fundamental building blocks of a governance structure, and therefore must be carefully examined when assessing the capacity and performance of the governance system. As previously stated, systems with low diversity, dynamic and complexity, with a well-defined boundary, and activities taking place in a small spatial scale, may be more governable than those that are highly diverse, complex and dynamic, and are ridden with boundary and scale issues. Yet, the latter systems can still be governable if the governing system is highly capable of performing its function, and it is organized to align with these characteristics and can respond in timely and effective manner.

2.1 The natural and social coastal SG

Coastal areas of Thailand are rich with many key aquatic ecosystems and habitats including mangroves, coral reefs, seagrass beds, sandy beach, muddy shore and rocky shore. Mangroves, coral reefs and seagrass beds, in particular, serve as feeding ground and nursery areas, for many aquatic organism. According to a recent report by DMCR (2022), mangrove covers an area of about 2,780 km^2, coral reefs 239 km^2, and seagrass beds 159 km^2. A total of 96 species of mangrove plants have been identified, with the dominance of *Rhizophora* spp. There are 273 species of coral, the majority of which are branching corals (*Acopora* spp.) and massive coral of the species *Porites lutea*. Two seagrass species, *Halophila ovalis* and *Enhalus acoroides*, are common among the 12 species found in Thailand (DMCR, 2022).

The rich natural coastal system supports diverse stakeholders with multiple uses in both coastal and marine areas. They provide food security and local livelihoods for coastal communities engaged in fisheries, aquaculture and tourism. Ports and shipping, oil and gas exploration and production, and coastal development are other activities taking place in these coastal areas. Fish and seafood are a key part of the Thai diet, with about 29 kg/year of fish being consumed per capita, which is higher than the world average of 21 kg/capita/year (FAO, 2020). The importance of fisheries, especially small-scale fisheries, cannot be under-estimated. Small-scale fisheries take place in all the 22 coastal provinces, and according to the latest catch survey statistics by the Department of Fisheries, the sector produced about 161,500 ton of marine fishery catch or about 11% of the country's total production (DOF, 2020). The number of fishers has also been estimated at 168,140 people actively fishing during peak season, with 57,800 households depending on fisheries livelihoods (DOF, 2016), the majority of which are involved in the small-scale fisheries value chain.

Threats to coastal and aquatic resources in Thailand have been increasing for decades and continue to grow. For instance, marine resources have been over-exploited, with some destructive fishing practices causing damage to habitats and marine mammals (PEMSEA, 2019). Coral reefs suffer damages from multiple causes including tourism, sedimentation, marine debris and untreated wastewater discharge. Sewage, sedimentation from coastal projects, destructive fishing, and shrimp farming have been reported to accelerate the decline of seagrass and other coastal vegetation. Loss of mangrove forests continues through deforestation and conversion to aquaculture, industrial development, construction of road, piers and other infrastructure, and agriculture. The mangrove forest area decreased from approximately 3,680 km^2 in 1961 to 1,680 km^2 in 1996. With reforestation programs carried out by government agencies, private sectors, and NGOs, mangroves have recovered with a reported area of about 2,780 km^2 in 2020 (DMCR, 2022).

2.2 Coastal GS

In line with how natural resources are generally governed in Thailand, coastal resources are governed under a decentralization system, with local government officials responsible for the day-to-day management and local decision-making since 1999 (Table S1).

In 2003, a bureaucratic reform took place, which resulted in an establishment of the new Ministry of Natural Resources and Environment (MONRE), designated as the main agency responsible for environmental and natural resource management in the country (Royal Gazette, 2003). The Department of Marine and Coastal Resources (DMCR) is one of the units under the ministry, in charge of promoting sustainable management and conservation of Thailand's marine and coastal resources, particularly mangrove forests, coral reefs, seagrass and marine endangered species. DMCR has a direct mandate for coastal resource management, but shares decision-making responsibility with other government agencies that also have jurisdiction in the coastal zone, such as the Department of National Parks, Wildlife and Plant

Conservation, and Office of Natural Resources and Environmental Policy and Planning under the MONRE, Department of Fisheries under the Ministry of Agriculture and Cooperatives, Marine Department (main authority for marine transportation and shipping) under the Ministry of Transport, Department of Public Works and Town Planning under the Ministry of Interior, and Office of the National Security Council under the Office of the Prime Minister. (Supplement A, upper box shows major institutions involved in governing marine and coastal resources at the national scale).

Prior to 2015, coastal resources were managed under a number of related laws (Table S1). Since March 2015, the Promotion of Marine and Coastal Resources Management Act (hereafter, 2015 Coastal Act) was enacted, with provisions for setting up institutions for managing coastal resources, either at the national or the local scale, and promoting community participation in coastal resources governance. In November of that year, the Royal Ordinance on Fishery came into effect, with the mandate of protecting fishery resources through similar institutional arrangement (i.e., national and provincial fishery committees) and promoting fishing communities' participation in fishery governance. In 2019, the National Park Act and the Marine Interest Protection Act are the two most recent laws, playing a supporting role in the governance of marine and coastal resources in Thailand (Table S1). We provide comprehensive details of direct governing institutions created under the 2015 Coastal Act as the second-order governance in section 3.2.

In sum, multiple government agencies have jurisdiction in the coastal zone and all have decision making authority at both national and provincial scales, thus creating a highly complex governing system (Supplement A). For instance, at the provincial scale (grey box in Supplement A), there are a minimum of three committees directly responsible for marine and coastal governance – the PMCRC (under the Coastal Act), the PFC (under the Royal Ordinance on Fisheries), and the PMECC (under the Marine Interest Protection Act). Additionally, two more committees will be added in the provinces that have environmental protected areas (the PCCME created under the National Environmental Quality Act) and marine protected areas (the PMNPC under the National Park Act), respectively.

2.3 Governing interaction

Several forms of interactions among several governing actors and the institutions (like the legal instruments) can be found, mostly in connection with the roles and responsibilities of different agencies, following principles such as participation, access to information, transparency and accountability. Specifically, there is a close connection and relationship between the Coastal Act and the Royal Ordinance on Fisheries, both of which have similar requirements to promote the participation and support of coastal communities (section 16) and local fishing communities (section 25) in the management, maintenance, conservation, restoration and exploitation of coastal and fishery resources. As in other areas, there are laws and legislations that can be drawn upon to enhance participation and interaction in the governance of coastal resources. For instance, the 1997 Official Information Act (Royal Gazette, 1997) establishes the right of people to access public information and makes all state agencies legally responsible for disseminating it. Additionally, the 2018 National Environmental Quality Act (second amendment, Royal Gazette, 2018a) requires that an environmental impact study be conducted on large-scale development projects that might affect coastal resources, with meaningful consultations with the communities to assess and mitigate impacts. There is also a mechanism that allows representatives of coastal communities to participate in committees at the provincial and national level.

While certain forms of interactions such as involving coastal communities in coastal decision making generally contribute to increasing coastal governability, quality of interactions and persons participating may affect the governance outcomes. This was the case with the plan to designate the dolphin conservation areas (under the 2015 Coastal Act) in Trat Province where the process began in 2018, but without much progress. Information about the causes of dolphin death was unclear, with the DMCR claiming that it was mostly caused by small-scale fishing gears, while fishers argued that the death was a result of plastic waste. Despite this, the DMCR began the planning process that did not lead to developing trust and agreement with the communities and fishers. This contrasts with a case in Trang Province, southern Thailand, where progress has been made to establish a marine protected areas (MPAs), taking into consideration local culture and sustainable use of local

people, and with an inclusive process with all relevant stakeholders sharing information (DMCR, 2021a).

3. GOVERNABILLITY IN THREE ORDERS

The ecological, social, economic and cultural importance of coastal systems makes it critical to get the governance right. As posited by the interactive governance theory, challenges and opportunities for governance, along with ways to improve governability, can be found in the system to be governed, governing system, governing interaction (section 2.1-2.3), and can be also found in the three orders of governance. We illustrate below what they imply in the context of Thai coastal zones.

3.1 Meta-order governance

The meta-order elements, i.e. values, images and principles underlying governance, are often implicit and not well articulated. Principles are the most explicit element among them and can be easily identified, at least on the face value. For instance, the five-year environmental management plan (Royal Gazette, 2017) lists twelve principles for natural resources and environment governance. These are: sustainable development, ecosystem approach, precautionary principle, polluters pay principle, beneficiaries pay principle, public-private partnership, good governance, extended producer responsibility, resource efficiency, human rights, integration, and environmental justice. The latter two principles, in particular, are emphasized in the upcoming five-year environmental management plan (2023-2027) under the Office of Natural Resources and Environmental Policy and Planning. Additionally, the sufficiency principle, originated more than 40 years ago by the late King Bhumibol Adulyadej, has been recognized as another key guiding principle for sustainable development envisaged in the SDGs, and has been incorporated in the Ninth National Economic and Social Development Plan since 2002 (NESDC, 2002).

The importance of meta-level governance, especially the sufficiency principle, in enhancing governability of many small-scale fishers in Thailand has been illustrated. Chuenpagdee and Juntarashote (2011) document how small-scale fisheries people in four provinces (Chantaburi, Prachuap Khiri Khan, Ranong and Krabi) adhered to the sufficiency principle, reflecting the positive image that they would like to portray along with their commitment to conservation. In these case studies, small-scale fisheries people were explicit in their agreement to abolish the use of illegal fishing gears and were active in their participation to protect and restore coastal resources. These actions contributed not only to maintaining the healthy marine environment but also to sustaining their livelihood and wellbeing.

Since the Rio+20 conference in 2012, the blue growth and blue economy concepts have been widely discussed and incorporated in the ocean development plans in many coastal states. Thailand has followed this trend in promoting blue economy as part of coastal and ocean sustainable development since 2015. The articulation of this concept can be found in several national strategies, including the 20 years National Strategy and the Master Plan (Royal Gazette, 2018b; Royal Gazette, 2019), and the 12th national social and economic plan (NESDC, 2016). Blue Economy is also incorporated in the DMCR action plan. Along with this is the incorporation of SDG14 (Life below water) targets in the national policy for protection and conservation of marine resources, which are implemented through, among other approaches, place-based tools such as marine spatial planning (MSP) and MPAs. These two are further discussed in section 3.2.

While principles are clearly articulated in the policy and planning documents, it is less obvious what or whose values underline them. It is also unclear what images drive the blue economy, nor whether key coastal and ocean stakeholders share them. So far the discussion about SDG14 in Thailand has been driven by the central government, and similar to other countries, the blue economy initiatives are mostly influenced by large-scale ocean-based sectors, including aquaculture, land development, industrial parks, tourism and industrial fisheries (Fabinyi et al., 2022). While there is an early attempt to provide small-scale fisheries people with alternative income (DMCR, 2021b), the most marginalized and vulnerable groups among them, such as women, will continue to be disadvantaged (Jentoft and Chuenpagdee, 2022).

3.2 Second-order governance

The second governance order refers to the institutional design and arrangement, formed in alignment with the meta-order, to enable the first order processes in problem-solving and opportunity creation. Kooiman et al. (2005) suggest that when designing or building these governing institutions, two questions must be considered: (1) whether the institutions form a proper framework for problem solving and opportunities creation; and (2) what a

division of tasks and responsibilities for each of them, or in combination between them, might look like.

As illustrated in the above, Thailand has a strong foundation of legal and policy instruments to support the sustainability of marine and coastal resources in the country (section 2.2). Through the 2015 Coastal Act, the NMCRC is inclusive in the approach to policy and planning for marine and coastal resources, with members representing 19 relevant ministries. Additionally, 12 academic or independent experts in fields related to coastal and marine resources are included in the committee, with a minimum of six individuals from coastal communities. The Prime Minister chairs the NMCRC and the DMCR Director-General serves as a secretariat, providing to a certain extent a high-level coordination and continuity to the coastal policy and planning process. The work of the NMCRC is done through eight sub-committees, which deal with specific issues (see Table S1 under the 2015 Coastal Act).

The 2015 Coastal Act also enables an establishment of the provincial level committee (PMCRC), with similar membership and response-bilities, as well as supports the registration of coastal community organizations, as another mechanism to enhance participation of coastal communities in resource governance. The involvement of community groups and local stakeholders in the provincial committees aligns well with what studies show about the importance of involving coastal actors in adapting and planning for change (see for instance Amarasinghe and Bavinck, 2011; Dearden et al., 2017; Prado et al., 2015).

In addition to setting up these institutions, the two spatial tools employed for coastal management in Thailand are worth noting in terms of their institutional design. Currently, Thailand has about 15,336 km^2 (close to 5% of the total maritime zone) designated as MPAs (NESDC, 2021), but is aiming to increase it to 10% by 2030. It is not clear, however, how the target will be met since coordination and harmonization among involved departments is highly problematic. The designation of an MPA in Thailand can be executed under three main laws including the Marine National Park Act (by DNP), the National Environment Quality Act (by ONEP), and the Coastal Act (by DMCR). Unavoidably, overlapping efforts and redundant work occur, causing confusion among coastal communities, especially about the different laws that allow or prohibit certain activities. The MPA designation has been delayed because of this lack of coordination.

Similar problems are likely to be observed in the MSP process, with two major laws related to its execution. The Marine Interest Protection Act provides power and authorities to the Office of the National Security Council in integrating multiple activities in the marine and coastal zone, and the Coastal Act enables protection of marine and coastal resources, but offers no direct power to DMCR to lead other institutions in integrating multiple activities in an area. Yet, without the legal responsibility to create an MSP, the DMCR has worked on drafting MSP plans for several areas in eastern and southern Thailand over the past five years. The Royal Thai Navy, an official institution in charge of mapping coastal seas, is also heavily involved in supporting the MSP process. Strong coordination between the lead agency and relevant institutions as related to MSP is imperative for an effective implenation of a place-based tool like MSP (DMCR, 2021c), especially in the context of Blue Ecnomy. As argued by Jentoft and Chuenpagdee (2022), MSP process must consider multi sectoral uses, and be inclusive of small-scale sectors, such as small-scale fishers and other vulnerable groups, to achieve just and equitable access and utilitzation of resources.

3.3 First-order governance

The first-order governance deals with day-to-day coastal management activities required to solve societal problems and to create societal opportunities. Principally speaking, when values, images and principles are well articulated and reflected in how the institutions are designed, actions at the first-order should follow correspondingly. Yet, many conditions are required for an efficient operation, most importantly the capability and capacity of governing actors and the shared understanding about the law and legal instruments among coastal stakeholders.

Across the country, staff persons in the two main agencies (local DMCR and the PMCRC) have limited skill to deal with complex problems, which are often interdisciplinary in nature. The local DMCR staffs are generally unequipped to tackle large-scale problems with multiple sources of threats to coastal and marine ecosystems. They are challenged by the need to approach coastal and marine degradation from the perspective of spatial integration, following MSP, and to identify the ways in which pressures from different sources are interconnected (Satumanatpan et

al., 2018). The reliance on familiar tools and approaches to deal with problems, and the lack of knowledge and opportunity to reflect on the root causes is a common challenge in coastal governance, not only in the case of Thailand (Eger et al., 2021).

A specific example is related to the operationalization of the Environmental Protected Areas (EPAs) in Phetchaburi and Prachuap Khiri Khan Provinces, and Koh Tao in Surat Thani Province, both of which were designated under the 1992 National Environmental Quality Act. EPAs is managed by the local governments (under the decentralized system) and is regulated through the EPAs committees, which comprise multi-stakeholders from relevant government agencies, local experts, private sectors, state enterprises and members of NGOs. The structure of the governing system is well defined and rather stable, which should facilitate the operationalization of the EPAs on the ground. Yet, a study by Satumanatpan and Chuenpagdee (2015) reveals that the EPAs do not function well, due mostly to the lack of understanding among the committee members about the natural and the coastal systems associated with the EPAs, the poor relationship and interaction between coastal stakeholders and the EPA committees, low enthusiasm and limited leadership from the EPA secretariat, and weak financial commitments for managing the EPA. Similarly, as revealed by Satumanatpan et al. (2017), the Koh Tao EPAs committees had limited understanding of the ministerial announcement about the Koh Tao EPAs, and their roles as decision makers, and had not held regular meetings but would convene only when there was a request for it. As such with all reported constraints, long-term goals for Koh Tao's sustainable development are unlikely to be achieved in a timely manner.

4. IMPLICATIONS FOR COASTAL GOVERNABILLITY

The above review illustrates how the coastal natural and social systems interact with the governing system in all three orders of governance, which then influences coastal governability. Certain features of the coastal systems, such as the rich habitats and multiplicity of coastal activities, are highly diverse, complex and dynamic, and operate at various scales, causing the coastal zones of Thailand to be difficult to govern effectively. When coupled with the highly complex and dynamic governing system, consisting of multiple agencies sharing responsibility and overlapping jurisdiction, and with limited staff capacity and poor coordination, the governability challenge is made even more difficult. Despite having the essential principles for good coastal governance, supported by laws and legislations, their operationalization is not straightforward, and coastal governance is often done without any good reflection about what it implies. In other words, the arrows in Jentoft and Chuenpagdee's figure (2022) go one way as a trickle down process from the meta-order, without any trickle up. The opportunity for interactive learning and adaptiveness is therefore limited. In this circumstance, some of the effective mechanisms to strengthen interaction between the orders would include communication and sharing information, along with a regular assessment of the alignment and correspondence. Further, governing interaction between the GS and SG can be facilitated through the participation mechanism in coastal governance, provided that it is meaningful and inclusive, and well facilitated and coordinated.

The interactive governance analytical approach offers opportunities to consider where in the governance system the coastal governability can be improved. First, at the meta-order governance, policy documents and vision for sustainable development need to be more explicit about principles such as social justice and equity. Specifically, better discussion with relevant coastal stakeholders about what Blue Economy means, what it should look like, and how to achieve it would be necessary. The same applies to the principles underlying the MSP process in a way that enables just and inclusive participation of small-scale fisheries and coastal communities. A broader conversation about the importance and values of coastal ecosystem, and the imminent role they play to support life and livelihoods of coastal people, is imperative.

In the second-order, serious considerations are required to examine the role and function of the different government agencies, making clear about their responsibility, authority and jurisdiction. Coordinating mechanisms need to be established to facilitate cooperation and harmonization, as well as to minimize duplication and confusion to increase credibility. Consideration should also be given to creating a process that recognizes the local culture and is respectful of the time and efforts of coastal community representatives involved in the governing committees. Coastal governability could also be enhanced through investment on relationship and trust building between governments and communities,

given the past experiences and the current political climate.

For the first-order, transdisciplinary training and capacity development programs need to be designed to enhance knowledge and skills of staff persons in the different government departments. The focus of the training is to build appreciation for the wicked nature in coastal governance, the reality of diverse worldviews agendas, and avoiding thus the application of technical fixes to favor iterative solutions co-creation. It is also about sensitizing staff persons with issues and concerns affecting coastal communities, and how they can work together to come up with innovative solutions for coastal sustainability. At the end, it is through mutual respect and collaborative efforts that would make governance work in the first-order.

5. CONCLUSION

This article uses the interactive governance theory, especially the three orders of governance, for examining coastal governance challenges, using the case of Thailand as an illustration. The findings can aid in understanding where governability challenges lie and how to enhance coastal governance. The study reveals the applicability of the interactive governance framework in other coastal developing countries that have similar contexts and that share the common goals to sustain marine and coastal resources.

ACKNOWLEDGEMENTS

The first author thanks the Faculty of Environment and Natural Resources, Mahidol University for providing time to working with this article. The study benefits from the discussion taken place as part of the Dried Fish Matters (DFM): Mapping the social economy of dried fish in South and Southeast Asia for enhance wellbeing and nutrition and the Vulnerability and Viability (V2V): Global Partnership for Building Strong Small-Scale Fisheries Communities, both are funded by the Social Sciences and Humanities Research Council of Canada. The paper is produced as part of the Too Big To Ignore Global Partnership for Small-Scale Fisheries Research (TBTI Global). Finally, we thank Dr. Pierre Echaubard for editing English of the manuscript.

REFERENCES

Amarasinghe A, Bavinck M. Building resilience: Fisheries cooperatives in Southern Sri Lanka. In: Jentoft S, Eide A, editors. Poverty Mosaics: Realities and Prospects in Small-Scale Fisheries. Dordrecht, Netherlands: Springer Science; 2011. p. 383-406.

Bennett N, Dearden P. From measuring outcomes to providing inputs: Governance, management, and local development for more effective marine protected areas. Marine Policy 2014; 50:96-100.

Burbridge PR. A critical review of progress towards integrated coastal management in the Baltic Sea Region. In: Schernewski G, Löser N, editors. Managing the Baltic Sea. United Kingdom: Coastline Report; 2004.

Celliers L, Scott D, Ngcoya M, Taljaard S. Negotiation of knowledge for coastal management? Reflections from a transdisciplinary experiment in South Africa. Humanities and Social Sciences Communication 2021;8:Article No. 207.

Cicin-Sain B, Knecht R. Integrated Coastal and Ocean Management: Concepts and Practice. Washington DC, USA: Island Press; 1988.

Cicin-Sain B, Belflore S. Linking marine protected areas to integrated coastal and ocean management: A review of theory and practice. Ocean and Coastal Management 2005;48:847-68.

Chuenpagdee R, Jentoft S. Governability assessment for fisheries and coastal systems: A reality check. Human Ecology 2009; 37:109-20.

Christie P, Lowry K, White A, Oracion EG, Sievanen L, Pomeroy R, et al. Key findings from a multidisciplinary examination of integrated coastal management process sustainability. Ocean and Coastal Management 2005;48:468-83.

Chuenpagdee R, Juntarashote K. Learning from the experts: Attaining sufficiency in small-scale fishing communities in Thailand. In: Jentoft S, Eide A, editors. Poverty Mosaics: Realities and Prospects in Small-Scale Fisheries. Dordrecht, Netherlands: Springer Science; 2011. p. 309-30.

Dearden P, Emphandhu D, Songpornwanich S, Ruksapol A. Koh Pitak a community based environment and tourism initiative in Thailand. In: Armitage D, Charles A, Berkes F, editors. Governing the Coastal Commons Communities, Resilience and Transformation. New York: Routlege; 2017. p 181-97.

Department of Marine and Coastal Resources (DMCR). The State of Marine and Coastal Resources and Coastal Erosion 2020. Bangkok, Thailand: Ministry of Natural Resources and Environment; 2022. (in Thai).

Department of Marine and Coastal Resources (DMCR). Marine and coastal protected areas of Trang Province (full report). [Internet]. 2021a [cited 2022 July 5]. Available from: https://projects.dmcr.go.th/miniprojects/174/download/113?page=1. (in Thai).

Department of Marine and Coastal Resources (DMCR). Guideline for Marine and Coastal Resources Utilization under the Blue Economy Framework of Trat Province. Bangkok, Thailand: Ministry of Natural Resources and Environment; 2021b. (in Thai).

Department of Marine and Coastal Resources (DMCR). Issues, Necessity and Scope of Authority for Marine Spatial Planning (MSP). Bangkok, Thailand: Ministry of Natural Resources and Environment; 2021c. (in Thai).

Department of Fisheries (DOF). Fisheries Statistics of Thailand 2014. Bangkok, Thailand: Department of Fisheries, Ministry of Agriculture and Cooperatives; 2016. (in Thai).

Department of Fisheries (DOF). Statistics of Aquatic Animals Catch from Artisanal Fishing 2019. Bangkok, Thailand: Department of Fisheries, Ministry of Agriculture and Cooperatives; 2020. (in Thai).

Eger SL, de Loe RC, Pitman J, Epstein G, Courtenay SC. A systematic review of integrated coastal and marine management progress reveals core governance characteristics for successful implementation. Marine Policy 2021;132:Article No. 104688.

Ehler C. Indicators to measure governance performance in integrated coastal management. Ocean and Coastal Management 2003;46:335-345.

Fabinyi M, Belton B, Dressler WH, Knudsen M, Adhuri DS, Aziz AA, et al. Coastal transitions: Small-scale fisheries, livelihoods, and maritime zone developments in Southeast Asia. Journal of Rural Studies 2022;91:184-94.

Food and Agriculture Organization (FAO). The State of World Fisheries and Aquaculture 2020: Sustainability in action. Rome, Italy: FAO; 2020.

Joint Group of Experts on the Scientific Aspects of Marine Environmental Protection (GESAMP). The Contributions of Science to Coastal Zone Management. Report and Student No. 61. Rome, Italy: FAO; 1996.

Graham J, Amos B, Plumptre T. Governance Principles for Protected Areas in the 21st Century. Ottawa, Canada: Institute on Governance; 2003.

Jentoft S, Chuenpagdee R. Blue Justice in three governance orders. In: Jentoft S, Chuenpagdee R, Said A, Isaacs M, editors. Blue Justice. MARE Publication Series Vol 26. Switzerland: Springer Chem; 2022. p 17-32.

Jentoft S, Chuenpagdee R. Fisheries and coastal governance as a wicked problem. Marine Policy 2009;33:553-60.

Kooiman J. Governing the Governance. London, United Kingdom: Sage Publication; 2003.

Kooiman J, Bavinck M, Jentoft S, Pullin R. Fish for Life: Interactive Governance for Fisheries. MARE Publication Series No. 3. Amsterdam: Amsterdam University Press; 2005.

Lockwood M, Davidson J, Curtis A, Stratford E, Griffith R. Governance principles for natural resources management. Society and Natural Resources 2010;23:986-1001.

Moore P, Zhang X, Triraganon R. Natural Resources Governance Trainers' Manual. Bangkok, Thailand: International Union for Conservation of Nature and Natural Resources (IUCN), The Center for People and Forests (RECOFT), and SNV Netherlands Development Organization (SNV); 2011.

Office of the National Economic and Social Development Council (NESDC). Progress Report on Thailand's Sustainable Development Goals (2016-2020). Bangkok, Thailand: NESDC; 2021. (in Thai).

Office of the National Economic and Social Development Council (NESDC). National Economic and Social Development Plan Twelfth Edition (2017-2021). Bangkok, Thailand: NESDC; 2016. (in Thai).

Office of the National Economic and Social Development Council (NESDC). National Economic and Social Development Plan Ninth Edition (2002-2006). Bangkok, Thailand: NESDC; 2002 (in Thai).

Olson S. Educating for the Governance of Coastal Ecosystems: the Dimensions of the Challenge. Ocean and Coastal Management 2000;43:331-41.

Partnership in Environmental Management for the Sea of East Asia (PEMSEA). National State of Oceans and Coasts 2018: Blue Economy Growth of Thailand. Quezon City, Philippines: PEMSEA; 2019.

Prado DS, Seixas CS, Berkes F. Looking back and looking forward: Exploring livelihood change and resilience building in a Brazilian coastal community. Ocean and Coastal Management 2015;113:29-37.

Rittel H, Webber M. Dilemmas in a general theory of planning. Policy Science 1973;4:155-69.

Royal Gazette. Announcement of the Prime Minister's Office: Announcing the Master Plan under the National Strategy (2018-2037). Volume 136, Part 51, Dated 18 Apr B.E. 2562. Bangkok, Thailand: Office of the Council of State; 2019. (in Thai).

Royal Gazette. National Environmental Quality Act (second amendment) 2018. Volume 135, Part 27, Dated 19 Apr B.E. 2561. Bangkok, Thailand: Office of the Council of State; 2018a. (in Thai).

Royal Gazette. National strategy (2018-2037). Volume 135, Part 81, Dated 13 Oct B.E. 2561. Bangkok, Thailand: Office of the Council of State; 2018b. (in Thai).

Royal Gazette. Environmental Management Plan (2017-2022). Volume 134, Part 67, Dated 3 Mar B.E. 2560. Bangkok, Thailand: Office of the Council of State; 2017 (in Thai).

Royal Gazette. Amending Ministry, Sub-Ministry and Department Act 2003. Volume 119, Part 99, Dated 2 Oct B.E. 2545. Bangkok, Thailand: Office of the Council of State; 2003. (in Thai).

Royal Gazette. Official Information Act 1997. Volume 114, Part 46, Dated 10 Sep B.E. 2540. Bangkok, Thailand: Office of the Council of State; 1997. (in Thai).

Satumanatpan S. Coastal management: Integration to sustainability. Nakorn Pathom, Thailand: Mahidol University Press; 2018.

Satumanatpan S, Moore P, Plathong S. Governance challenges for the sustainability of marine and coastal resources. In: Trisurat Y, Shrestha RP, Havmoller P, editors. Thailand, Environmental Resources, Social Issues and Related Politics. New York, USA: Nova Publishers; 2018. p. 219-39.

Satumanatpan S, Moore P, Lentisco A, Kirkman H. An assessment of governance of marine and coastal resources on Koh Tao, Thailand. Ocean and Coastal Management 2017;148:143-57.

Satumanatpan S, Chuenpagdee R. Assessing governability of environmental protected areas in Phetchaburi and Prachuap kirikhan, Thailand. Maritime Studies 2015;14:Article No. 17.

Satumanatpan S, Sanawongse P, Thansuporn V, Kirkman H. Enhancing management effectiveness of environmental protected areas, Thailand. Ocean and Coastal Management 2014;89:1-10.

Singh A. Environmental governance in small island developing states. [Internet]. 2014 [cited 2022 Mar 25]. Available from: http://www.cries.org/wp-content/uploads/2014/11/23-sha.pdf.

United Nations. United Nations convention on the law of the Sea (UNCLOS). New York, USA: Office of Legal Affairs, United Nations; 1982.

White A, Deguit E, Jatulan W, Eisma-Osorio L. Integrated coastal management in Philippine local governance: Evolution and benefits. Coastal Management 2006;34:287-302.

Soil Contamination by Phthalate Esters in Cultivated and Non-Cultivated Soils in North African Arid Regions: A Tunisian Case Study

Abdelhakim Bouajila*, Zohra Omar, Rim Saoud, and Rami Rahmani

Faculty of Sciences of Gabes, Gabes University, Cité Erriadh Zrig 6072, Gabes, Tunisia

ARTICLE INFO

Received: 29 Mar 2022
Received in revised: 30 Jun 2022
Accepted: 7 Jul 2022
Published online: 15 Aug 2022
DOI: 10.32526/ennrj/20/202200049

Keywords:
Soil/ Phthalate esters/ Plastic films/ Arid regions/ Tunisia

*** Corresponding author:**
E-mail:
bouajilaabdelhakim@gmail.com

ABSTRACT

Over the last decades, several studies showed that phthalic acid esters (PAEs) were ubiquitous environmental contaminants and became a major threat to human health. This study provided the first case study about the concentration and the potential sources of soil's PAEs, both in Tunisia and North Africa. Soil samples were collected from four cultivated (CS) and two adjacent native soils (NS) at 0-10 cm and 10-30 cm layers in southeastern Tunisia. The PAEs concentrations were analyzed using a gas chromatography-mass spectrometry (GC-MS) system. Results showed that the total concentration of PAEs ranged from 2.40 to 11.05%. Higher values were detected in NS in the 0-10 cm layer contrary to CS which showed higher PAEs concentration in 10-30 cm depth. The di-n-butyl phthalate (DBP) and di-(2-ethylhexyl) phthalate (DEHP) were the most abundant PAEs. In the 0-10 cm layer, PAEs concentration was highly related to the age of the plastic film in CS. We observed a positive association between PAEs concentration and conductivity (EC) values. The PAEs concentrations were affected by the presence of soil organic matter (SOM) in CS. This decrease of PAEs in CS compared to the NS may be related to the microbial decomposition activity stimulated by the presence of fresh organic residues and fertilizers. These results showed that CS and adjacent NS in the studied regions were contaminated by PAEs which is probably a result of agricultural activities. More investigations on PAEs concentrations in various soil managements are needed to confirm these results.

1. INTRODUCTION

Intensive use of plastic films can induce contamination of microplastics and phthalate esters (PAEs) (Li et al., 2021). Reduction of microplastics contamination is related to the management and mitigation of microplastics pollution (Rahmayanti et al., 2022). However, Phthalic acid esters (PAEs) are extensively used in plastic materials (Zhu et al., 2022), such as, polyvinyl chloride, medical product, cosmetics, clothing, building materials, paints, pesticides, fertilizers, food packaging (Staples et al., 1997; Xu et al., 2008; Wang et al., 2013). As a result of their large scale use, the global PAEs consumption per annum is estimated to 6.0×10^6 tons (Xie et al., 2007). In recent times, there has been an increasing concern over the risk of phthalate exposure leading to adverse effects to human health and the environment (Das et al., 2021).

Several studies have reported health concerns related to endocrine disruptive problems and confirmed that human exposure to PAEs causes particularly cancer and reproductive effects (Hens and Caballos, 2003; Guo and Kannan, 2011). Therefore, they are considered as one of the widespread classes of organic pollutants (Kong et al., 2012) and classified as priority environmental contaminants (USEPA, 2013).

The presence of PAEs is confirmed in various environmental media, such as, air (Wang et al., 2012), water (Xie et al., 2007), sediment, soils (Ma et al., 2013; Kong et al., 2012) and many types of plant species (Fu and Du, 2011). Soils are considered as the main environmental matrices, highly affected by anthropogenic activities, and they act as natural sinks for pollutants, which can lead to the pollution of other spheres of the ecosystems and the human food chain.

Citation: Bouajila A, Omar Z, Saoud R, Rahmani R. Soil contamination by phthalate esters in cultivated and non-cultivated soils in North African Arid regions: A Tunisian case study. Environ. Nat. Resour. J. 2022;20(6):553-562. (https://doi.org/10.32526/ennrj/20/202200049)

Actually, irrigation methods, the application of pesticides, and the impact of surrounding pollutant sources, waste and diversity of manure may lead to the differences of PAEs concentrations in various types of soils (Kong et al., 2012). Fertilizers contain between 0.01 to 2.8 mg/kg of PAEs as reported by Mo et al. (2008). It can lead to the accumulation of PAEs in the soil (Fu and Du, 2011). Plastic film used in agricultural field is associated to the increase of PAEs contamination (Pedersen et al., 2008). The use modes, and the amount of plastic films, as well as the age of the greenhouse, are the principal sources of PAEs soil contamination. Thus, they are the main factors controlling the PAEs concentration's variation in soil (Guo and Wu, 2011).

Soil contamination by PAEs is controlled by various factors, such as, soil properties and soil uses (Xu et al., 2008; Zeng et al., 2009), as well as the meteorological conditions (Cai et al., 2008; Kong et al., 2012). Zhang et al. (2015) demonstrated that high PAEs concentrations are detected in the summer.

DEHP and DBP are the most identified contaminants in cultivated soils and in multiple environment compartments like surface waters (Kelly et al., 2010). In fact, DEHP and DBP are the dominant components in plastic film (Wang et al., 2013). Moreover, longer/branching alkyl-chain PAEs such as DEHP improve polymer flexibility and they have been extensively used in the polymer industry as plasticizers (Hens and Caballos, 2003). DEHP is a principal component in most widely used-fertilizers (Mo et al., 2008). High concentration of DBP and DEHP in agricultural soils have already been detected in Chinese soils (Ma et al., 2003; Xu et al., 2008).

Our study was carried out in the Gabès Governorate, which is an industrial and commercial town with a population of about 374,300 inhabitants. However, since the foundation of one of the biggest Tunisian industrial complexes in Gabes City (1972), several studies showed that many wastes are produced by the industrial complex and have been directly dumped in the near coastal environment of Gabes region which is considered one of the most polluted areas in the Mediterranean Basin (El Zrelli et al., 2021). In addition, in Gabès region oasis agrosystems and other agricultural soil play a vital role in the life of the local communities. Actually, date palms are one of the most important crops in oasis ecosystems, providing a major source of income for local farmers and for the national economy. Seasonal crops in this region, where soils are poor quality, use fertilizers and greenhouse vegetables are extensively grown. However, in many developing countries, there is a large quantity of agricultural wastes that cause severe pollution problems (El-Hassanin et al., 2020). Hence, degrees of damage on the ecosystem and on human health are detected. We believe that the contamination of atmosphere, groundwater and soils are behind several health damages such as birth defects, negative effects on neurodevelopment and growth in children, cancer, and so on, in the Gabès population. Actually, industrial towns worldwide and particularly in arid regions are subjected to several environmental threats because temperature and wind spread pollutants over large areas. According to Wei et al. (2020) PAEs were detected in all the soil and vegetable samples collected in the economically developed YRD region of China. The main objective of this preliminary study, being the first one in the field in North Africa, is to determine the concentration and the potential sources of soil PAEs under cultivated greenhouse and adjacent non-cultivated native soils. More considerable attention should be given to the PAEs contamination status in soils and potential effects on local resident health (Tao et al., 2020).

2. METHODOLOGY

2.1 Studied sites and sampling method

All studied sites were located in southeastern arid region of Tunisia, precisely in Gabès governorate (Figure 1). The climate is Mediterranean, dry, hot in summer and mild in winter. The average annual temperatures ranged between 17 and 45°C and irregular precipitation (237 mm/year) is concentrated in the winter. Soils in southren regions of Tunisia are classified as Arenosols or Gypsisols in the WRB classification (Jones et al., 2013; Labiadh et al., 2013). However, in the current study, sampled soils in both sites were classified as Gypsisols. Soil samples were taken from the 0-10 cm and 10-30 cm layers of the profile using pre-cleaned iron soil shovel. In each greenhouse, three profiles were sampled: the first one was about 1m from the door of the greenhouse, the second is at the middle and the third is in the back of the greenhouse. In the laboratory, the three samples from each depth were sieved and mixed to produce composite samples which were reduced and used for analyses. Soil samples were stored in glass bottles and air-dried in a ventilated place at room temperature. Before analysis, samples were sieved through a 2 mm stainless steel sieve to remove plant debris and rock fragments. Six profiles were selected in four vegetable

greenhouse cultivated soils (CS1, CS2, CS3, and CS4) and two adjacent native soils (NS1 and NS2). The ages of the vegetable greenhouses were 8, 10, 15, and 30 years for, respectively, CS1, CS2, CS3, and CS4. In these greenhouses (each one covering 504 m^2, length=56 m, width=9 m) (Figure 2), farmers produce seasonal crops, particularly tomato, pepper, cucumber, melon. The planting date is depending on type of crops.

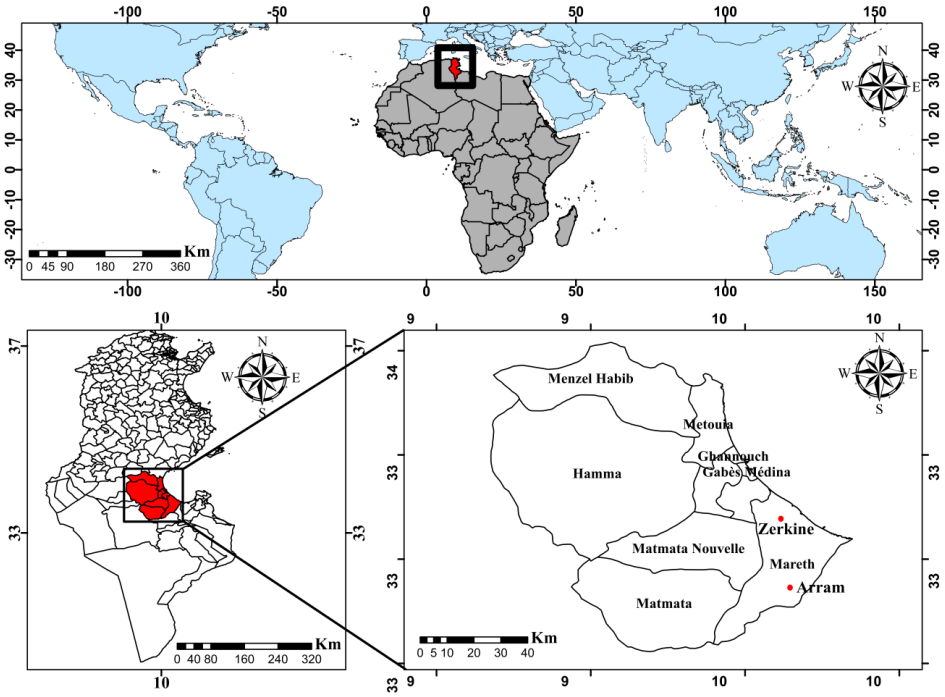

Figure 1. Localization map of the study area in Gabès Governorate

(a)

(b)

Figure 2. The sampling sites of soils (a) Arram (vegetable greenhouse CS1, CS2, and NS1) and (b) Zerkine (vegetable greenhouse CS3, CS4, and NS2)

2.2 Soil analysis

The total soil organic carbon (SOC) was determined by $K_2Cr_2O_7 \cdot H_2SO_4$ oxidation method of Walkey and Black (Nelson and Sommers, 1982) then the soil organic matter (SOM) content was calculated by multiplying SOC content by 1.72 (Dabin, 1967). Soil pH and EC were measured in a 1:5 soil:water suspension. Calcium carbonate ($CaCO_3$) content was estimated by the method of calcimetry (Nelson, 1982). Soil particle size distribution was determined by Robinson's method (Robinson, 1922).

2.3 Organic compounds extraction

Soil organic compounds were obtained by maceration of 50 g of air-dried soil (<2 mm) in 250 mL of methanol (MeOH) for 2 h at room temperature. After filtration, the solvent was evaporated under vacuum at 35°C, using a rotary evaporator (IKA, RV 10 auto V, Germany). The obtained dry concentrated organic residues were placed in hemolysis tubes and stored at -20°C until further analysis (Rahmani et al., 2020).

2.4 Gas chromatography-mass spectrometry (GC-MS)

Gas chromatography-mass spectrometry analysis (a gas chromatography system (7890A) coupled to a mass spectrometry system (5975C, MSD) (Agilent Technologies, USA), was used to identify the volatile compounds from soil organic extracts (Rahmani et al., 2020) (Figure 2).

3. RESULTS AND DISCUSSION

3.1 Soil properties

The cultivated soils and native soils were slightly alkaline because pH values were between 8.12 and 8.90. Specifically, the cultivated soils showed high EC values. However, SOM concentrations were from 0.39 to 1.39% and from 0.55 to 0.87%, respectively, in cultivated soils and in native soils (Table 1). Among soils low concentrations of $CaCO_3$ and gypsum were recorded. The soil textures were loamy sand.

The pH values can be attributed to the high levels of carbonate calcium and gypsum (Corti et al., 2020). Similar pH values are detected by Mlih et al. (2019) and Omar et al. (2020) in the same regions under cultivated and non-cultivated soils. However, higher EC value in CS can be explained particularly by the use of saline water in irrigation (2.5 g/L to 4 g/L) (Omar et al., 2017; Corti et al., 2020). The presence of $CaCO_3$ and gypsum in arid soils of Tunisia was related to the alteration of geological parent materials (Mtimet, 2001). Low SOM concentrations observed in studied regions are similar to the average of SOM contents in soils of arid regions characterized by little accumulation of organic residues and high mineralization rate. SOM concentrations ranged between 0.39 and 1.39%; and between 0.55 and 0.87%, respectively, in CS and NS. Our results are in agreement with those detected by Mlih et al. (2019), Omar et al. (2020), and Znaidi et al. (2020) in soils of arid regions of Tunisia, by Elbasiouny et al. (2017) in reclaimed cultivated soils of the Nile Delta, Egypt and by Shahabinejad et al. (2019) in arid regions of Iran.

Table 1. Main characteristics of the vegetable greenhouse cultivated soils (CS1, CS2, CS3, and CS4) and adjacent native soils (NS1 and NS2).

		pH	EC (mS/cm)	Clay (%)	Silt (%)	Sand (%)	SOM (%)	$CaCO_3$ (%)	Gypsum (%)
CS1	0-10 cm	8.19±0.03	2.67±0.02	5.6	7.8	83.9	1.37±0.03	10.09±1.36	1.10±0.28
	10-30 cm	8.20±0.04	2.62±0.08	4.2	18	77.1	0.49±0.02	6.25±1.10	1.10±0.56
CS2	0-10 cm	8.17±0.12	6.89±0.61	6.7	7.2	83.5	0.39±0.05	6.25±1.30	8.70±0.74
	10-30 cm	8.18±0.08	6.23±0.45	8.1	7.7	83.9	0.96±0.06	5.28±1.30	12.25±0.42
CS3	0-10 cm	8.12±0.05	5.27±0.09	13.3	6.5	78.1	1.39±0.04	7.70±0.90	1.25±0.09
	10-30 cm	8.14±0.04	5.90±0.05	12.9	4.8	79.5	1.04±0.03	7.20±1.87	1.77±0.10
CS4	0-10 cm	8.39±0.04	9.40±1.10	14.2	3.3	80.9	0.73±0.03	8.18±1.91	2.06±0.12
	10-30 cm	8.28±0.03	12.20±1.80	12.5	4.5	81.6	0.84±0.03	7.24±2.44	0.44±0.01
NS1	0-10 cm	8.12±0.09	2.92±0.02	6.6	8.8	82.9	0.55±0.01	3.63±1.51	0.44±0.05
	10-30 cm	8.13±0.06	1.65±0.03	6.2	16.7	77.3	0.67±0.02	10.90±2.86	0.22±0.02
NS2	0-10 cm	8.19±0.02	1.48±0.01	14.9	5.3	78.9	0.87±0.01	8.20±2.55	0.29±0.02
	10-30 cm	8.38±0.02	2.36±0.02	13.5	5.1	81.5	0.60±0.03	8.60±3.22	0.44±0.02

C: cultivated; N: Native; EC: electrical conductivity; SOM: soil organic matter

3.2 PAEs soil concentrations and sources

Four types of PAEs are detected in studied soils DBP, DEHP, Dimethyl phthalate (DMP), and Dipentyl phthalate (DPP), which indicated that studied soils, as expected, were polluted by PAEs (Table 2). The total PAEs concentrations (∑PAEs) are ranging from 2.40 to11.05%. Across depth, PAEs concentration in CS was between 2.40 and 8.33% and in NS between 5.01 and 11.05%. Several previous studies have reported that soils of various agrosystems and uncultivated surrounding soil are contaminated by PAEs (Zhang et al., 2015). However, in our study as unexpected in NS the ∑PAEs was more than two or three times higher compared to CS. For example the ∑PAEs in NS2 in 0-10 cm was equal to 10.05% but in CS1 and CS2 we recorded, respectively, 2.4 and 3.97%. This finding is in agreement with those by Zhang et al. (2014) which found that total PAEs and individual concentrations of phthalate contaminants were all relatively low in the areas that used plastic films compared with other samples. They considered this fact is due to the greatest usage amount of plastic

products in people's daily lives and other factors like diffusion of PAEs in the atmosphere. In our study, probably, these differences can be the result of the impact of factors controlling PAEs accumulation in soil, such as, distance from a pollution source, soil type and properties, land use, rainfall and temperature, which can make transverse, vertical and seasonal changes (He et al., 2015). Xu et al. (2008) thought that precipitation, atmospheric deposition, drainage, or seepage could cause PAEs contaminations in cultivated and uncultivated soils. Moreover, building materials and domestic garbage at surroundings can cause native PAEs soil contamination. Actually, high concentrations of PAEs in urban soils were observed for roadside sites (Kong et al., 2012). Moreover, the less PAEs in cultivated soils in the present study is probably because sampling in the present study was performed in summer when fewer agricultural activities were involved, leading to less PAEs input. In addition, in CS, we hypothesize that the presence of organic matter (Gao et al., 2021), water and fertilizers increase microbial activity in CS which in turn increases organic matter and PAEs mineralization (Boll et al., 2020; Das et al., 2021; Wang et al., 2020). Microbial degradation could efficiently reduce the residue of organic pollutants in soil and crop plants (Liu et al., 2022; Wang et al., 2020). This is perhaps why in CS the PAES concentration is low than in NS.

Table 2. The concentrations (%) of different PAEs detected in the vegetable greenhouse cultivated soils (CS1, CS2, CS3, and CS4) and adjacent native soils (NS1 and NS2)

Soil	CS1		CS2		CS3		CS4		NS1		NS2	
	8years		10years		15years		30 years					
	0-10 cm	10-30 cm	0-10 cm	10-30 cm	0-10 cm	10-30 cm	0-10 cm	10-30 cm	0-10 cm	10-30 cm	0-10 cm	10-30 cm
DEHP (%)	2.40	6.00	3.97	4.99	4.30	5.39	5.34	6.38	7.12	3.30	6.74	5.30
DBP (%)	ND	1.74	ND	0.78	0.97	1.26	0.00	1.95	1.05	1.33	3.40	3.00
DPP (%)	ND	0.41	ND	ND	ND	ND	ND	ND	ND	ND	ND	ND
DMP (%)	ND	ND	ND	ND	ND	ND	0.59	ND	ND	0.38	0.91	0.00
Total (%)	2.40	8.15	3.97	5.77	5.27	6.65	5.93	8.33	8.17	5.01	11.05	8.30

C: cultivated; N: native; DEHP: di-(2-ethylhexyl) phthalate; DBP: di-n-butyl phthalate; DPP: dipentyl phthalate; DMP: dimethyl phthalate; ND: not detected

Among different sampled soils four types of phthalates were detected DBP, DEHP, DPP, and DMP which showed different concentrations. The DPP is closely present in CS1 in Arram region. However, the DMP was detected in NS and cultivated soil CS4. The DEHP and DBP are the most abundant PAEs in NS and CS but varied widely between sites and across soil depth. This result is in agreement with those found by Ma et al. (2020). The DEHP and DBP are the principal components of wide ranges of industrial products. For example, according to Mo et al. (2008) and Kong et al. (2012), the concentrations of DBP and DEHP were influenced by fertilizers and plastic films, as well as differences in the use of irrigation mode. An increase in the annual average temperature causes the reduction in bond strength of the plasticizer and Polyvinyl chloride (PVC) chain thus leading to increased discharge of PAEs into the surrounding soil (Chen et al., 2011). DEHP is not easily biodegradable; therefore, it easily accumulates in the soil at high levels (Cartwright et al., 2000). An increase in the annual average temperature causes the reduction in bond strength of the plasticizer and PVC chain thus leading to increased discharge of PAEs particularly into the surrounding soil (Chen et al., 2011). That is probably why sampled soils showed relatively high accumulation of DEHP and DBP.

3.3. The DEHP and DBP concentrations and repartition across depth

Among sites, the DEHP concentration ranged between 2.40 and 7.12% and 3.30 and 6.38% in 0-10 cm and 10-30 cm depth, respectively. Native soils showed the highest contamination by DEHP which was located at surface layer (0-10 cm) (Figure 3(a)). In 0-10 cm the largest proportion of DEHP in cultivated soil (5.34%) was detected in CS4 which showed also the greatest DEHP percentage (6.38%) in 10-30 cm depth. Soil cultivation increases deep layer contamination by PAEs. For example, in CS1 the DEHP concentration in 10-30 cm depth was more than two times higher than in 0-10 cm depth. Conversely, in NS the surface layer 0-10 cm concentrated more DEHP than the 10-30 cm layer depth. Contrarily to

DEHP, the presence of DBP is recorded in only four samples at 0-10 cm depth and five samples in 10-30 cm (Figure 3(b)). The maximum of DBP concentration was detected in NS2 with 3.40 and 3.00%, respectively, in 0-10 cm depth and 10-30 cm depth. However, in the cultivated sites, the DBP concentration did not exceed 2%. Our results are in agreement with those found by Chai et al. (2014) who indicated that the maximum of PAEs concentration was detected in 10-20 cm layer in soils of vegetable greenhouses. Also, sampled soils from different regions of China, showed that the DEHP and DBP are concentrated in 0-20 or 0-30 cm layer, but DEHP was the dominant congener at 20 cm to 40 cm depth (Chai et al., 2014; Zhang et al., 2015).

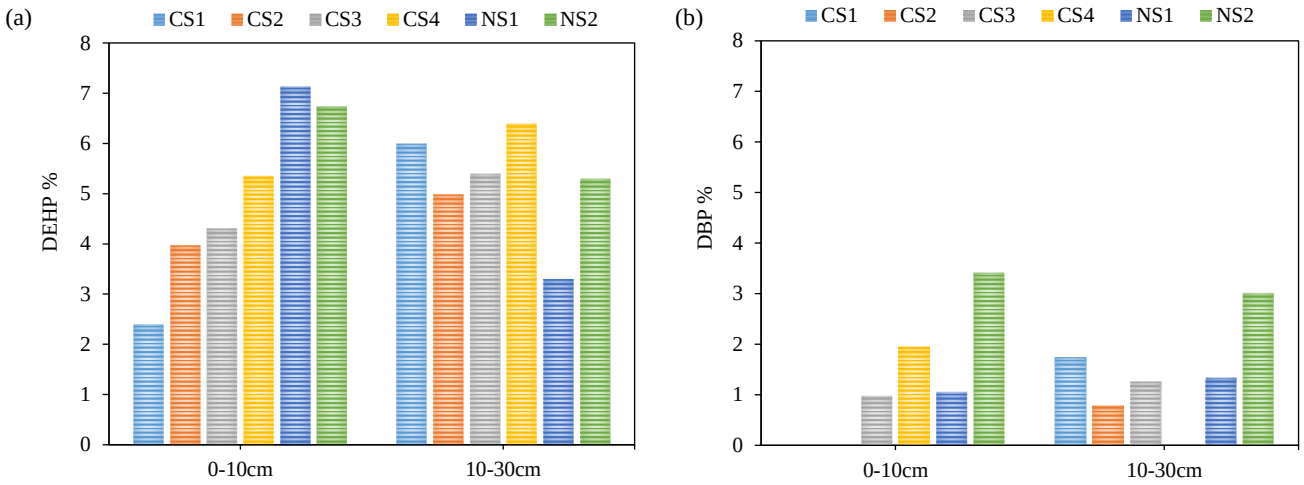

Figure 3. The (a) DEHP and (b) DBP concentrations of different sampled soil

Actually, the consumption of plastic films would lead to the continuous input of the PAEs into the soil, which leads to an increase in the concentration of DBP and DEHP in the soil (Tao et al., 2020). DEHP and DBP are the dominant components in plastic films (Wang et al., 2013, Tao et al., 2020). The amount of DEHP added in flexible PVC products could reach up to 40% (Chao and Cheng, 2007). DEHP is a principal component in most widely used-fertilizers (Mo et al., 2008), and it is typically used in plastic products in high volume compared to DBP (Zeng et al., 2009; Chai et al., 2014). In recent studies (Tao et al., 2020; Wei et al., 2020; Zhou et al., 2021) in Chinese soils the DBP and DEHP were the dominant pollutants among large numbers of PAEs.

Our results were in agreement with the finding of the Chinese study which concluded that cultivation is a principal source of soil's contamination by DBP and DEHP. However, in the current study we found that less DBP and DEHP concentrations were recorded in cultivated soils which are in disagreement with the previously mentioned study in China. For example the DBP and DEHP levels for cultivated fields were about 3.5 fold higher than those for non-cultivated fields in Chinese soils (Xu et al., 2008). We can suggest that differences between soil properties in arid Tunisia and in China make the studied CS show low concentrations of PAEs compared to surrounding soils. The higher accumulation in surface layer was the result of the rapprochement to the source of contamination. Actually, in 0-10 cm depth we remark a strong relationship between DEHP and DBP percentages (Figure 4). This supports our suggestion that these two compounds have the same source.

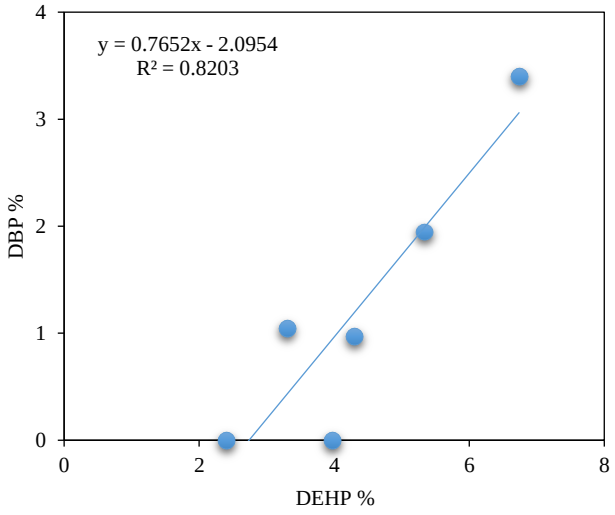

Figure 4. Relationship between the DEHP and the DBP percentages in different vegetable greenhouse cultivated soils

3.4. Effect of plastic film use period on PAEs concentration

As shown in Figure 5, the PAEs concentration appears to be related to the period of plastic film use. Interestingly, in 0-10 cm layer, the PAEs concentration increases with the age of the used plastic film. Similarly, Fu and Du (2011), remarked that the variation of PAEs concentration in soil could be related to the age of plastic greenhouse or the amounts of remaining plastic film residues. Due to the use of a large amount of agricultural film, greenhouse vegetable soil has become a key area of PAE pollution, and it has also become a pollution source of PAEs (Zhou et al., 2021).

According to Wang et al. (2013), the time over which the soil is exposed to the plastic film and the use mode can influence PAEs concentration. Larger value of PAEs concentrations in soils at 0-10 cm and 10-20 cm appeared in the region with a long history of vegetable production and particularly for extensive greenhouse cultivation (Chai et al., 2014). In their previous study, Wang et al. (2013) found that Chinese soil exhibited elevated levels of PAEs caused by large amounts of plastic film and compost fertilizers, which had been used for several years. In addition, they demonstrated that in soil covered with new plastic film the PAEs concentration is high. High PAEs levels have been previously reported in soils with residual plastic film (Kong et al., 2012). In addition, it was noticed that the PAEs soil concentration is significantly correlated to the period of plastic film coverage because the PAEs compounds in plastic films are released to the soils with the passage of time (Hens and Caballos, 2003). Soils using plastic mulch for long or using black plastic mulch were found to have a relatively higher PAEs content. The application of large amounts of plastic film over long periods of time can raise PAEs concentrations and environmental risk in soils (Wang et al., 2013). Guo and Wu (2011) and Chai et al. (2014) demonstrated that DBP and DEHP contents in soils were high with long periods of plastic film utilization or the use of greenhouse vegetable cultivation over years. Recently, Wang et al. (2022) confirmed that the duration of plastic film used and air temperature affect phthalate soil-air migration. In our study this positive relationship between soil PAEs concentrations and the period of use of plastic film strongly supports the hypothesis that plastic films are the main source of the contamination by PAEs.

However, PAEs concentration in 10-30 cm showed no link with the age of plastic film use. In the deeper layer from 10-30 cm depth the concentration of PAEs was not correlated to the period of plastic film use and fertilizers addition. The current results were in agreement with those found by Chai et al. (2014) which record a low correlation between PAEs and the age of vegetable greenhouses in deeper soil layer. This may be due to the soil properties, soil land use or the soil leaching by water, which caused the migration of PAEs through the soil (Chai et al., 2014). Soil leaching of studied soils is considered high because of their coarse texture (developed porosity).

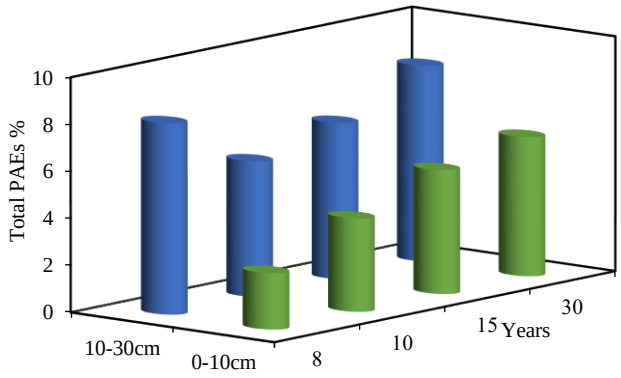

Figure 5. Effect of period of plastic film use of vegetable greenhouse on total PAEs concentrations across soil depth in cultivated soils.

3.5. Relation between soil properties and PAEs concentration

Globally, the soil properties and the soil use types affect largely the concentration, mobility and the decomposition rate of pollutants. According to Zeng et al. (2009), the soil's PAEs concentration levels and variation were, also, affected by many factors, such as, land use and soil properties.

As shown in Figures 6 and 7 we can draw positive correlations between PAES concentrations and particular soil properties in the current study. Indeed, Figure 6(a) shows positive relationship (R^2=0.16) between PAEs concentrations and EC (soil salinity) in CS. Similarly positive association (R^2=0.28) was observed between DEHP percentages and EC values (Figure 6(b)). However, we recorded negative correlation between the amount of SOC in CS and the PAEs and DEHP percentages in soil (Figure 7 and Figure 7(b)). Similar positive correlations with similar R-squared are recorded by Li et al. (2016), particularly between SOM and PAEs in contrast with our study. It means that these soil properties affect directly or indirectly the concentration of PAEs of soil in studied region. Though, these weak associations between soil

properties and PAEs in this work make it hard to draw any conclusive statements on the observed values. We can make hypothesis about the origins of this correlation. Generally, soil salinity, in arid regions, is related to the soil irrigation by saline water and the use of PVC irrigation system increases the soil's PAEs concentration by dissolved plastic compounds in the water. In addition, several studies indicated the presence of PAEs in water used for irrigation in polluted regions (Zeng et al., 2009; Wang et al., 2012). Hence we can consider that irrigation increases simultaneously EC and PAEs concentration in soil which can explain the association between them. Similarly, the negative association between SOC and PAEs or DEHP concentrations is in contrast with both results found by Zhang et al. (2015) and Li et al. (2022) which recorded high significant positive correlation between PAEs and organic matter. We can suggest that the difference in results can be related to other soil properties such as soil microbiology or CEC, the type of fertilizers and the type of agro-systems. This makes it crucial to start further studies to give more accurate data about factors controlling PAEs concentration, origins and dynamic in soil of Tunisia and MENA regions.

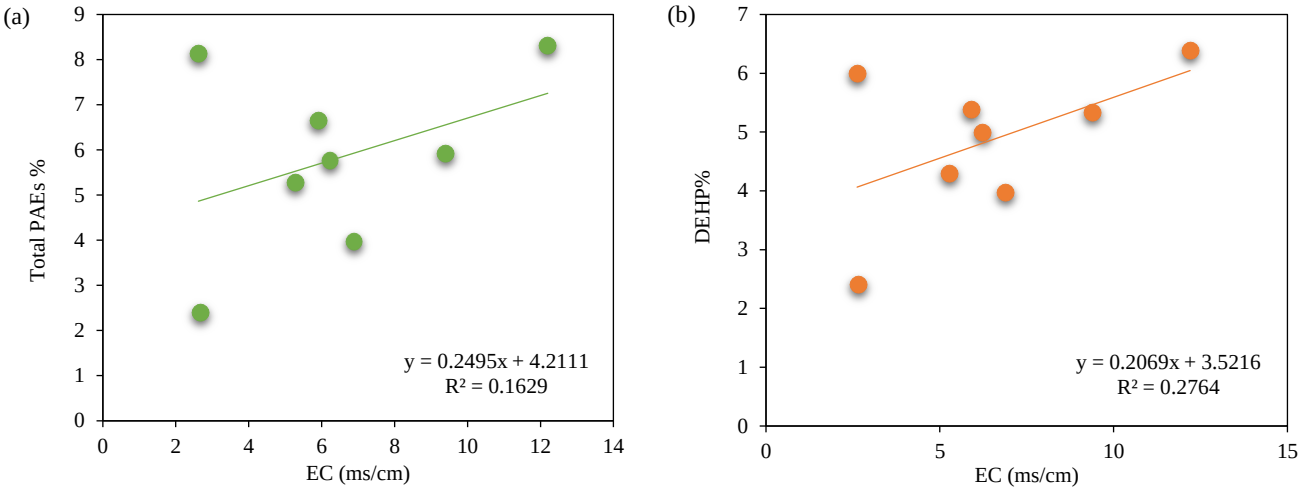

Figure 6. Relationships between soil's electrical conductivity EC (a) Total PAEs concentrations and (b) the DEHP concentrations in vegetable greenhouse cultivated soils

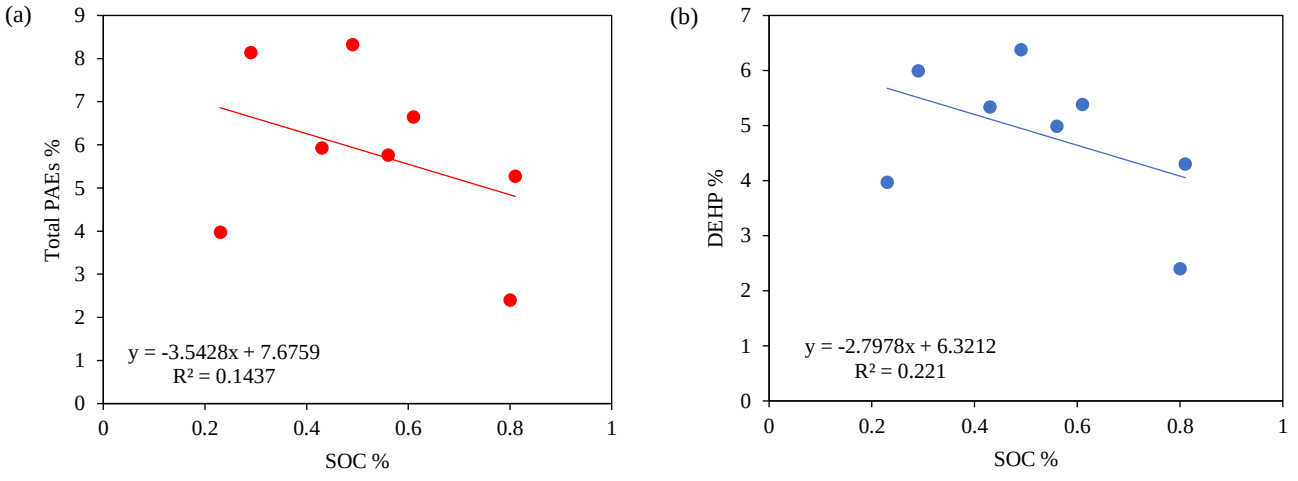

Figure 7. Relationships between SOC and (a) total PAEs concentrations and (b) the DEHP concentrations in vegetable greenhouse cultivated soils

4. CONCLUSION

The current preliminary study has provided baseline information about the concentration and distribution of phthalate acid esters (PAEs) in the soils of arid regions of Tunisia. Only four types of PAEs were detected with different concentrations. Cultivated soils under greenhouses showed low PAE concentrations than in adjacent native soils. The main PAEs detected were DBP and DEHP. Soil PAEs, DBP and DEHP concentrations seem to be related to the age

of greenhouses, the EC and to the SOC content. This primary data confirmed that PAEs are emerging organic contaminants in agricultural soils of Tunisia. Data on PAEs in various types of soils in different regions and in various types of irrigation water are needed for future research on human exposure to these emerging toxic contaminants. Effective measures should be taken to control the migration of PAEs from soil to plants. The soil pollution by PAEs and human health threats should receive more attention in developed country in MENA regions.

ACKNOWLEDGEMENTS

The authors are grateful to the Tunisian Ministry of Higher Education and Research which supported this study. In addition, our deepest gratitude goes to the anonymous reviewers for their careful work and thoughtful suggestions that have substantially improved this paper.

REFERENCES

Boll M, Geiger R, Junghare M, Schink B. Microbial degradation of phthalates: Biochemistry and environmental implications. Environmental Microbiology Reports 2020;12(1):3-15.

Cai QY, Mo CH, Wu QT, Katsoyiannis A, Zeng QY. The status of soil contamination bysemivolatile organic chemicals (SVOCs) in China: A review. Science of the Total Environment 2008; 389(2-3):209-24.

Cartwright CD, Thompson IP, Burns RG. Degradation and impact of phthalate plasticizers on soil microbial communities. Environmental Toxicology and Chemistry 2000;19(5):1253-61.

Chai C, Cheng H, Ge W, Ma D, Shi Y. Phthalic acid esters in soils from vegetable greenhouses in Shandong Peninsula, East China. PloS One 2014;9:Article No. 95701.

Chao WL, Cheng CY. Effect of introduced phthalate-degrading bacteria on the diversity of indigenous bacterial communities during di-(2-ethylhexyl) phthalate (DEHP) degradation in a soil microcosm. Chemosphere 2007;67:482-8.

Chen YS, Luo YM, Zhang HB, Song J. Preliminary study on PAEs pollution of greenhouse soils. Acta Pedologica Sinica 2011; 48:516-23.

Corti G, Cocco S, Hannachi N, Cardelli V, Weindorf DC, Marcellini M, et al. Assessing geomorphological and pedological processes in the genesis of pre-desert soils from southern Tunisia. Catena 2020;187:Article No. 104290.

Dabin B. Application de dosage automatique à l'analyse des sols, 3éme partie. Cahier ORSTOM, Série Pédologie 1967;7:257-63. (in French).

Das MT, Kumar SS, Ghosh P, Shah G, Malyan SK, Bajar S, et al. Remediation strategies for mitigation of phthalate pollution: Challenges and future perspectives. Journal of Hazardous Materials 2021;409:Article No. 124496.

Elbasiouny H, Bowaly A, Gad A, Abu-Alkheir A, Elbehiry F. Restoration and sequestration of carbon and nitrogen in the degraded northern coastal area in Nile Delta, Egypt for climate change mitigation. Journal of Coastal Conservation 2017;21: 105-14.

El- Hassanin AS, Samak MR, Radwan SR, El- Chaghaby GA. Preparation and characterization of biochar from rice straw and its application in soil remediation. Environment and Natural Resources Journal 2020;18(3):283-9.

El Zrelli R, Baliteau JY, Yacoubi L, Castet S, Grégoire M, Fabre S, et al. Rare earth elements characterization associated to the phosphate fertilizer plants of Gabes (Tunisia, Central Mediterranean Sea): Geochemical properties and behavior, related economic losses, and potential hazards, Science of the Total Environment 2021;791:Article No. 148268.

Fu XW, Du QZ. Uptake of di-(2-ethylhexyl) phthalate of vegetables from plastic film greenhouses. Journal of Agricultural and Food Chemistry 2011;59:11585-8.

Gao M, Chang X, Xu Y, Guo Z, Song Z. Effects of Fe-Mn impregnated biochar on enzymatic activity and bacterial community in phthalate-polluted brown soil planted with wheat. Environmental Pollution 2021;284:Article No. 117179.

Guo Y, Kannan K. Comparative assessment of human exposure to phthalate ethers from house dust in China and the United States. Environmental Science and Technology 2011;45:3788-94.

Guo DM, Wu Y. Determination of phthalic acid esters of soil in south of Xinjiang cotton fields. Arid Environmental Monitoring 2011;25:76-9.

He L, Gielen G, Bolan N, Zhang X, Qin H, Huang H, et al. Contamination and remediation of phthalic acid esters in agricultural soils in China: A review. Agronomy for Sustainable Development 2015;35:519-34.

Hens AG, Caballos MPA. Social and economic interest in the control of phthalic acid esters. Trends in Analytical Chemistry 2003;22:847-57.

Jones A, Breuning-Madsen H, Brossard M, Dampha A, Deckers J, Dewitte O, et al. Soil Atlas of Africa: An Introduction to the First Ever Soil Atlas of Africa. Luxembourg: European Commission: Publications Office of the European Union; 2013.

Kelly MA, Reid AM, Quinn-Hosey KM, Fogarty AM, Roche JJ, Brougham CA. Investigation of the estrogenic risk to feral male brown trout (*Salmotrutta*) in the Shannon International River Basin District of Ireland. Ecotoxicology and Environmental Safety 2010;73:1658-65.

Kong S, Ji Y, Liu L, Chen L, Zhao X, Wang J, et al. Diversities of phthalate esters in suburban agricultural soils and wasteland soil appeared with urbanization in China. Environmental Pollution 2012;170:161-8.

Labiadh M, Bergametti G, Kardous M, Perrier S, Grand N, Attoui B, et al. Soil erosion by wind over tilled surfaces in South Tunisia. Geoderma 2013;202-203:8-17.

Li K, Ma D, Wu J, Chai C, Shi Y. Distribution of phthalate esters in agricultural soil with plastic film mulching in Shandong Peninsula, East China. Chemospher 2016;164:314-21.

Li Q, Zeng A, Jiang X, Gu X. Are microplastics correlated to phthalates in facility agriculture soil? Journal of Hazardous Materials 2021;412:Article No. 125164.

Li X, Li N, Wang C, Wang A, Kong W, Song P, et al. Occurrence of phthalate acid esters (PAEs) in protected agriculture soils and implications for human health exposure. Research Square 2022:preprint;1-11.

Liu LH, Yuan T, Zhang JY, Tang GX, Huixiong Lü, Zhao HM, et al. Diversity of endophytic bacteria in wild rice (*Oryza meridionalis*) and potential for promoting plant growth and degrading phthalates. Science of the Total Environment 2022;806(1):Article No. 150310.

Ma LL, Chu SG, Xu XB. Phthalate residues in greenhouse soil from Beijing suburbs, People' s Republic of China. Bulletin of Environmental Contamination and Toxicology 2003;71:394-9.

Ma TT, Christie P, Luo YM. Phthalate esters contamination in soil and plants on agricultural land near an electronic waste recycling site. Environmental Geochemistry and Health 2013;35:465-76.

Ma T, Zhou W, Chen L, Li Y, Luo Y, Wu P. Phthalate esters contamination in vegetable-soil system of facility greenhouses in Jingmen, Central China and the assessment of health risk. Environmental Geochemistry and Health 2020;36:505-15.

Mlih R, Gocke MI, Bol R, Berns AE, Fuhrmann I, Brahim N. Soil organic matter composition in coastal and continental date palm systems-insights from Tunisian oases. Pedosphere 2019;29:444-56.

Mo CH, Cai QY, Li YH, Zeng QY. Occurrence of priority organic pollutants in the fertilizers, China. Journal of Hazardous Materials 2008;152:1208-13.

Mtimet A. Soils in Tunisia. In: Zdruli P, Steduto P, Lacirigola C, Montanarella L, editors. Soil Resources of Southern and Eastern Mediterranean Countries, Options Méditerranéennes: Serie B. Etudes et Recherche; 2001. p. 243-62. (in French).

Nelson R. Carbonate and gypsum. In: Page AL, editor. Methods of Soil Analysis. 2nd ed. Madison, USA: American Society of Agronomy and Soil Science Society of America; 1982. p. 181-97.

Nelson DW, Sommers LE. Total carbon, organic carbon, and organic matter In: Page AL, editors. Methods of Soil Analysis. 2nd ed. Madison, USA: American Society of Agronomy and Soil Science Society of America; 1982. p. 539-77.

Omar Z, Bouajila A, Brahim N, Grira M. Soil property and soil organic pools and stocks of soil under oases in arid regions of Tunisia. Environmental Earth Science Journal 2017;76: Article No. 415.

Omar Z, Bouajila A, Bouajila J, Rahmani R, Besser H, Hamed Y. Spectroscopic and chromatographic investigation of soil organic matter composition for different agrosystems from arid saline soils from Southeastern Tunisia. Arabian Journal of Geosciences 2020;13:Article No. 524.

Pedersen GA, Jensen LK, Fankhauser A, Biedermann S, Petersen JH, Fabech B. Migration of epoxidized soybean oil (ESBO) and phthalates from twist closures into food and enforcement of the overall migration limit. Food Additives and Contaminants 2008;25:503-12.

Rahmani R, Bouajila J, Jouaidi M, Debouba M. African mustard (*Brassica tournefortii*) as source of nutrients and nutraceuticals properties. Journal of Food Science 2020;85:1856-71.

Rahmayanti R, Adji BK, Nugroho AP. Microplastic pollution in the inlet and outlet networks of Rawa Jombor Reservoir: Accumulation in aquatic fauna, interactions with heavy metals, and health risk assessment. Environment and Natural Resources Journal 2022;20(2):192-208.

Robinson GW. A new method for mechanical analysis of soil and other dispersion. Journal of Agricultural and Food Chemistry 1922;212:306-21.

Shahabinejad N, Mahmoodabadi M, Jalalian A, Chavoshi E. In situ field measurement of wind erosion and threshold velocity in relation to soil properties in arid and semiarid environments. Environmental Earth Sciences. 2019;78:Article No. 501.

Staples CA, Peterson DR, Urbanerton TF, Adams WJ. The environmental fate of phthalate esters: a literature review. Chemosphere 1997;35:667-749.

Tao H, Wang Y, Liang H, Zhang X, Liu X, Li J. Pollution characteristics of phthalate acid esters in agricultural soil of Yinchuan, northwest China, and health risk assessment. Environmental Geochemistry and Health 2020;42:4313-26.

United States Environmental Protection Agency (USEPA). Electronic Code of Federal Regulations (e-CFR), Part 423-Steam electric power generating point source category: Appendix A to part 423-126, Priority pollutants [Internet]. 2013 [cited 2021 Jun]. Available from: https://www.law.cornell.edu/cfr/text/40/appendix-A_to_part_423.

Wang J, Luo YM, Teng Y, Ma WT, Christie P, Li ZG. Soil contamination by phthalate esters in Chinese intensive vegetable production systems with different modes of use of plastic film. Environnemntal Pollution 2013;180:265-73.

Wang Q, Wu X, Jiang L, Fang C, Wang H, Chen L. Effective degradation of di-nbutyl phthalate by reusable, magnetic Fe_3O_4 nanoparticle- immobilized *Pseudomonas* sp. W1 and its application in simulation. Chemosphere 2020;250: Article No. 126339.

Wang W, Zhang Y, Wang S, Fan CQ, Xu H. Distributions of phthalic esters carried by total suspended particulates in Nanjing, China. Environmental Monitoring and Assessment 2012;184:6789-98.

Wang X, Zhang Y, Huang B, Chen Z, Zhong M, Lu Q, et al. Phthalate pollution and migration in soil-air-vegetable systems in typical plastic agricultural greenhouses in northwestern China. Science of the Total Environment 2022;809: Article No. 151101.

Wei L, Li Z, Sun J, Zhu L. Pollution characteristics and health risk assessment of phthalate esters in agricultural soil and vegetables in the Yangtze River Delta of China. Science of the Total Environment 2020;726:Article No. 137978.

Xie Z, Ebinghaus R, Temme C, Lohmann R, Caba A, Ruck W. Occurrence and air-sea exchange of phthalates in the Arctic. Environmental Science and Technology 2007;41:4555-60.

Xu G, Li FS, Wang QH. Occurrence and degradation characteristics of dibutylphthalate (DBP) and di-(2-ethylhexyl) phthalate (DEHP) in typical agricultural soils of China. Science of the Total Environment 2008;393:333-40.

Zeng F, Cui KY, Xie ZY, Wu LN, Luo DL, Chen LX, et al. Distribution of phthalate esters in urban soils of subtropical city, Guangzhou, China. Journal of Hazardous Materials 2009; 164:1171-8.

Zhang Z, He G, Peng X, Lu L. Distribution and sources of phthalate esters in the topsoils of Beijing, China. Environmental Geochemistry and Health 2014;36:505-15.

Zhang Y, Wang P, Wang L, Sun G, Zhao J, Zhang H, et al. The influence of facility agriculture production on phthalate esters distribution in black soils of northeast China. Science of the Total Environment 2015;506-507:118-25.

Zhou B, Zhao L, Sun Y, Li X, Weng L, Li Y. Contamination and human health risks of phthalate esters in vegetable and crop soils from the Huang-Huai-Hai region of China. Science of the Total Environment 2021;778:Article No. 146281,

Zhu Z, Rao R, Zhao Z, Chen J, Jiang W, Bi F, et al. Research progress on removal of phthalates pollutants from environment. Journal of Molecular Liquids 2022;355:Article No. 118930.

Znaidi A, Brahim N, Ibrahim H, Bol R, Chaouachi M. Comparison of organic carbon stock of Regosols under two different climates and land use in Tunisia. Arabian Journal of Geosciences 2020;13:Article No. 1011.

Spatial and Temporal Habitat Use by the Main Prey Species of Tigers in Two Protected Areas of Thailand's Southern Western Forest Complex

Sasi Suksavate[1], Yutthapong Dumsrisuk[2], Paitoon Indarabut [2], Alexander Godfrey[3], Sutasinee Saosoong[4], Abishek Harihar[3], Imran Samad[3], Ronglarp Sukmasuang[1], and Prateep Duengkae[1*]

[1]Department of Forest Biology, Faculty of Forestry, Kasetsart University, Bangkok 10900, Thailand
[2]Department of National Parks, Wildlife and Plant Conservation, Ratchaburi 70110, Thailand
[3]Panthera Corporation, New York 10018, USA
[4]Panthera South and Southeast Asia, Kanchanaburi 71000, Thailand

ARTICLE INFO

Received: 22 Feb 2022
Received in revised: 8 Jul 2022
Accepted: 12 Jul 2022
Published online: 1 Aug 2022
DOI: 10.32526/ennrj/20/202200046

Keywords:
Camera trap/ Tigers's prey/ Occupancy/ sWEFCOM/ Khuean Srinagarindra National Park/ Salakphra Wildlife Sanctuary

*** Corresponding author:**
E-mail: prateepd@hotmail.com

ABSTRACT

Tigers (*Panthera tigris*) have disappeared from over 90% of their historical range, and extant populations face habitat loss, direct poaching, and prey depletion in otherwise suitable habitats. In Thailand, tiger numbers continue to decline due to prey depletion, yet a few strongholds remain. Recently, tigers have been detected in the Southern Western Forest Complex (sWEFCOM), following intensification of conservation efforts. However, there is still a lack of primary data on the status of tigers and their prey in the sWEFCOM. To fill this knowledge gap, we conducted camera trapping surveys between 2019 and 2020 in Khuean Srinagarindra National Park (KSR) and Salakphra Wildlife Sanctuary (SLP). Located near a tiger source population in Thungyai Naresuan and Huai Kha Khaeng, these areas are potential areas for tiger recovery. In particular, our study assessed the status of prey, a prerequisite to the persistence and recovery of tigers. Based on relative abundance indices, time overlap and occupancy models, we analysed the effect of anthropogenic and ecological factors on the spatial and temporal habitat use of the main prey species. We highlight that anthropogenic factor impacted species-specific habitat relationships. Mainly, shifts in ungulate temporal and spatial habitat use was linked to human activities. These relationships, however, differed between the two protected areas. As tiger recovery depends on prey recovery, we suggest that increased conservation law enforcement and greater engagement with villages within and adjacent to protected areas are essential to minimising unsustainable resource use practices that currently affect prey.

1. INTRODUCTION

Thailand's Western Forest Complex (WEFCOM) is the largest remaining tract of forest in mainland Southeast Asia and is currently home to the largest known population of Indochinese tigers (*Panthera tigris corbetti*) (DNP, 2010a; WEFCOM, 2004). The WEFCOM lies at the heart of the Dawna Tenasserimm mountain range that straddles the border with Myanmar and includes the Kaeng Krachan Forest Complex to the south. The Thung Yai-Huai Kha Khaeng (TY-HKK) World Heritage Site, established in 1991, covering an area of approximately 6,000 km^2, constitutes the core of the WEFCOM (WEFCOM, 2004; UNESCO, 2020). In 2005 the government of Thailand established an intensive patrolling system to protect and recover its most significant source of wild tigers in Huai Kha Khaeng Wildlife Sanctuary. Duangchantrasiri et al. (2016) conducted photographic capture-recapture from 2006 to 2012 to estimate tiger abundances annually and reported an increase in abundance from 35 to 58 tigers, with high individual survival (ranging from 79.60% to 95.50%), and substantial recruitment of 25 individuals. In large part, this increase is attributed to better management and protection of ungulate species, the tiger's main prey within the protected area, and the intensification of

Citation: Suksavate S, Dumsrisuk Y, Indarabut P, Godfrey A, Saosoong S, Harihar A, Samad I, Sukmasuang R, Duengkae P. Spatial and temporal habitat use by the main prey species of tigers in two protected areas of Thailand's Southern Western Forest Complex. Environ. Nat. Resour. J. 2022;20(6):563-574. (https://doi.org/10.32526/ennrj/20/202200046)

patrols and wildlife protection efforts. Consequently, the increase in tiger density during this period appears to have created the need for tigers to disperse to other forested areas adjacent to the wildlife sanctuaries (Phumanee et al., 2021a). In light of some reports from Khuean Srinagarindra National Park (KSR) and Salakphra Wildlife Sanctuary (SLP) south of TY-HKK, it is critical to assess the potential for these sites to support tiger recovery (Panthera, 2018).

Tigers are large carnivores and prey primarily on ungulates within the weight range of 10 to 250 kg (Hayward et al., 2007). However, over 50% of ungulate species that tigers prey upon are threatened, and over 80% of these species have declining population trends on account of habitat loss and degradation, being hunted for human consumption, and coming into conflict with agriculturalists due to damages to crops (Wolf and Ripple, 2016; Wolf and Ripple, 2017). Hence, understanding the status of prey at sites constitutes a crucial first step in evaluating the site's potential to support tiger recovery and suggest appropriate interventions to meet recovery objectives. In the TY-HKK World Heritage Site (WHS), a broad assemblage of ungulates are present, ranging from muntjac (18 kg) to gaur/banteng (600-1,200 kg). And, studies report the tigers' diet is primarily composed of large prey (with 89.80% biomass consumed being banteng, sambar, gaur, and domestic water buffalo). In contrast, small prey species (<100 kg) in the tiger's diet was 10.20% (Simcharoen et al., 2018). However, studies highlight that prey occupancy outside the WHS is low, especially for large ungulates (Duangchatrasiri et al., 2019). Therefore, it is critical to understand the status of prey outside of the WHS to evaluate the sites recovery potential (Harihar et al., 2018). With Phumanee et al. (2020) and Phumanee et al. (2021b) highlighting that the status of prey to the north of the WHS is poor, we aim to assess the status of prey to the south in the protected areas of KSR and SLP to inform tiger population recovery efforts. For the most part, both KSR and SLP are surrounded by settlements, with a few relatively large communities also existing within the boundaries of the protected areas. Furthermore, data from the DNP (2019) confirmed the occurrence of offenses directly affecting the population of wildlife in the study area (19 cases in KSR and two cases in SLP), which indicates that species may be threatened at these sites from anthropogenic influences. Furthermore, Lahkar et al. (2020) report that chronic anthropogenic disturbances such as unsustainable natural resource harvesting have a detrimental effect on ungulate populations, with a consequence on carnivore populations as well, and Amorntiyangkul et al. (2022) report that human activity near villages in protected areas has a negative effect on wildlife populations. Therefore, understanding the nature of human-wildlife relationships is essential when considering conservation measures and natural resource management policies. Currently, no scientific studies having been conducted to examine the spatial and temporal influence of humans on the prey species of tigers in the sWEFCOM. Therefore, understanding the impacts of human disturbances and interactions with carnivores and their prey is vital to formulate appropriate conservation action in the region (Widodo et al., 2022).

Since SLP may be a potential recovery site for breeding populations and KSR may provide critical connectivity between TY-HKK and SLP, this study aims to understand the determinants of prey species occurrence and behavior in relation to ecological and anthropogenic factors. As part of our assessment of the status of prey in these two protected areas, we estimated the relative abundance indices, time activity and occupancy of the tigers' main prey and the influence of anthropogenic and ecological factors on their spatial and temporal distribution.

2. METHODOLOGY

2.1 Study area

This study was carried out in two protected areas, Khuean Srinagarindra National Park (KSR) and Salakphra Wildlife Sanctuary (SLP), located in the West of Thailand (Figure 1). The rainy season runs from May to October, with an average rainfall of 1,628.8 mm/year. The highest temperature is around 44-45ºC in April. The minimum temperature is about 8-9ºC in December. With an average temperature of approximately 27ºC.

KSR, established in the early 1980s, is bisected by a large reservoir, covering an area of 1,532 km^2 (15.80% of the NP); 76.22% of the national park is forested, consisting of 56.06% mixed deciduous forest, 7.30% bamboo forest, 6.43% dry-dipterocarp forest, 5.64% dry-evergreen forest, 0.78% evergreen forest, and 1.41% grassland and natural forest restoration (WEFCOM, 2004). The remaining 7.98% comprises agricultural lands and communities. There are 42 villages within the National Park boundaries with 1,716 households and approximately 8,415 people, most farmers (WEFCOM, 2004). The

reservoir construction caused a large-scale relocation of local communities from the flooded plain to higher areas. The displacement and subsequent expansion of communities in the higher regions, as well as related agricultural and subsistence activities such as farming, livestock grazing and hunting, has caused a decrease in the occurrence of wildlife species in the area and potentially constricting connectivity (Knight and Cole, 1995; Suttidate et al., 2021). Important perennial watersheds flow into KSR Reservoir, including large basins such as the Mae Klong River and Huai Kha Khaeng Stream.

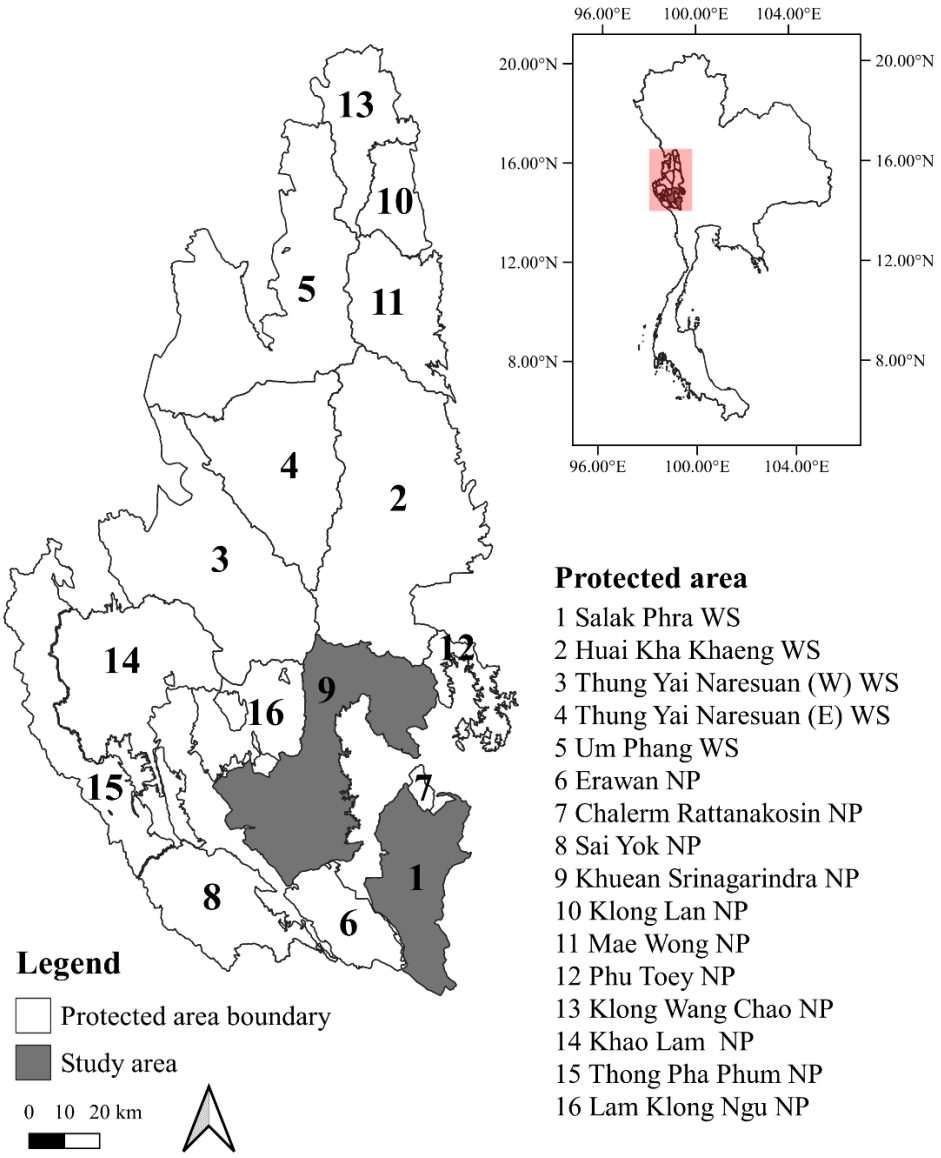

Figure 1. Protected areas in the Western Forest Complex (WEFCOM) in West Central Thailand

SLP, Thailand's first wildlife sanctuary, established in 1965, forms the southernmost tip of the Western Forest Complex, and covers an area of approximately 858.55 km^2, consisting of 60% mixed deciduous forest, 30% dry-dipterocarp forest, and 10% dry-evergreen forest (WEFCOM, 2004). Seven villages with 833 households and 3,483 individuals are located inside the sanctuary. Within the 3-km buffer from the boundary, there are 17 villages with 937 households and 3,937 individuals (WEFCOM, 2004). Critical perennial watersheds flow through SLP, including Huai Sadong, Huai Lam Esu, Huai Mae Lamoon, and Huai Mae Plasoi. SLP supports, gaur, sambar, muntjac, and wild pig. Additionally, banteng was locally extinct in SLP, and a reintroduction program was carried out between 2015 and 2016 to repopulate the park (Chaiyarat et al., 2020). While tigers inhabited SLP historically, no photographic evidence was recorded until 2014. However, a camera trap study, using similar methods to those used in the

World Heritage Site and carried out by the Zoological Society of London (ZSL) in collaboration with the DNP and Panthera, confirmed the presence of one female tiger. Cross-referencing with the Khao Nang Ram research stations tiger database revealed that this individual had dispersed from HKK, travelling over 130 km. This dispersal likely occurred through Khuean Srinagarindra National Park (KSR). In 2015, ZSL and Panthera collaborated with the DNP to survey the Northeastern part of KSR and identified three tigers, one of which, a young male, had also dispersed from HKK. The other two tigers, both females, had not been identified previously in HKK and were, therefore, new records for Thailand. In 2019 and 2022, surveys were replicated in KSR and SLP, respectively. Based on previous research studying the dietary preferences of tigers in HKK (Simcharoen et al., 2018), wild ungulates represent the main prey for tigers, with five species comprising the majority of wild tigers' diet in Thailand, banteng (*Bos javanicus*), gaur (*Bos gaurus*), sambar (*Rusa unicolor*), northern red muntjac (*Muntiacus vaginalis*), and the wild pig (*Sus scrofa*). Hence in this study, we assess the status of these species from camera trapping surveys.

2.2 Camera trap survey

We conducted systematic camera trap gridded surveys in sWEFCOM covering an area of 572 km^2 in north KSR and 557 km^2 in SLP, respectively, placing camera traps to optimize detections of tigers and their prey. The surveys were carried out in KSR from January to May 2019 with 76 camera trap stations and in SLP from November 2019 to February 2020 with 69 stations (Figure 2).

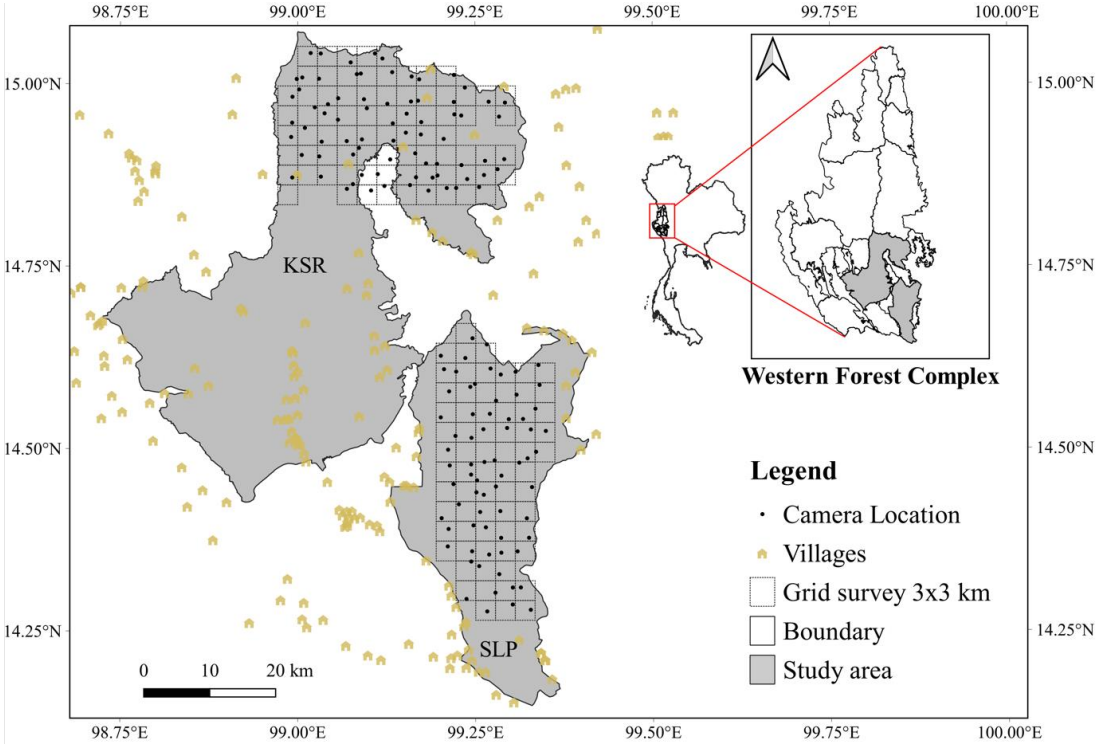

Figure 2. Camera trap stations in Khuean Srinagarindra National Park (KSR) from January to May 2019 and Salakphra Wildlife Sanctuary from November 2019 to February 2020, the map also shows the 9 km^2 grid cells (gray-filled squares) that were surveyed.

While the two surveys were not undertaken simultaneously, they were carried out in the same year in the dry season and, therefore subject to similar seasonal conditions and diurnal patterns. Although the effective trapping period was approximately 90 days for each survey, the remoteness and steepness of the terrain in KSR required longer deployment and collection periods when compared to SLP.

Camera trap stations consisted of a pair of motion-triggered PantheraCam V-series camera traps positioned opposite each other and fixed approximately 40-50 cm above the ground. Cameras were set to have a minimum of 15 seconds between trigger events and were continuously active during the survey period. To maximize the probability of detecting our target species, camera-trap stations were

placed in a grid 3×3 km along dirt roads, streams, animal trails and routes commonly used by tiger and their prey. Camera traps were mounted on trees located 3-5 m from the trail, clearing vegetation that might obstruct the camera's field of view. We did not use any baits to attract wildlife. Camera traps were not moved during the individual surveys.

After collecting the images from camera traps, we categorized the photos using Panthera's "Camera trap File Manager" software (Olliff et al., 2014). First, we identified the animal species in each image, referring to Francis (2019). If a species could not be identified, the image was categorized as "unidentified species". Next, all images of the same species captured within 30 min were grouped into independent events, following the principle described by O'Brien et al. (2003). Finally, a photo with multiple individuals of the same species in the frame were counted as single detection for that species.

2.3 Data analysis

2.3.1 Photographic capture rate index (PCRI)

For each station, we calculated the photographic capture rate index (PCRI) using independent event captures of individuals of the same species taken at more than 30 minutes time intervals (O'Brien et al., 2003). We then divided the number of independent event captures obtained at each trap by the number of camera trap nights and expressed the estimate per 100 trap nights (Carbone et al., 2001). Finally, PCRI values of each camera trap were calculated and mapped using the open-source software QGIS. To create the map and assess the difference in PCRI of prey species between KSR and SLP, we summarized species-specific PCRI of each area. We finally visualised the magnitude of the capture rate with higher rates of capture shown as larger dots.

2.3.2 Temporal activity

We used the 'overlap' package (Ridout and Linkie, 2009) in the program R to fit kernel density functions to times of observations of human and five prey species and to estimate the coefficient of overlapping, a quantitative measure the continuous ranging from 0 (no overlap) to 1 (identical activity patterns). The coefficient is defined as the area under the curve. Confident intervals for coefficients of overlap were calculated by 1,000 bootstraps.

2.3.3 Influence of ecological and anthropogenic factors on species occupancy

- Ecological and anthropogenic covariate

We examined the effects of ecological and anthropogenic covariates to explain the probability of occupancy in each grid. Across the two PAs we included (a) distance to closest village, (b) average distance to closest road, (c) distance to closest stream, (d) distance to park boundary, (e) distance to reservoir, (f) human PCRI, (g) elevation, (h) NDV, and (i) distance to closest patrol path, all factors shown in Table 1. All distances, except for roads were calculated from the centroid of each grid. We suppose that all species might occur nearby water (survey in the dry season) and further from anthropogenic factors (poaching pressure is higher closer to villages) (Phumanee et al., 2020). NDVI is a remotely sensed measure for vegetation productivity, nitrogen content, and other aspects of high-quality food for herbivores and is widely used to predict herbivore distribution and abundance (Pettorelli et al., 2011).

Table 1. Factors hypothesized to influence of detection probability and occupancy of prey species in sWEFCOM, Thailand

Covariate	Description	Source
a	Distance to closest village	WEFCOM (2004)
b	Average distance to closest road	WEFCOM (2004)
c	Distance to closest stream	WEFCOM (2004)
d	Distance to protected area boundary	WEFCOM (2004)
e	Distance to reservoir	WEFCOM (2004)
f	Human PCRI	Camera trap data
g	Elevation	Google engine (Gorelick et al., 2017)
h	NDVI	Google engine (Gorelick et al., 2017)
i	Distance to closest patrol path	SMART patrol database

- Unmarked occupancy model

Capture data for the main prey species was formatted into detection/non-detection data format with 14 occasions, with each occasion representing one week time. If a species was detected in one or more days of the week, it was recorded as detected (1), else it was recorded as not-detected (0) for the particular occasion. For SLP, data was available from 4/11/2019 to 5/02/2020 (14 weeks) for 69 sites. Accordingly, data for KSR was truncated to 14 weeks (15/01/2020 to 22/04/2020) and included 70 sites. Each site was represented by a grid of 3×3 km^2, and sites from both protected areas were combined in a single occupancy analysis as data was scarce for PA specific models. Effort, in terms of the number of days each camera trap was active during the study period, was used as a covariate to explain heterogeneity in detection probability.

Ten models were set up independently for each site to explain occupancy and detection probabilities for the different species. The first five models included (a) null model with no covariates for either occupancy or detection probability (NULL), (b) a full model with all covariates used to explain occupancy, (c) a habitat model including only covariates for habitat characteristics, i.e., distance to stream and elevation, (d) an environment model including NDVI, and (e) a human intervention model including covariates a, b, d, f, and i. The second set of five models were the same, with detection probability additionally being modelled as a function of effort.

Highly correlated variables (Pearson's correlation coefficient ≥0.7) were checked for and removed before further analysis. Variables 'distance to reservoir' and 'NDVI' were removed for KSR, while variables 'NDVI' and 'distance to road' were removed for SLP. However, since NDVI was the only variable used to explain occupancy in 'environment' models, it was only removed from the 'full' models. All covariates were centre scaled. All analyses were conducted in R using the package 'unmarked' (MacKenzie et al., 2002).

Models were ranked according to their AIC values and weights. However, all models were averaged for further inference on occupancy, detection probability and effect sizes of covariates on them. Site-wise occupancy and site/occasion-wise detection probabilities were estimated using the 'predict' function in R, which were used to calculate mean occupancy and detection probability values for each species at each site.

3. RESULTS AND DISCUSSION

3.1 Survey effort and photo captured rate

3.1.1 Khuean Srinagarindra National Park (KSR)

Our survey in KSR had 75 camera stations (one location did not yield data because the cameras were stolen), totalling 8,751 camera trap nights. No tigers were detected during this survey. However, Panthera's previous survey revealed a tiger to have been photographed at TY-HKK. This indicates that the tigers from TY-HKK disperse toward KSR. The main prey animals detected included gaur, banteng, sambar, muntjac, and wild pig. According to the event per 100 camera trap nights, wild pig was the most detected species, with 3.77 events per 100 camera trap nights, followed by muntjac, gaur, sambar, and banteng with 3.57, 0.38, 0.30, and 0.15 events per 100 trap nights, respectively (Table 2). The majority of captures were of small prey species while large prey capture rates were low, especially banteng. Capture records indicated that banteng occurred in a small area covered by seven camera stations close to each other. Sambar was primarily distributed along the edge of the reservoir. Guar was found mainly in the upland areas adjacent to the TY-HKK forest. We found small prey species (wild pigs and muntjac) distributed throughout the area.

Table 2. Number of photo capture event per 100 trap nights in KSR and SLP

Species	KSR		SLP	
	No. of capture event	No. of event per 100 trap nights	No. of capture event	No. of event per 100 trap nights
Gaur	33	0.38	47	1.07
Banteng	13	0.15	3	0.07
Sambar	26	0.30	209	4.77
Muntjac	312	3.57	356	8.12
Wild Pig	330	3.77	382	8.71

3.1.2 Salakphra Wildlife Sanctuary (SLP)

We placed 69 camera stations in part of SLP, totalling 4,384 camera trap nights. Three tigers were found and, comparing the tiger individual with the DNP tiger database, we found that two tigers dispersed from the TY-HKK World Heritage Site, and one tiger had never been detected previously. However, we detected gaur, banteng (reintroduced species), sambar, muntjac, and wild pig amongst ungulate species. The wild pig was the most detected species with 8.71 events per 100 camera trap nights, followed by muntjac, sambar, gaur, and banteng were 8.12, 4.77, 1.07, and 0.07 events per 100 camera trap nights, respectively. Banteng were detected at two locations, one at the release site of the reintroduction, and another to the south of the protected area, suggesting the spread of the population. Sambar was detected in flat areas located in the middle PA. Muntjac and wild pig were distributed throughout the site.

Overall, most prey species at SLP had a higher capture rate than KSR. The number of banteng found in both areas was low. In addition, based on the camera trap image data, a calf of banteng was detected. The two smaller prey (wild pig and muntjac) were common throughout both areas. Similarly, in another protected area in WEFCOM, wild pig and muntjac were the most commonly detected than large prey, observed >50% of camera locations, sambar <22%, and gaur <19% (Phumanee et al., 2020). Additionally, strong habitat protection in some protected areas has resulted in more gaurs occurring near the borders of the protected area (Prayoon et al., 2021), explaining the distribution of gaur in the upper area adjacent to HKK (Figure 3).

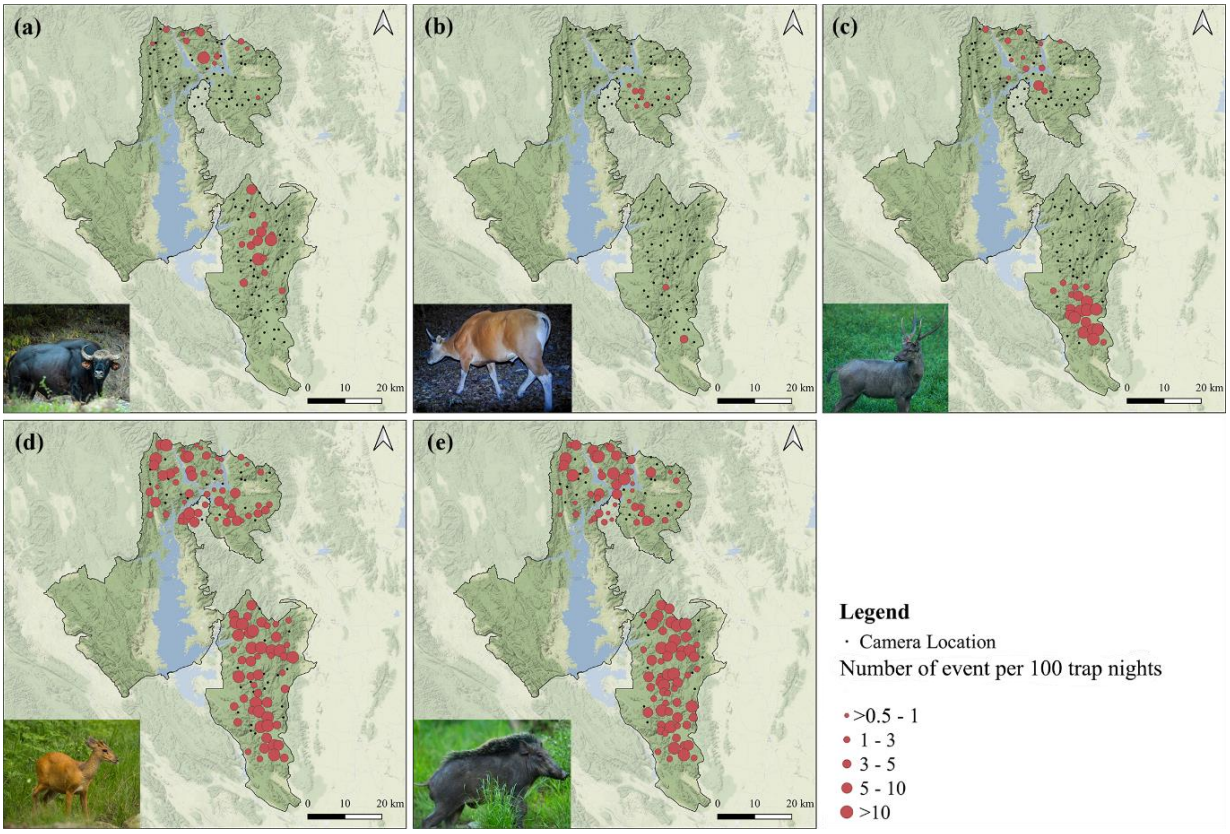

Figure 3. Photographic capture rate index (PCRI) of prey species in KSR and SLP including: (a) gaur, (b) banteng, (c) sambar, (d) northern red muntjac, and (e) wild pig

3.2 Temporal activity

In our study areas, the peak of human activity was recorded at mid-day, as illustrated by the dotted line in Figure 4. The shaded area in Figure 4 represents the estimated temporal overlap in activity for humans and prey species. Camera trap data has revealed the widespread movement of people throughout the protected areas. In KSR, large prey species, gaur, banteng, and sambar, were more active during the hours of darkness compared to smaller species such as muntjac and wild pig, whose peak activity periods were during the day. In SLP, sambar, muntjac, and wild pig showed similar temporal activity patterns to their conspecifics in KSR, while gaur and banteng

appeared to be active day and night. As a result, the species with the highest temporal overlap with humans in both areas is the wild pig, (KSR; 0.763 (0.70-0.82) and SLP; 0.607 (0.51-0.70)), while sambar was the species with the lowest temporal overlap in both areas, (KSR; 0.439 (0.29-0.60) and SLP; 0.194 (0.11-0.28)).

In Khao Yai National Park, Khoewsree et al. (2020) found that sambar mainly was active during the night while most human, muntjac, and wild pig activity was recorded during the daylight hours resulting in low temporal overlap, similar to the findings of this study. Furthermore, Johann et al. (2020) reported that large areas with low levels of human disturbance were linked with higher daytime activity of wild pigs than smaller areas with relatively higher levels of disturbance. Similarly, Ohashi et al. (2013) also reported human activity in the Southwestern part of Tochigi, Japan, significantly affected the activity patterns of wild pigs. Additionally, in a study of the spatial and temporal distribution of leopards and their prey in Thailand's Western Forest Complex, Saisamorn et al. (2019) reported that sambar and banteng were nocturnal while wild pig and muntjac were diurnal.

Our results indicate that gaur activity in KSR peaks around 00:00, while in SLP, the peak period is around 18:00. Similarly, Vinitpornsawan and Fuller (2020) also found similar patterns of activity, with most detections between 17:00 and 18:00 and 59% of overall gaur activity in the daytime. Their study recorded most human activity around noon, with only a few detections after 18:00 hours, causing overlaps of activity with nocturnal wildlife species.

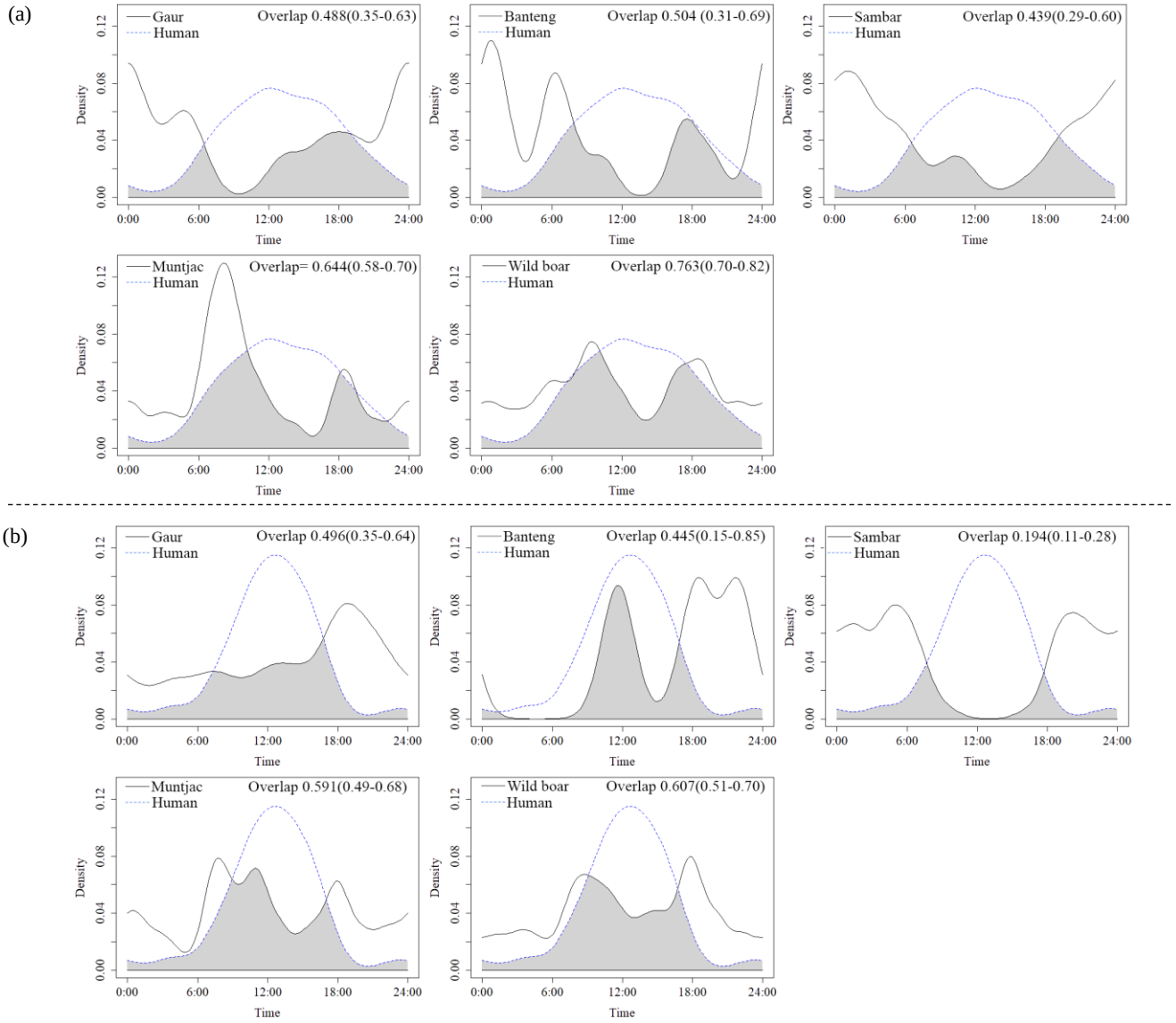

Figure 4. Time overlaps plot of human and tiger's prey species in (a) KSR and (b) SLP, the estimated overlap is shown by the grey area.

3.3 Influence of covariates on occupancy model

3.3.1 Gaur

The model averaged estimate of gaur occupancy across the two protected areas was 29% (Table 3). The top model included human influence covariates with distance to closest patrol path and road having the most significant effect (Table S1 and S2). Differing from studies in HKK, Jornburom et al. (2020) reported the best model for gaur is higher elevation and avoidance of shallow slope areas within a 1 km buffer of streams. In addition to this, McShea et al. (2011) reported that gaur in Thailand required grassland and open areas of moist evergreen, dry evergreen, semi-evergreen, and mixed deciduous forests. Paansri et al. (2022) however found that gaur was detected in both open and closed forests.

In the past, both study areas had a greater distribution of gaur (Srikosamatara and Suteethorn, 1995). Currently, there is a threat to the population from hunting. Around and within both areas there are human settlements and this might be causal to the relationship.

Table 3. Detection probability and occupancy estimates of prey species in KSR and SLP, Thailand, 2019-2020

Species	Detection probability			Occupancy probability		
	Mean	2.50%	97.50%	Mean	2.50%	97.50%
Gaur	0.11	0.07	0.11	0.29	0.01	0.98
Banteng	0.08	0.03	0.08	0.10	0.07	0.14
Muntjac	0.27	0.10	0.30	0.77	0.74	0.82
Sambar	0.31	0.13	0.33	0.23	0.00	0.94
Wild pig	0.29	0.05	0.32	0.73	0.08	1.00

3.3.2 Banteng

The model averaged estimate of banteng occupancy was low (10%) across the two PAs (Table 3). Banteng detections in our study were likely too few to run the model effectively (Table S1 and S2). Jornburom et al. (2020) simulated a map of predicted occupancy for banteng in WEFCOM in the absence of poaching, and estimated ~6,400 km^2 of ecologically suitable habitat that could support reintroduction of banteng in other protected areas and reports banteng used low elevations and low slopes. Furthermore, Mae Wong National Park confirms the return of banteng after an absence of over 40 years, likely dispersed from HKK (Phoonjampa et al., 2021).

Three replications of camera trap surveys in KSR since 2016 have confirmed that banteng is present in only one relatively small area of the protected area. In SLP, Banteng were distributed throughout the park, however, there were no reports of sightings for more than 30 years (personal communication with park rangers). Therefore, banteng was reintroduced in 2015. Currently, the reintroduced population of 13 have increased to 19 and is concentrated near the release area. With improved protection, this population is expected to increase.

3.3.3 Sambar

The model averaged estimate of sambar occupancy across the parks is 23% (Table 3). Habitat covariates such as distance to reservoir, elevation and NDVI had a significant relationship on the occupancy suggesting that sambar was far the reservoir, at lower elevation and in more open habitats (Table S1 and S2). Our results are similar to that reported from HKK, where occupancy of sambar was negatively correlated to elevation, with the majority of detections distributed in lower altitude grasslands (Simcharoen et al., 2014). Duangchatrasiri et al. (2019) found that livestock was negatively correlated with tiger and sambar occupancy in HKK. Furthermore, Paansri et al. (2021) found that sambar occupancy was directly related to grass biomass and also avoided human disturbance factors. From our study, sambar avoid the reservoirs. This might be because the KSR reservoir area has a traffic of villagers' boats, fishing, and livestock. Livestock grazing in forested areas was expected to negatively impact ecosystems and wildlife, such as competition for forage, pollution of water resources. (Chaiyarat and Srikosamatara, 2009).

3.3.4 Northern red muntjac

The model averaged estimate of occupancy from the muntjac is 77% across the two PAs (Table 3). The human influence model was top ranked suggesting that (although non-significant) human capture rate negatively influenced muntjac occupancy (Table S1 and S2). Similar to a study in Mae Wong-Khlong Lan National Park in northern WEFCOM,

none of the variables in the top model set were statistically significant, (Phumanee et al., 2020). Likely as muntjac has non-specific habitats and can be detected in all forest types, agricultural areas, and abandoned farm (DNP, 2010b). The negative correlation with photo capture rate of human shows that muntjac although widely distributed are susceptible to human influence.

3.3.5 Wild pig

Model averaged occupancy estimate of wild pig across the two PAs was 73% (Table 3). The top models included human influence covariates, particularly noting higher occupancy away from roads and the reservoir (Table S1 and S2). Consistent with studies of ungulates in Mae Wong and Khlong Lan, where wild pig was associated with avoidance of villages (Phumanee et al., 2020). The wild pig is a resilient species, distributed throughout the area. It has the highest reproduction rate among ungulates and therefore a high resilience to hunting pressure (Gaillard et al., 1993; Steinmetz et al., 2010) and is a habitat generalist (Spitz and Janeau, 1995).

While our study provides an assessment of species occupancy in the sWEFCOM, these estimates are relatively lower compared to HKK (Duangchatrasiri et al., 2019). Tiger occupancy is strongly influenced by prey availability and often choose larger ungulates as diet (sambar, gaur, and banteng) (Simcharoen et al., 2018). Given large prey occupnacy was low in KSR and SLP this may limit the recovery of tigers and conservation measures should therefore focus on mitigating the factors that limit the presence of large tiger prey (Duangchantrasiri et al., 2016).

4. CONCLUSION

This study provides evidence of the impact of ecological and anthropogenic factors on the spatial and temporal habitat use patterns of the tigers' wild prey across KSR and SLP, and emphasizes the importance of initiating and maintaining conservation measures to support prey recovery to ensure the recovery of tigers. To be more specific, we first demonstrate that the abundance indices of prey (PCRI) across the two protected areas indicate that small prey appear to be more abundant than large prey. Nevertheless, large prey species, such as sambar and gaur, registered higher PCRI estimates in SLP than in KSR, suggesting that the site might be a better habitat for tigers. Secondly, we demonstrate through the analysis of time activity patterns that most prey avoided periods of high human activity. At both protected areas, this was most prominent among the large prey animals, gaur and sambar. While the smaller prey, which are more abundant, overlap more widely with human activity. Finally, the results of our occupancy analysis confirm that small prey (muntjacs and wild pigs) occupy more area than large prey (sambars, gaurs, and bantengs), demonstrating the importance of large prey recovery if tiger recovery is to be supported across the PAs.

The results of this study and other similar analysis suggest that most tiger prey species tend to avoid anthropogenic activity. The detection in the southern WEFCOM of at least two tigers having dispersed from the Thungyai Naresuan-Huai Kha Khaeng World Heritage Site has highlighted the importance of sWEFCOM for the long-term viability of tiger populations in Thailand. Our results will also help protected area managers better understand the ecological and anthropogenic factors affecting ungulate, allowing them to make more informed decisions regarding the management and regulation of the protected areas.

- Management implications

Many studies have shown that the abundance of tigers often depends on the health and abundance of large ungulates. Sambar, banteng, and gaur composed 95.10% of biomass of these kills in HKK (Pakpien et al., 2017), It can be noticed that tigers tend to choose large prey (>100 kg). Based on our surveys within KSR and SLP, populations of large prey species should be of concern. Strengthening efforts should be made to protect the remaining small red bull populations and to preserve the area. Since communities are settled throughout around KSR and SLP, human activities impacting wildlife distribution and abundance should be regulated through a combination of patrolling and community engagement aimed at reducing, where possible, spatial and temporal overlap between human activities and wildlife. There should be a zoning arrangement for villagers who come to use forest resources to reduce disturbances in wildlife habitats, including livestock. At present, the outbreak of lumpy skin disease affects both domestic and wild cattle in Thailand (Arjkumpa et al., 2021). There should be surveillance for diseases transmitted from domestic animals to wild animals. Wildlife conservation depends on habitat maintenance (Reed, 2004). KSR connects to HKK and are suitable for gaur population. Most suitable gaur habitat was

connected to large patches (Prayoon et al., 2021). Therefore, it should be managed to reduce the threat in order to support population of gaur that spread from nearby areas. To increase the large ungulate populations throughout the area, salt lick sources need attention, because the tiger's prey is herbivorous, causing sodium and other nutrient deficiencies. (Emmons and Stark, 1979). Furthermore, the presence of salt licks in WEFCOM is associated with gaur and other ungulate species (Jornburom et al., 2020; Phumanee et al., 2020). Finally, these studies should provide information that can be used by management for the establishment of conservation areas to develop plans to conserve gaur and banteng to support tiger habitat.

ACKNOWLEDGEMENTS

This study was supported by Officer of Khuean Srinagarindra National Park and Salakphra Wildlife Sanctuary, Department of National Park, Wildlife and Plant Conservation, Panthera Corporation, Zoological Society of London (ZSL), US Fish and Wildlife Services-Rhino, and Tiger Conservation Fund and Khao Nang Rum Wildlife Research Station.

REFERENCES

Amorntiyangkul P, Pattanavibool A, Ochakul W, Chinnawong W, Klanprasert S, Aungkeaw C, et al. Dynamic occupancy of wild Asian Elephant: A case study based on the SMART database from the Western Forest Complex in Thailand. Environment and Natural Resources Journal 2022;20(3):310-22.

Arjkumpa O, Suwannaboon M, Boonrod M, Punyawan I, Liangchaisiri S, Laobannue P, et al. The first lumpy skin disease outbreak in Thailand (2021): Epidemiological features and spatio-temporal analysis. Frontiers in Veterinary Science 2021;8:Article No. 799065.

Carbone C, Christie S, Conforti K, Coulson T, Franklin N, Ginsberg JR, et al. The use of photographic rates to estimate densities of tigers and other cryptic mammals. Animal Conservation 2001;4(1):75-9.

Chaiyarat R, Srikosamatara S. Populations of domesticated cattle and buffalo in the Western Forest Complex of Thailand and their possible impacts on the wildlife community. Journal of Environmental Management 2009;90(3):1448-53.

Chaiyarat R, Sakchan P, Panprayun G, Thongthip N, Nakbun S. Monitoring of forage and nutrition before and after reintroduction of banteng (*Bos javanicus* d'Alton, 1823) to Salakphra Wildlife Sanctuary, Thailand. Scientific Reports 2020;10(1):Article No. 11135.

Department of National Parks, Wildlife and Plant Conservation (DNP). Summary of Forestry Case Reports: Fiscal Year 2019. Bangkok, Thailand: Ministry of Natural Resources and Environment; 2019. (in Thai).

Department of National Parks, Wildlife and Plant Conservation (DNP). Thailand Tiger Action Plan 2010-2022. Bangkok, Thailand: Ministry of Natural Resources and Environment; 2010a.

Department of National Parks, Wildlife and Plant Conservation (DNP). Status of Large Mammals in Thailand. Bangkok, Thailand: Ministry of Natural Resources and Environment; 2010b.

Duangchantrasiri S, Umponjan M, Simcharoen S, Pattanavibool A, Chaiwattana S, Maneerat S, et al. Dynamics of a low-density tiger population in Southeast Asia in the context of improved law enforcement. Conservation Biology 2016; 30(3):639-48.

Duangchatrasiri S, Jornburom P, Jinamoy S, Pattanvibool A, Hines JE, Arnold TW, et al. Impact of prey occupancy and other ecological and anthropogenic factors on tiger distribution in Thailand's Western Forest Complex. Ecology and Evolution 2019;9(5):2449-58.

Emmons LH, Stark NM. Elemental composition of a natural mineral lick in Amazonia. Biotropica 1979;11(4):311-3.

Francis C. Field Guide to the Mammals of South-East Asia. London, UK: Bloomsbury Publishing; 2019.

Gaillard JM, Brandt S, Jullien JM. Body weight effect on reproduction of young wild boar (*Sus scrofa*) females: A comparative analysis. Folia Zoologica (Brno) 1993;42(3): 204-12.

Gorelick N, Hancher M, Dixon M, Ilyushchenko S, Thau D, Moore R. Google earth engine: Planetary-scale geospatial analysis for everyone. Remote Sensing of Environment 2017;202:18-27.

Harihar A, Chanchani P, Borah J, Crouthers RJ, Darman Y, Gray TN, et al. Recovery planning towards doubling wild tiger Panthera tigris numbers: Detailing 18 recovery sites from across the range. PLoS One 2018;13(11):e0207114.

Hayward MW, O'Brien J, Kerley GI. Carrying capacity of large African predators: Predictions and tests. Biological Conservation 2007;139:219-29.

Johann F, Handschuh M, Linderoth P, Dormann CF, Arnold J. Adaptation of wild boar (*Sus scrofa*) activity in a human-dominated landscape. BMC Ecology 2020;20(1):1-4.

Jornburom P, Duangchantrasiri S, Jinamoy S, Pattanavibool A, Hines JE, Arnold TW, et al. Habitat use by tiger prey in Thailand's Western Forest Complex: What will it take to fill a half-full tiger landscape? Journal for Nature Conservation 2020;58:Article No. 125896.

Khoewsree N, Charaspet K, Songsasen N, Pla-Ard M, Thongbantum J, Kongchaloem W, et al. Abundance, prey, and activity period of dholes (*Cuon alpinus*) in Khao Yai National Park, Thailand. Biodiversitas Journal of Biological Diversity 2020;21(1):345-54.

Knight RL, Cole DN. Wildlife and recreationists: Coexistence through management and research. In: Knight RL, Gutzwiller KJ, editers. Wildlife Responses to Recreationists. Washington DC, USA: Island Press; 1995.

Lahkar D, Ahmed MF, Begum RH, Das SK, Harihar A. Responses of a wild ungulate assemblage to anthropogenic influences in Manas National Park, India. Biological Conservation 2020;243:Article No. 108425.

MacKenzie DI, Nichols JD, Lachman GB, Droege S, Andrew Royle J, Langtimm CA. Estimating site occupancy rates when detection probabilities are less than one. Ecology 2002; 83(8):2248-55.

McShea WJ, Davies SJ, Bhumpakphan N. The Ecology and Conservation of Seasonally Dry Forests in Asia. Washinton DC, USA: Smithsonian Institution Scholarly Press; 2011.

O'Brien TG, Kinnaird MF, Wibisono HT. Crouching tigers, hidden prey: Sumatran tiger and prey populations in a tropical forest landscape. Animal Conservation 2003;6(2):131-9.

Ohashi H, Saito M, Horie R, Tsunoda H, Noba H, Ishii H, et al. Differences in the activity pattern of the wild boar *Sus scrofa* related to human disturbance. European Journal of Wildlife Research 2013;59(2):167-77.

Olliff ERR, Cline CW, Bruen D, Yarmchuk EJ, Pickles RSA, Hunter L. The panthercam-a camera-trap optimized for monitoring wild felids. Wild Felid Monitor 2014;7(2):21-8.

Paansri P, Sangprom N, Suksavate W, Chaiyes A, Duengkae P. Spatial modeling of forage crops for tiger prey species in the area surrounding highway 304 in the Dong Phayayen-Khao Yai Forest Complex. Environment and Natural Resources Journal 2021;19(3):220-9.

Paansri P, Suksavate W, Chaiyes A, Chanteap P, Duengkae P. Use of Bayesian, lasso binary quantile regression to identify suitable habitat for tiger prey species in Thap Lan National Park, Eastern Thailand. Environment and Natural Resources Journal 2022;20(3):266-78.

Pakpien S, Simcharoen A, Duangchantrasiri S, Chimchome V, Pongpattannurak N, Smith JL. Ecological covariates at kill sites influence tiger (*Panthera tigris*) hunting success in Huai Kha Khaeng Wildlife Sanctuary, Thailand. Tropical Conservation Science 2017;10:1-7.

Panthera. Enabling the Recovery and Conservation of Tiger and Tiger Prey in Southern Western Forest Complex (sWEFCOM): Annual Report 2018. Karnchanaburi, Thailand: Panthera Corporation; 2018.

Pettorelli N, Ryan S, Mueller T, Bunnefeld N, Jedrzejewska B, Lima M, et al. The normalized difference vegetation index (NDVI): Unforeseen successes in animal ecology. Climate Research 2011;46(1):15-27.

Phoonjampa R, Steinmetz R, Phumanee W, Bunchornratana K, Kaewsrisod T, Srirattanaporn S, et al. Recolonization of former range by endangered banteng *Bos javanicus* in Mae Wong National Park, Thailand. Tropical Conservation Science 2021;14:1-6.

Phumanee W, Steinmetz R, Phoonjampa R, Bejraburnin T, Grainger M, Savini T. Occupancy-based monitoring of ungulate prey species in Thailand indicates population stability, but limited recovery. Ecosphere 2020;11(9):e03208.

Phumanee W, Steinmetz R, Phoonjampa R, Weingdow S, Phokamanee S, Bhumpakphan N, et al. Tiger density, movements, and immigration outside of a tiger source site in Thailand. Conservation Science and Practice 2021a;3(12): e560.

Phumanee W, Steinmetz R, Phoonjampa R, Bejraburnin T, Bhumpakphan N, Savini T. Coexistence of large carnivore species in relation to their major prey in Thailand. Global Ecology and Conservation. 2021b;32:e01930.

Prayoon U, Suksavate W, Chaiyes A, Winitpornsawan S, Tunhikorn S, Faengbubpha K, et al. Past, present and future habitat suitable for gaur (*Bos gaurus*) in Thailand. Agriculture and Natural Resources 2021;55(5):743-56.

Reed DH. Extinction risk in fragmented habitats. Animal Conservation 2004;7(2):181-91.

Ridout MS, Linkie M. Estimating overlap of daily activity patterns from camera trap data. Journal of Agricultural, Biological, and Environmental Statistics 2009;14(3):322-37.

Saisamorn A, Duengkae P, Pattanavibool A, Duangchantrasiri S, Simcharoen A, Smith JL. Spatial and temporal analysis of leopards (*Panthera pardus*), their prey and tigers (*Panthera tigris*) in Huai Kha Khaeng Wildlife Sanctuary, Thailand. Folia Oecologica 2019;46(2):73-82.

Simcharoen A, Savini T, Gale GA, Roche E, Chimchome V, Smith JL. Ecological factors that influence sambar (*Rusa unicolor*) distribution and abundance in western Thailand: Implications for tiger conservation. Raffles Bulletin of Zoology 2014; 62:100-6.

Simcharoen A, Simcharoen S, Duangchantrasiri S, Bump J, Smith JLD. Tiger and leopard diets in western Thailand: Evidence for overlap and potential consequences. Food Webs 2018;15:e00085.

Spitz F, Janeau G. Daily selection of habitat in wild boar (*Sus scrofa*). Journal of Zoology 1995;237(3):423-34.

Srikosamatara S, Suteethorn V. Populations of gaur and banteng and their management in Thailand. Natural History Bulletin of the Siam Society 1995;43(1):55-83.

Steinmetz R, Chutipong W, Seuaturien N, Chirngsaard E, Khaengkhetkarn M. Population recovery patterns of Southeast Asian ungulates after poaching. Biological Conservation 2010;143(1):42-51.

Suttidate N, Steinmetz R, Lynam AJ, Sukmasuang R, Ngoprasert D, Chutipong W, et al. Habitat connectivity for endangered Indochinese tigers in Thailand. Global Ecology and Conservation 2021;29:e01718.

United Nations Educational, Scientific and Cultural Organization (UNESCO). World Heritage list: Thungyai-huai kha khaeng wildlife sanctuaries [Internet]. 2020 [cited 2020 Jan 20]. Available from: https://whc.unesco.org/en/list/591/.

Vinitpornsawan S, Fuller TK. Spatio-temporal correlations of large predators and their prey in Western Thailand. Raffles Bulletin of Zoology 2020;68.118-31.

Western Forest Complex (WEFCOM). GIS Database and Its Applications for Ecosystem Management. Bangkok, Thailand: Department of National Park, Wildlife, and Plant Conservation; 2004.

Widodo FA, Imron MA, Sunarto S, Giordano AJ. Carnivores and their prey in Sumatra: Occupancy and activity in human-dominated forests. PLoS One 2022;17(3):e0265440.

Wolf C, Ripple WJ. Prey depletion as a threat to the world's large carnivores. Royal Society Open Science 2016;3(8):Article No. 160252.

Wolf C, Ripple WJ. Range contractions of the world's large carnivores. Royal Society Open Science 2017;4(7):Article No. 170052.

Bacterial Community of Klong Tub Mangrove Forest in Chonburi Province, Thailand

Papon Ganjanasiripong[1], Pimmnapar Neesanant[2], Thongchai Taechowisan[1], Nakarin Kitkumthorn[3], and Thanaporn Chuen-im[1*]

[1]Department of Microbiology, Faculty of Science, Silpakorn University, SanamChandra Palace, Nakhon Pathom 73000, Thailand
[2]The Thai Association for Biotech Industries, 88 Chaloemphrakiat Rama IV, Nongbon, Prawet, Bangkok 10250, Thailand
[3]Department of Oral Biology, Faculty of Dentistry, Mahidol University, Bangkok 10400, Thailand

ARTICLE INFO

Received: 9 Mar 2022
Received in revised: 6 Jul 2022
Accepted: 18 Jul 2022
Published online: 24 Aug 2022
DOI: 10.32526/ennrj/20/202200058

Keywords:
Microbial diversity/ Actinomycetes/ Mangrove forest/ Narrowleaf cattail wetland/ *Typha angustifolia* L.

*** Corresponding author:**
E-mail: suy85@hotmail.co.uk

ABSTRACT

Mangrove forests are located in the transition zone of terrestrial and river/marine ecosystems, making these forests a unique environment harbouring diverse microbes. This study investigated the bacterial community of Klong Tub Mangrove Forest in Chonburi Province, Thailand. The distinct feature of this forest is its nearby location to a narrowleaf cattail wetland. Assessment of the abiotic parameters of the sediments from site#1 nearby the narrowleaf cattail wetland and site#2 in the mangrove forest revealed differences in pH and salinity values between these two sites. Biochemical identification of bacterial isolates (n=233) indicated that these species belonged to 16 families and 29 genera as follows: *Moraxellaceae* (17.60%) > *Vibrionaceae* (16.31%) > *Paenibacillaceae* (15.88%) > *Staphylococcaceae* and *Bacillaceae* (9.87% each) > *Aeromonadaceae* and *Pseudomonadaceae* (8.58% each) > *Enterobacteriaceae* (4.29%) > *Lactobacillaceae* (2.58%) > *Moraxellaceae* (2.15%) > *Comamonadaceae* (1.72%) > *Alcaligenaceae* (0.86%) > *Morganellaceae*, *Burkholderiaceae*, *Pasteurellaceae* and *Streptococcaceae* (0.43% each). Among the genera, 12 were commonly isolated from both sites. Bacterial strains from 7 and 10 genera were detected only in site#1 and site#2, respectively. Analysis of the partial 16s rRNA gene sequence of four filamentous gram-positive isolates showed their high sequence similarity to three genera, including three novel species, *Streptomyces* sp. NA03103, *Micromonospora fluminis* sp. nov. and *Bacillus velezensis* sp. nov. In conclusion, the Klong Tub Mangrove Forest possesses high microbial diversity, and the bacterial taxon in the sediments differ between the narrowleaf cattail wetland and mangrove forest. Several bacterial isolates from the forest show a high biotechnological potential.

1. INTRODUCTION

Mangrove forests harbour a unique environment with microbial diversity because they are located in the transition zone of terrestrial and river/marine ecosystems. Mangroves with high microbial diversity are a potential natural resource for various biotechnological fields, such as industry, agriculture, and medicine. In the past decade, mangrove ecosystems have become a hotspot in the study of natural products (Azman et al., 2015; Katili and Retnowati, 2017). Several novel species, particularly actinomycetes, have been found in marine ecosystems; this breakthrough led to the discovery of newly bioactive compounds, some of which are promising drug candidates (Pathomaree et al., 2006; Hong et al., 2009; Gong et al., 2018; Shi et al., 2019; Xavier et al., 2021). Other mangrove-associated bacteria with high potential biotechnological interests were also documented, including an extracellular hydrolytic enzyme producer *Vibrio alginolyticus* Jme3-20, a diverse metabolic intermediate producer *Bacillus velezensis* sp. nov. and a new lipopeptide biosurfactant and mosquitocidal agent producer *Aneurinibacillus aneurinilyticus* (Das et al., 2016; Balan et al., 2017; Abouelkheir et al., 2020; Mamangkey et al., 2021). Exploring the bacterial strains in mangroves is crucial for biotechnology applications and deep understanding of the ecosystem, such as the interaction between microorganisms and

Citation: Ganjanasiripong P, Neesanant P, Taechowisan T, Kitkumthorn N, Chuen-im T. Bacterial community of Klong Tub Mangrove Forest in Chonburi Province, Thailand. Environ. Nat. Resour. J. 2022;20(6):575-584. (https://doi.org/10.32526/ennrj/20/202200058)

their environment and the dynamics of microbial population resilience in response to seasonality (Fuhrman et al., 2015). The abiotic factors of each site vary and can influence its microbial taxonomy and structure (Stottmeister et al., 2003; Oguh et al., 2021). Hence, the various aspects of a mangrove forest, including status, microbial diversity and ecosystem interaction webs, are crucial in establishing policies for its protection, rehabilitation and sustainable use (Allard et al., 2020).

The Klong Tub Mangrove Forest is well preserved under the care of the Air and Costal Defense Command, Royal Thai Navy. It covers a small area of 0.0112 km^2 but contains a high diversity of plant species from at least 15 genera, including *Rhizophora*, *Acrostichum*, *Lumnitzera*, *Ceriops*, *Clerodendrum*, *Sonneratia*, *Bruguiera*, *Avicennia*, *Hibiscus*, *Xylocarpus*, *Nypa*, *Flagellaria*, *Barringtonia*, *Wollastonia*, and *Derris* (Mangrove Forest at Air and Coastal Defense Command, 2014). This forest has distinct characteristics because it is located near a narrowleaf cattail (*Typha angustifolia* L.) wetland whose rhizopheric bacterial colonies exhibit high taxon richness (Gao and Shi, 2018). The Klong Tub Mangrove is also an undisturbed and unpolluted forest because it is isolated from the community, tourists and any other activities. Several publications have reported anthropogenic effects on the biodiversity of mangrove ecosystems, including the alternation and abundance of their bacterial communities (Ghizelini et al., 2012; Mishra et al., 2012; Oguh et al., 2021; Palit et al., 2022). Given that it is undisturbed by any human activity, contains a variety of plant species and is located close to a narrowleaf cattail wetland, the Klong Tub Forest may possess high microbial diversity and contain bacterial strains with high biotechnological potential. This study aimed to investigate the bacterial diversity of Klong Tub Mangrove Forest and to compare the structure of bacterial community in the sediments between near the narrowleaf cattail wetland and close to the Sattahip Bay. The findings will be used in the evaluation of the forest status and the establishment of management plan for sustainable uses in biotechnological applications.

2. METHODOLOGY

2.1 Sample collection

Klong Tub Mangrove Forest, Sattahip District, Chonburi Province, Thailand is located on the coast of Sattahip Bay, the Upper Gulf of Thailand (Figure 1) and about 30 km from Pattaya City, a famous touring place in Eastern Thailand. This forest has a distinct environment because it is located in the interface of a marine ecosystem and a narrowleaf cattail (*Typha angustifolia* L.) wetland. Sampling was carried out in two sites (Figure 1): site#1 samples were collected nearby *T. angustifolia* wetland, and site#2 samples were from the mangrove area close to the Sattahip Bay. Soil samples were collected at the depth of 5 cm from the surface, placed in sterile bags, kept on ice during transportation, and maintained at 4°C until microbiological examination. Three sediment samples were collected about 2 m apart for each site, and their temperature was measured at the time of sampling using a glass thermometer. Salinity and pH were measured at the laboratory using a portable salinity/resistivity metre (SUNTEX, model SC-110, Taiwan).

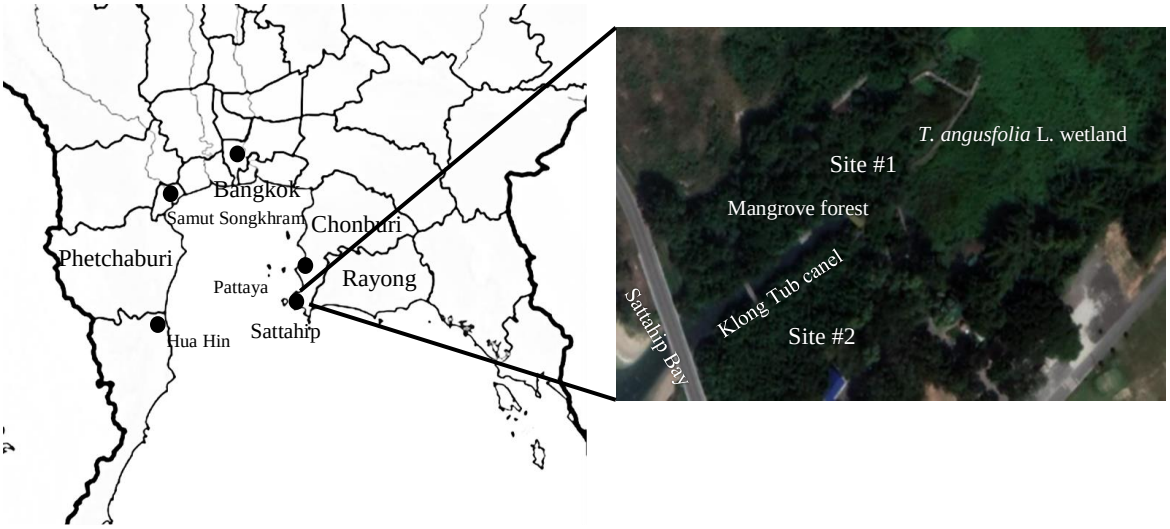

Figure 1. Map of Klong Tub Mangrove Forest, Sattahip District, Chonburi Province, Thailand and sample sites in this study (modified from Google map and own work based on Nordwest). Site#1: 12º38′48.7″N 100º55′53.7″E and site#2: 12º38′46.4″N 100º55′50.9″E

2.2 Bacterial isolation

Bacterial strains were isolated within 12 h after sample collection using the modified protocol of Jalal et al. (2010). Briefly, 1 g of each soil sample was suspended in 9 mL of sterile distilled water. The mixture was shaken to thoroughly combine the suspension before centrifugation to collect the supernatant. The supernatant of each sample was diluted by 10-fold serial dilution method to obtain 10^{-1}-10^{-5} dilutions. For the total plate count of heterotrophic bacteria, 100 µL of each dilution was spread on nutrient agar supplemented with 1% NaCl (NA+1% NaCl). The plates were incubated at 37°C for 24-48 h and used for bacterial identification.

Actinomycetes were isolated and characterised using ISP medium#2 (ISP-2) containing 10 g/L glucose, 5 g/L meat extract, 4 g/L malt extract, and 18 g/L agar-agar with pH 7.0 and incubated at 30°C (Taechowisan et al., 2017). Actinomycete colonies, evidenced by a filamentous growth pattern, were then subjected to amplified partial 16S rRNA gene sequencing for identification.

2.3 Biochemical test for the identification of bacterial isolates

For bacterial strain identification, colonies were randomly selected according to their morphological differences and streaked on NA+1% NaCl. The pure culture was observed for the presence of Gram's reaction. The strains were subsequently identified using the following morphological and standard biochemical features/tests: carbohydrate fermentation, triple-sugar iron agar, indole production, methyl red and Voges-Proskauer tests, citrate utilisation, motility, urease, oxidase, catalase and decarboxylation. Primary bacterial identification was performed using the ABIS online tool available at https://www.tgw1916.net/ (Sorescu and Stoica, 2021). According to the guidelines of the ABIS online tool, the bacteria were identified according to the isolates' metabolic characteristics, cultural and phenotypical characteristics, ecology data and similarity percentage (≥87.00).

2.4 Identification of bacteria by 16S rRNA PCR

Genomic DNA was extracted using the modified protocol of Taechowisan et al. (2017). Briefly, the isolates were cultured in ISP-2 broth by shaking at 100 rpm and 28°C for 7-14 days. After centrifugation at 6,000 rpm for 15 min, the mycelial pellet was ground to powder in liquid nitrogen using mortar and pestle. The powder was mixed with 400 µL of lysozyme (20 mg/mL) and then incubated at 25°C for 20 min. Subsequently, the mixture was added with 20 µL of 25% (w/v) SDS and 10 µL of RNase (100 mg/mL) and incubated at 37°C for 30 min, followed by protein digestion with 50 µL of proteinase K (20 mg/mL) at 37°C for 2 h. Finally, the mixture was subjected to phenol:chloroform (1:1) extraction and subsequent DNA precipitation with 2 volume of absolute ethanol and 0.1 M NaCl. The DNA pellet was rinsed with 70% ethanol and resuspend in TE buffer. DNA concentration was measured using Nano drop (Thermo Fisher Scientific, USA), followed by PCR.

The 16S rRNA gene was amplified using primers A7-26f (5′-CCGTCGACGAGCTCA GAGTTTGATCCTGGCTCAG-3′) and B1523-1504r (5′-CCCGGGTACCAAGCTTAAGGAGGTGATC-CAGCCGCA-3′), and the thermal cycle for PCR was described by Taechowisan et al. (2017). The PCR condition was started with denaturation at 95°C for 5 min, followed by 35 cycles of denaturation at 95°C for 1 min, annealing at 56°C for 1 min, extension at 73°C for 1 min, and a final extension at 72°C for 10 min. The PCR products were then subjected to sequence analysis (Illumina Miseq, Celemics, South Korea). The resulting sequences were submitted to the National Center for Biotechnology Information database using Basic Local Alignment Search Tool (BLAST) algorithm (Zhang et al., 2000; Morgulis et al., 2008), Ribosomal Database Project (RDP) (Wang et al., 2007) and EzBioCloud (Yoon et al., 2017).

3. RESULTS AND DISCUSSION

3.1 Abiotic parameters of the sediments from Klong Tub Mangrove Forest

Three abiotic parameters influencing micro-organism growth were measured in the sediment samples from the Klong Tub Forest. The pH of site#1 sediments was higher than that of site#2 sediments with ranges of 7.55 to 8.12 and 7.11 to 7.53, respectively. Meanwhile, the salinity of site#1 sediments ranged from 0.54 to 1.20 ppt and was lower than that of site#2 sediments at 18.40 to 23.42 ppt. The temperature of site#1 sediments was between 28°C and 30°C, and that of site#2 sediments was between 26°C and 28°C.

3.2 Determination of microbial diversity in the sediments from Klong Tub Mangrove Forest

According to the experiment using spread plate technique on NA+1%NaCl, the total plate count of

heterotrophic bacteria in site#1 and site#2 sediments ranged from 2.39 log CFU/mL to 4.39 log CFU/mL and from 2.47 log CFU/mL to 3.07 log CFU/mL, respectively. The bacterial colonies on NA+1% NaCl were categorised on the basis of morphology, such as shape, size and colour, and then randomly selected for identification. A total of 233 bacterial isolates were subsequently identified using biochemical tests and were found to belong to 16 families and 29 genera (Figure 2). The first-, second-, and third-most identified isolates were in families *Moraxellaceae* (41 isolates; 17.60%), *Vibrionaceae* (38 isolates; 16.31%), and *Paenibacillaceae* (37 isolates; 15.88%), respectively.

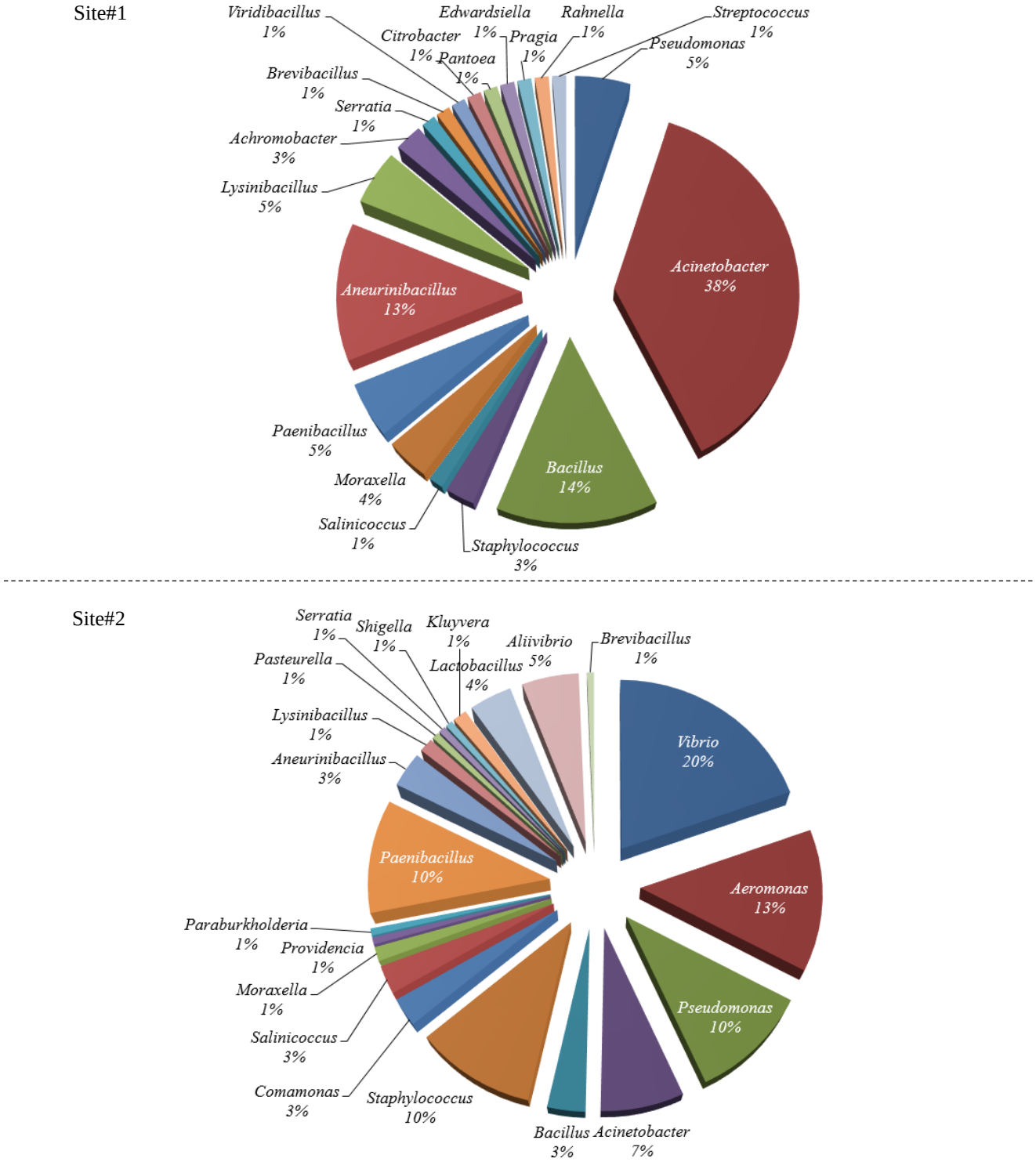

Figure 2. Taxonomy of bacterial strains isolated from Klong Tub Mangrove Forest at sites#1 (nearby the narrowleaf cattail wetland) and site#2 (in the mangrove)

Comparison of bacterial isolates in site#1 and site#2 sediments revealed differences in bacterial structure and composition (Figure 2). Identification of isolates from site#1 sediments (n=80) revealed that the bacteria belonged to nine families and 19 genera. The first-, second-, and third-most frequently identified isolates were in genera *Acinetobacter* (38%), *Bacillus* (14%), and *Aneurinibacillus* (13%), respectively. One isolate each from six genera including *Citrobacter*, *Panoea*, *Edwardsiella*, *Pragia*, *Rahnella*, and *Streptococcus* and two isolates of *Achromobacter* spp. were identified in site#1 sediments but not in site#2 samples. For site#2 sediments, 153 of the isolates belonged to 14 families and 21 genera. The first- and second-most frequently identified isolates were in genera *Vibrio* (20%) and *Aeromonas* (13%), and the third-most frequently identified isolates were bacterial strains from three genera *Pseudomonas*, *Staphylococcus*, and *Paenibacillus* (10% each). The following bacterial strains from nine genera were detected only in site#2 sediments: *Vibrio* spp. (30 isolates), *Aliivibrio* spp. (8 isolates), *Lactobacillus* spp. (6 isolates), *Commamonas* spp. (4 isolates), *Kluyvera* spp. (2 isolates), *Shigella* sp. (1 isolate), *Providencia* sp. (1 isolate), *Paraburkholderia* sp. (1 isolate), and *Pasteurella* sp. (1 isolate).

Figure 3 shows the colony morphology of four bacterial isolates (A.1, B.1, C.1, and D.1) identified using 16s rRNA sequence analysis. Isolate A.1 showed a mucous, transparent spread out, edged shape with chalk-like colour. For isolate B.1, the morphology was power-like colony with pink colour in the centre. Isolate C.1 was a small, orange-brown-coloured colony covered with thick slime. Finally, isolate D.1 appeared as a powder-like colony with whitish to greyish aerial mycelium. Results from the alignment of partial 16s rRNA sequences using three different tools, BLAST, EzBioCloud, and RDP classifier, are shown in Table 1. The alignment of all sequences gave high similarity values (≥99.65%). Isolates A.1 and C.1 were closely related to *Streptomyces platensis* strain ATCC 23948 and *Streptomyces* sp. NA03103, respectively. The other two isolates, B.1 and D.1, shared sequence similarity to *Micromonospora* sp. A38 (100.00%) and *Bacillus velezensis* strain KKLW (≥99.86%), respectively. Accordingly, isolates A.1 and C.1 were identified as *Streptomyces* spp. and isolates B.1 and D.1 were *Micromonospora* sp. and *Bacillus* sp., respectively.

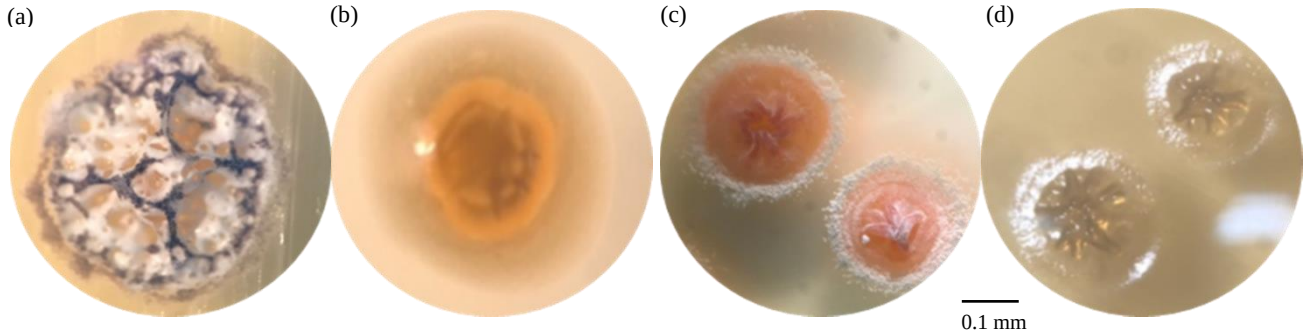

Figure 3. Colonial appearance of bacterial isolates on ISP-2 agar (a) isolate A.1, (b) isolate B.1, (c) isolate C.1, and (d) isolate D.1

Table 1. Closely related species shared similarity to the partial 16s rRNA sequence of isolates A.1, B.1, C.1, and D.1 as analysed by three different tools

Isolate	Best blast match with known taxa by BLAST (% identity)	Top-hit taxon by EzBioCloud (% similarity)	Genus predicted by RDP classifier at 95% confidence threshold (% probability)
A.1	*Streptomyces platensis* strain ATCC 23948 (100.00%)	*Streptomyces platensis* JCM 4662 (99.93%)	*Streptomyces* (100%)
B.1	*Micromonospora* sp. A38 (100.00%)	*Micromonospora fluminis* A38 (100.00%)	*Micromonospora* (100%)
C.1	*Streptomyces* sp. NA03103 (100.00%)	*Streptomyces ardesiacus* (99.65%)	*Streptomyces* (100%)
D.1	*Bacillus velezensis* strain KKLW (100.00%)	*Bacillus velezensis* CR-502 (99.86%)	*Bacillus* (100%)

4. DISCUSSION

This study investigated the microbial diversity of Klong Tub Mangrove Forest. Observation of heterotrophic bacteria in aerobic condition was conducted in 5 cm-deep sediments because the oxygen level in the sediments at this level is higher than that of the sediments in low depths, leading to high microbial diversity (Dias et al., 2009; Somerfield et al., 1998). A total of 233 bacterial isolates were isolated and identified using biochemical approaches and ABIS online tools (Bhagobaty, 2020; Kayode et al., 2020; Dumitru et al., 2021; Ndukwu et al., 2021; Vansia et al., 2021). The results showed that the bacteria belonged to 29 genera and 16 families. The dominant strains in the microbial community were in descending ranked order as follows: *Moraxellaceae* (17.60%), *Vibrionaceae* (16.31%), *Paenibacillaceae* (15.88%), *Staphylococcaceae* (9.87%), *Bacillaceae* (9.87%), *Aeromonadaceae* (8.58%), and *Pseudomonadaceae* (8.58%). Moreover, phosphate-solubilizing bacteria that were commonly found in mangroves, namely, *Bacillus*, *Paenibacillus*, *Kluyvera*, *Pseudomonas*, *Burkholderia*, *Serrtia*, and *Acinetobacter* species, were predominant in this forest (Thatoi et al., 2013; Teymouri et al., 2016). The Klong Tub Mangrove Forest is located in the transition zone between a narrowleaf cattail wetland and Sattahip Bay (Figure 1). Assessment of abiotic parameters revealed differences in abiotic values between the two site samples. Compared with site#2 samples, site#1 samples had higher pH and lower salinity. Differences in taxonomic structures were also detected between the bacterial communities. The first-, second-, and third-most frequently identified isolates from site#1 samples were from genera *Acinetobacter* (38%), *Bacillus* (14%), and *Aneurinibacillus* (13%), respectively. *Acinetobacter* spp. and *Bacillus* spp. have been reported as two of the top 26 genera associated with narrowleaf cattail rhizospheric samples (Gao and Shi, 2018). For site#2 samples, the predominant bacterial strains were *Vibrio* (20%), *Aeromonas* (13%), *Pseudomonas* (10%), *Staphylococcus* (10%), and *Paenibacillus* (10%). These bacterial groups are commonly found in marine and estuarine environments (Thompson et al., 2004; Sousa et al., 2006; Stevens et al., 2007). This study provided evidence on the influence of environmental conditions, including abiotic parameters and types of plants, on determining the compositions and diversity patterns of bacterial communities (Stottmeister et al., 2003; Oguh et al., 2021).

The microbial community in site#1 sediments (19 genera, n=80) showed higher diversity than those in site#2 sediments (21 genera, n=153). Gao and Shi (2018) investigated the taxonomic structure of seed, root and rhizospheric bacterial microbiota of narrowleaf cattail *T. angustifolia* using Illumina-based sequencing. They found that the rhizospheric bacterial community exhibited higher taxon richness compared with the seed and root endophytes. Similarly, a study of ammonium/ammonia-oxidizing prokaryote (AOP) communities in Hong Kong revealed more complex AOP community structures in man-made freshwater wetland than in natural coastal marine wetland (Wang and Gu, 2013). The authors concluded that the high diversity in freshwater AOP community was affected by narrowleaf cattail *T. angustifolia* which enhanced AOP abundances in the rhizophere area. This finding suggested that presence of narrowleaf cattail nearby the Klong Tub Mangrove Forest may influence the high microbial diversity in site#1 sediments.

Four filamentous Gram-positive isolates were isolated from the sediment in the studied mangrove forest. Partial 16s rRNA sequence analysis using three different similarity-based search tools, BLAST, EzBioCloud, and RPD Classifier, revealed three presumptive genera with a similarity value of ≥99.65%. Two isolates, A.1 and C.1, shared high 16s rRNA gene sequence similarity with *Streptomyces platensis* and *Streptomyces* sp. NA03103, respectively. *Streptomyces platensis* produces a variety of antibiotics, including oxytetracycline, platensimycin, migrastatin, isomigrastatin, platencin, dorrigocin A and B and terramycine (Ju et al., 2005; Smanski et al., 2012). Genome mining of *Streptomyces* sp. NA03103 revealed the presence of an orphan nonribosomal peptide synthetase (NRPS) gene cluster (*asm*) encoding for two novel cyclopeptides ashimides A and B (Shi et al., 2019). Ashimide B has been classified as an organic compound, namely, benzoxazine. Several studies have reported the biological activities of benzoxazine derivatives in various aspects, including anti-inflammatory, antimicrobial, anticancer and anti-malaria (Akhter et al., 2011; Foto et al., 2014; Sharma et al., 2018). This finding is consistent with the study of Xavier et al. (2021) who analysed the genomic DNA of *Streptomyces* sp. NA03103 using anti-SMASH v5.2.0 and found a number of predictive BCGs which may implicate diverse secondary metabolic biosynthesis, such as polyketides, nonribosomal peptides, terpenes, and lanthipeptides

(Xavier et al., 2021). Further experiments are required to investigate the function of this potential bacterial strain on the synthesis of marine natural products.

In addition to *Streptomyces*, one rare actinomycete strain was isolated from the sediments in Klong Tub mangrove forest. Analysis of partial 16s rRNA sequence showed 100.00% similarity to *Micromonospora* sp. A38 (Table 1). Strain A38 has been classified as a novel species named *Micromonospora fluminis* sp. nov. (Pozo et al., 2020). *M. fluminis* strain was isolated from freshwater, the Carpintero River in Cuba. Meanwhile, the isolated strain in the present study was from a marine environment, implying its ability to adopt to a wide range of environmental conditions. To our knowledge, the secondary metabolites of this novel strain has never been reported.

A number of bacterial strains isolated from the Klong Tub Mangrove Forest have been documented for their biotechnological potentials. One of which was *Bacillus*, one of the abundant genera detected in the rhizosphere communities of mangroves (Sebastianes et al., 2017; Jeyanny et al., 2020). In the present study, a rhizophere bacterium named *Bacillus velezensis*, a novel species of *Bacillus*, was isolated. *B. velezensis* produces diverse metabolic intermediates with wide applications, such as in surfactant production, antagonistic activities against phytopathogens, promotion of seed development and plant growth, antibiotics, iron chelators, antioxidants, and anticancer agents (Ruiz-García et al., 2005; Meena et al., 2018; Aloo et al., 2019; Rabbee et al., 2019). *B. velezensis* SMR isolated from seawater can produce nanocellulose, a promising material for various industries, such as medicine, food and agriculture (Abouelkheir et al., 2020). In Thailand, a number of *Bacillus* spp., such as *Bacillus aquimaris* strain TF-12 and *B. aryabhattai* strain B8W22, have been isolated from mangrove forest sediments (Foophow and Tangjitjaroenkun, 2014). These isolates can produce proteases, enzymes that are widely used in various industries (Razzaq et al., 2019). In addition to *Bacillus* spp., *Aeromonas* spp. were documented for their biotechnological potentials, particularly extracellular proteases that are involved in the degradation of different proteinaceous compounds, such as albumin, fibrin and gelatine (Liu, 2014). For the genus *Acinetobacter*, the predominant bacterial strains isolated from site#1 sediments have the abilities of hydrocarbon degradation, ester production and biosurfactant production (Jung and Park, 2015). The other genus was *Comamonas* spp. which can be found in soil and water. The recent isolation and investigation of *Comamonas aquatica* from mangrove swamps in Rayong Province, Thailand revealed its ability to degrade polycyclic aromatic hydrocarbons (PAHs) (Chantarasiri, 2021). *C. aquatica* can also promote plant growth via the production of indole-3-acetic acid as their metabolites (Al-Mamari et al., 2020). Moreover, the *C. aquatica* strain isolated from the root of freshwater plant *Pistia stratiotes* exhibited the efficient removal of heavy metal, Ni and Cu in the environment, implying the potential of this bacterial genera in phytoremediation technology (Ghosh et al., 2020). *Aneurinibacillus aneurinilyticus* is another bacterial strain displaying various biotechnological interests. It was recognised as a plant growth-promoting rhizobacteria and also exhibited antifungal activity (Chauhan et al., 2014). Its marine strain has been recently evaluated for a new lipopeptide biosurfactant (Balan et al., 2017). Interestingly, the secondary metabolite of this bacterium has mosquitocidal potential to control mosquito-borne diseases (Das et al., 2016).

The Klong Tub Mangrove Forest is located near Pattaya City, Chonburi Province, Thailand, a famous coastal city on the Upper Gulf of Thailand. Bacterial identification revealed that none of the isolates were enterococci and *Escherichia coli*, bacterial indicators of faecal contamination (U.S. EPA, 2012). The absence of faecal contamination was confirmed by spread plate technique on eosin methylene blue agar (Abbu and Lyimo, 2009). On the basis of these results were, the Klong Tub Mangrove Forest in Sattahip, Chonburi Province, Thailand possesses high microbial diversity with minimal anthropogenic effects, making it a valuable natural resource in terms of industrial enzymes and secondary metabolite producers. Particularly, the three Actinomycete isolates require further investigation to determine their potential in biotechnological applications.

5. CONCLUSION

This study investigated the microbial community in sediments from Klong Tub Mangrove Forest. The results indicated that the forest possesses a number of bacterial strains. Comparison of the structure of bacterial microbiota between site#1 (nearby the narrowleaf cattail wetland) and site#2 (the mangrove forest close to the sea) revealed differences in their predominant bacterial species and compositions. This finding implied the significance of

environmental conditions on determining bacterial community compositions and diversity patterns. Moreover, two actinomycete strains (*Streptomyces* sp. and *Streptomyces* sp. NA03103) and a rare actinomycete *Micromonospora* sp. were isolated. The production of bioactive compounds from these isolates are currently under investigation. Several bacterial isolates from the mangrove forest have been documented for their biotechnological potentials, including plant growth promotion, antibiotics, antifungal and PAH degradation. According to our observation, the Klong Tub Mangrove Forest possesses high microbial diversity with minimal anthropogenic effects and high potentials for biotechnological applications.

ACKNOWLEDGEMENTS

We are grateful to the Air and Costal Defense Command, Royal Thai Navy for their kind support during sampling. This research was financially supported by Thailand Science Research and Innovation (TSRI), National Science, Research and Innovation Fund (NSRF), (Fiscal Year 2021), Grant no. 48857.

REFERENCES

Abbu AA, Lyimo TJ. Assessment of fecal bacteria contamination in sewage and non-sewage impacted mangrove ecosystems along the coast of Dar es salaam. Tanzania Journal of Science 2009;33(1):27-40.

Abouelkheir SS, Kamara MS, Atia SM, Amer SA, Youssef MI, Abdelkawy RS, et al. Novel research on nanocellulose production by a marine *Bacillus velezensis* strain SMR: A comparative study. Scientific Reports 2020;10(1):Article No. 14202.

Akhter M, Husain A, Akhter N, Khan MSY. Synthesis, anti-inflammatory and antimicrobial activity of some new 1-(3-phenyl-3,4-dihydro-2H-1,3-benzoxazin-6-yl)-ethanone derivatives. Indian Journal of Pharmaceutical Sciences 2011; 73(1):101-4.

Al-Mamari SNH, Al-Sadi AM, Babu SPS, Al-Mahmooli IH, Velazhahan R. *In vitro* antagonistic potential, plant growth-promoting activity and indole-3-acetic acid producing trait of bacterial isolates from button mushroom (*Agaricus bisporus*) spent substrate. Journal of Agricultural and Marine Sciences 2020;25(2):22-9.

Allard SM, Costa MT, Bulseco AN, Helfer V, Wilkins LGE, Hassenrück C, et al. Introducing the mangrove microbiome initiative: Identifying microbial research priorities and approaches to better understand, protect, and rehabilitate mangrove ecosystems. Applied and Environmental Science 2020;5(5):e00658-20.

Aloo BN, Makumba BA, Mbega ER. The potential of bacilli rhizobacteria for sustainable crop production and environmental sustainability. Microbiological Research 2019;219:26-39.

Azman AS, Othman I, Velu SS, Chan KG, Lee LH. Mangrove rare actinobacteria: Taxonomy, natural compound, and discovery of bioactivity. Frontiers in Microbiology 2015;6:Article No. 856.

Balan SS, Kumar CG, Jayalakshmi S. Aneurinifactin, a new lipopeptide biosurfactant produced by a marine *Aneurinibacillus aneurinilyticus* SBP-11 isolated from Gulf of Mannar: Purification, characterization and its biological evaluation. Microbiological Research 2017;194:1-9.

Bhagobaty RK. Hydrocarbon-utilizing bacteria of natural crude oil seepages, Digboi oilfield, Northeastern region of India. Journal of Sedimentary Environments 2020;5:177-85.

Chantarasiri A. Enrichment and identification of phenanthrene-degrading bacteria isolated from the oil-stained engine sediment in the mangrove swamps of Thailand. Applied Science and Engineering Progress 2021;14(2):206-18.

Chauhan A, Balgir PP, Shirkot CK. Antifungal potential of native strain isolated from rhizosphere soil of *Valeriana jatamansi* from temperate regions of Himachal Pradesh. Journal of Applied Horticulture 2014;16(2):131-5.

Das D, Chatterjee S, Dangar TK. Characterization and mosquitocidal potential of the soil bacteria *Aneurinibacillus aneurinilyticus* isolated from Burdwan, West Bengal, India. Proceedings of the National Academy of Sciences India Section B - Biological Sciences 2016;86:707-13.

Dias ACF, Andreote FD, Dini-Andreote F, Lacava PT, Sá ALB, Melo IS, et al. Diversity and biotechnological potential of culturable bacteria from Brazilian mangrove sediment. World Journal of Microbiology Biotechnology 2009;25(7):1305-11.

Dumitru M, Ciurescu G, Hăbeanu M. Evaluation of *Lactobacillus* spp. based on phenotypical profile as direct-fed microbial candidate for poultry nutrition. Archiva Zootechnica 2021; 24(2):150-66.

Foophow T, Tangjitaroenkun J. Screening and identification of protease producing halophilic bacteria isolated from mangrove forest sediments in Chanthaburi. Proceedings of the 26th Annual Meeting of the Thai Society for Biotechnology and International Conference; 2014 Nov 26-29; Mae Fah Luang University, Chiang Rai: Thailand; 2014.

Foto E, Ozen C, Zilifdar F, Yilmaz S, Alper-Hayta S, Yildiz I, et al. Inhibitory effects of some benzoxazine derivatives on human DNA topoisomerase I. Proceedings of the 2nd International Bau-Drug Design Symposium, Novel Methods and Emerging Targets in Drug Discovery and Patented Drug Development; 2014 Apr 17-19; Bahçeşehir University, Istanbul: Turkey; 2014.

Fuhrman JA, Cram JA, Needham DM. Marine microbial community dynamics and their ecological interpretation. Nature Reviews Microbiology 2015;13:133-46.

Gao T, Shi XY. Taxonomic structure and function of seed-inhabiting bacterial microbiota from common reed (*Phragmites australis*) and narrowleaf cattail (*Typha angustifolia* L.). Archives of Microbiology 2018;200:869-76.

Ghizelini AM, Mendonça-Hagler LCS, Macrae A. Microbial diversity in Brazilian mangrove sediments: A mini review. Brazilian Journal of Microbiology 2012;43(4):1242-54.

Ghosh A, Ali S, Mukherjee SK, Saha S, Kaviraj A. Bioremediation of copper and nickel from freshwater fish *Cyprinus carpio* using rhiozoplane bacteria isolated from *Pistia stratiotes*. Environmental Processes 2020;7:443-61.

Gong B, Chen S, Lan W, Huang Y, Zhu X. Antibacterial and antitumor of actinomycetes isolated from mangrove soil in the

Maowei Sea of the Southern Coast of China. Iranian Journal of Pharmaceutical Research 2018;17(4):1339-46.

Hong K, Gao AH, Xie QY, Gao H, Zhuang L, Lin HP, et al. Actinomycetes for marine drug discovery isolated from mangrove soils and plants in China. Marine Drugs 2009;7:24-4.

Jalal KCA, Fatin UTN, Mardiana MA, John BA, Kamaruzzaman YB, Shahbudin S, et al. Antibiotic resistance microbes in tropical mangrove sediments, East Coast Peninsular Malaysia. African Journal of Microbiology Research 2010;4:640-5.

Jeyanny V, Norlia B, Getha K, Nur-Nabilah A, Lee S, Rozita A, et al. Bacterial communities in a newly regenerated mangrove of Sungai Haji Dorani mangroves in the west coast of Selangor, Malaysia. Journal of Tropical Forest Science 2020;32(3):268-82.

Ju J, Lim SK, Jiang H, Seo JW, Shen B. Iso-migrastatin congeners from *Streptomyces platensis* and generation of a glutarimide polyketide library featuring the dorrigocin, lactimidomycin, migrastatin, and NK30424 scaffolds. Journal of the American Chemical Society 2005;127:11930-1.

Jung J, Park W. *Acinetobacter* species as model microorganisms in environmental microbiology: Current state and perspective. Applied Microbiology and Biotechnology 2015;99:2533-48.

Katili AS, Retnowati Y. Isolation of actinomycetes from mangrove ecosystem in Torosiaje, Gorontalo, Indonesia. Biodiversitas Journal of Biological Diversity 2017;18:826-33.

Kayode A, Okunrounmu P, Olagbende A, Adedokun O, Hassan AW, Atilol G. High prevalence of multiple drug resistant enteric bacteria: Evidence from a teaching hospital in Southwest Nigeria. Journal of Infection and Public Health 2020;13:651-6.

Liu D. Aeromonas. In: Yi-Wei T, Sussman M, Liu D, Poxton I, Schwartzman J, editors. Molecular Medical Microbiology. 2nd ed. Elsevier; 2014. p. 1099-110.

Mamangkey J, Suryanto D, Munir E, Mustopa AZ, Sibero MT, Mendes LW, et al. Isolation and enzyme bioprospection of bacteria associated to *Bruguiera cylindrica*, a mangrove plant of North Sumatra, Indonesia. Biotechnology Reports 2021;30:e00617.

Mangrove Forest at Air and Coastal Defense Command. Diverse of species [Internet]. 2014 [cited 2021 Nov 26]. Available from: http://www.thainavyland.com/ecology/mangrove-forest-park01/.

Meena KR, Tandon T, Sharma A, Kanwar SS. Lipopeptide antibiotic production by *Bacillus velezensis* KLP2016. Journal of Applied Pharmaceutical Science 2018;8:91-8.

Mishra RR, Swain MR, Dangar TK, Thatoi H. Diversity and seasonal fluctuation of predominant microbial communities in Bhitarkanika, a tropical mangrove ecosystem in India. Revista de Biología Tropical 2012;60(2):909-24.

Morgulis A, Coulouris G, Raytselis Y, Madden TL, Agarwala R, Schäffer AA. Database Indexing for Production MegaBLAST Searches. Bioinformatics 2008;24:1757-64.

Ndukwu CLC, Akani NP, Wemedo SA, Sampson T. Public health implications of coliform contaminants in non-packaged, commercially hawked herbal remedies sold in port harcourt. Journal of Advances in Microbiology 2021;21(9):79-87.

Oguh CE, Obiwulu ENO, Umezinwa OJ, Ameh SE, Ugwu CV, Sheshi IM. Ecosystem and ecological services; Need for biodiversity conservation: A critical review. Asian Journal of Biology 2021;11(4):1-14.

Palit K, Rath S, Chatterjee S, Das S. Microbial diversity and ecological interactions of microorganisms in the mangrove ecosystem: Threats, vulnerability, and adaptations. Environmental Science and Pollution Research 2022; 29(1):32467-12.

Pathom-aree W, Nogi Y, Ward AC, Horikoshi K, Bull AT, Goodfellow M. *Dermacoccus barathri* sp. nov. and *Dermacoccus profundi* sp. nov., novel actinomycetes isolated from deep-sea mud of the Mariana Trench. International Journal of Systematic and Evolutionary Microbiology 2006; 56(10):2303-7.

Pozo MIC, Wieme AD, Pérez SR, Maury GL, Peeters C, Snauwaert C, et al. *Micromonospora fluminis* sp. nov., isolated from mountain river sediment. International Journal of Systematic and Evolutionary Microbiology 2020;70(12):6428-36.

Rabbee MF, Ali MS, Choi J, Hwang BS, Jeong SC, Baek K. *Bacillus velezensis*: A valuable member of bioactive molecules within plant microbiomes. Molecules 2019;24:Article No. 1046.

Razzaq A, Shamsi S, Ali A, Ali Q, Sajjad M, Malik A, et al. Microbial proteases applications. Frontiers in Bioengineering and Biotechnology 2019;7:Article No. 110.

Ruiz-García C, Béjar V, Martínez-Checa F, Llamas I, Quesada E. *Bacillus velezensis* sp. nov., a surfactant-producing bacterium isolated from the river Velez in Malaga, southern Spain. International Journal of Systematic and Evolutionary Microbiology 2005;55(1):191-5.

Sebastianes FLS, Azevedo JL, Lacava PT. Diversity and biotechnological potential of endophytic microorganisms associated with tropical mangrove forests. In: Azevedo JL, Quecine MC, editors. Diversity and Benefits of Microorganisms from the Tropics. Switzerland: Springer International Publishing; 2017. p. 37-56.

Sharma V, Amarnath N, Shukla S, Ayana R, Kumar N, Yadav N, et al. Benzoxazine derivatives of phytophenols show anti-plasmodial activity via sodium homeostasis disruption. Bioorganic and Medicinal Chemistry Letters 2018;28(9): 1629-37.

Shi J, Zeng YJ, Zhang B, Shao FL, Chen YC, Xu X, et al. Comparative genome mining and heterologous expression of an orphan NRPS gene cluster direct the production of ashimides. Chemical Sciences 2019;10:Article No. 3042.

Smanski MJ, Peterson, RM, Shen B. Platensimycin and platencin biosynthesis in *Streptomyces platensis*, showcasing discovery and characterization of novel bacterial diterpene synthases. Methods in Enzymology 2012;515:163-86.

Somerfield PJ, Gee JM, Aryuthaka C. Meiofaunal communities in a Malaysian mangrove forest. Journal of the Marine Biological Association of the United Kingdom 1998;78(3):717-32.

Sorescu I, Stoica C. Online advanced bacterial identification software, an original tool for phenotypic bacterial identification. Romanian Biotechnological Letters 2021;26(6):3047-53.

Sousa OV, Macrae A, Menezes FGR, Gomes NCM, Vieira RHSF, Mendonça-Hagler LCS. The impact of shrimp farming effluent on bacterial communities in mangrove waters, Ceará, Brazil. Marine Pollution Bulletin 2006;52(12):1725-34.

Stevens H, Brinkhoff T, Rink B, Vollmers J, Simon M. Diversity and abundance of gram positive bacteria in a tidal flat ecosystem. Environmental Microbiology 2007;9(7):1810-22.

Stottmeister U, Wieβner A, Kuschk P, Kappelmeyer U, Kästner M, Bederski O, et al. Effects of plants and microorganisms in constructed wetlands for wastewater treatment. Biotechnology Advances 2003;22:93-117.

Taechowisan T, Chaisaeng S, Phutdhawong W. Antibacterial, antioxidant and anticancer activities of biphenyls from

Streptomyces sp. BO-07: An endophyte in *Boesenbergia rotunda* (L.). Mansf A. Food and Agricultural Immunology 2017;28(6):1330-46.

Teymouri M, Akhtari J, Karkhane M, Marzban A. Assessment of phosphate solubilisation activity of rhizobacteria in mangrove forest. Biocatalysis and Agricultural Biotechnology 2016; 5:168-72.

Thatoi H, Behera BC, Mishra RR, Dutta SK. Biodiversity and biotechnological potential of microorganisms from mangrove ecosystems: A review. Annals of Microbiology 2013;63:1-19.

Thompson FL, Iida T, Swings J. Biodiversity of vibrios. Microbiology and Molecular Biology Reviews 2004; 68(3):403-31.

United States Environmental Protection Agency (U.S. EPA). Recreational water quality criteria, Office of Water 820-F-12-058 [Internet]. 2012 [cited 2021 Sep 24]. Available from: https://www.epa.gov/sites/default/files/2015-10/documents/rwqc2012.pdf.

Vansia A, Patel R, Dudhagara P. Analysis of multidrug resistance profile of *Escherichia coli* from clinical samples from companion animals and bird retrospect to five-year (2015-2019) literature data. Biointerface Research in Applied Chemistry 2021;11(5):12506-15.

Wang Q, Garrity GM, Tiedje JM, Cole JR. Naïve Bayesian classifier for rapid assignment of rRNA sequences into the new bacterial taxonomy. Applied and Environmental Microbiology 2007;73(16):5261-7.

Wang YF, Gu JD. Higher diversity of ammonia/ammonium-oxidizing prokaryotes in constructed freshwater wetland than natural coastal marine wetland. Applied Microbiology and Biotechnology 2013;97:7015-33.

Xavier RKM, Xu D, McCarthy PJ, Yang S, Wang G. Genome sequence of *Streptomyces* sp. strain HB-N217, isolated from the marine sponge *Forcepia* sp. Microbiology Resource Announcements 2021;10(8):e01410-20.

Yoon SH, Ha SM, Kwon S, Lim J, Kim Y, Seo H, et al. Introducing EzBioCloud: A taxonomically united database of 16S rRNA and whole genome assemblies. International Journal of Systematic and Evolutionary Microbiology 2017;67(5):1613-7.

Zhang Z, Schwartz S, Wagner L, Miller W. A greedy algorithm for aligning DNA sequences. Journal of Computational Biology 2000;7(1-2):203-14.

Evaluating Ecological Risk Associated with Heavy Metals in Agricultural Soil in Dong Thap Province, Vietnam

Nguyen Thanh Giao*, Huynh Thi Hong Nhien, and Phan Kim Anh

College of Environment and Natural Resources, Can Tho University, Ninh Kieu District, Can Tho City 900000, Vietnam

ARTICLE INFO

Received: 20 May 2022
Received in revised: 15 Jul 2022
Accepted: 21 Jul 2022
Published online: 16 Aug 2022
DOI: 10.32526/ennrj/20/202200114

Keywords:
Agricultural soil/ Ecological risks/ Dong Thap/ Heavy metals/ Source identification

*** Corresponding author:**
E-mail: ntgiao@ctu.edu.vn

ABSTRACT

Heavy metal pollution in soil has received more attention in recent years because of an increase in human activities and its potential effects on ecology and human health. This study assessed the occurrence of heavy metals (As, Pb, Cu, Zn, and Cd) in different cultivated land and their ecological risk in Dong Thap Province, Vietnam. Seventeen samples collected in paddy, vegetable, perennials, and ornamental soils were measured for heavy metal concentrations and soil structure. The data were analyzed using Pearson correlation, principal component analysis (PCA), cluster analysis (CA), Nemerow pollution index (PI_N), geoaccumulation index (I_{geo}), pollution load index (PLI), and potential ecological risk index (RI). The results revealed that the soil structure was clay loam and silt clay loam. Heavy metal concentrations were within the national limits with the order of Zn>Cu>Pb>As>Cd. Pearson correlation and PCA indicated that heavy metals were strongly correlated, and agriculture and soil formation were responsible for their presence in soil. The sampling sites were divided into four groups using CA, in which paddy and crop soils had the highest content of heavy metals. Based on PI_N values (0.82-2.92), the heavy metal pollution ranged from warning to moderate level. As had the highest accumulation potential in the soil, with the I_{geo} values ranging from 0.12-2.05. The risk of heavy metal pollution in agricultural soil to ecology was low to moderate. Despite that, it is recommended to annually monitor the occurrence of heavy metals in agricultural soils to have proper solutions to protect public health.

1. INTRODUCTION

Heavy metals are defined as metallic elements whose density is at least five times higher than water (Fergusson, 1990). Based on this definition, heavy metals include metalloids such as arsenic (As) with a density of 5.73 g/cm^3 (Duffus, 2002; Tchounwou et al., 2012). Heavy metals are naturally occurring elements in the earth's crust. As a result of rapid urbanization and industrialization, an increase in heavy metal pollution has become a significant concern (Apostol et al., 2021; Fei et al., 2022). Heavy metals are persistent and non-biodegradable, which are likely to disperse and accumulate in ecosystems, eventually entering the human body through the food chain (Klinsawathom et al., 2017; Rashed, 2018). Some heavy metals, such as cadmium (Cd), chromium (Cr), arsenic (As), mercury (Hg), lead (Pb), copper (Cu), zinc (Zn), and nickel (Ni), have been listed as priority pollutants for control by the United States Environmental Protection Agency (USEPA) (Cravotta and Brady, 2015). Heavy metal accumulation in the human body can cause serious diseases, such as Cd damaging kidney function (Liu et al., 2022) and As causing cardiovascular disease, diabetes, and cancer (Li et al., 2016). Therefore, it is necessary to evaluate heavy metal contamination in soil and determine their potential risks.

The presence of heavy metals in soil is attributed to two primary sources. Firstly, natural processes such as weathering and volcanism are associated with heavy metal pollution (Fei et al., 2022; Cui et al., 2021). The impacts of anthropogenic activities are prominent, including mining and smelting industries, metal-based industries, domestic wastes, and agriculture (Wei and Yang, 2010; Huan et al., 2017; Guan et al., 2019; Cui et al., 2021; Fei et al., 2022). In terms of the impact of agricultural activities, applying heavy metal-

Citation: Giao NT, Nhien HTH, Anh PK. Evaluating ecological risk associated with heavy metals in agricultural soil in Dong Thap Province, Vietnam. Environ. Nat. Resour. J. 2022;20(6):585-597. (https://doi.org/10.32526/ennrj/20/202200114)

containing pesticides and herbicides greatly contributes to soil pollution. For example, As contamination in cultivated land was associated with the excessive application of pesticides (Cai et al., 2019; Jiang et al., 2020; Fei et al., 2022). Using phosphate fertilizers and pesticides is a reason for the high content of Cd in Shanghai (Fei et al., 2022). In addition, using contaminated water for irrigation has caused the enrichment of heavy metals in the agricultural system (Hung and Thom, 2016). In recent years, many countries have intensively increased agricultural activities to ensure food safety which is one of 17 sustainable development goals (SDGs). This has led to a high risk of heavy metal contamination in the agricultural soil. There are several factors that control the concentrations of heavy metals in soil: wind direction, topography, and particle size distribution (Lou et al., 2022). However, the number of studies on heavy metals in agricultural soils and their potential environmental risks are limited (Fei et al., 2022).

In recent studies, different indices have been introduced to assess the extent of pollution and the potential pollution of agricultural soil by heavy metals, such as Nemerow pollution index (PI_N), geoaccumulation index (I_{geo}), pollution load index (PLI), and potential ecological risk index (RI) (Fei et al., 2022; Kowalska et al., 2018; Cui et al., 2021; Kang et al., 2020). PI_N is calculated to evaluate the overall pollution of soil and determine the most polluted parameters (Kowalska et al., 2018). Similar to PI_N, PLI is used to assess the pollution levels or the levels of heavy metals in soil, which can be used to compare the soil quality between different study areas (Nazzal et al., 2021; Ferreira et al., 2022). I_{geo} index is employed to assess the pollution extent in soil by each heavy metal, which can compare the changes in the soil problems in the past and the present (Kowalska et al., 2018; Nazzal et al., 2021; Ferreira et al., 2022). To evaluate the potential risks to ecology by heavy metal-contaminated soils, RI is employed with the consideration of toxic level, ecological sensitivity, and synergy effects of heavy metals (Cui et al., 2021; Ferreira et al., 2022). These indices are deemed effective tools to comprehensively evaluate soil contamination and predict the effects on ecology (Kowalska et al., 2018). However, the application of a single index could not provide a full understanding of the pollution extent (Kowalska et al., 2018; Fei et al., 2022). Thus, it is required to combine different indices to generate comprehensive information related to soil pollution by heavy metals, which supports policymakers in developing sustainable development strategies.

In Vietnam, agricultural production is one of the most important economic sectors, especially in two primary deltas (Red River delta and Mekong Delta). In the Red River delta, high As content was found in vegetable land (Ha et al., 2016). Collected soil samples in the vegetable growing area showed the signal of Cu, Cd, and Pb contamination (Huan et al., 2017). In Mekong Delta, the natural land area is mainly used for agricultural cultivation, about 2,615.6 thousand hectares, accounting for approximately 64.08% of the total area (General Statistics Office of Vietnam, 2022). According to Huynh et al. (2022), several heavy metals (As, Pb, Cu, Zn) were detected in An Giang Province. Nevertheless, studies about heavy metals in different agricultural soils in the Mekong Delta remain limited. Thus, this study was conducted to evaluate soil characteristics and identify sources and ecological risk associated with the occurrence of heavy metals in agricultural soil using multivariate statistics, Nemerow pollution index (PI_N), geological accumulation index (I_{geo}), pollutant load index (PLI) and ecological potential risk index (RI). The findings could provide helpful information on the agricultural soil pollution levels in Dong Thap Province to formulate strategies for agricultural safety and sustainability.

2. METHODOLOGY

2.1 Description of the study area

Dong Thap is located in Mekong Delta with the coordinates of 10°07′ to 10°58′ North latitude and 105°12′ to 105°56′ East longitude, which is adjacent to Cambodia (North), Vinh Long Province and Can Tho City (South), An Giang Province (West), Long An and Tien Giang Provinces (East). Dong Thap has a fairly flat terrain, and the whole province is located in the delta region. The elevation difference is not large, with an average of about 2 m. The province has three types of terrain: natural dykes along the Tien and Hau Rivers, behind the dyke, and low-lying fields (closed floodplains). Land resources of Dong Thap Province are classified into four main soil types. Alluvial and alkaline soils have the largest area, with an area of 183.9 thousand hectares and 92.4 thousand hectares, respectively. They are distributed mainly along the Tien and Hau Rivers (alluvial soil), Tam Nong and Thap Muoi Districts (alkaline soil). Gray soil is mainly found in Tan Hong District bordering Cambodia and Tam Nong District, about 26.5 thousand hectares.

Sandy soil is distributed in Thap Muoi and Cao Lanh Districts with 0.067 thousand hectares.

The structure of land use in agriculture in Dong Thap Province in 2019 is divided into two categories: annual cropland (accounting for 227.3 thousand hectares) and perennial cropland (accounting for 32.80 thousand hectares). The annual cropland is used mainly for rice cultivation, with about 221.5 thousand hectares (accounting for 65.47%). Dong Thap Province has a total natural land area in 2019 of 338.4 thousand hectares, of which agricultural production land accounts for 76.84% with 260.1 thousand hectares (DoNRE, 2021). Therefore, it is considered one of the provinces with agricultural land accounting for a high proportion of the total natural land area. The agricultural system of Dong Thap Province is diverse with many other agricultural cultivation models, such as rice, vegetables, fruit trees, and ornamental plants.

2.2 Soil sample collection and analysis

Seventeen agricultural soil samples (D01-D17) were collected twice in 2020. The sampling sites are presented in Figure 1. The soil samples were collected at different agricultural cultivation areas in Dong Thap Province, including rice, vegetables, perennials, and ornamental plants. These collected soil samples were then analyzed for soil structure and heavy metals (As, Pb, Cu, Zn, and Cd). Soil samples were collected and preserved according to the standards specified in the national standard TCVN 5297:1995 on Soil Quality-Sampling-General requirements (MOST, 1995) and the national standard TCVN 7538-2:2005 in the Soil Quality-Sampling-Part 2: Guidance on sampling techniques (MOST, 2005). The collected soil samples were dried in an oven and then ground to pass through a 0.5 mm stainless steel mesh. The heavy metal concentrations in the soil were measured according to the national standard TCVN 6496:2009 on Soil quality - Determination of cadmium, chromium, cobalt, copper, lead, manganese, nickel, and zinc in aqua regia extracts of soil - Flame and electrothermal atomic absorption spectrometric methods (Varian SpectrAA Model 220FS, US) (MOST, 2009). The detection limits of these heavy metals were 0.01 mg/kg. The sample collection and analysis were strictly conducted to ensure quality assurance/quality control (QA/QC). Three field samples were obtained from one location and preserved in a separate container. In the laboratory, blank samples, verification standard samples, and duplicate laboratory samples were measured.

2.3 Data processing

2.3.1 Statistical analysis

The data of heavy metals were analyzed to determine the values of min, max, mean, standard deviation, and coefficient of variation (CV). To assess the current status and evolution of soil environmental quality in Dong Thap Province, the heavy metals in the soil were compared with QCVN 03-MT:2015/BTNMT-National technical regulation on heavy metal content for agricultural soil (MoNRE, 2015). Correlation analysis was performed to determine the relationship between soil properties and heavy metals (Qishlaqi and Moore, 2007; Zhu et al., 2017). In addition, the principal component analysis (PCA) and cluster analysis (CA) were applied based on the mean of the parameters. PCA aims to determine the most significant parameters affecting soil quality. On the other hand, PCA was also used to determine the origin of heavy metals in the soil. Moreover, CA can group the sampling locations with similar soil properties (Yang et al., 2014; Zhang et al., 2016; Nazzal et al., 2021). The analytical methods were performed using the statistical software Statgraphics Centurion version XVI (Statgraphics Technologies Inc., Virginia, USA).

2.3.2 Ecological risk and pollution level calculation

The Nemerow pollution index (PI_N), cumulative geographic index (I_{geo}), pollution load index (PLI), and potential ecological risk index (RI) were applied to quantify pollution level and potential risk of heavy metals in agricultural soil.

The single pollution index (PI) is used to evaluate the pollution level of each heavy metal in soil (Kowalska et al., 2018). Meanwhile, the accumulation level of each heavy metal in the soil was assessed by geoaccumulation index (I_{geo}) (Kowalska et al., 2018; Cui et al., 2021). The values of indexes were calculated by the equation (1) and (2):

$$PI = \frac{C_n}{GB} \quad (1)$$

$$I_{geo} = \log_2 \left(\frac{C_n}{1.5GB}\right) \quad (2)$$

The spatial variation of I_{geo} values was conducted by the Arcgis version 10.2 software. It was based on interpolation with the inverse distance weighted method.

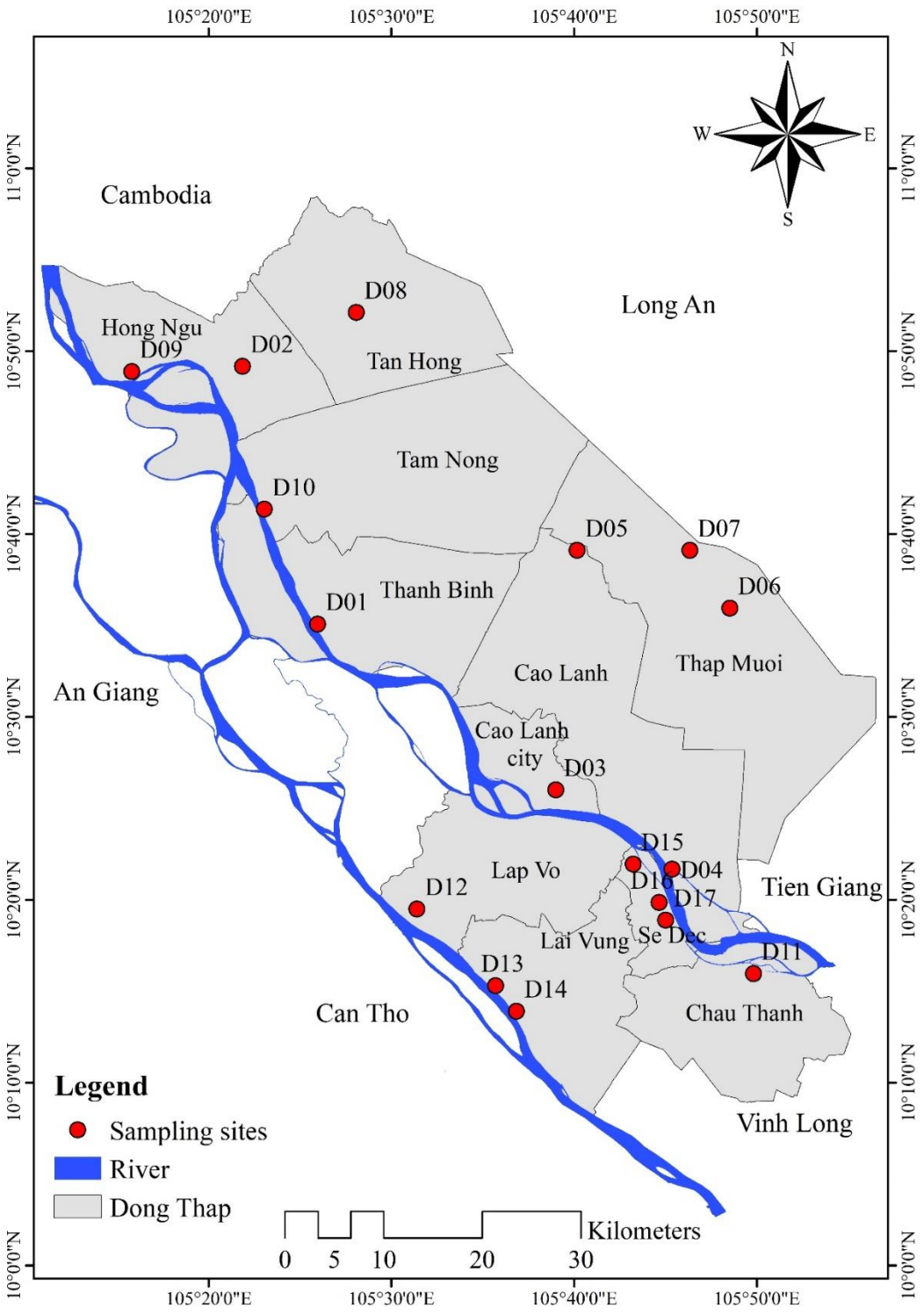

Figure 1. Location of soil sample collection in Dong Thap Province

The overall pollution level of heavy metals in the soil was determined through two indexes (PI_N and PLI). These two indexes were calculated by formulas (3) and (4) (Kowalska et al., 2018; Mamut et al., 2018; Kang et al., 2020):

$$PI_N = \sqrt{\frac{\left(\frac{1}{n}\sum_{i-1}^{n} PI\right)^2 + PI_{max}^2}{n}} \quad (3)$$

$$PLI = \sqrt[n]{PI_1 \times PI_2 \times PI_3 \times ... \times PI_n} \quad (4)$$

In addition, the potential ecological risk (RI) was used to assess potential risks that heavy metals pose to the ecology of the study area (Hakanson, 1980; Ramdani et al., 2018):

$$RI = \sum_{i=1}^{n} E_r^i = \sum_{i=1}^{n} T_r^i \times PI \quad (5)$$

Where, C_n is heavy metal content in analyzed soil samples; GB is the value of the geochemical background corresponding to As, Pb, Cu, Zn, and Cd are 0.67, 27, 38.9, 70, and 0.41 mg/kg, respectively (Kabata-Pendias, 2010; Kowalska et al., 2018); PI_{max} is the maximum value of single pollution index (PI); PI is value of single pollution index; n is the number of heavy metals; E_r^i is potential ecological risk factor for each metal; T_r^i is the toxicity coefficient of metal corresponds to As, Pb, Cu, Zn, and Cd are 10, 5, 5, 1, and 30, respectively (Hakanson, 1980). The reference values of each index in the study are detailed in Table 1.

Table 1. Pollution and risk rating scale

Index	Values	Rating	Index	Values	Rating
PLI	PLI≤1	No pollution	RI	RI<50	Low
	1<PLI≤2	Moderate		50≤RI<100	Moderate
	2<PLI≤3	High		100≤RI<200	High
	PLI>3	Extremely high		RI≥200	Very high
PI_N	PI_N≤0.7	Safe level	I_{geo}	I_{geo}≤0	No pollution
	0.7<PI_N≤1	Warning limit		0<I_{geo}≤1	No to moderate
	1<PI_N≤2	Slight pollution		1<I_{geo}≤2	Moderate
	2<PI_N≤3	Moderate pollution		2<I_{geo}≤3	Moderate to high
	PI_N > 3	Heavy pollution		3<I_{geo}≤4	High
				4<I_{geo}≤5	High to very high
				5<I_{geo}	Extreme pollution

3. RESULTS AND DISCUSSION

3.1 Soil structure properties

The change in soil structure is considered a factor affecting the fluctuation in soil chemical composition (Wang et al., 2018). The analysis results of the structure of agricultural soil are presented in Figure 2. The percentage of clay and silt was high in this study area, which was about 32.57±3.82% and 44.87±5.87%, respectively. Meanwhile, that of sand only fluctuated around 22.56±4.95%. Based on the soil structure triangle classified by Soil Survey Staff (1999), the results showed that the soil in Dong Thap mainly belongs to the clay loam and silty clay loam groups (Figure 2). Soil particle-size distribution will affect the organic matter content in the soil (Wang et al., 2018). This can affect the mobility and accumulation of heavy metals in the soil. Specifically, agricultural land in the study area is assessed to have a higher ability to absorb and retain nutrients and heavy metals (Wang et al., 2018).

3.2 Concentrations of heavy metals

In agricultural soils, heavy metal pollution can negatively impact soil properties, reduce the yield and quality of agricultural products, and consequently affect human and animal health (Hung and Thom, 2016). The results of heavy metal concentration in agricultural soils in Dong Thap Province are shown in Table 2. The Cu content fluctuated in the range of 18.53-44.48 mg/kg, with an average of 27.28±7.24 mg/kg. In Mekong Delta, the Cu concentration varied from 20.1-43.0 mg/kg (Nguyen et al., 2020), which is consistent with the current study. However, the Cu concentration in agricultural soils along the Tarim basin (Xinjiang, China) is generally lower than in the present study area, ranging from 16.4±3.22 to 21.97±7.6 mg/kg (Fan et al., 2019). High Cu concentration in agricultural land is attributed to weathering and trace fertilizers. In addition, the high concentration of Cu in the soil is partly due to the influence of domestic wastewater (Thu et al., 2018).

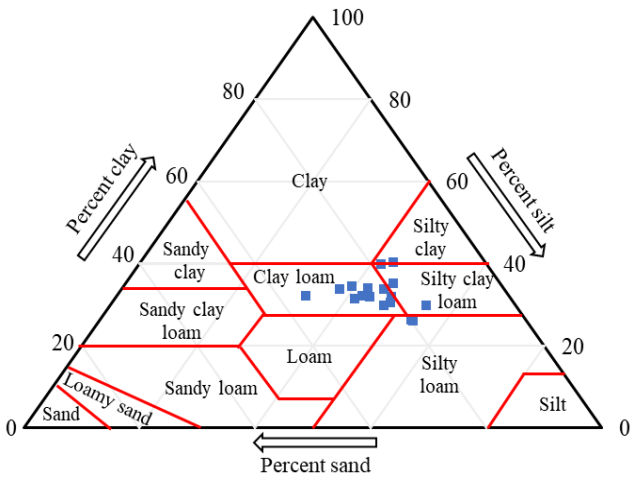

Figure 2. Triangle of soil structure in the study area

In the earth's crust, the Zn concentration is about 75 mg/kg and about 50 mg/kg in soil (Nazzal et al., 2021). The results revealed that the relatively high Zn content was found in the range of 104.30 to 195.49 mg/kg, with an average of 143.96±29.62 mg/kg. According to Marrugo-Negrete et al. (2017), the Zn content in the soil Sinu River Basin (Colombia) was found to be the highest among other heavy metals. This is consistent with the results of the present study. In the Mekong Delta, the Zn concentration was recorded at about 90 mg/kg in soil (Nguyen et al., 2020). In addition, the previous study by Ramdani et al. (2018) found that Zn in the agricultural area ranged from 52.5 to 1,952.5 mg/kg, with an average of 126.8±510.7 mg/kg. This analysis indicated that Zn concentration increased significantly in agricultural soil in Dong Thap Province. This range of Zn concentration could be affected by anthropogenic sources (Ramdani et al., 2018).

Table 2. The concentration of heavy metals in agricultural soil in the study area

Parameters	Range	Minimum	Maximum	Mean	Standard deviation	%CV	Vietnamese standard
Cu	25.95	18.53	44.48	27.28	7.24	26.54	100
Zn	91.19	104.30	195.49	143.96	29.62	20.58	200
As	3.08	1.09	4.17	2.51	0.93	37.16	15
Pb	6.39	5.98	12.37	8.56	1.82	21.27	70
Cd	0.08	0.05	0.12	0.07	0.02	30.41	1.5

The concentration of Pb varied from 5.98 to 12.37 mg/kg, reaching an average of 8.56±1.82 mg/kg. The lowest and highest concentration was both found in soil for farming vegetables. It can be seen that the concentration of Pb in the soil depends on the soil characteristics and the doses of agrochemicals used or wastes from the surrounding areas. Compared with the study of Nguyen et al. (2020) and Ha et al. (2016), the Pb concentration in agricultural soil in the Mekong Delta region (28.6±18.5 mg/kg) and Hanoi Capital (17.3-42.0 mg/kg) was higher than that in the study area. The use of herbicides, insecticides, and gasoline combustion in treating rice straws are the potential sources of Pb generation in the soil (Guan et al., 2019).

The arsenic concentrations ranged from 1.01 to 4.17 mg/kg, with an average of 2.51±0.93 mg/kg. Compared with the study of Hung and Thom (2016), the As concentration in agricultural soil fluctuated higher from 2.56 to 5.15 mg/kg, and the highest concentration was found in the paddy field. According to Nguyen et al. (2020), the As concentration was found in the range of 8.3-28.9 mg/kg in the Mekong Delta region, which was significantly higher than that of the study area. Ren et al. (2019) and Rostami et al. (2021) suggested that As concentration in agricultural soil increased after using phosphate fertilizers and pesticides over long periods of time.

The average Cd concentration in the study area was 0.07±0.02 mg/kg, ranging from 0.05 to 0.12 mg/kg. The lowest was found at position D12, and the highest was found at location D8. Former studies found that higher Cd concentrations ranging from 2.20 to 2.72 mg/kg exceeded the permissible limit (Huan et al., 2017). However, the Cd contents in the Mekong Delta varied from 0.16-0.43 mg/kg (Nguyen et al., 2020). According to Pan et al. (2016), the application of phosphate fertilizers is considered a major source of Cd in the environment. In addition, inorganic fertilizers such as nitrogen or potassium have significant Cd concentrations, which are sources of Cd in the soil (Cai et al., 2012). Other Cd sources are wastewater, sewage sludge, pesticides, fertilizers, and industrial emissions (Aboubakar et al., 2021).

It was found that the heavy metal contents in agricultural soil in Dong Thap province increased gradually in the order of Cd<As<Pb<Cu<Zn. Based on the coefficient of variation, the contents of heavy metals showed obvious spatial variability with the range of 20.58-37.16%. Spatial variability of heavy metals was explained by different types of agriculture having different effects on the concentration of heavy metals in the soil (Ren et al., 2019). The enrichment of heavy metals in agricultural soil is related to the supply of inputs for agricultural production, such as fertilizers and pesticides (Aboubakar et al., 2021). Compared with the national standard in QCVN 03-MT:2015/BTNMT-agricultural soil (MoNRE, 2015), the concentration of heavy metals is still within limits.

3.3 Correlation between soil parameters in the study area

The results of the Pearson correlation analysis between heavy metals in soil are presented in Table 3. There was a positive correlation between As, Pb, Cu, and Zn ($p<0.01$). Meanwhile, Cd was only found to be positively correlated with Pb ($r=0.55$) and Cu ($r=0.45$) in soil. The strong correlation between heavy metals showed that these elements are derived from the same source, which is human activities (Marrugo-Negrete et al., 2017; Wu et al., 2022). In addition, the high content of As, Pb, Cu, and Zn also indicated that pollution level is affected not only by the intrinsic properties of the soil but also by long-term agricultural activities (Zhu et al., 2017; Wu et al., 2022). In addition, the analysis also showed a high correlation of soil particles, including sand, clay and silt. However, the results only recorded a significant correlation between the percentage of sandy soil and Cu, which had a negative correlation ($r=-0.48$).

Table 3. Correlation between heavy metals and soil structure in agricultural soil

Parameter	As	Pb	Cu	Zn	Cd	Sand	Silt
Pb	0.56**						
Cu	0.49**	0.73**					
Zn	0.63**	0.6**	0.41**				
Cd	0.34	0.55**	0.45**	0.23			
Sand	-0.39	-0.33	-0.48**	-0.28	-0.26		
Silt	0.34	0.13	0.22	0.09	0.08	-0.68**	
Clay	-0.06	0.15	0.2	0.17	0.17	-0.112	-0.66**
Range	-1			0			1

**Correlation is significant at the level of 0.01; *Correlation is significant at the level of 0.05.

3.4 The main factors affecting the soil quality in the study area

PCA analysis was used to extract principal components (PCs) that can detect and identify sources of heavy metal contamination. In this analysis, only the components with eigenvalues greater than 1 are retained (Nazzal et al., 2021). The analysis results showed that there were three main components extracted, explaining 82.14% of the variations of heavy metals in the study area (Table 4).

Table 4. Principal component analysis results

Variable	PC1	PC2	PC3	PC4	PC5	PC6	PC7
As	0.40	-0.12	-0.42	0.13	0.05	-0.75	-0.25
Pb	0.45	0.16	-0.14	-0.07	-0.26	0.49	-0.66
Cu	0.43	0.08	0.17	-0.31	-0.67	-0.13	0.48
Zn	0.38	0.08	-0.52	-0.19	0.47	0.33	0.46
Cd	0.32	0.28	0.23	0.85	0.04	0.08	0.20
Sand	-0.37	0.28	-0.53	0.18	-0.37	0.04	0.08
Silt	0.23	-0.64	0.22	0.05	0.09	0.11	0.01
Clay	0.11	0.62	0.35	-0.31	0.34	-0.22	-0.12
Eigenvalues	3.74	1.82	1.02	0.57	0.41	0.30	0.14
%Variation	46.70	22.75	12.69	7.12	5.17	3.76	1.81
Cum.%Variation	46.70	69.44	82.14	89.26	94.43	98.19	100.00

The first principal component (PC1) explained 46.70% of the total variance of heavy metals. PC1 had positive loadings for As (0.40), Pb (0.45), Cu (0.43), Zn (0.38), Cd (0.32), and was the most important component. PC1 could explain the anthropogenic origin of heavy metals, specifically related to long-term agricultural activities in the study area. Several previous studies have noted that P-containing fertilizers used in vegetable cultivation also contain Pb, Cd and others (Yang et al., 2014; Wu et al., 2022). In addition, the contribution of heavy metals in this PC can originate from the formation of soil structure in the

study area, namely Cd. The second principal component (PC2) accounted for 22.75% of total variance, which was contributed by the ratio of clay (0.62) and silt (-0.64). This component describes the effects of soil structure in the study areas. PC3 explained 12.69% of the variation correlated with As (-0.42) and Zn (-0.52). Although the presence of As and Zn may be the results of anthropogenic activities, this probably comes from different sources with previous PCs. The eigenvalues of PC4 were less than 1, accounting for 7.10% of the variation. However, PC4 was very strongly correlated with Cd (-0.85). In general, the heavy metals have contributed to soil quality variability in the study area. Excessive use of pesticides and inorganic fertilizers in farming can lead to the formation of heavy metals such as Cu, Zn, Pb, Cd, and As in the soil (Huang et al., 2010; Yang et al., 2014).

3.5 Clustering soil quality based on heavy metal concentrations

Four groups of sampling locations were obtained from CA method and the characteristics of each group are presented in Figure 3 and Table 5. Group I consisted of four sites D01, D05, D11, and D15, with relative similar soil quality (accounted for 25.53% of the total locations), which were located in the rice-growing areas. The average concentrations of As, Pb and Cu were 2.74, 8.35, and 24.13 mg/kg, respectively. The concentrations of Zn and Cd in this group were 154.25 and 0.08 mg/kg, respectively. Group III had 3 sampling sites (D02, D06, and D07), accounting for 17.65% of the total locations. These sites were also identified in the rice cultivation area. However, the proportion of clay and silt particles was higher than in Group I. Meanwhile, Group II gathered seven locations with similar soil quality, namely D03, D04, D12, D13, D14, D16, and D17, accounting for 41.18%. The locations in Group II have been identified as perennial crops, vegetables and ornamental plants. Group II had the lowest concentration of heavy metals in the soil. Finally, Group IV included D08, D09, and D10, accounting for 17.65%. The heavy metal content in group IV was the highest among the four soil groups.

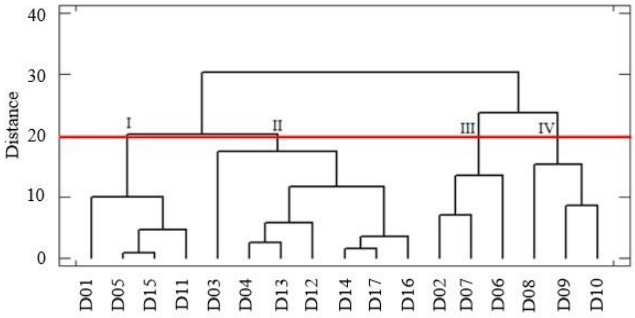

Figure 3. Clustering soil quality in the study area

Table 5. Heavy metals concentrations in the identified groups

Cluster	As (mg/kg)	Pb (mg/kg)	Cu (mg/kg)	Zn (mg/kg)	Cd (mg/kg)	Sand (%)	Silt (%)	Clay (%)
I	2.74	8.35	24.13	154.25	0.08	23.86	43.00	33.16
II	1.67	7.22	22.22	121.47	0.05	25.43	42.48	32.10
III	3.56	9.63	31.44	157.98	0.07	18.38	54.20	27.44
IV	3.12	10.89	39.13	168.70	0.09	18.37	43.63	38.01

3.6 Assessment of pollution levels and ecological risks in the study area

The PI_N is an index used to assess the aggregate influence of heavy metals on the quality of the soil environment (Cui et al., 2021). The results showed that the PI_N fluctuated in the range of 0.82-2.92. This assessed heavy metals from a warning level to moderate pollution (Figure 4). Only D14 and D17 were recorded at a warning level, accounting for 11.76% of total samples. Eight soil samples (D03, D04, D05, D11, D12, D13, D15, and D16) were slightly contaminated, which accounted for 47.06%. These sites are found mainly in the southern part of Dong Thap Province, with the dominance of perennial crops. Meanwhile, seven sampling sites (D01, D02, D06, D07, D08, D09, and D10) for cultivating rice and vegetable crops were evaluated at moderate pollution levels, accounting for 41.18% of the total sampling sites. In addition, Figure 4 also shows that the average heavy metal pollution was distributed mainly in the north of Dong Thap Province. The findings were consistent with the cluster analysis by groups III and IV, which show the highest soil heavy metal content. It can be seen that agricultural cultivation activities have greatly affected the soil quality in the area. Therefore, it is necessary to take appropriate measures to improve and implement sustainable production in agriculture.

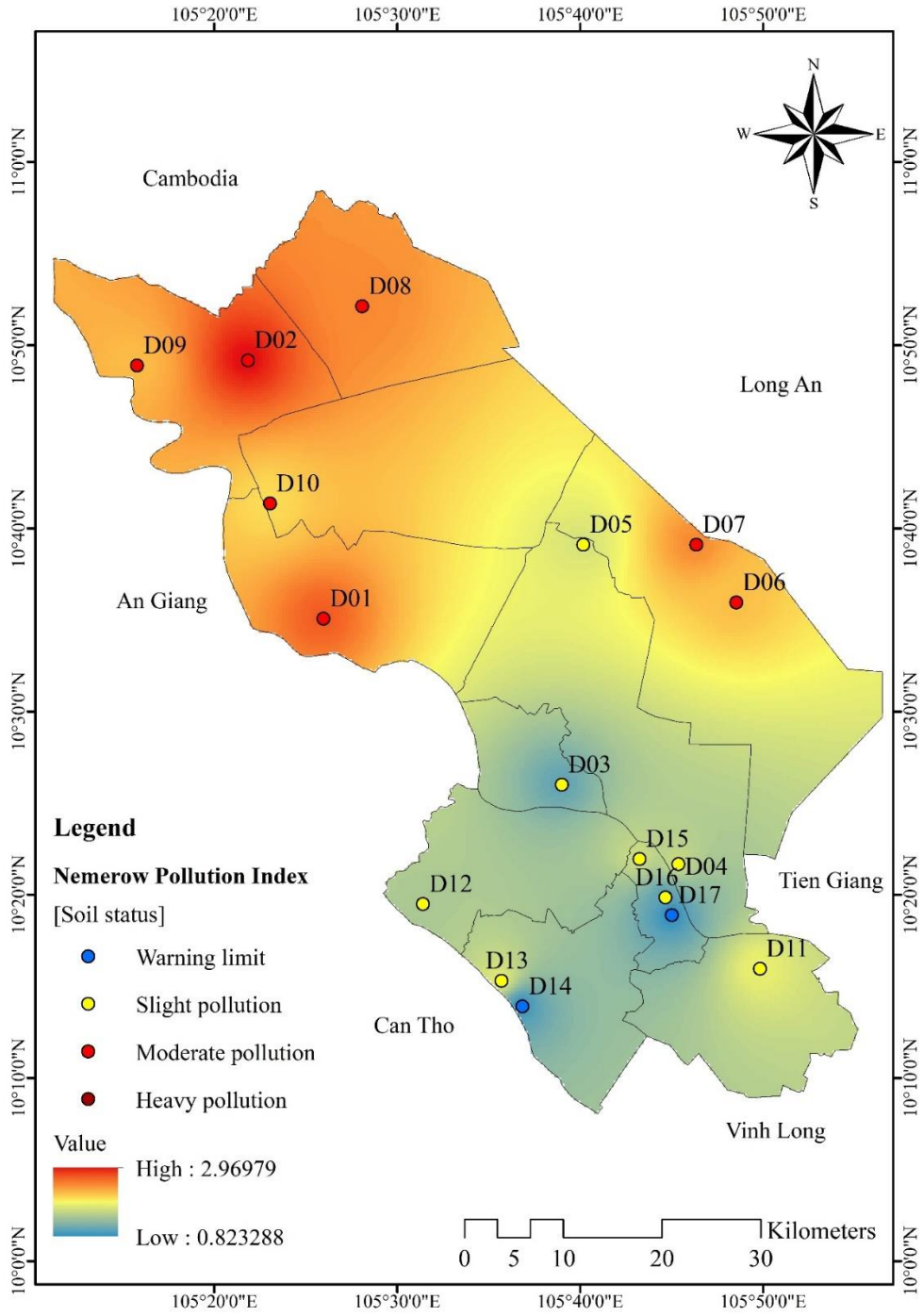

Figure 4. Values of PI_N at the study area

The I_{geo} values of Cu, Pb, and Cd were lower than 0; that is, there was no pollution of these heavy metals in soil. The contamination extent of As fluctuated from moderate to high, with the I_{geo} ranges of 0.12-2.05. The I_{geo} values of Zn were slightly lower than those of As, ranging from -0.01 to 0.90. The level of Zn pollution in soil was moderate. Specifically, the average values of I_{geo} index increased gradually from Cd(-3.20)<Pb(-2.27)<Cu(-1.14)<Zn(0.43)<As(1.21). The I_{geo} values of As and Zn in soil are presented in Figure 5(a) and Figure 5(b), respectively. The analysis results found that As and Zn accumulation was highest at D02 and D01 in rice-growing areas. According to Cai et al. (2012), As accumulated in agricultural soils is mainly derived from human activities, such as the inappropriate use of pesticides and fertilizers containing calcium and sodium arsenate. In superphosphate and granular fertilizers, Zn concentrations were approximately two and seven times higher, respectively, than the maximum

tolerable concentrations (Rostami et al., 2021). The trend of heavy metals accumulation was higher in the northern part of Dong Thap Province. This is explained by the soil structure is mainly clay and silt particles, which are more likely to accumulate heavy metals than sandy soils.

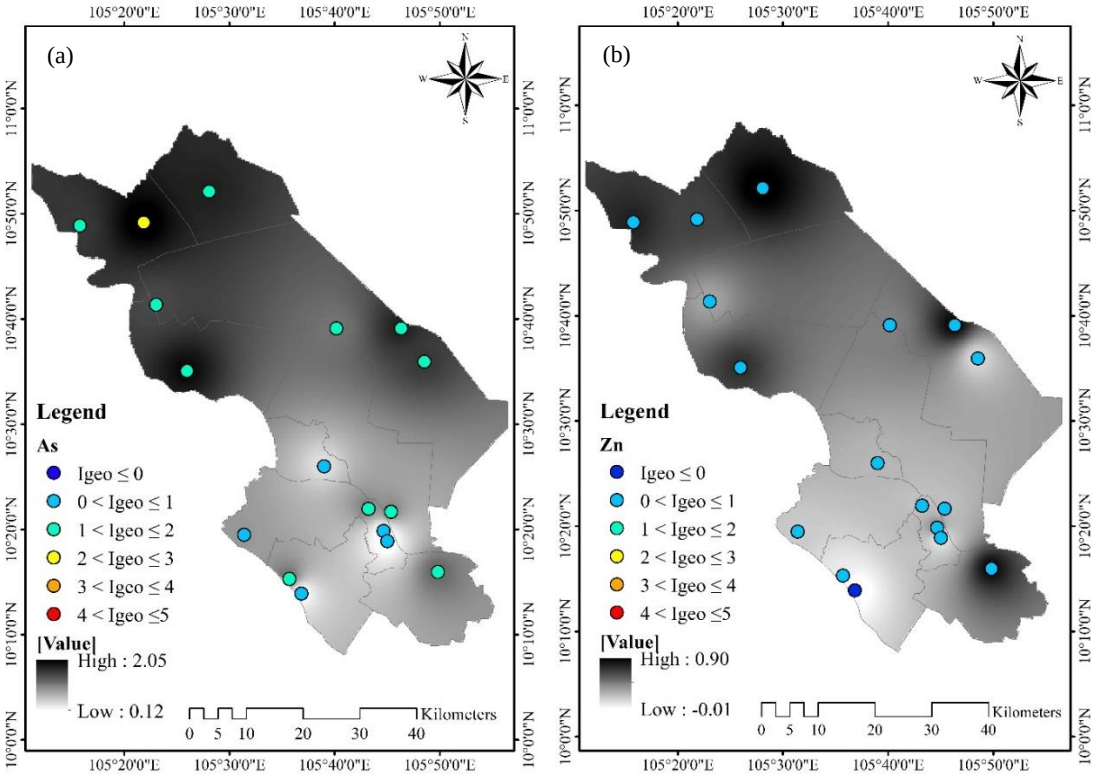

Figure 5. The values of I_{geo} of As (a) and Zn (b) in soil

The values of PLI ranged from 0.53 to 1.11 (Figure 6). Heavy metals in agricultural soils in the study area were at a non-polluted (94.1%) to moderately polluted level (5.9%). In addition, the values of RI ranged from 26.73 to 74.80. This has shown the potential ecological risk of heavy metals ranging from low (47.06%) to moderate (52.94%). It can be deduced that agricultural farming negatively impacts heavy metal contamination and risk to ecosystems. Excessive use of phosphate fertilizers increases the amount of phosphorus in the soil and leads to the accumulation of heavy metals in agricultural soils and pesticides (Marrugo-Negrete et al., 2017; Rostami et al., 2021). This information is useful for environmental managers in the agricultural sector to reconsider the cropping patterns and agricultural practices for sustainable development.

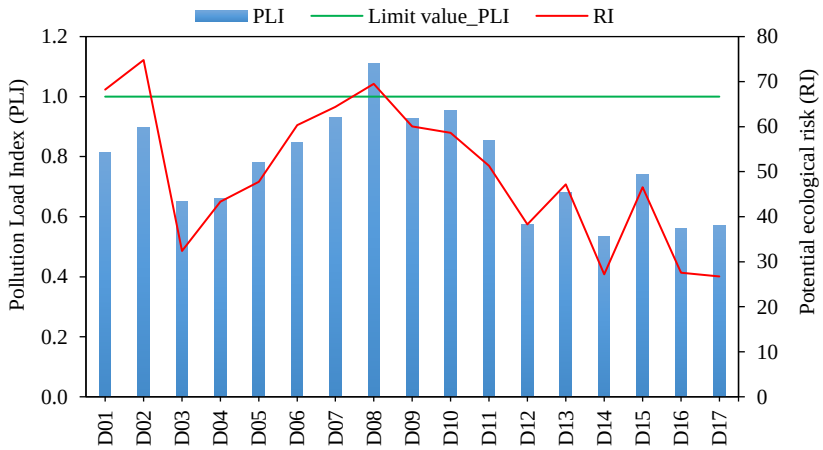

Figure 6. The values of PLI and RI in the study area

4. CONCLUSION

This study evaluated heavy metal contamination in various cultivated lands (rice, vegetables, perennials, ornamental plants) and potential ecological risks using multivariate statistics and pollution indices in Dong Thap Province, Vietnam. The soil structure in the study area was characterized by clay loam and silty clay loam groups. The results showed that the contents of heavy metals in agricultural soil were within the Vietnamese standard. Heavy metals (As, Pb, Cu, Zn, Cd) were strongly positively correlated. The results of PCA identified that agricultural practices contributed to the heavy metal pollution in the study area, especially in rice and vegetable-cultivated areas. Four different groups of sampling locations were obtained from CA, representing the effects of different agricultural practices on the presence of heavy metals. The PI_N index showed that the soil pollution by heavy metals was at the warning limit to moderate levels. As had the highest contribution to soil pollution in the study area. The PLI index reflected heavy metals in the soil ranging from non-polluted to moderately polluted. The ecological risk of heavy metal pollution was low to moderate. It should be noted that the impacts of heavy metals are cumulated, and the occurrence of several metals at the same time could accelerate the negative repercussions. Therefore, it is suggested to continue monitoring the concentration of heavy metals in soils for timely solutions to prevent the effects on ecology and human health.

ACKNOWLEDGEMENTS

The authors would like to thank the Department of Natural Resources and Environment of Dong Thap Province for providing the monitoring data. In this study, all analyses and assessment are based on the authors' scientific perspectives without the intervention of the views of the data provider.

REFERENCES

Aboubakar A, Douaik A, Mewouo YCM, Madong RCBA, Dahchour A, El Hajjaji S. Determination of background values and assessment of pollution and ecological risk of heavy metals in urban agricultural soils of Yaoundé, Cameroon. Journal of Soils and Sediments 2021;21:1437-54.

Apostol M, Hlihor RM, Daraban GM, Zaleschi LH, Simion IM. Heavy metal pollution in the environment and their effects to ornamental plants. Proceedings of the 2021 International Conference on e-Health and Bioengineering (EHB); 2021 Nov 18-19; Manhattan, New York: United States; 2021.

Cai L, Xu Z, Ren M, Guo Q, Hu X, Hu G, et al. Source identification of eight hazardous heavy metals in agricultural soils of Huizhou, Guangdong Province, China. Ecotoxicology and Environmental Safety 2012;78:2-8.

Cai LM, Jiang HH, Luo J. Metals in soils from a typical rapidly developing county, Southern China: levels, distribution, and source apportionment. Environmental Science and Pollution Research 2019;26:19282-93.

Cravotta CA, Brady KBC. Priority pollutants and associated constituents in untreated and treated discharges from coal mining or processing facilities in Pennsylvania, USA. Applied Geochemistry 2015;62:108-30.

Cui X, Geng Y, Sun R, Xie M, Feng X, Li X, et al. Distribution, speciation and ecological risk assessment of heavy metals in Jinan Iron and Steel Group soils from China. Journal of Cleaner Production 2021;295:Article No. 126504.

Department of Natural Resources and Environment of Dong Thap province (DoNRE). Report on Environmental Status of Dong Thap Province in 5 Years, Period 2016-2020. Dong Thap, Vietnam: DoNRE; 2021. (in Vietnamese).

Duffus JH. "Heavy metals" a meaningless term? (IUPAC Technical Report). Pure and Applied Chemistry 2002;74:793-807.

Fan W, Zhou J, Zhou Y, Wang S, Du J, Chen Y, et al. Heavy metal pollution and health risk assessment of agricultural land in the Southern Margin of Tarim Basin in Xinjiang, China. International Journal of Environmental Health Research 2019;31:835-47.

Fei X, Lou Z, Xiao R, Ren Z, Lv X. Source analysis and source-oriented risk assessment of heavy metal pollution in agricultural soils of different cultivated land qualities. Journal of Cleaner Production 2022;341:Article No. 130942.

Fergusson JE. The Heavy Elements: Chemistry, Environmental Impact and Health Effects. Oxford, UK: Pergamon Press, 1990.

Ferreira SL, da Silva Junior JB, dos Santos IF, de Oliveira OM, Cerda V, Queiroz AF. Use of pollution indices and ecological risk in the assessment of contamination from chemical elements in soils and sediments-Practical aspects. Trends in Environmental Analytical Chemistry 2022;35:e00169.

General Statistics Office of Vietnam. Land use by province (As of 31 December 2018) by Cities, provinces and land use [Internet]. 2019 [cited 2022 May 10]. Available from: https://www.gso.gov.vn/px-web-2/?pxid=V0103&theme=%C4%90%C6%A1n%20v%E1%BB%8B%20h%C3%A0nh%20ch%C3%ADnh%2C%20%C4%91%E1%BA%A5t%20%C4%91ai%20v%C3%A0%20kh%C3%AD%20h%E1%BA%ADu. (in Vietnamese).

Guan Q, Zhao R, Pan N, Wang F, Yang Y, Luo H. Source apportionment of heavy metals in farmland soil of Wuwei, China: Comparison of three receptor models. Journal of Cleaner Production 2019;237:Article No. 117792.

Ha NN, Phuong NP, Anh NM. Assessment of current soil quality and the accumulation of heavy metals and nitrate in cultivated vegetables in Yen Nghia, Ha Dong, Hanoi. VNU Journal of Science: Earth and Environmental Sciences 2016;32:118-24. (in Vietnamese).

Hakanson L. An ecological risk index for aquatic pollution control: A sedimentological approach. Water Research 1980;14:975-1001.

Huan NH, Hai NX, Viet NQ, Anh NTP. Assessment of pollution index of Cu, Cd, and Pb in soil environment in the intensive cultivation areas of vegetables, flower in Tay Tuu ward, Bac Tu Liem District, Hanoi. VNU Journal of Science: Earth and Environmental Sciences 2017;33:179-84.

Huang Y, Lan Y, Thomson SJ, Fang A, Hoffmann WC, Lacey RE. Development of soft computing and applications in agricultural and biological engineering. Computers and Electronics in Agriculture 2010;71:107-27.

Hung PQ, Thom TTH. Assessment of soil properties and contamination soil in Nhue River Basin in Duy Tien District, Ha Nam Province. Vietnam Journal of Agricultural Sciences 2016;14:1741-52. (in Vietnamese).

Huynh NTH, Le DMT, Giao NT. Ecological risk assessment for occurrence of toxic elements in various land use types in Vietnamese Mekong Delta Province. Journal of Ecological Engineering 2022;23:121-30.

Jiang HH, Cai LM, Wen HH, Hu GC, Chen LG, Luo J. An integrated approach to quantifying ecological and human health risks from different sources of soil heavy metals. Science of the Total Environment 2020;701:Article No. 134466.

Kabata-Pendias A. Trace Elements in Soils and Plants. Florida, USA: CRC Press; 2010.

Kang Z, Wang S, Qin J, Wu R, Li H. Pollution characteristics and ecological risk assessment of heavy metals in paddy fields of Fujian Province, China. Scientific Reports 2020;10:1-10.

Klinsawathom T, Songsakunrungrueng B, Pattanamahakul P. Heavy metal concentration and risk assessment of soil and rice in and around an open dumpsite in Thailand. EnvironmentAsia 2017;10:53-64.

Kowalska JB, Mazurek R, Gąsiorek M, Zaleski T. Pollution indices as useful tools for the comprehensive evaluation of the degree of soil contamination: A review. Environmental Geochemistry and Health 2018;40:2395-420.

Li Y, Ye F, Wang A, Wang D, Yang B, Zheng Q, et al. Chronic arsenic poisoning probably caused by arsenic-based pesticides: findings from an investigation study of a household. International Journal of Environmental Research and Public Health 2016;13:Article No. 133.

Liu L, Wu Q, Miao X, Fan T, Meng Z, Chen X, et al. Study on toxicity effects of environmental pollutants based on metabolomics: A review. Chemosphere 2022;286:Article No. 131815.

Lou X, Wu C, Lin Y, Li W, Deng M, Tan J, et al. Soil heavy metal pollution from Pb/Zn smelting regions in China and the remediation potential of biomineralization. Journal of Environmental Sciences 2022;125:662-77.

Mamut A, Eziz M, Mohammad A. Pollution and ecological risk assessment of heavy metals in farmland soils in Yanqi County, Xinjiang, Northwest China. Eurasian Soil Science 2018;51: 985-93.

Marrugo-Negrete J, Pinedo-Hernández J, Díez S. Assessment of heavy metal pollution, spatial distribution and origin in agricultural soils along the Sinú River Basin, Colombia. Environmental Research 2017;54:380-8.

Ministry of Natural Resources and Environment (MoNRE). National Technical Regulation on the Allowable Limits of Heavy Metals in the Soils: QCVN 03-MT:2015/BTNMT. Hanoi, Vietnam: MoNRE; 2015. (in Vietnamese).

Ministry of Science and Technology of Vietnam (MOST). Soil Quality - Determination of Cadmium, Chromium, Cobalt, Copper, Lead, Manganese, Nickel and Zinc in Aqua Region Extracts of Soil - Flame and Electrothermal Atomic Absorption Spectrometric Methods (TCVN 6496:2009). Hanoi, Vietnam: Ministry of Science and Technology of Vietnam; 2009. (in Vietnamese).

Ministry of Science and Technology of Vietnam (MOST). Soil Quality - Sampling - General Requirements (TCVN 5297:1995). Hanoi, Vietnam: Ministry of Science and Technology of Vietnam; 1995. (in Vietnamese).

Ministry of Science and Technology of Vietnam (MOST). Soil Quality - Sampling - Part 2: Guidance on Sampling Techniques (TCVN 7538-2:2005). Hanoi, Vietnam: Ministry of Science and Technology of Vietnam; 2005. (in Vietnamese).

Nazzal Y, Bărbulescu A, Howari F, Al-Taani AA, Iqbal J, Xavier CM, et al. Assessment of metals concentrations in soils of Abu Dhabi emirate using pollution indices and multivariate statistics. Toxics 2021;9:Article No. 95.

Nguyen TP, Ruppert H, Pasold T, Sauer B. Paddy soil geochemistry, uptake of trace elements by rice grains (*Oryza sativa*) and resulting health risks in the Mekong River Delta, Vietnam. Environmental Geochemistry and Health 2020;42: 2377-97.

Pan L, Ma J, Hu Y, Su B, Fang G, Wang Y, et al. Assessments of levels, potential ecological risk, and human health risk of heavy metals in the soils from a typical county in Shanxi Province, China. Environmental Science and Pollution Research 2016;23:19330-40.

Qishlaqi A, Moore F. Statistical analysis of accumulation and sources of heavy metals occurrence in agricultural soils of Khoshk River Banks, Shiraz, Iran. American-Eurasian Journal of Agriculture and Environmental Science 2007;2:565-73.

Ramdani S, Amar A, Belhsaien K, El Hajjaji S, Ghalem S, Zouahri A, et al. Assessment of heavy metal pollution and ecological risk of roadside soils in Tlemcen (Algeria) using flame-atomic absorption spectrometry. Analytical Letters 2018;51:2468-87.

Rashed ARA. The environmental impacts of kabd landfill on the soil and groundwater in Kuwait: A case study. International Journal of Geosciences 2018;9:255-71.

Ren Z, Xiao R, Zhang Z, Lv X, Fei X. Risk assessment and source identification of heavy metals in agricultural soil: A case study in the coastal city of Zhejiang Province, China. Stochastic Environmental Research and Risk Assessment 2019;33:2109-18.

Rostami S, Kamani H, Shahsavani S, Hoseini M. Environmental monitoring and ecological risk assessment of heavy metals in farmland soils. Human and Ecological Risk Assessment 2021;27:392-404.

Soil Survey Staff. Soil Taxonomy: A Basic System for Soil Classification for Making and Interpreting Soil Surveys. 2nd ed. Washington DC, USA: USDA Handbook; 1999.

Tchounwou PB, Yedjou CG, Patlolla AK, Sutton DJ. Heavy metal toxicity and the environment. In: Luch A, editor. Molecular, Clinical and Environmental Toxicology. Switzerland: Springer; 2012. p. 133-64.

Thu TTM, Tuan TA, Tien TM. Investigation of heavy metal contamination in agricultural soils in Bac Ninh Province. Journal off Vietnam Agricultural Science and Technology 2018;8:102-7. (in Vietnamese).

Wang Y, Chen F, Zhang M, Chen S, Tan X, Liu M, et al. The effects of the reverse seasonal flooding on soil texture within the hydro-fluctuation belt in the Three Gorges reservoir, China. Journal Soils Sediments 2018;18:109-15.

Wei B, Yang L. A review of heavy metal contaminations in urban soils, urban road dusts and agricultural soils from China. Microchemical Journal 2010;94:99-107.

Wu Y, Li X, Yu L, Wang T, Wang T, Liu T. Review of soil heavy metal pollution in China: Spatial distribution, primary sources,

and remediation alternatives. Resources, Conservation and Recycling 2022;181:Article No. 106261.

Yang P, Yang M, Mao R, Shao H. Multivariate-statistical assessment of heavy metals for agricultural soils in northern China. The Scientific World Journal 2014;2014:1-7.

Zhang J, Wang Y, Liu J, Liu Q, Zhou Q. Multivariate and geostatistical analyses of the sources and spatial distribution of heavy metals in agricultural soil in Gongzhuling, Northeast China. Journal of Soils and Sediments 2016;16:634-44.

Zhu G, Guo Q, Xiao H, Chen T, Yang J. Multivariate statistical and lead isotopic analyses approach to identify heavy metal sources in topsoil from the industrial zone of Beijing Capital Iron and Steel Factory. Environmental Science and Pollution Research 2017;24:14877-88.

Exploration of Potential Indigenous Non-phytopathogenic Fungi for Bio-organic Fertilizer Recycling from Organic Waste

Abul Hossain Molla[1*], Hasnat Zahan[1], M. M. H. Oliver[2], and M. Khaled Mosharaf[1]

[1]*Department of Environmental Science, Bangabandhu Sheikh Mujibur Rahman Agricultural University, Gazipur-1706, Bangladesh*
[2]*Department of Agricultural Engineering, Bangabandhu Sheikh Mujibur Rahman Agricultural University, Gazipur-1706, Bangladesh*

ARTICLE INFO

Received: 12 May 2022
Received in revised: 8 Jul 2021
Accepted: 25 Jul 2022
Published online: 18 Aug 2022
DOI: 10.32526/ennrj/20/202200110

Keywords:
Fungi/ Mixed culture/ Organic wastes/ *Penicillium*/ Seed germination/ *Trichoderma*

*** Corresponding author:**
E-mail: ahmolla@bsmrau.edu.bd

ABSTRACT

Using potential microbes in biodegradable solid waste management is an emerging science. Microbes play a significant role in recycling of organic solid wastes. Therefore, the present project was carried out to isolate indigenous potential non-phytopathogenic fungi from local relevant decomposed substrates for the purpose of organic waste recycling as bio-organic fertilizer (BOF). A total of thirteen fungal strains were isolated. Seven of them were identified as *Trichoderma* spp., and the rest were *Penicillium* spp. Germination of mung bean (*Vigna radiata*), mustard (*Brassica campestris*), and wheat (*Triticum aestivum*) seeds were assessed by application of 13 fungal isolate suspensions. Significant increase of germination percent was achieved in mung bean (98.35%), mustard (96.65%), and wheat (93.35%) by fungal treatments RW-T02, PL-P01, and CD-T01/MSW-T05, respectively, compared to the controls. But radicle and plumule lengths were not promoted by fungal treatments in the majority of cases. Significantly, the longest radicle and plumule lengths of mung bean and mustard were found in control treatments. Conversely, in wheat the longest radicle and plumule length were achieved in treatments MSW-T05 and RW-T03, respectively. Based on superior performances of percent germination and radicle/plumule length, six fungal isolates were selected for compatibility performance in mixed cultures. In the compatibility tests, two fungal combinations (ABF and BCE) presented superior mutual intermingle appearances. Perhaps these combinations may play significant roles in biodegradation of organic wastes.

1. INTRODUCTION

Waste is not waste, but may be treated as a resource, if it is managed properly. Proper management of waste offers value added product and its recycling conserves congenial environment. One of the most acceptable and viable options of organic waste management is composting, which offers good quality product recognized as bio-organic fertilizer (Kauser and Khwairakpam, 2022). Bio-organic fertilizer (BOF) is not simply bio-fertilizer but it is rich in both beneficial microbes and organic substances. Well decomposed, fully biomatured and sanitized compost with potential microbes are known as bio-organic fertilizer, which is beneficial for soil health improvement and to ensure agricultural yield with high nutritional values (Heerden et al., 2002; Barua et al., 2018; Castiglione et al., 2021). Microbes enriched BOF is not only rich in decomposed organic substances but also beneficial microbes which enhance yield and nutritional qualities of the crop, and obviously it is superior to simply organic fertilizer (Molla et al., 2012).

Bangladesh is an agro-based and densely populated country. Therefore, a significant volume of waste is generated every day. In Dhaka City, approximately 4,000-4,500 tons of solid waste is generated per day (Bari et al., 2007), where the majority is biodegradable for composting. Proper environmentally friendly and economically viable disposal of such waste is a great concern to the relevant authority. Generation of potential technology for production of quality BOF may reduce the load of excessive usages of chemicals fertilizers for agronomic practices, as well as opening an avenue of sustainable environmentally friendly recycling of bio-decomposable wastes.

The potential microbes play vital roles in composting/bioconversion of organic wastes treated

Citation: Molla AH, Zahan H, Oliver MMH, Mosharaf MK. Exploration of potential indigenous non-phytopathogenic fungi for bio-organic fertilizer recycling from organic waste. Environ. Nat. Resour. J. 2022;20(6):598-610. (https://doi.org/10.32526/ennrj/20/202200110)

by a reliable process of waste management to reduce the aforesaid problems (Molla et al., 2006; Cerda et al., 2018). Additionally, the roles of microbes in biodegradation are considered as an important factor (Jung and Kim, 2016; Srivastava et al., 2020). Proper attention on using biological agents for composting is important, otherwise the obtained end product of composting (i.e., BOF) may cause severe damage to the applied crop. This implies that the use of microbes for composting (biodegradation) should be non-phytopathogenic. In biodegradation processes of organic wastes, the microbes used have greater degradation ability if they originated from a similar environment (Meda et al., 2021).

Moreover, the food toxicities/adulteration is a common phenomenon due to excessive usage of agrochemicals for agronomic practices. Continuous consumption of adulterated foods may invite several fatal diseases to human as well as other living beings. Possible alternatives to ensure the supply of bio-based plant growth enhancers (i.e., value added BOF) may help to produce safe food (crops) production by reducing usages of chemical fertilizers. Accordingly, the current interest of using bio-organic fertilizers and phyto-stimulators is inspiring the enhancement of crop yield and protection against crop damages as green technologies (Adesemoye et al., 2008; Castiglione et al., 2021). Moreover, degradation of organic substrates was enhanced more by application of a microbial consortia than a monoculture (Li et al., 2021). The most important determinant in the biodegradation process is a compatible consortium of microbes, which ensure quality compost for crop growth and development (Gutierrez-Correa and Tengerdy, 1997; Molla et al., 2004; Devi and Anu-Appaiah, 2021).

Therefore, the present study was undertaken to find potential, but non-phytopathogenic fungal isolates and compatible consortia which will be efficient for future use in degradation of organic wastes into bio-organic fertilizer as well as reduce the load of inorganic fertilizer usage, promote safe food production and conserve congenial friendly environment.

2. METHODOLOGY

2.1 Collection of relevant wastes for isolation of native filamentous fungal isolates

Six types of decomposed organic wastes materials were collected from local sources for filamentous fungal strains isolation. These were (1) Decomposed cow dung (CD), (2) Rotten rice straw (RW), (3) Decomposed poultry litter (PL), (4) Rotten wood (RW), (5) Decomposed municipal solid waste (MSW), and (6) Decomposed leaf litter (LL).

2.2 Isolation of fungal isolates as pure culture

The Rose Bengal Agar (RBA) media and technique was used for isolation of indigenous fungal strains (Martin, 1950). All reagents of RBA were dissolved in distilled water by subsequent stirring and gentle heating before being autoclaved (121ºC for 15 min). Exactly 2 mL of sterile (filtered) streptomycin (50 mg/mL) was added aseptically to molten RBA and mixed homogeneously. One milliliter of the 1,000-fold diluted sample (substrate used for isolation of fungi) was poured into a petri dish followed by approximately 15 mL of molten RBA and allowed to solidify. The plates were incubated at room temperature (28±2ºC) for 2 weeks and observed every day. The colonies (i.e., colony forming unit) were transferred onto 3.9% potato dextrose agar (PDA, Oxoid) plate for subculture to obtain the pure strains.

2.3 Identification of isolated fungal strains

Visual observation of petri dish cultures and macro and micro-morphological features of the reproductive organs of well grown fungal isolates/strains in slide culture (Molla et al., 2002a) were adopted for identification of fungal species by viewing in microscope and image processing unit. For visual observation the isolates were grown in 3.9% PDA (Oxoid) for 10 days and for studying reproductive organs in slide culture, the slides were kept 2-4 days at room temperature based on description of Molla (2002). The mode of mycelial growth, color, odor, and changes of medium color of each isolate were examined daily. The relevant code number was assigned to the tentatively identified fungal isolates based on source of origin and genus.

2.4 Preparation of fungal spore suspensions for screening against crop seed germination

A total of 13 fungal isolates/strains were selected based on fast and vigorous growth appearance in PDA plates. The fungal isolate was subcultured on potato dextrose agar (PDA, 3.9% Merck) plate for seven days at ambient temperature (28±2ºC). For preparing spore suspension/culture filtrate, each plate of fungal culture was washed with 10 mL of sterilized 0.01% Tween 20 solution, diluted twenty-fold with sterile water and filtered by 12.5 cm Whatman#1 filter

paper. The stocks of spore suspensions were preserved at 4ºC until used for subsequent activities.

2.5 Seed sterilization and germination of seeds against fungal spore suspensions

The germination of three crop seeds [Mung bean (*Vigna radiata*), Mustard (*Brassica campestris*), and Wheat (*Triticum aestivum*)] were examined by applying fungal spore suspensions. Uniform disease free crop seeds were surface sterilized by washing one minute in 95% ethanol followed by 2-3 min in 2% sodium hypochloride and finally washing six times with sterile distilled water (Molla et al., 2001a). Twenty-five seeds were soaked on filter paper with fungal spore suspensions in glass petri dishes. However, the filter of each petri dish was soaked with 5 mL of fungal suspension based on treatment before placing seeds on the petri dishes. Each fungal isolate was considered as a treatment and replicated five times. Sterile water soaked filter paper was used as a control treatment. Seeds were allowed to germinate in aseptic environment to attain a constant number of germinated seeds in a seed germinator in the Seed Technology Laboratory of BSMRAU (Bangabandhu Sheikh Mujibur Rahman Agricultural University). Concurrently, germination performance was recorded. Approximately more than 2 mm of radicle emerging from a seed coat was considered as a germinated seed. Germination percent, germination index, radicle length and plumule length were recorded and percent infected/spotted seedlings were considered for evaluation of induced phytopathogenic study of seedlings by fungi in seeds germination. Germination index was calculated based on the procedure of Islam et al. (2018).

2.6 Compatibility of fungal mixed culture

The six fungal isolates/strains were designated as A=CD-T01 (*Trichoderma* sp.), B=MSW-T04 (*Trichoderma* sp.), C=RW-T02 (*Trichoderma* sp.), D=RS-P01 (*Penicillium* sp.), E=MSW-T05 (*Trichoderma* sp.), and F=PL-P01 (*Penicillium* sp.) and selected from 13 fungal isolates/strains based on crop seeds germination.

A total of 12 combinations designated as ABC, ABF, ACE, ACF, ADE, ADF, BCE, BCF, BDE, BDF, CDE, and CDF using six isolates/strains (A, B, C, D, E, and F) were evaluated for compatibility performance. Each combination was replicated five times. Equal sizes of three different fungal blocks were placed in a freshly prepared PDA plate and allowed to grow in an incubator at 28ºC for 5-7 days. The study was exercised by adopting the technique described by Molla et al. (2001b).

The inoculated fungal plates were monitored daily after the second day of inoculation. Fungal isolates combinations with proper intermingled growth were selected for subsequent research activities.

2.7 Experimental design and statistical analysis

The experiments were done in glass petri dishes in an aseptic environment in factorial completely randomized design with five replications. Simple statistical tools along with R-software (version 4.1.3) were used for analysis of variance and mean comparison (LSD). Finally, the processed data were presented in tables and figures.

3. RESULTS AND DISCUSSION

3.1 Isolation and identification of filamentous fungal isolates/strains

Several numbers of filamentous fungal strains were isolated from six decomposed sources of organic substrates rich in cellulose and hemicellulose (Figure 1), but, finally, 13 pure cultures of filamentous fungal strains were recorded (Table 1). Others isolates were discarded based on their almost similar appearance at plate culture. Generally, cow dung, poultry litter, municipal solid wastes (MSW), etc. are being used for composting with the addition of bulking materials rich in cellulose and hemicellulose as carbon source such as rice straw, saw dust etc. Fungal isolates originated from cellulose and hemicellulose rich substrates would be effective for degradation of bulking materials as compost.

Among the isolated fungal strains, the species of *Trichoderma* and *Penicillium* were monitored, and the species *Trichoderma* was higher in number than the *Penicillium*. Only these two genera of fungal strains were recorded from six sources. Several authors reported different species and number of filamentous fungi isolated from different substrates. Findings of our previous study reported a maximum number of *Trichoderma* spp. in decomposed POME (Palm Oil Mill Effluent) wreckages and *Penicillium* spp. in decomposed sludge (Molla et al., 2002a). In another study, Ahirwar et al. (2017) isolated 5, 10, and 11 thermophilic and thermotolerant fungi from 6, 11, and 12 samples of litter, wheat straw and compost, respectively. Thirty-six fungal isolates under seven genera were isolated from four biogas plants and DNA sequences tools were used for their identification

(Young et al., 2018). The macro/micro-morphological structures of the reproductive organs of the studied fungi were used to identify the genera (Rifai, 1969; Bohacz and Kornillowicz-Kowalska, 2020).

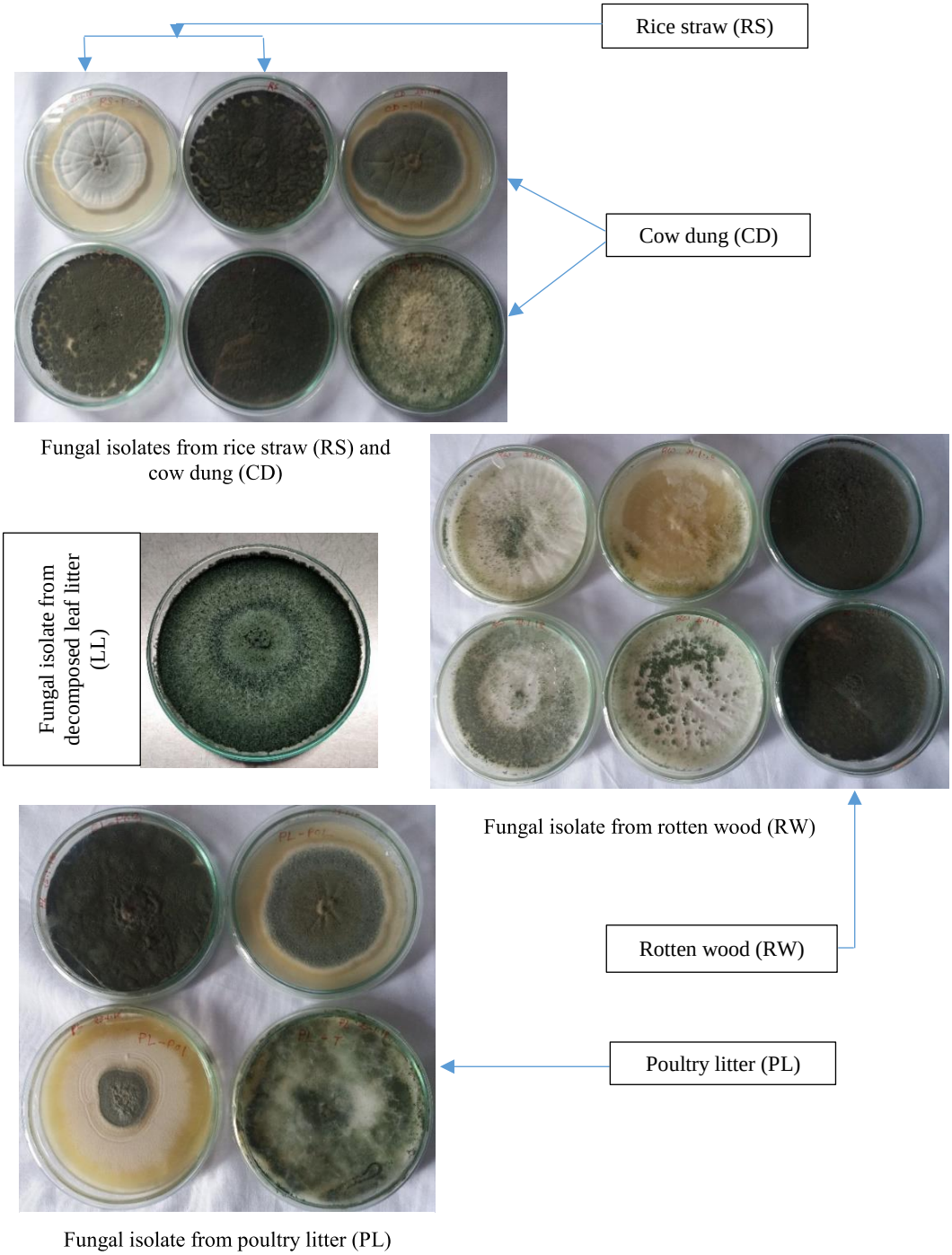

Figure 1. Isolated fungal species from different related native sources

3.2 Germination of crop seeds

Thirteen fungal isolates/species were used for three crop seeds [Mung bean (*Vigna radiata*), Mustard (*Brassica campestris*), and Wheat (*Triticum aestivum*)] germination to evaluate its performance (Figure 2). Performances of the applied 13 fungal isolates/species were examined by studying the parameters of percent germination, germination index, radicle length, and plumule length. The findings of the study have been presented and discussed below.

Table 1. Tentatively identified fungal isolates/strains

Isolate code	View in plate	Morphological description	Tentative identification
CD-P01		Smooth and uniform growth of fungal strain, initial color was dark ash, the central matured part became whitish. The young margin was relatively more off-white in color.	*Penicillium* sp.
CD-P03	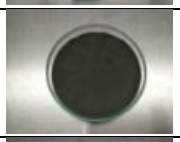	It's growth was also smooth and uniform but color was more dark ask. Slow growing fungal strain.	*Penicillium* sp.
CD-T01		Relatively compact white i.e., milk colored, fast growing fungal mycelia mat was observed within 3-4 days after inoculation in PDA plate. Later sporadic green fungal biomass was developed.	*Trichoderma* sp.
RW-T02	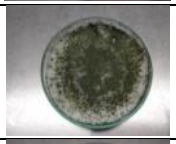	Fluffy milk-colored fungal mycelia in nature. But the mycelia color was changed as olive green in color within 3-4 days and the green portion was expanded in mature stage.	*Trichoderma* sp.
RW-T03		Relatively green colored mycelia were appeared and later on the middle portion became whitish in color. The peripheral portion was quite green.	*Trichoderma* sp.
PL-P01		Smooth and uniform fungal mycelial growth was appeared. The matured central portion of mycelia became whitish in color. The peripheral young mycelia were off-white.	*Penicillium* sp.
PL-P03	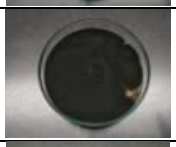	Slow growing deep olive colored mycelial smooth mat was appeared and uniform growth and colored was maintained.	*Penicillium* sp.
PL-T01		Closely similar pattern of fungal mycelial growth was observed as CD-T01.	*Trichoderma* sp.
RS-P01	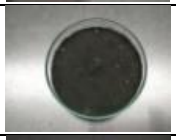	Slightly rough, harsh, deep greenish to olive colored slow growing mycelia was observed. At matured stage loose power of spores was noticed on mycelial mat.	*Penicillium* sp.
RS-P02		Almost similar pattern of fungal mycelial growth was observed as PL-P01. But the color of the whole was almost uniform.	*Penicillium* sp.
LL-T04		Initially deep green colored fluffy mycelial growth was observed. But at mature stage, the fungal biomass of central part of the plate became comparatively whitish in color and peripheral portion was quite green.	*Trichoderma* sp.
MSW-T04		Quite fluffy and fast growing white colored mycelial was appeared at early stage. But after 2-3 day later it was turned into olive color.	*Trichoderma* sp.
MSW-T05		More or less uneven but smooth fungal mycelial growth was observed. Moreover, it was slowing growing in nature.	*Trichoderma* sp.

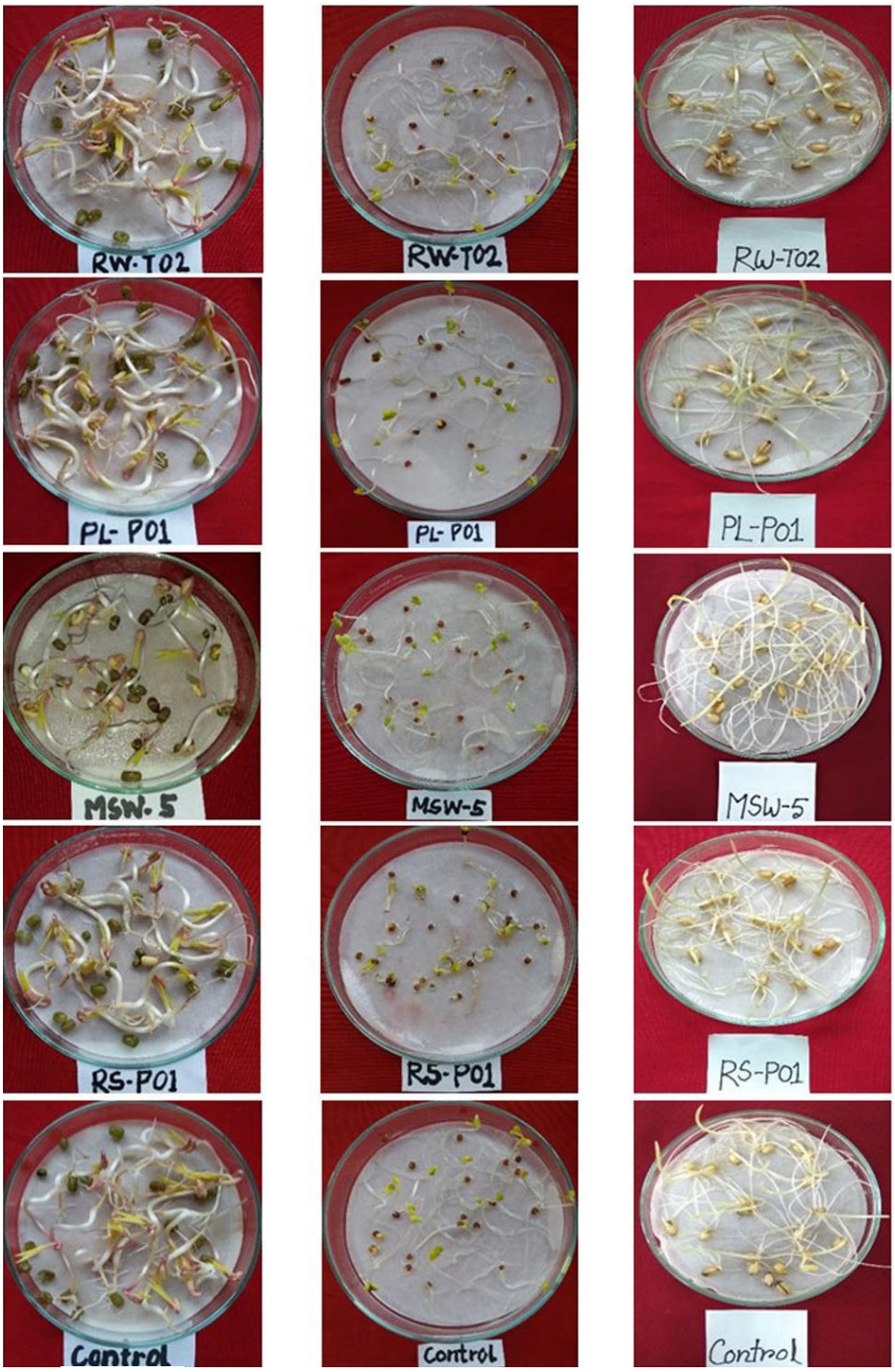

Figure 2. Germination performance of mung bean, mustard and wheat seeds at spores suspension of different fungal isolates/strains in petri dishes. (A-mung bean seed, B-mustard seed, and C-wheat seed)

3.2.1 Germination percentage

No germination of mung bean seeds (*Vigna radiata*) was noticed after 24 h, but at 48 h more than 30% seeds were germinated in all treatments (Table 2). Next, 60% germination of seeds was recorded at 72 h, and at 96 h the percent germination in all treatments was above 80%, except the treatment CD-P03 which was around 76%. The treatment RW-T02 provided the highest (98.35) percent of germination at 96 h (Table 2 and Figure 3) and the second highest (96.65%) was monitored at PL-P01 treatment. However, the control (water) treatment provided 91.61% of mung bean seed germination at 96 h.

Table 2. Germination percent of three crop seeds by application of several fungal suspensions

Treatment*	Germination (%) of three crop seeds											
	Mung bean				Mustard				Wheat			
	24 h	48 h	72 h	96 h	24 h	48 h	72 h	96 h	24 h	48 h	72 h	96 h
CD-P01	0.00	43.30	68.35	81.65^{e}	1.67	48.35	86.65	93.35^{abc}	26.65	80.00	86.65	86.65^{cd}
CD-P03	0.00	35.00	65.00	76.65^{f}	0.00	65.00	90.00	95.00^{ab}	46.65	85.00	85.00	85.00^{cd}
CD-T01	0.00	58.30	73.35	85.00^{de}	0.00	41.65	85.00	93.35^{abc}	18.35	88.35	93.35	93.35^{a}
RW-T02	0.00	71.65	95.00	98.35^{a}	0.00	33.35	73.35	91.65^{bcd}	26.65	80.00	83.35	83.35^{d}
RW-T03	0.00	35.00	78.35	83.35^{de}	0.00	25.00	78.35	93.35^{abc}	31.65	83.35	86.65	86.65^{cd}
PL-P01	0.00	75.00	91.65	96.65^{ab}	0.00	55.00	95.00	96.65^{a}	26.65	85.00	86.65	86.65^{cd}
PL-P03	0.00	41.65	70.00	83.35^{de}	1.67	58.35	85.00	90.00^{cd}	35.00	81.65	83.35	83.35^{d}
PL-T01	0.00	46.65	68.35	83.35^{de}	0.00	56.65	88.35	91.65^{bcd}	33.35	85.00	86.65	86.65^{cd}
RS-P01	0.00	58.30	80.00	81.65^{e}	0.00	35.00	51.65	75.00^{e}	33.35	90.00	91.65	91.65^{ab}
RS-P02	0.00	66.65	76.65	86.65^{d}	0.00	46.65	90.00	93.35^{abc}	30.00	85.00	88.35	88.35^{bc}
LL-T04	0.00	63.30	76.65	85.00^{de}	0.00	23.35	71.65	91.65^{bcd}	8.35	75.00	85.00	85.00^{cd}
MSW-T04	0.00	75.00	90.00	93.35^{bc}	0.00	31.65	71.65	91.65^{bcd}	31.65	85.00	86.65	86.65^{cd}
MSW-T05	0.00	56.65	70.00	81.65^{e}	0.00	46.65	88.35	90.00^{cd}	28.35	90.00	93.35	93.35^{a}
Control	0.00	56.65	91.65	91.65^{c}	0.00	38.35	80.00	88.35^{d}	36.65	76.65	78.35	78.35^{e}
				(p≤0.1)				(p≤0.001)				(p≤0.01)

*N.B. Fungal strains isolated from decomposed/rotten (CD-Cow dung, RW-Rotten wood, PL-Poultry litter, RS-Rice straw, LL-Decomposed leaf litter, and MSW-Municipal solid waste); P-*Penicillium* sp. and T-*Trichoderma* sp.

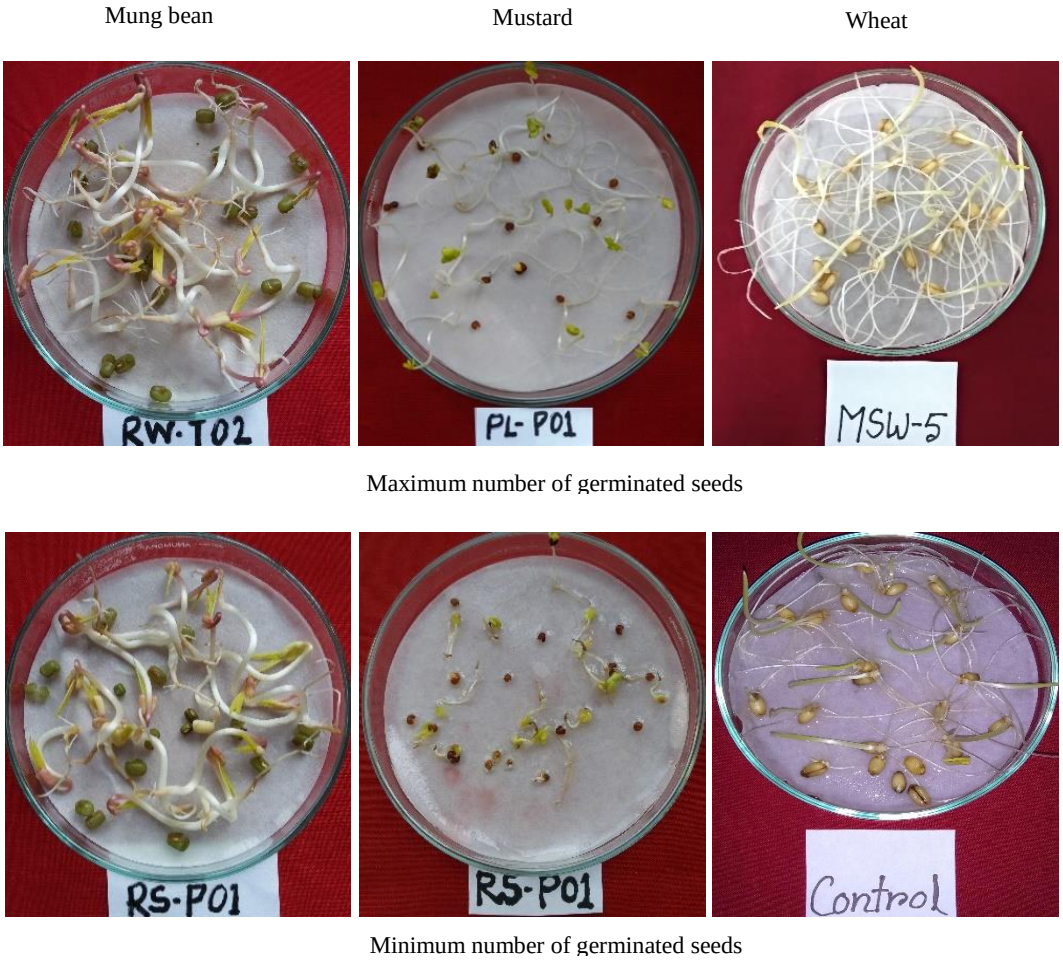

Figure 3. Maximum and minimum germination percent of three crop seeds while germination allowed by application of fungal suspension

In the case of mustard (*Brassica campestris*) at 24 h, 1.67% germination was monitored in treatments CD-P01 and PL-P03 (Table 2). After 48 h, 25% or more germinated seeds were recorded in all treatments. At 72 h, more than 50% germinated seeds were noticed. While at 96 h the percent germination in all treatments was above 88%, except the treatment RS-P01 which was around 75%. The treatment PL-P01 provided the highest (96.65) percent of germination at 96 h and second highest (95%) was treatment CD-P03. On the other hand, the treatment RW-T03 provided above 93% of seeds germination. But in control (water) treatment, only 88.35% of mustard seed germination was achieved at 96 h.

In wheat (*Triticum aestivum*) seed germination, the responses were not like mung bean and mustard. Germination of wheat seed was responded earlier at 24 h and completed by day 72 h and at 96 h the germination record was same as at 72 h (Table 2). At 72 h above 80% germination was recorded in all the treatments except the control (78.35%). The highest 93.35% germination was recorded in the treatments CD-T01 and MSW-T05. The second highest (91.65%) was achieved at treatment RS-P01. In all cases the germination percent of all crop seeds was significantly higher than the control treatment.

The applied fungal spore suspension treatment influenced germination of seed and germination index. Germination of some seeds by some isolates/strains was quite encouraging. The obtained findings conveyed that no particular isolate positively influenced in germination of all tested crop seeds. In the present study, the influence on germination of seeds by fungal suspension was crop specific. However, the germination of *Brassica campestris* seeds was promoted when a fungal suspension was applied (Molla and Khan, 2018). Microbes release different bio-molecules/growth promoting substances, i.e., phyto-hormones, which influence or promote germination of seeds and growth of seedlings (Kagithoju et al., 2013; Castiglione et al., 2021). In the present study, the fungal isolates PL-P01 and RW-T02 played remarkable roles in crop seeds germination in most of the cases. It implied that these isolates might release useful bio-enhancer plant metabolites which promote germination. Yue et al. (2019) studied seed germination and mortality of desert winter annual plants (*Brassica tournefortii*; *Plantago ovata*) with soil-borne fungi, and used fungi induced substantial seed germination and mortality in summer with ten strains demonstrating host-specificity. Increasing and decreasing of seeds germination were noticed by fungal application due to species host-specificity (Li et al., 2021). *Trichoderma* spp. promote seed germination and alleviated biotic and abiotic stresses in germinating seeds and seedlings by inducing physiological protection in plants against oxidative damage (Mastouri et al., 2010; Delgado-Sánchez et al., 2013). Like *Triochoderma* spp., *Penicillium* spp. promotes seed germination and seedling growth (Yamaji et al., 2005; Tamura et al., 2008; Delgado-Sánchez et al., 2013), and protects seedlings by producing antifungal compounds to keep antifungal activity under competitive condition (Yamaji et al., 2005). In another study, seed germination of *Strychnos potatorum* with *Penicillium* and *Aspergillus* species that the significant increase and early germination was noticed due to the culture exudates on metabolic activities that promote cell division of pre-germinated seeds, as well as production of growth regulating substances like gibberellins and auxins (Yoneyama et al., 1998; Kagithoju et al., 2013; Khokhar et al., 2013). In the present study, early germination appeared in wheat (*Triticum aestivum*), which may be most responsive to the released metabolites by the applied fungal isolates.

3.2.2 Germination index (GI)

No germination was recorded at 24 h in the case of mung bean. So, the germination index was zero for all the treatments at 24 h. The germination index at 72 h was 100 or above in each treatment. The treatment RW-T02 provided the highest (107.31) germination index at 96 h and a closer index (second highest) was recorded 105.46 for PL-P01 at the same period. Whereas the germination index of 100 was recorded in control treatment (Table 3). Conversely, the lowest GI (83.63) was monitored for the CD-P03 treatment.

In the case of mustard, at 24 h the germination index was zero for all the treatments, similar to mung bean (Table 3). However, the highest germination index was 118.75 and 109.39 recorded in treatment PL-P01 at 72 and 96 h, respectively. The second highest GI (107.53) was found in treatment CD-P03 at 96 h. On the other hand, the germination index in control treatment was 100.

In wheat seed (Table 3) germination, the responses were not like mung bean or mustard. Wheat seed germination was noticed at 24 h and completed by 72 h. At 72 h the highest germination index was recorded in the treatments CD-T01 and MSW-T05 (119.14), whereas in control it was 100 as usual. The

second highest GI (116.98) was recorded in treatment RS-P01 at 72 h.

The germination index (GI) is the percent expression of multiplied results of percent germination (Molla et al., 2002b). Therefore, it follows the similar trends as the germination percent. But GI is treated as a dependable measurement of phytotoxicity levels of seeds germination (DeVleeschauwer et al., 1981; Rao et al., 2014). Seed germination by fungal application either enhances (germination) due to release of growth regulating substances like gibberellins and auxins (Khokhar et al., 2013) or decreases due to liberation of mycotoxins (Khokhar et al., 2011; Rao et al., 2014), which is dependent on the strains of microbes. In the present study, the GI of mustard and wheat were influenced more than the control by all fungal treatment, but mung bean was affected by only some of the fungal isolates.

Table 3. Germination index of three crop seeds in germination with application of several fungal suspensions

Treatment*	Germination index (GI) of three crop seeds											
	Mung bean				Mustard				Wheat			
	24 h	48 h	72 h	96 h	24 h	48 h	72 h	96 h	24 h	48 h	72 h	96 h
CD-P01	0.00	76.43	74.58	89.09	0.00	126.08	108.31	105.66	72.72	104.37	110.59	110.59
CD-P03	0.00	61.78	70.92	83.63	0.00	169.49	112.50	107.53	127.29	110.89	108.49	108.49
CD-T01	0.00	102.91	80.03	92.75	0.00	108.60	106.25	105.66	50.07	115.26	119.14	119.14
RW-T02	0.00	126.48	103.66	107.31	0.00	86.96	91.69	103.74	72.72	104.37	106.38	106.38
RW-T03	0.00	61.78	85.49	90.94	0.00	65.19	97.93	105.66	86.36	108.74	110.59	110.59
PL-P01	0.00	132.39	100.00	105.46	0.00	143.42	118.75	109.39	72.72	110.89	110.59	110.59
PL-P03	0.00	73.52	76.38	90.94	0.00	152.15	106.25	101.87	95.49	106.52	106.38	106.38
PL-T01	0.00	82.35	74.58	90.94	0.00	147.72	110.44	103.74	90.99	110.89	110.59	110.59
RS-P01	0.00	102.91	87.29	89.09	0.00	91.26	64.56	84.89	90.99	117.42	116.98	116.98
RS-P02	0.00	117.65	83.63	94.55	0.00	121.64	112.50	105.66	81.86	110.89	112.76	112.76
LL-T04	0.00	111.74	83.63	92.75	0.00	60.89	89.56	103.74	22.78	97.85	108.49	108.49
MSW-T04	0.00	132.39	98.19	101.85	0.00	82.53	89.56	103.74	86.36	110.89	110.59	110.59
MSW-T05	0.00	100.00	76.38	89.09	0.00	121.64	110.44	101.87	77.35	117.42	119.14	119.14
Control	0.00	100.00	100.00	100.00	0.00	100.00	100.00	100.00	100.00	100.00	100.00	100.00

*N.B. Fungal strains isolated from decomposed/rotten (CD-Cow dung, RW-Rotten wood, PL-Poultry litter, RS-Rice straw, LL-Decomposed leaf litter, and MSW-Municipal solid waste); P-*Penicillium* sp. and T-*Trichoderma* sp.

3.2.3 Length of radicle and plumule

Radicle and plumule length of mung bean, mustard and wheat are shown in Table 4. In case of mung bean, the longest radicle length was observed in control treatment (9.08 cm) and which was followed by the treatment LL-T04 (9.06 cm). The shortest radicle length was recorded in the treatment PL-P03 (6.37 cm). In the case of mustard, the longest radicle length was observed in control treatment (5.89 cm) also which was followed by the treatment PL-T01 (4.47 cm). The shortest radicle length was recorded in the treatment RW-T03 (0.8 cm). Conversely, in wheat the longest radicle length was observed in treatment MSW-T05 (6.87 cm) which was followed by the control treatment (6.09 cm). The shortest radicle length was recorded in the treatment RW-T03 (3.18 cm).

In Table 4 the longest plumule length of mung bean was observed in control treatment (1.98 cm) which was followed by the treatment MSW-T05 (1.93 cm). The shortest plumule length was recorded in the treatment CD-T01 (1.43 cm). In mustard the longest plumule length was observed in control treatment (3.25 cm) which was followed by the treatment PL-P03 (2.62 cm). Conversely the shortest plumule length was recorded in the treatment RS-P01 (0.90 cm). On the other hand, in wheat the longest plumule length was observed in treatment RW-T03 (3.08 cm) which was followed by the control treatment (2.91 cm). The shortest plumule length was recorded in the treatment CD-P03 (2.15 cm). Both radicle and plumule length of mustard and mung bean attained significant height in the control than other treatments. It might happen that the fungal treatments released some sorts of metabolites that arrested the growth of radicle and plumule to some extent. Conversely in wheat the longest radicle and plumule lengths were recorded in MSW-T05 and RW-T03, respectively; which were statistically insignificant to the results attained in

control treatment. Moreover, both radicle and plumule length in wheat were enhanced by the treatments containing *Trichoderma* spp.

The germination of Millet (Dami Mallit) seeds by application of *Trichoderma* spp. and *Penicillium* sp. were examined and the *Trichoderma* strains enhanced the plumule length whereas, *Pencillium* strain decreased the plumule growth of all varieties in all concentrations compared to control (Hassan et al., 2013). In another study, the coleoptile length of *Elymus sibiricus* increased with application of endophytic fungi supernatant (Li et al., 2017). In the present study, the longest plumule length was achieved using fungal treatment (RW-T03) in wheat, but it was statistically similar to control and most of the fungal treatments presented the statistically similar results also. Mustard had the longest plumule length in the control, but it was statistically similar to most of the treatments. In mung bean, relatively poor plumule length was noticed in the most fungal treatments compared to control, perhaps due to release of some mycotoxins by the applied fungi (Khokhar et al., 2011). Among eight fungal treatments, *Fusarium oxysporum* and *Aspergillus flavus* presented reduced radicle and plumule length on fenugreek seed germination (Khokhar et al., 2011). It implied that responses of fungal suspension/supernatant are not similar to all crop seed germination, but seems to be crop specific. Besides, the radicle and plumule growth are more responsive to mycotoxins than germination of seeds.

Table 4. Radicle and plumule length of mung bean, mustard and wheat germinated seeds by different fungal isolates suspension at last day of observation

Treatment*	Radicle length (cm) at 96 h of germination			Plumule length (cm) at 96 h of germination		
	Mung bean	Mustard	Wheat	Mung bean	Mustard	Wheat
CD-P01	7.62^{ab}	3.81^{bc}	5.40^{bc}	1.73^{abc}	2.28^{ab}	2.39^{bcd}
CD-P03	7.64^{ab}	2.49^{de}	5.35^{bc}	1.77^{abc}	2.54^{ab}	2.15^{cd}
CD-T01	7.21^{ab}	1.60^{efg}	5.58^{abc}	1.43^{d}	1.84^{bc}	2.83^{ab}
RW-T02	6.68^{b}	4.39^{b}	5.21^{bc}	1.69^{bcd}	2.04^{abc}	2.16^{d}
RW-T03	8.01^{ab}	0.80^{g}	3.18^{d}	1.77^{abc}	1.43^{bc}	3.08^{a}
PL-P01	8.07^{ab}	4.41^{b}	5.40^{bc}	1.68^{bcd}	2.22^{ab}	2.31^{bcd}
PL-P03	6.37^{b}	1.23^{g}	5.52^{bc}	1.64^{cd}	2.62^{ab}	2.70^{abcd}
PL-T01	8.15^{ab}	4.47^{b}	4.97^{bc}	1.56^{cd}	2.07^{abc}	2.45^{bcd}
RS-P01	6.69^{b}	1.19^{g}	4.88^{bc}	1.71^{bc}	0.90^{c}	2.54^{abcd}
RS-P02	7.72^{ab}	3.53^{bcd}	5.58^{abc}	1.76^{abc}	2.30^{ab}	2.50^{abcd}
LL-T04	9.06^{a}	1.29^{fg}	4.61^{c}	1.82^{abc}	1.64^{bc}	2.57^{abcd}
MSW-T04	7.12^{ab}	2.77^{cd}	5.92^{ab}	1.73^{abc}	2.42^{ab}	2.80^{abc}
MSW-T05	7.41^{ab}	2.42^{def}	6.87^{a}	1.93^{ab}	2.27^{ab}	2.85^{ab}
Control	9.08^{a}	5.89^{a}	6.09^{ab}	1.98^{a}	3.25^{a}	2.91^{ab}
	($p \leq 0.1$)	($p \leq 0.001$)	($p \leq 0.01$)	($p \leq 0.05$)	($p \leq 0.1$))	($p \leq 0.1$)

*N.B. Fungal strains isolated from decomposed/rotten (CD-Cow dung, RW-Rotten wood, PL-Poultry litter, RS-Rice straw, LL-Decomposed leaf litter, and MSW-Municipal solid waste); P-*Penicillium* sp. and T-*Trichoderma* sp.

3.3 Compatibility performance of fungal mixed culture

A total of 12 combinations designated as ABC, ABF, ACE, ACF, ADE, ADF, BCE, BCF, BDE, BDF, CDE, and CDF using six fungal isolates (A, B, C, D, E, and F) were examined for their performance as mixed fungal growth. Compatible mixed cultures, which might ensure multiple enzymes in bioprocess system for enhancement of biodegradation, are more highly efficient than monocultures (Gutierrez-Correa and Tengerdy, 1997; Rahman et al., 2002). However, both mutual intermingle as well as inhibitory growth of fungal isolates were noticed. The combination ABF and BCE presented the maximum mutual intermingle growth (Figure 4). Mixed cultures of microbes can strengthen and accelerate the bioconversion process and the most important determinants in mixed culture are strain compatibility and nutritional status (Duenas et al., 1995; Gutierrez-Correa and Tengerdy, 1997; Molla et al., 2001b). Accordingly, these two combinations are considered for future research activities.

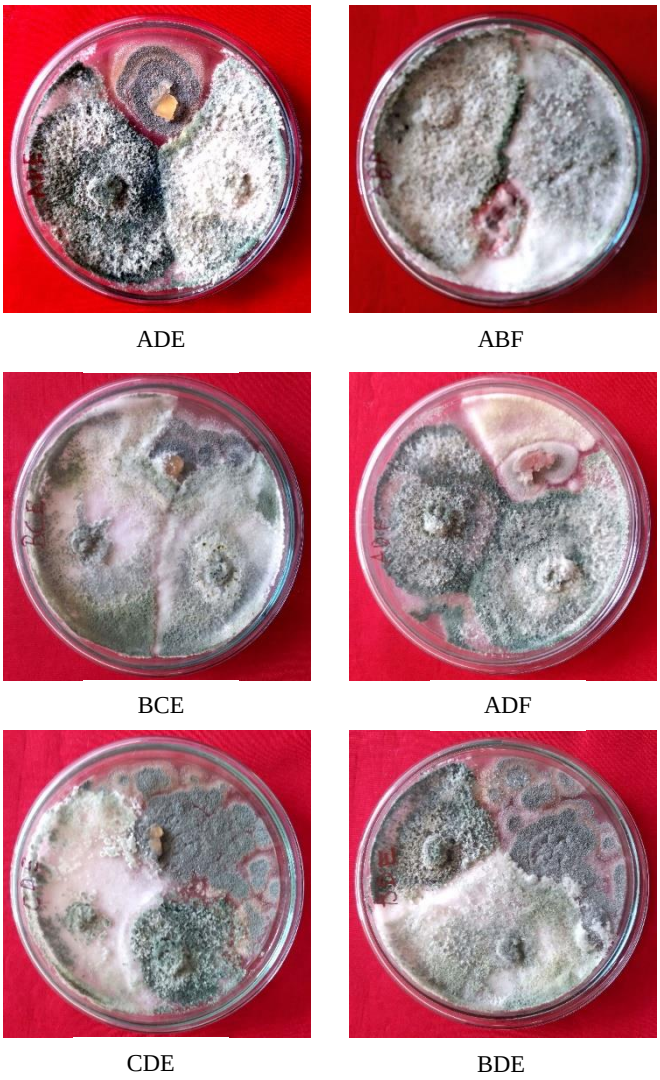

Figure 4. Features of mixed culture growth of different fungal isolate on PDA plates

4. CONCLUSION

Responses of fungal isolates/strains isolated from six native habitats showed dissimilar trends in germination of different seeds. Isolates/strains showed significant response to a crop seed germination, but not equally to all seed types. An isolate/strain significantly increased percent germination but did not affect radicle/plumule length. Discoloration and abnormal symptoms of germinated seeds were not noticed. ABF and BCE combinations of fungal isolates/strains may respond successfully in organic wastes degradation as a mixed culture due to its excellent intermingle performance. Perhaps these combinations (ABF and BCE) of fungal isolates may play significant roles in biodegradation of organic wastes into compost that will reduce load of inorganic fertilizers usages along with improved yield and quality of crop in future research.

ACKNOWLEDGEMENTS

The authors are grateful and extend sincere thanks to Research Management Wing (RMW) of Bangabandhu Sheikh Mujibur Rahman Agricultural University (BSMRAU), Gazipur, Bangladesh for extending their cooperation and providing required fund to conduct research.

REFERENCES

Adesemoye AO, Torbert HA, Kloepper JW. Enhanced plant nutrient use efficiency with PGPR and AMF in an integrated nutrient management system. Canadian Journal of Microbiology 2008;54(10):876-86.

Ahirwar S, Soni H, Prajapati BP, Kango N. Isolation and screening of thermophilic and thermotolerant fungi for production of hemicellulases from heated environments. Mycology 2017; 8(3):125-34.

Bari MN, Alam MZ, Rahman MM. Soild waste management of Dhaka City using composting process. Proceedings of the International Conference on Biotechnology Engineering; 2007 May 8-10; ICBioE'07, Kuala Lumpur: Malaysia; 2007.

Barua S, Molla AH, Haque MM, Alam MS. Performance of *Trichoderma*-enriched bio-organic fertilizer in N supplementation and bottle gourd production in field condition. Horticulture International Journal 2018;2(3):106-14.

Bohacz J, Kornillowicz-Kowalska T. Modification of post-industrial lignin by fungal strains of the genus *Trichoderma* isolated from different composting stages. Journal of Environmental Management 2020;266:Article No. 110573.

Castiglione AM, Mannino G, Contartese V, Bertea CM, Ertani A. Microbial biostimulants as response to modern agriculture needs: Composition, role and application of these innovative products. Plants 2021;10(8):Article No. 1533.

Cerda A, Artola A, Font X, Barrena R, Gea T, Sánchez A. Composting of food wastes: Status and challenges. Bioresource Technology 2018;248:57-67.

Delgado-Sánchez P, Jiménez-Bremont JF, Guerrero-González ML, Flores J. Effect of fungi and light on seed germination of three *Opuntia* species from semiarid lands of central Mexico. Journal of Plant Research 2013;126:643-9.

Devi A, Anu-Appaiah KA. Mixed malolactic co-culture (*Lactobacillus plantarum* and *Oenococcus oeni*) with compatible Saccharomyces influences the polyphenolic, volatile and sensory profile of Shiraz wine. LWT-Food Science and Technology 2021;135:Article No. 1102456.

DeVleeschauwer D, Verdonck O, Assche PV. Phytototoxicity of refuse compost. Biocycle 1981;1-2:44-6.

Duenas R, Tengerdy RP, Gutierrez-Correa M. Cellulase production by mixed fungi in solid-substrate fermentation of bagasse. World Journal of Microbiology and Biotechnology 1995;11:333-7.

Gutierrez-Correa M, Tengerdy RP. Production of cellulase on sugar cane bagasse by fungal mixed culture solid substrate fermentation. Biotechnology Letters 1997;19(7):665-7.

Hassan MM, Daffalla HM, Modwi HI, Osman MG, Ahmed II, Gani MEA, et al. Effects of fungal strains on seeds germination of Millet and Striga Hermonthica. Universal Journal of Agricultural Research 2013;2(2):83-8.

Heerden IV, Cronjé C, Swart SH, Kotzé JM. Microbial, chemical and physical aspects of citrus waste composting. Bioresource Technology 2002;81:71-6.

Islam MM, Kayesh E, Zaman E, Urmi TA, Haque MM. Evaluation of rice (*Oryza sativa* L.) genotypes for drought tolerance at germination and early seedling stage. The Agriculturists 2018;16(1):44-54.

Jung HY, Kim JK. Eco-friendly waste management of mackerel wastewater and enhancement of its reutilization value. International Biodeterioration and Biodegradation 2016; 111:1-13.

Kagithoju S, Sheikh AH, Godishala V, Nanna RS. Role of fungi and fungal extract on *Strychnos potatorum* seed germination. Research Journal of Biotechnology 2013;8(11):33-6.

Kauser H, Khwairakpam M. Organic waste management by two-stage composting process to decrease the time required for vermicomposting. Environmental Technology and Innovation 2022;25:Article No. 102193.

Khokhar I, Haider MS, Mukhtar I, Ali A, Mushtaq S, Ashfaq M. Effect of *Penicillium* species culture filtrate on seedling growth of wheat. International Research Journal of Agricultural Science and Soil Science 2013;3(1):24-9.

Khokhar M, Rawal P, Mathur AC. Effect of fungal metabolites on seed viability and seedling vigour of fenugreek (*Trigonella foenum graecum*). Jurnal of Mycology and Plant Pathology 2011;41(4):543-5.

Li X, Song M, Yao X, Chai Q, Simpson WR, Li C, et al. The effect of seed-borne fungi and epichloë endophyte on seed germination and biomass of *Elymus sibiricus*. Frontiers in Microbiology 2017;8:Article No. 2488.

Li Y, Chen L, Tian X, Lin L, Ding R, Yan W, et al. Functional role of mixed-culture microbe in photocatalysis coupled with biodegradation: Total organic carbon removal of ciprofloxacin. Science of the Total Environment 2021;784:Article No. 147049.

Martin JP. Use of acid, rose bengal and streptomycin in the plate for estimating soil fungi. Soil Science 1950;69:215-32.

Mastouri F, Björkman T, Harman GE. Seed treatment with *Trichoderma harzianum* alleviates biotic, abiotic, and physiological stresses in germinating seeds and seedlings. Phytopathology 2010;100:1213-21.

Meda A, Sangwan P, Bala K. In-vessel composting of HMX and RDX contaminated sludge using microbes isolated from contaminated site. Environmental Pollution 2021;285:Article No. 117394.

Molla AH, Fakhru'l-Razi A, Abd-Aziz S, Hanafi MM, Alam MZ. *In-vitro* compatibility evaluation of fungal mixed culture for bioconversion of domestic wastewater sludge. World Journal of Microbiology and Biotechnology 2001b;17(9):849-56.

Molla AH, Fakhru'l-Razi A, Abd-Aziz S, Hanafi MM, Roychoudhury PK, Alam MZ. A potential resource for bioconversion of domestic wastewater sludge. Bioresource Technology 2002a;85:263-72.

Molla AH, Fakhru'l-Razi A, Alam MZ. Evaluation of solid-state bioconversion of domestic wastewater sludge as a promising environmental-friendly disposal technique. Water Research 2004;38:4143-52.

Molla AH, Fakhru'l-Razi A, Alam MZ. Solid state bioconversion (SSB): An effective process for safe disposal and recycling of domestic wastewater sludge as compost. The Journal of the Agricultural Engineering Society of Sri Lanka 2006;9(1): 57-71.

Molla AH, Fakhru'l-Razi A, Hanafi MM, Abd-Aziz S, Alam MZ. Potential non phytopathogenic filamentous fungi for bioconversion of domestic wastewater sludge. Journal of Environmental Science and Health 2002b;A37(8):1495-507.

Molla AH, Haque MM, Haque MA, Ilias GNM. *Trichoderma*-enriched biofertilizer enhances production and nutritional quality of tomato (*Lycopersicon esculentum* Mill.) and minimizes NPK fertilizer use. Agricultural Research 2012;1(3):265-72.

Molla AH, Khan HI. Detoxification of textile effluent by fungal treatment and its performance in agronomic usages. Environmental Science and Pollution Research 2018; 25:10820-8.

Molla AH, Shamsuddin ZH, Halimi MS, Morziah M, Puteh AB. Potential for enhancement of root growth and nodulation of soybean co-inoculated with *Azospirillum* and *Bradyrhizobium* in laboratory systems. Soil Biolology and Biochemistry 2001a;33:457-63.

Molla AH. Solid State Bioconversion of Domestic Wastewater Treatment Plant Sludge into Compost by Screened Filamentous Fungi [dissertation]. Faculty of Engineering, Universiti Putra Malaysia, Malaysia; 2002.

Rahman KSM, Banat IM, Thahira J, Thayumanavan T, Lakshmanaperumalsamy P. Bioremediation of gasoline contaminated soil by a bacterial consortium amended with

poultry litter, coir pith and rhamnolipid biosurfactant. Bioresource Technology 2002;81:25-32.

Rao VK, Girisham S, Reddy SM. Influence of different species of *Penicillium* and their culture filtrates on seed germination and seedling growth of sorghum. Journal of Biochemistry and Technology 2014;5(4):832-7.

Rifai MA. A revision of the genus *Trichoderma*. Mycological Papers No. 116. Kew, Surrey, England: Commonwealth Mycological Institute; 1969.

Srivastava B, Khatri M, Singh G, Arya SK. Microbial keratinases: An overview of biochemical characterization and its eco-friendly approach for industrial applications. Journal of Cleaner Production 2020;252:Article No. 119847.

Tamura T, Hashidoko T, Ogita N, Limin SH, Tahara S. Requirement for particular seed-borne fungi for seed germination and seedling growth of *Xyris complanata*, a pioneer monocot in topsoil-lost tropical peatland in Central Kalimantan, Indonesia. Ecological Research 2008;23:573-9.

Yamaji K, Hashidoko Y, Fukushi Y, Tahara S. Chemical response of *Picea glehnii* seed-epiphytic *Penicillium* species to *Pythium vexans* under in vitro competitive conditions for mycelial growth. Journal of Chemical Ecology 2005;31:805-17.

Yoneyama K, Takeuchi Y, Ogasawara M, Konnai M, Sugimoto Y, Sassa T. Cotylenins and fusicoccins stimulate seed germination of *Striga hermonthica* (Del.) Benth and *Orobanche minor* Smith. Journal of Agricultural and Food Chemistry 1998;46:1583-6.

Young D, Dollhofer V, Callaghan TM, Reitberger S, Lebuhn M, Benz JP. Isolation, identification and characterization of lignocellulolytic aerobic and anaerobic fungi in one- and two-phase biogas plants. Bioresource Technology 2018;268:470-9.

Yue MLi, Shaffer JP, Hall B, Ko H. Soil-borne fungi influence seed germination and mortality, with implications for coexistence of desert winter annual plants. PLoS One 2019;31:1-21.

Biochar Derived from *Sesbania sesban* Plant as a Potential Low-Cost Adsorbent for Removal of Methylene Blue

Nguyen Trung Hiep[1], Ta Thi Hoai Thu[2], Lam Thi Thanh Quyen[2], Phan Dinh Dong[1], Tran Tuyet Suong[1], and Thai Phuong Vu[1*]

[1]Research Institute for Sustainable Development, Ho Chi Minh University of Natural Resources and Environment, 236B Le Van Sy, Tan Binh District, Ho Chi Minh City 700000, Vietnam
[2]Faculty of Environment, Ho Chi Minh University of Natural Resources and Environment, 236B Le Van Sy, Tan Binh District, Ho Chi Minh City 700000, Vietnam

ARTICLE INFO

Received: 29 May 2022
Received in revised: 13 Jul 2022
Accepted: 1 Aug 2022
Published online: 14 Sep 2022
DOI: 10.32526/ennrj/20/202200119

Keywords:
Biochar/ Low-cost adsorbent/ Methylene blue/ *Sesbania sesban*

*** Corresponding author:**
E-mail: tpvu@hcmunre.edu.vn

ABSTRACT

In this study, biochar made from the *Sesbania sesban* plant, under slow pyrolysis at 300°C was used to adsorb methylene blue (MB) in aqueous solution. The biochar properties were clarified by diverse analytical methods such as FTIR, SEM, and BET. The results indicated that the surface of biochar was relatively smooth, had porous texture, and stacked evenly. In addition, the biochar had a large specific surface area of 561.8 m^2/g and the pH_{pzc} value was 6.9. The effect of adsorbent dosage, initial pH, contact time, and concentration of dye solution on biochar were investigated. The optimum conditions for MB adsorption were found at the MB concentration of 50 mg/L, initial pH of 11, biochar mass of 0.6 mg, and contact time of 30 min. Under these optimal conditions, MB dye removal efficiency was above 90%. Adsorption isotherm data were fitted with the Langmuir isotherm model (R^2=0.897) suggesting the adsorption was monolayer, and its maximum adsorption capacity was about 6.6 mg/g. The adsorption kinetic models showed that the linear pseudo-second-order by R^2=0.999 was well fitted. The results indicated the enormous potential of *Sesbania sesban* plant to produce biochar as a low-cost and rather high-effective adsorbent for dye removal from wastewater as well as water quality improvement.

1. INTRODUCTION

Presently, removing color from industrial wastewater, particularly from textile and color manufacturers, is an important pollution control measure. Dye wastewater dumped into natural receiving waters may render them unfit for human consumption due to the toxicological challenges caused by harmful dyes to the environment and human health. Methylene blue (MB), for example, is a synthetic dye that is widely employed in medical staining agents, diagnostic examination, and fiber coloring agents in the textile industry (Ahmad et al., 2020). A high dose of MB dye produces major skin problems, eye discomfort, vomiting, decreases cardiac output, renal blood flow, and other side effects (Rahman-Setayesh et al., 2019). Furthermore, MB has poor biodegradability, so it needs to be treated before being discharged into the environment.

The standard water treatment solutions cannot effectively decolorize dyes because of their complex chemical structure and resistance to oxidizing chemicals and light. Hence, these dyes are processed using a variety of procedures commonly employed in industrial effluent treatment, such as membrane process (Liu et al., 2020; Rashidi et al., 2015), solidification (Khayat and Zali-Boeini, 2019), ion exchange (Joseph et al., 2020), electrochemical oxidation (Rodríguez-Narváez et al., 2021), and absorption (Nouri et al., 2021; Saleh et al., 2021). However, among present treatment methods, adsorption is the most effective solution for removing contaminants from an aquatic environment due to its ease of usage and high efficiency (Nodehi et al., 2022; Sarbisheh et al., 2017; Tran et al., 2020). Absorption techniques can especially deal with different types of color. There are many adsorbents have been studied such as activated carbon (Hameed et al., 2007), graphene oxide (Zhang et al., 2011), carbon

Citation: Hiep NT, Thu TTH, Quyen LTT, Dong PD, Suong TT, Vu TP. Biochar derived from *Sesbania sesban* plant as a potential low-cost adsorbent for removal of methylene blue. Environ. Nat. Resour. J. 2022;20(6):611-620. (https://doi.org/10.32526/ennrj/20/202200119)

nanotubes (Li et al., 2013), bentonite (Oussalah and Boukerroui, 2020), and diatomite (Du and Danh, 2021). Furthermore, a numerical study on using low-cost and regeneration adsorbents have been investigated (Abdul et al., 2021; Alorabi et al., 2021; Hussain et al., 2022; Misran et al., 2022).

In recent years, biochar has been evaluated as a highly effective, environmentally safe and cost-effective adsorbent, which is used for water purification and removal of various contamination (Nguyen et al., 2021; Sutar et al., 2022). Biochar is produced by pyrolysis of organic raw materials under conditions in the absence or limitation of oxygen (Meyer et al., 2011). As reported by Lee et al. (2020), the biochar adsorption process is heavily influenced by biomass type, pyrolysis conditions, porosity, and surface functionalities. Moreover, the biochar has distinct qualities such as a huge surface area, a highly porous structure, enhanced surface functional groups, and mineral components. In order to produce biochar, various other biomass has been investigated such as agricultural organic waste, botanical biomass, and animal waste (Ahmad et al., 2020; Liu et al., 2012; Lonappan et al., 2016). However, to our knowledge, the preparation of biochar from *Sesbania sesban* plant has not been studied yet. Therefore, biochar generated from *S. sesban* plant is considered as a new type of biomass with properties that need to be explored. *S. sesban* plant is a scrub that fixes atmospheric N_2 and has both commercial and biological importance (Farghaly et al., 2022; Kwesiga et al., 1999). In Vietnam, the leaves of *S. sesban* are used as feed to augment rice straw in animal diets and as much in home gardens (Dan et al., 2011). *S. sesban* thrives rapidly in wetland areas in the Mekong Delta. Notably, the stem of *S. sesban* has a porous structure, light, and water absorption capacity. It is these unique properties that make *S. sesban* a potential biomass to produce biochar.

This study was carried out to figure out the adsorption potential of biochar derived from *S. sesban* biomass based on the experiments on methylene blue (MB) adsorption. The MB dye was thought as a model for visible pollution due to its strong adsorption onto the materials. The absorption process was carried out at different batch adsorption conditions (adsorbent dosage, initial MB concentration, contact time, and pH) and calculated through adsorption isotherms and kinetics. The biochar was characterized by Fourier transform infrared spectroscopy (FT-IR), scanning electron microscope (SEM) images, and Brunauer-Emmett-Teller (BET) analysis. This research advances our understanding of a new material and suggests a possible adsorbent for the treatment of dye-rich wastewater.

2. METHODOLOGY

2.1 Preparation of biochar and adsorbate

The *S. sesban* plant was harvested from the Mekong delta region in southwestern Vietnam and used to make biochar. *S. sesban* stalks were stripped of their shells and leaves, cut into small pieces, and dried outside for 2-4 days before being cleaned to remove contaminants. Next, the material was dried at 105°C in 24 h. To make biochar from *S. sesban*, the materials were placed in inox cups with lids and heated under oxygen-limited conditions in a muffle furnace (Nabertherm GmbH, model B410, Germany). This muffle furnace was set to heat to 300°C at a rate of 10°C/min, and it was kept there for 2 h. Lastly, the biochar was crushed into small particles and then screened through sieves with a mesh size of 0.15 mm. The biochar derived from *S. sesban* plant was abbreviated as BSS. It was kept in an airtight container until used in adsorption experiments.

Methylene Blue (MB), a cationic dye with a chemical formula of $C_{16}H_{18}ClN_3S$, was chosen as the adsorbate in this research. It was purchased from Xilong Chemical Co., Ltd., China. The MB stock solution (1,000 mg/L) was made with distilled water. The working solutions were made by diluting this stock solution with distilled water to the required concentration.

2.2 Analysis of the biochar characterization

The pH value at the point of zero charge (pH_{pzc}) of the biochar was determined using the solid addition method. Accordingly, around 50 mL of 0.1 M NaCl was prepared in a series of 100 mL Erlenmeyer flasks. The initial pH values (pH_i) were roughly adjusted in the pH range of 2-12 by adding 0.1 M HCl or 0.1 M NaOH solution. Then, 1 g of biochar was added to each 50 mL conical flask. After 24 h of shaking using a rotary shaker at room temperature, the final pH values (pH_f) of the solution were determined. Finally, the difference between pH_i and pH_f ($\Delta pH = pH_i - pH_f$) was plotted against pH_i. The point of zero charge (pH_{pzc}) was defined as the intersection of the plot and the X-axis.

The microscopic surface texture of biochar was examined using a Scanning Electron Microscope (Thermo Scientific, model Prisma E SEM, USA). The functional groups present in the material were

characterized by Fourier Transform Infra-Red spectrometer (Thermo Scientific, model Nicolet iS5, USA). In addition, the specific surface areas of the adsorbent were measured by the Brunauer-Emmett-Teller (BET) method using nitrogen gas adsorption at -196°C as an analyzer.

2.3 Adsorption experiments

Batch experiments were conducted to investigate the efficiency of MB removal in an aqueous solution. The influence of varied reaction conditions on MB removal efficiency were examined by altering the pH solution (viz., 4, 5, 6, 7, 8, 9, 10, 11), contact time (viz., 0, 10, 20, 30, 40, 50, 60 min), biochar dosage (viz., 0.2, 0.4, 0.6, 0.8, 1.0, 1.2 g), and initial MB solution concentration (viz., 20, 30, 40, 50, 60, 70, 80 mg/L). Adsorption studies were carried out in Erlenmeyer flasks containing 50 mL of MB solution in a rotary shaker (Jeio Tech, model OS-2000, Korea) at 150 rpm and 30±2°C. After adsorption, the filter paper was used to get the adsorbent from the suspension. The concentration of filtrate was analyzed by measuring the MB absorbance using a UV-Vis spectrophotometer (Thermo Scientific, model Evolution 350, USA) at a wavelength of maximum absorbance (665 nm). All of the experiments were carried out in triplicates.

The amount of adsorbate at equilibrium, at a particular time and MB removal efficiency, were calculated using the equations (1-3), respectively (Tehubijuluw et al., 2021).

$$\text{The adsorption capacity at equilibrium: } q_e = \frac{C_0 - C_e}{m} \times V \quad (1)$$

$$\text{The adsorption capacity at a particular time: } q_t = \frac{C_0 - C_t}{m} \times V \quad (2)$$

$$\text{Removal efficiency: } H\% = \frac{C_0 - C_e}{C_0} \times 100 \quad (3)$$

Where; q_e is the adsorption capacity at equilibrium, q_t is the adsorption capacity at a particular time, C_0 is the initial MB solution concentration (mg/L), C_e is the equilibrium MB solution concentration (mg/L), C_t is the MB solution concentration (mg/L) at time t, V is the volume of solution (L), and m is the mass of the biochar (g).

2.4 Adsorption isotherm and kinetic models

The Langmuir and Freundlich (Assimeddine et al., 2022; Shayesteh et al., 2016) adsorption isotherm models were used to study the adsorption performance at equilibrium. The non-linear forms of the isotherm models are shown in Equations (4-5).

$$\text{Langmuir adsorption isotherm model: } q_e = \frac{Q_{max} K_L C_e}{1 + K_L C_e} \quad (4)$$

$$\text{Freundlich adsorption isotherm model: } q_e = K_F C_e^{(1/n)} \quad (5)$$

Where; C_e (mg/L) is the equilibrium concentration of the MB, q_e (mg/g) is the amount of MB adsorbed per unit mass of biochar, Q_{max} is maximum adsorption capacity (mg/g), K_L (L/mg) is the Langmuir constant related to the heat of adsorption, K_F [(mg/g)/(mg/L)$^{1/n}$] is the Freundlich adsorption capacity, and 1/n (dimensionless) is a Freundlich intensity parameter.

In terms of adsorption kinetics, pseudo-first-order kinetic model and pseudo-second-order kinetic model were applied to investigate MB adsorption capability onto each adsorbent surface (Shayesteh et al., 2016). The formulas of the models are expressed in non-linear form as follows:

$$\text{Pseudo-first-order kinetic model: } q_t = q_e\left(1 - \exp^{-k_1 t}\right) \quad (6)$$

$$\text{Pseudo-second-order kinetic model: } q_t = \frac{q_e^2 k_2 t}{1 + q_e k_2 t} \quad (7)$$

Where; q_e (mg/g) is the adsorbed amount at equilibrium, q_t (mg/g) the adsorbed amount at time t (min). In addition, k_1 (1/min) and k_2 (g/mg.min) were respectively the rate constants of the two kinetic models.

3. RESULTS AND DISCUSSION

3.1 Characterization of adsorbent

3.1.1 Fourier transforms infrared analysis (FTIR)

The presence of organic functional groups on the surface of BSS were characterized using FTIR analysis. Figure 1 shows the FTIR spectrum of BSS. The broad absorption band at 3,500-3,300 cm^{-1} was expressed with a peak band of about 3,451 cm^{-1} due to O-H vibrations of alcohols, phenols, and carboxylic acids, as in cellulose and lignin. As a result, phenolic and acidic groups were responsible for the adsorption of MB dye on BSS. The small peaks at 2,937 and 2,869 cm^{-1} can be attributed to the C-H stretching (Bhattacharya et al., 2021). The absorption band near 1,640 cm^{-1} corresponds to the C=C stretching vibration from conjugated alkene groups. The peak at 1,450 cm^{-1} may be regarded as a C-H bending vibration caused by the

methyl group. Another band was found at about 1,222 cm^{-1}, which was associated with C-O stretching.

3.1.2 Scanning electron microscopy (SEM)

The morphology of the BSS is presented in the SEM image (Figure 2). The surface of BSS is relatively smooth, porous texture, and stacks evenly. This unique morphological result led to a high surface area. In addition, the block pore structure facilitated MB adsorption.

3.1.3 Specific surface area

The physical properties of BSS were analyzed in order to confirm the specific surface area, pore diameter, and total pore volume (Table 1). The BET results have shown a huge surface area of up to 561.8 m^2/g. This surface area is higher than that of other non-modified biochar. Therefore, it is envisaged that they will have a high adsorption capability to the MB dye in an aqueous solution.

3.1.4 pH zero charge point (pH_{pzc})

The pH_{pzc} (zero charge point pH) describes the pH value at which the surface charge of the adsorbent is zero. This is a vital parameter in adsorption processes that demonstrates the comprehensive effects of functional groups on the surface of biochar. Essentially, when the pH_{pzc} is greater than the solution pH, the adsorbent surface becomes positively charged; conversely, when the pH_{pzc} is less than the solution pH, the adsorbent surface becomes negatively charged. The result of this research showed that the pH_{pzc} value of the BSS was roughly 6.9 (Figure 3). When the solution pH was above 6.9, the surface of the adsorbent was negatively charged. As a result, the BSS efficiently adsorb a cationic MB dye.

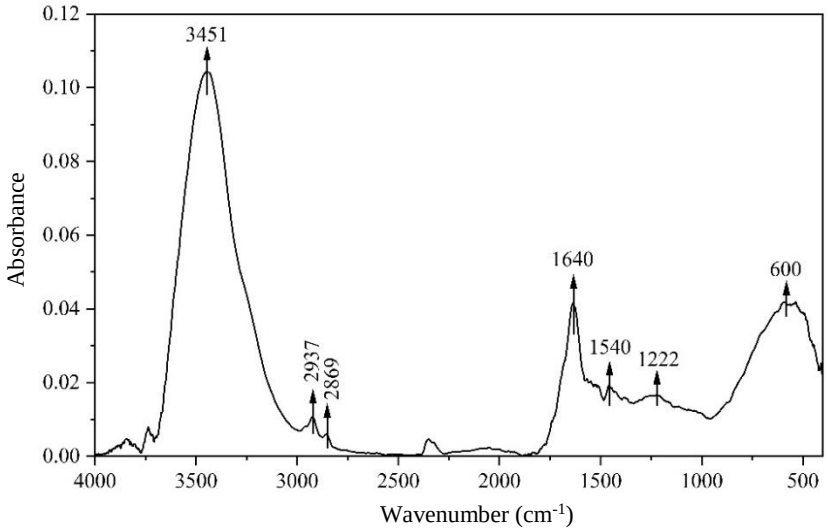

Figure 1. FTIR spectra of biochar

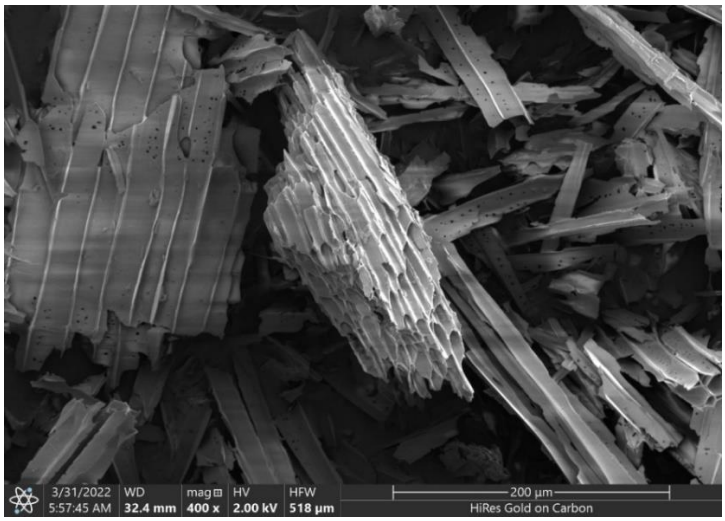

Figure 2. The SEM morphology of BSS

Table 1. The physical properties of BSS for N_2 adsorption

Parameters	Value
BET specific surface area (m^2/g)	561.8
Total pore volume (cm^3/g)	0.5
Pore diameter (nm)	3.7

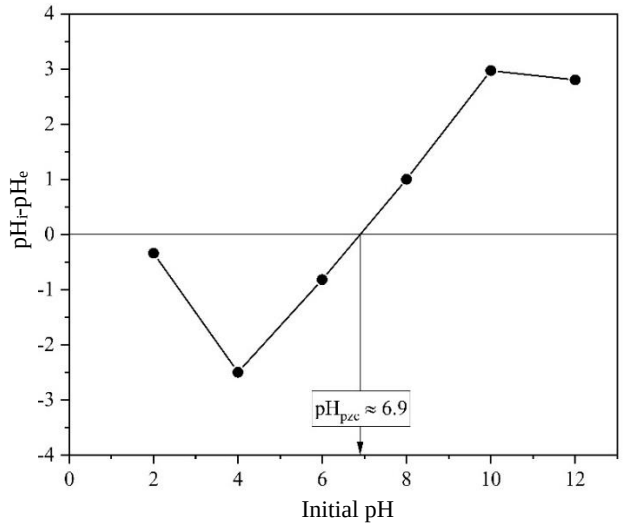

Figure 3. The pH zero charge point (pH_{pzc}) of BSS

3.2 Adsorption performance

3.2.1 Influence of pH on adsorption

The initial solution pH is a vital parameter in the adsorption process which can affect the surface charge of the biochar as well as the chemistry of the adsorbate. Furthermore, the influence of pH on MB adsorption might reveal information on adsorption mechanisms. Figure 4(a) shows the experimental performance of MB adsorption at different pH conditions. The results present an increasing trend in the MB removal efficiency and adsorption capacity of biochar as the pH increased from 4 to 11. This trend was consistent with the results of previous studies (Assimeddine et al., 2022; Dawood et al., 2016; Huang et al., 2018). The removal efficiency of MB was low ~66% at acidic pH (range 4-5). As the pH of the MB solution approached 11, the removal efficiency was approximately 90% and the adsorption capacity reached 3.4 mg/g. These results can be explained when the solution pH is above 6.9 ($pH_{solution} > pH_{pzc}$), the biochar surface is negatively charged, which promotes adsorption of the MB dye. This adsorption is principally caused by electrostatic attraction between the surface adsorbent and the positive charge MB molecules.

3.2.2 Influence of contact time on adsorption

The MB dye adsorption of biochar was investigated in the contact time of 10-60 min, pH of 11, and the adsorbent dosage of 0.4 g was mixed with the initial MB concentration of 30 mg/L. As indicated in Figure 4(b), the MB dye removal efficiency and adsorption capacity of biochar increased rapidly in the first 10 min, and then progressively stabilized. The first quick adsorption is caused by a physical mechanism involving solid-to-liquid mass transfer. The ensuing stabilization phase shows deterioration in physical adsorption with equilibrium and minor desorption of MB dye. In this study, the acceptable contact time for adsorption to reach an equilibrium state was 30 min. At this time, MB adsorption efficiency and adsorption capacity of biochar reached approximately 94% and 3.5 mg/g, respectively.

3.2.3 Influence of biochar dosage on adsorption

The MB dye adsorption performance at the different dosages of biochar is shown in Figure 4(c). The removal efficiency of MB dye increased rapidly (from 62.7±2.7% to 92.1±0.4%) when the biochar dosage was in the range of 0.2-0.4 g (per 50 mL of MB solution). The rise in adsorption efficiency with increasing adsorbent dosage was explained by the enhancement in the higher number of adsorption sites. When biochar dosage was increased from 0.4 to 0.8 g, the performance gradually stabled. However, when the biochar mass was increased to 1.2 g, the treatment efficiency tended to decrease slightly. The MB dye adsorption was enhanced insignificantly when the biochar dose was raised to a specified amount because the adsorbent layers overlapped and concealed the adsorbent active sites. The tendency to simultaneously increase the adsorption capacity and MB removal efficiency when increasing the amount of adsorbent was also found in some previous studies (Inyang et al., 2014; Lonappan et al., 2016; Sun et al., 2013). In this study, to save adsorbent cost, biochar in the amount of 0.6 g was suggested to be used for further experiments. At an adsorbent dosage of 0.6 g (per 50 mL of MB solution), MB dye adsorption efficiency and adsorption capacity of biochar reached approximately 95% and 3.6 mg/g, respectively.

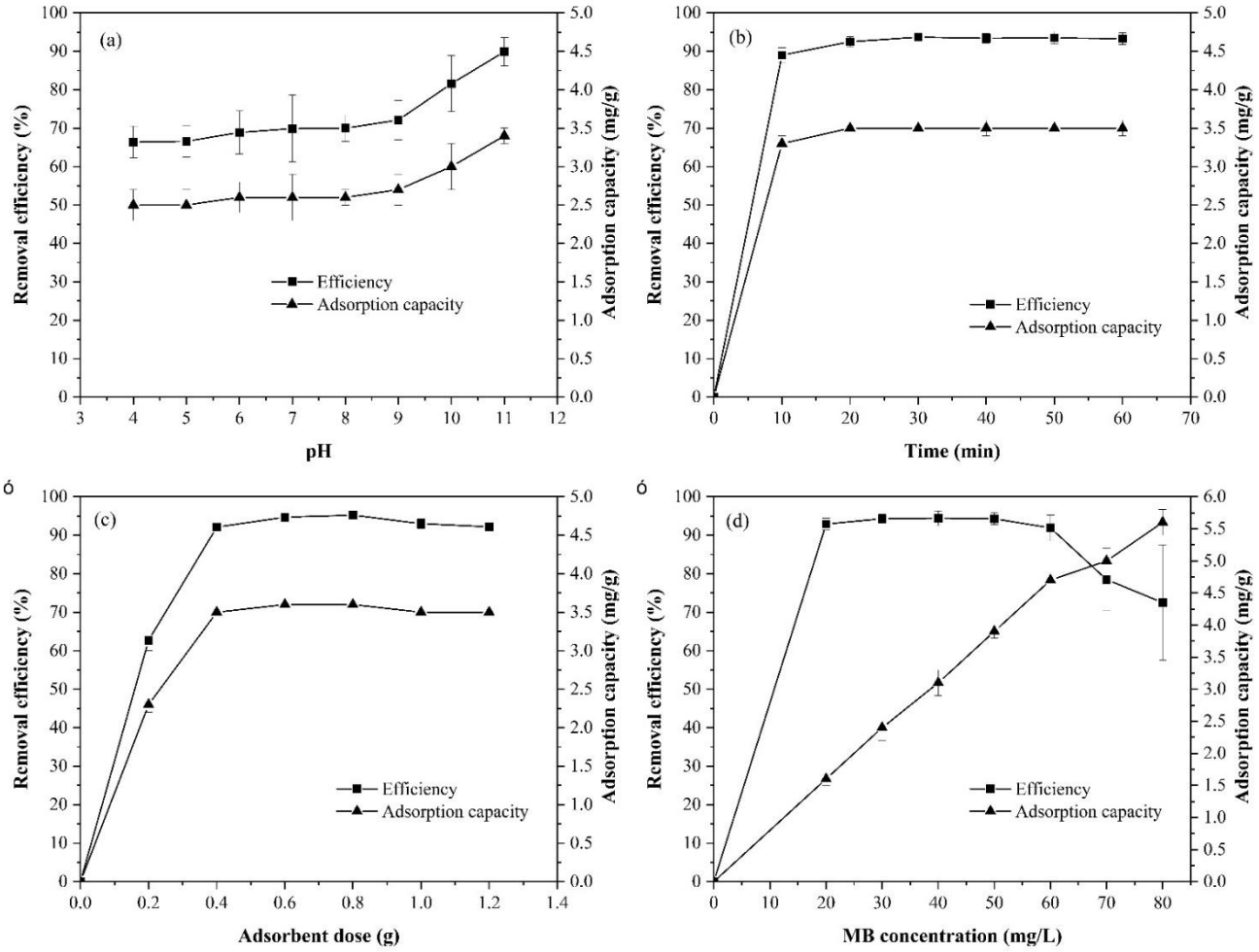

Figure 4. The influence of different experimental conditions on MB adsorption by biochar: (a) Initial pH solution, (b) Contact time, (c) Biochar dosage, and (d) MB concentration

3.2.4 Influence of initial MB concentration on adsorption

The effect of initial concentrations is an important factor for MB dye adsorption. In this study, MB concentrations were investigated in the range of 20-80 mg/L. As observed in Figure 4(c), the MB removal efficiency was over 90% when the initial dye concentration rose from 20 to 60 mg/L. Simultaneously, the adsorption capacity also enhanced from 1.6 to 4.7 mg/g in this MB concentration range. However, at the initial concentration of 80 mg/L, the treatment efficiency tended to decline sharply. This result was explained because the active sites of the adsorbent decreased compared to the increasing MB concentration. In contrast, the adsorption capacity continued to increase as MB concentration increased from 60 to 80 mg/L. According to Assimeddine et al. (2022), increasing the initial MB concentration improves the interaction between the MB molecules and the biochar particles, resulting in an increase in adsorption capacity. A similar trend was also reported in previous studies (Dawood et al., 2016; Phihusut and Chantharat, 2017; Subratti et al., 2021) on dye adsorption of biochar. In general, raising the concentration of MB enhanced adsorption capacity but decreased MB removal efficiency. Therefore, in this case, the appropriate initial MB concentration for the study was 50 mg/L. At this concentration, the removal efficiency reached 94.3±1.5%.

3.2.5 Adsorption isotherms

In essence, adsorption isotherms describe the relationship between MB concentration and adsorption capacity for a given biochar dose and temperature. Various isotherm models were applied to fit the experimental data and assess their usefulness for adsorption (Ayawei et al., 2017). In this study, the experimental data points were compared to theoretical Langmuir and Freundlich isotherms due to the simplicity of their model parameters. It can be seen in Figure 5 that Langmuir model symbolled the adsorption process on biochar better than Freundlich

model did because its values were close to the experimental value. In contrast, the values in the Freundlich model deviate further from the experimental value rendering it unsuitable. In addition, the parameters and correlation coefficients of these two isotherm models provided in Table 2 confirmed that the studied adsorption process fitted to the Langmuir model due to its higher correlation coefficient (R^2). Therefore, the monolayer adsorption occurred and the adsorption sites are identical and energetically equivalent.

Table 2. The parameters of the Langmuir and Freundlich isotherm models for MB adsorbed onto BSS at 30±2°C

Isotherm models	Parameters value	Correlation coefficient (R^2)
Langmuir	Q_m = 6.6 (mg/g) K_L = 0.414 (L/g)	0.897
Freundlich	n = 2.4 K_F = 0.332 × [(mg/g)/(mg/L)$^{1/n}$]	0.725

Table 3 shows the comparison of the MB absorption capabilities of BSS to those of other adsorbents. It was well known that there are many factors influencing the adsorbent capacity of biochar, such as its surface property and particle size, adsorbate and solution properties, and temperature. Therefore, the comparison between the adsorption capacity of BSS biochar and other types of adsorbents was difficult because of their different research conditions. However, the adsorption capability of biochar generated in this study outperformed that of biochar derived from pine wood, coir pith carbon, and eucalyptus (Kavitha and Namasivayam, 2007; Lonappan et al., 2016; Sun et al., 2013).

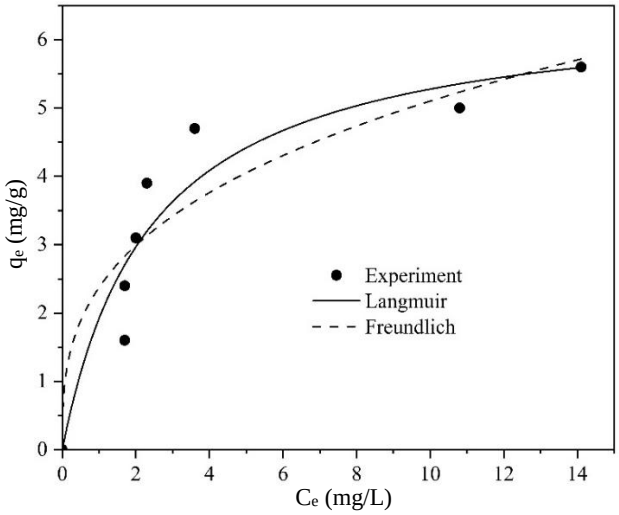

Figure 5. The adsorption isotherm models of MB dye onto BSS at 30±2°C

Table 3. The adsorption capabilities of various adsorbents for the elimination of MB dye

Adsorbents	Pyrolysis temperature (°C)	Heating time (h)	Q_{max} (mg/g)	References
Sesbania sesban	300	1	6.6	This research
Cedrela odorata (capsule-like interior)	400	1	158.5	Subratti et al. (2021)
Pine wood	525	-	3.9	Lonappan et al. (2016)
Eucalyptus	400	1	2.1	Sun et al. (2013)
Coir pith carbon	700	1	5.8	Kavitha and Namasivayam (2007)

3.2.6 Adsorption kinetic

The two kinetic models namely, pseudo-first-order and pseudo-second-order, have been analyzed to find out the kinetics and mechanism of the MB adsorption process. The results of the kinetic models are illustrated in Figure 6 and Table 4. According to the results, the two models matched the experimental data well, with a high correlation coefficient. However, chi-square values (χ^2) were analyzed to determine the best-fit kinetic models. The χ^2 values were near zero when the data derived using models were similar to that in (Ho and Wang, 2008). The constants, correlation coefficients, and χ^2 values of the kinetic models were shown in Table 4. The chi-square values of the pseudo-second-order (χ^2=0.001) were significantly lower than the pseudo-first-order (χ^2=2.106). Thus, the pseudo-second-order model was more correct in describing the adsorption process of BSS, whereas the pseudo-first-order model can only be suitable to describe the kinetics in the early stages of the adsorption process.

Table 4. The kinetic parameters for MB adsorption by BSS (non-linearized method)

Kinetic models	Parameters value	R^2	χ^2
Pseudo-first-order	$q_{e,exp}$ = 3.5 (mg/g) $q_{e,cal}$ = 3.5 (mg/g) k_1 = 0.29 (1/min)	0.999	2.106
Pseudo-second-order	$q_{e,exp}$ = 3.5 (mg/g) $q_{e,cal}$ = 3.6 (mg/g) k_2 = 0.39 (g/mg/min)	0.999	0.001

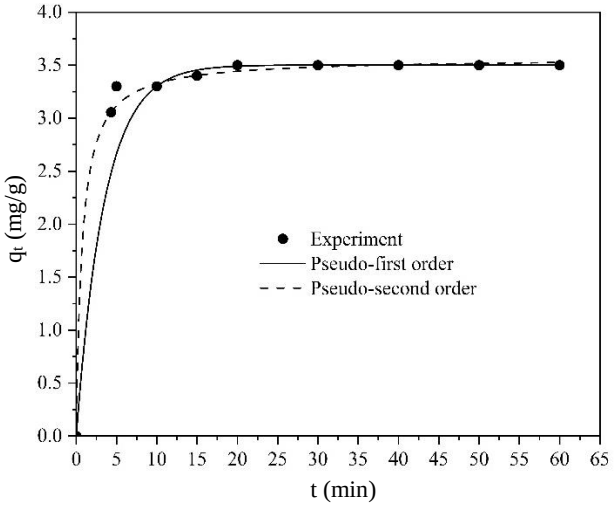

Figure 6. The adsorption kinetic models of MB dye onto BSS

4. CONCLUSION

Slow temperature pyrolysis resulted in BSS with a larger specific surface area and a more complex pore structure, indicating a strong adsorption potential. The adsorption factors, namely, initial pH, contact time, biochar dosage, and MB concentration, all had a substantial impact on MB adsorption. The equilibrium data fit well to the Langmuir isotherm model with the maximum adsorption capacity of 6.6 mg/g. The reaction achieved equilibrium in 30 minutes, and the adsorption kinetics followed the pseudo-second-order model. In general, the current investigation has demonstrated that the BSS looks to be a promising adsorbent candidate for the decolorization of dye-containing effluents. Furthermore, the BSS can be regenerated using the proper processes. If it is not economically feasible to regenerate the BSS, it must be treated according to hazardous waste procedures. Therefore, the regeneration of BSS also needs to be further studied to find an economically appropriate method and efficient reuse of materials.

ACKNOWLEDGEMENTS

The authors would like to thank the Center Laboratory of Research Institute for Sustainable Development, Ho Chi Minh University of Natural Resources and Environment for providing research facilities.

REFERENCES

Abdul RAR, Mohsin HM, Chin KBL, Johari K, Saman N. Promising low-cost adsorbent from desiccated coconut waste for removal of Congo red dye from aqueous solution. Water, Air, and Soil Pollution 2021;232(9):1-11.

Ahmad A, Khan N, Giri BS, Chowdhary P, Chaturvedi P. Removal of methylene blue dye using rice husk, cow dung and sludge biochar: Characterization, application, and kinetic studies. Bioresource Technology 2020;306:Article No. 123202.

Alorabi AQ, Hassan MS, Alam MM, Zabin SA, Alsenani NI, Baghdadi NE. Natural clay as a low-cost adsorbent for crystal violet dye removal and antimicrobial activity. Nanomaterials 2021;11(11):Article No. 2789.

Assimeddine M, Abdennouri M, Barka N, Elmoubarki R, Sadiq Mh. Natural phosphates characterization and evaluation of their removal efficiency of methylene blue and methyl orange from aqueous media. Environment and Natural Resources Journal 2022;20(1):29-41.

Ayawei N, Ebelegi AN, Wankasi D. Modelling and interpretation of adsorption isotherms. Journal of Chemistry 2017;2017: Article No. 3039817.

Bhattacharya S, Bar N, Rajbansi B, Das SK. Adsorptive elimination of Cu (II) from aqueous solution by chitosan-nanoSiO_2 nanocomposite: Adsorption study, MLR, and GA modeling. Water, Air, and Soil Pollution 2021;232(4):1-23.

Dan TH, Chiem NH, Brix H. Treatment of high-strength wastewater in tropical constructed wetlands planted with *Sesbania sesban*: Horizontal subsurface flow versus vertical downflow. Ecological Engineering 2011;37(5):711-20.

Dawood S, Sen TK, Phan C. Adsorption removal of Methylene blue (MB) dye from aqueous solution by bio-char prepared from *Eucalyptus sheathiana* bark: Kinetic, equilibrium, mechanism, thermodynamic and process design. Desalination and Water Treatment 2016;57(59):28964-80.

Du PD, Danh HT. Single and binary adsorption systems of Rhodamine B and methylene blue onto alkali-activated Vietnamese diatomite. Adsorption Science and Technology 2021;2021:Article No. 1014354.

Farghaly MM, Youssef IM, Radwan MA, Hamdon HA. Effect of feeding *Sesbania sesban* and reed grass on growth performance, blood parameters, and meat quality of growing lambs. Tropical Animal Health and Production 2022;54(1):1-13.

Hameed B, Ahmad A, Latiff K. Adsorption of basic dye (methylene blue) onto activated carbon prepared from rattan sawdust. Dyes and Pigments 2007;75(1):143-9.

Ho YS, Wang CC. Sorption equilibrium of mercury onto ground-up tree fern. Journal of Hazardous Materials 2008;156(1-3):398-404.

Huang W, Chen J, Zhang J. Adsorption characteristics of methylene blue by biochar prepared using sheep, rabbit, and pig manure. Environmental Science and Pollution Research 2018;25(29):29256-66.

Hussain Z, Chang N, Sun J, Xiang S, Ayaz T, Zhang H, et al. Modification of coal fly ash and its use as low-cost adsorbent for the removal of directive, acid and reactive dyes. Journal of Hazardous Materials 2022;422:Article No. 126778.

Inyang M, Gao B, Zimmerman A, Zhang M, Chen H. Synthesis, characterization, and dye sorption ability of carbon nanotube-biochar nanocomposites. Chemical Engineering Journal 2014;236:39-46.

Joseph J, Radhakrishnan RC, Johnson JK, Joy SP, Thomas J. Ion-exchange mediated removal of cationic dye-stuffs from water using ammonium phosphomolybdate. Materials Chemistry and Physics 2020;242:Article No. 122488.

Kavitha D, Namasivayam C. Experimental and kinetic studies on methylene blue adsorption by coir pith carbon. Bioresource Technology 2007;98(1):14-21.

Khayat Z, Zali-Boeini H. Phase selective amphiphilic super-gelators for oil spill solidification and dye removal. Soft Materials 2019;17(2):150-8.

Kwesiga F, Franzel S, Place F, Phiri D, Simwanza C. *Sesbania sesban* improved fallows in eastern Zambia: Their inception, development and farmer enthusiasm. Agroforestry Systems 1999;47(1):49-66.

Lee T, Nam IH, Jung S, Park YK, Kwon EE. Synthesis of nickel/biochar composite from pyrolysis of *Microcystis aeruginosa* and its practical use for syngas production. Bioresource Technology 2020;300:Article No. 122712.

Li Y, Du Q, Liu T, Peng X, Wang J, Sun J, et al. Comparative study of methylene blue dye adsorption onto activated carbon, graphene oxide, and carbon nanotubes. Chemical Engineering Research and Design 2013;91(2):361-8.

Liu H, Zhang J, Lu M, Liang L, Zhang H, Wei J. Biosynthesis based membrane filtration coupled with iron nanoparticles reduction process in removal of dyes. Chemical Engineering Journal 2020;387:Article No. 124202.

Liu Y, Zhao X, Li J, Ma D, Han R. Characterization of bio-char from pyrolysis of wheat straw and its evaluation on methylene blue adsorption. Desalination and Water Treatment 2012; 46(1-3):115-23.

Lonappan L, Rouissi T, Das RK, Brar SK, Ramirez AA, Verma M, et al. Adsorption of methylene blue on biochar microparticles derived from different waste materials. Waste Management 2016;49:537-44.

Meyer S, Glaser B, Quicker P. Technical, economical, and climate-related aspects of biochar production technologies: A literature review. Environmental Science and Technology 2011;45(22):9473-83.

Misran E, Bani O, Situmeang EM, Purba AS. Banana stem based activated carbon as a low-cost adsorbent for methylene blue removal: Isotherm, kinetics, and reusability. Alexandria Engineering Journal 2022;61(3):1946-55.

Nguyen XC, Nguyen TTH, Nguyen THC, Van Le Q, Vo TYB, Tran TCP, et al. Sustainable carbonaceous biochar adsorbents derived from agro-wastes and invasive plants for cation dye adsorption from water. Chemosphere 2021;282:Article No. 131009.

Nodehi R, Shayesteh H, Rahbar-Kelishami A. Fe_3O_4@ NiO core-shell magnetic nanoparticle for highly efficient removal of Alizarin red S anionic dye. International Journal of Environmental Science and Technology 2022;19(4):2899-912.

Nouri H, Azin E, Kamyabi A, Moghimi H. Biosorption performance and cell surface properties of a fungal-based sorbent in azo dye removal coupled with textile wastewater. International Journal of Environmental Science and Technology 2021;18(9):2545-58.

Oussalah A, Boukerroui A. Alginate-bentonite beads for efficient adsorption of methylene blue dye. Euro-Mediterranean Journal for Environmental Integration 2020;5(2):1-10.

Phihusut D, Chantharat M. Removal of methylene blue using agricultural waste: A case study of rice husk and rice husk ash from chaipattana rice mill demonstration center. Environment and Natural Resources Journal 2017;15(2):30-8.

Rahman-Setayesh MR, Rahbar Kelishami A, Shayesteh H. Equilibrium, kinetic, and thermodynamic applications for methylene blue removal using *Buxus sempervirens* leaf powder as a powerful low-cost adsorbent. Journal of Particle Science and Technology 2019;5(4):161-70.

Rashidi HR, Sulaiman NMN, Hashim NA, Hassan CRC, Ramli MR. Synthetic reactive dye wastewater treatment by using nano-membrane filtration. Desalination and Water Treatment 2015;55(1):86-95.

Rodríguez-Narváez OM, Picos AR, Bravo-Yumi N, Pacheco-Alvarez M, Martínez-Huitle CA, Peralta-Hernández JM. Electrochemical oxidation technology to treat textile wastewaters. Current Opinion in Electrochemistry 2021; 29:Article No. 100806.

Saleh AK, El-Gendi H, Ray JB, Taha TH. A low-cost effective media from starch kitchen waste for bacterial cellulose production and its application as simultaneous absorbance for methylene blue dye removal. Biomass Conversion and Biorefinery 2021;preprint:1-13.

Sarbisheh F, Norouzbeigi R, Hemmati F, Shayesteh H. Application of response surface methodology for modeling and optimization of malachite green adsorption by modified sphagnum peat moss as a low cost biosorbent. Desalination and Water Treatment 2017;59:230-42.

Shayesteh H, Rahbar-Kelishami A, Norouzbeigi R. Evaluation of natural and cationic surfactant modified pumice for congo red removal in batch mode: Kinetic, equilibrium, and thermodynamic studies. Journal of Molecular Liquids 2016;221:1-11.

Subratti A, Vidal JL, Lalgee LJ, Kerton FM, Jalsa NK. Preparation and characterization of biochar derived from the fruit seed of *Cedrela odorata* L. and evaluation of its adsorption capacity with methylene blue. Sustainable Chemistry and Pharmacy 2021;21:Article No. 100421.

Sun L, Wan S, Luo W. Biochars prepared from anaerobic digestion residue, palm bark, and eucalyptus for adsorption of cationic methylene blue dye: Characterization, equilibrium, and kinetic studies. Bioresource Technology 2013;140:406-13.

Sutar S, Patil P, Jadhav J. Recent advances in biochar technology for textile dyes wastewater remediation: A review. Environmental Research 2022;209:Article No. 112841.

Tehubijuluw H, Subagyo R, Yulita MF, Nugraha RE, Kusumawati Y, Bahruji H, et al. Utilization of red mud waste into mesoporous ZSM-5 for methylene blue adsorption-desorption studies. Environmental Science and Pollution Research 2021;28(28):37354-70.

Tran TH, Le AH, Pham TH, Nguyen DT, Chang SW, Chung WJ, et al. Adsorption isotherms and kinetic modeling of methylene

blue dye onto a carbonaceous hydrochar adsorbent derived from coffee husk waste. Science of the Total Environment 2020;725:Article No. 138325.

Zhang W, Zhou C, Zhou W, Lei A, Zhang Q, Wan Q, et al. Fast and considerable adsorption of methylene blue dye onto graphene oxide. Bulletin of Environmental Contamination and Toxicology 2011;87(1):86-90.

Methane and Nitrous Oxide Emissions from Lowland Rice as Affected by Farmers' Adopted Fertilizer Applications under Two Crop Establishment Methods in Myanmar

Myo Thet Tin[1], Amnat Chidthaisong[2], Nathsuda Pumijumnong[1], Noppol Arunrat[1], and Monthira Yuttitham[1*]

[1]Faculty of Environment and Resource Studies, Mahidol University, Nakhon Pathom 73170, Thailand
[2]The Joint Graduate School of Energy and Environment, King Mongkut's University of Technology Thonburi, 126 Prachauthit Rd, Bangmod, Tungkru, Bangkok 10140, Thailand

ARTICLE INFO

Received: 12 Apr 2022
Received in revised: 22 Jul 2022
Accepted: 2 Aug 2022
Published online: 6 Sep 2022
DOI: 10.32526/ennrj/20/202200095

Keywords:
Greenhouse gas emissions/ Fertilizer application/ CH_4/ N_2O/ Rice cropping establishment

*** Corresponding author:**
E-mail:
monthira.yut@mahidol.ac.th;
monthira.yut@mahidol.edu

ABSTRACT

Identifying the optimal rice establishment option combined with specific fertilizer application can lower the global warming potential (GWP) and greenhouse gases intensity (GHGI) of rice production. In this study, methane (CH_4) and nitric oxide (N_2O) emissions and rice yields under different fertilizer application methods and two different planting methods, transplanted rice (TPR) and wet bed direct seeded rice (WDSR), was measured. Field experiments using a split plot design and closed chamber-GC method for gas flux measurements were conducted. CH_4 and N_2O emissions ranged from 1.83-4.68 mg/m^2/h and 0.073-0.135 mg/m^2/h, respectively. Minimum CH_4 and N_2O emissions were observed at 48-69 days after seedling (DAS) (tiller stage), while maximum emissions were generally found at 90 DAS or early primordial initiation (EPI) stage. It was found that TPR produced more CH_4 and N_2O than WDSR across fertilizers methods almost each growth stage throughout the growing period. Regarding GHGs emission factors, CH_4 emissions were negatively correlated with soil pH (-0.35*, N=18). At higher soil pH, lower CH_4 emissions were found in early growth stages. The N_2O emissions did not correlate with soil pH (-0.04 ns, N=18). The highest average CH_4 emission was reached in 90 days after seedling and EPI when the soil temperature was maximal at 34.8°C. The correlation coefficient (r) between CH_4 emission and soil temperature was 0.48*, N=18, indicating a positive correlation.

1. INTRODUCTION

The addition of greenhouse gases (GHGs) to the global atmosphere has been ascending since the very first days of civilization. Among the several GHGs, the two major gases are methane (CH_4) and nitrous oxide (N_2O) which have global warming potentials (GWP) 28 and 265 times higher than carbon dioxide(CO_2) equivalent in a 100 year time horizon, respectively (Pachauri et al., 2014). Methane emissions from anthropogenic activities has been increasing at a rate from 0.5% to 1% per year and reached 16% of the total anthropogenic GHGs emissions in 2010. An additional 6% of the anthropogenic GHGs emission was from N_2O emissions (Pachauri et al., 2014).

The agriculture sector is the one of the main causes of anthropogenic GHGs emissions and accounts for 1.5% of global anthropogenic GHGs emissions (Lam et al., 2017; Mosier et al., 1998; Timilsina et al., 2020; Tubiello et al., 2013). Methane (CH_4) and nitrous oxide (N_2O) are released from agricultural practices and are considered as the major source of greenhouse gases producing 60% of global N_2O emission and 50% of CH_4 emission (Linquist et al., 2012; Shukla et al., 2019). In the case of GHGs emission from the agricultural sector, rice cultivation is one important source of emitting CH_4 (Zhang et al., 2020) and N_2O (Lam et al., 2017; Mosier et al., 1998; Timilsina et al., 2020). Globally, rice is mostly grown and consumed in Asia and it will continue to influence

Citation: Tin MT, Chidthaisong A, Pumijumnong N, Arunrat N, Yuttitham M. Methane and nitrous oxide emissions from lowland rice as affected by farmers' adopted fertilizer applications under two crop establishment methods in Myanmar. Environ. Nat. Resour. J. 2022;20(6):621-633. (https://doi.org/10.32526/ennrj/20/202200095)

the world rice economy as per capita rice consumption of Asia increased from 85 kg per year in the early 1960s to nearly 103 kg in the early 1990s (Chauhan et al., 2017). Moreover, rice production in Asia accounts for 90% of total rice production (Bandumula, 2018).

The major cause of CH_4 emissions from agriculture land is biologically mediated processes of methanogenesis bacteria as a consequence of organic matter decomposition especially in anaerobic soil conditions (Conrad, 2002; Sass et al., 2002) while nitrification and denitrification of soil influence N_2O emissions (Smith, 2010). Therefore, mitigation strategies of CH_4 and N_2O emissions are considered on the management of soil submergence duration or irrigation practices and controlling the carbon inputs, for instance, crop establishment management and fertilizer application (Linquist et al., 2012; Yan et al., 2005). Additionally, The rice cultivation practice including selection of rice cultivar crop variety, fertilizer management and water management are the determinant factors of these emissions (Sun et al., 2013).

Myanmar is traditionally an agricultural country and this sector contributes 20.1% of the national Gross Domestic Profit (GDP) (MoALI, 2019). Among the diverse crops, rice is major crop and yield maximization strategies are given as high priority for domestic consumption and for exports as well. Two popular practices for local farmers are transplanted rice (TPR) and wet bed direct seeded rice (WDSR). Generally, TPR method utilizes intensive inputs and large amounts of water and labor resulting in a high cost of production (Chauhan et al., 2017; MoALI, 2019). Meanwhile, WDSR method seeded directly on non-puddle soil has become very popular since it can solve water shortage and labor scarcity problems. It also has a high cost-benefit ratio (Janz et al., 2016; Pathak et al., 2013). Several studies have indicated that crop establishment using WDSR with appropriate water management will be a potentially better CH_4 mitigation strategy than TPR (Liu et al., 2014). Gupta et al. (2016) also highlighted the average CH_4 emission from TPR practice was more than 80% greater than the WDSR practice in two year experiments. In addition, WDSR with midseason drainage probably reduced the CH_4 emission rate up to 50% (Wassmann et al., 2004). WDSR may be easily accepted by different levels of rice farmers through less requirement of water and lower cost of production. The capacity for adaptation to climate change may also be good using WDSR which is relatively tolerant to drought and water stress (Pathak et al., 2013).

Concerning GHGs emissions from paddy fields in Myanmar, there are no robust research programs that have investigated the GHGs emissions from rice fields under different conditions. Both private and public sector have still overlooked that the agricultural sector can harm the environment. The Ministry of Natural Resources and Environmental Conservation (MONREC) issued the Environmental Conservation Law in 2012. This law has totally ignored GHGs emission from the agriculture sector and only paid attention upon the industrial sector, urbanization, tourism, and mining sectors. Furthermore, the System of Rice Intensification (SRI) policy was issued in 2018 as a national plan by the Ministry of Agriculture, Livestock and Irrigation (MOALI), Department of Planning (DoP) with two main objectives, securing national food security and increasing rice exports through developing agricultural economics, without consideration of environmental problems. As a consequence of current circumstances in Myanmar, it is truly necessary to initiate primary field experiments that underline the GHGs emission from the agricultural sector.

In this regard, the objective of this study was to answer the following question: Among the rice establishment methods and fertilizer applications currently practiced by the farmers in lowland rice system, is there a combination that significantly mitigates CH_4 and N_2O emissions?

If a particular rice establishment option or fertilizer application method can result in less CH_4 or N_2O emissions without reducing rice yield, it would be a valuable practice for cost effective GHGs mitigation strategy in sustainable rice production. Furthermore, the desired mitigation strategy should be compatible with the ongoing processes of farmers and can improve their current system to achieve systemic change for GHGs mitigation.

2. METHODOLOGY

2.1 Study area

The field experiment was carried out at Kyaukse research station in Kyaukse Township, Mandalay region, Myanmar (Figure 1) situated at 21º36′47″N 96º7′49″E and 77 m above average sea level, where many varieties of agricultural practices have been traditionally exercised by the farmers. Soil property of this area is carbonated Alluvial (Gleysol) in FAO/UNESCO system with very fine texture and

shallow soil profile. There is good water drainage and high water percolation but low moisture retaining capacity. The soil is suitable for cultivation of field crops with paddy-upland cropping system: green gram, chickpea, and sesame, sunflower as upland crops and rice as lowland crop.

As per lab analysis, soil texture in top soil is clay loam consisting of sand (34.2%), silt (38%), and clay (27.8%) with soil organic matter (2.9%). Soil reaction is moderately alkaline with a pH of (8.1) and electrical conductivity (EC) is 0.12 d/Sm. Low, medium and high rating of available N (59 mg/kg), K (225 mg/kg), and P (30 mg/kg), respectively. Relatively high exchangeable Calcium (12.4 cmole/kg) and exchangeable magnesium (11.9 cmole/kg) are contained in this soil. Calcium extractable SO_4-S was found to be sufficient (11 mg/kg) and DTPA extractable Zn (0.6 mg/kg), and Fe (53 mg/kg) could be rated as marginal and adequate, respectively, but exchangeable Mn (6.8 mg/kg) was rated as adequate in soil.

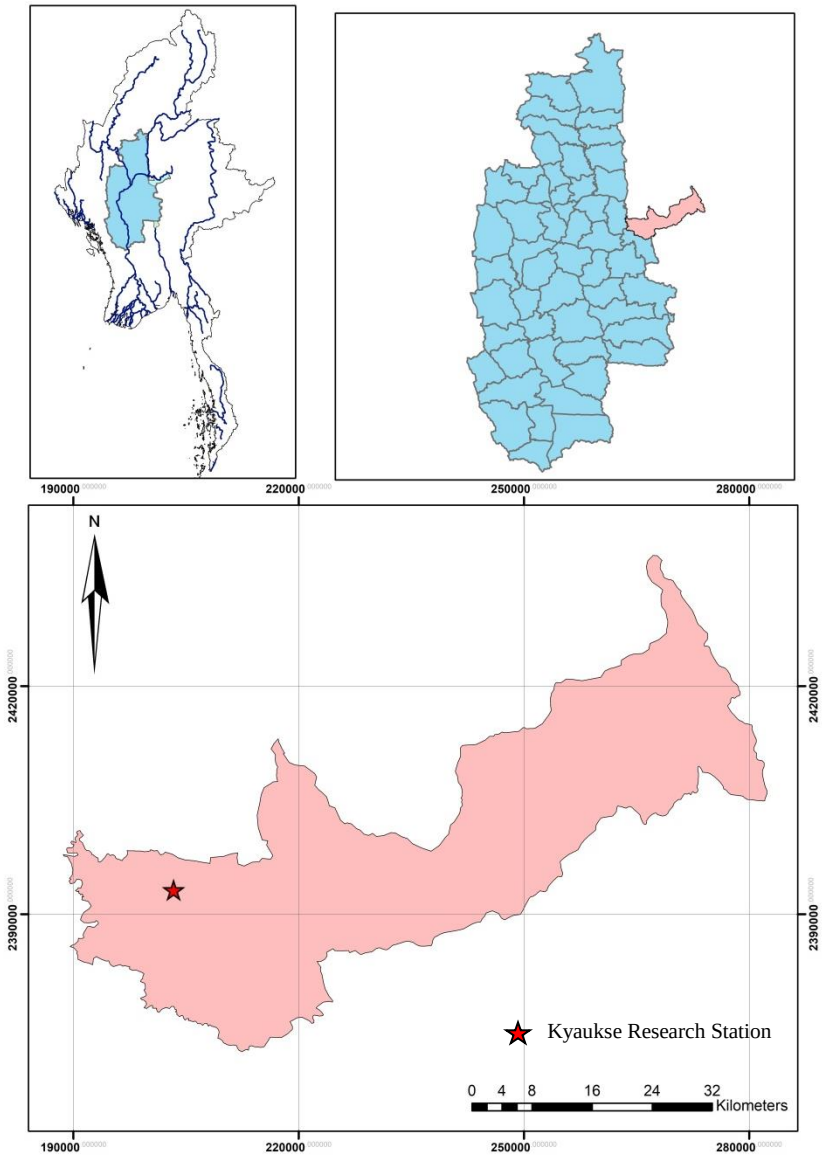

Figure 1. Location map of Kyaukse Township in Mandalay Region

2.2 Field experiment design, treatments, and layout

The two factors based on current local farmers' existing practices were designated as Crop establishment factor (Transplanted rice-TPR and Wet direct seeded rice-WDSR) and Fertilizer factor (F0, F1, and F2). The experimental design had two factors with three replications as a split plot design (Figure 2). The crop establishment and fertilizer application methods adopted in this experiment followed the local farmers' practices of rice cultivation.

As of crop establishment factor, the TPR was cultivated under wet condition and made puddling.

Twenty day-old seedlings of SinThuKha (IRYn1068-7-1 (Manawthukha/IRBB21) were transplanted and kept in flooded water as deep as 10 cm until one week before maturity but irrigated again whenever water reached 1 cm above soil level. The WDSR was grown under wet condition and made puddling and leveling. The same variety of rice, 70 kg/ha seed rate was sown with sprouted seeds through manual line sowing after thorough land leveling and draining water. Water was irrigated when seedlings were well survived and kept water level at about 3-5 cm. Flooded water was kept at about 10 cm depth and irrigated again when ever water reached 1 cm above soil level.

Regarding fertilizer factor, there were three treatments: Control (1) F0=No nitrogen + 63 kg TSP/ha (28 kg P_2O_5/ha) + 63 kg MOP/ha (37 kg K_2O/ha); (2) F1=Urea alone 189 kg urea/ha (86 kg N/ha) + 63 kg TSP/ha (28 kg P_2O_5/ha) + 63 kg MOP/ha (37 kg K_2O/ha); and (3). F2=124 kg/ha compound fertilizer (15:15:15), NPK were supplemented with 145 kg urea/ha (67 kg N/ha), 20 kg TSP/ha (9 kg P_2O_5/ha) and 30 kg MOP/ha (18 kg K_2O/ha).

TPR Plot	WDSR Plot
F1	F2
F0 (Control)	F1
F2	F0 (Control)

TPR Plot	WDSR Plot
F0 (Control)	F2
F1	F0 (Control)
F2	F1

TPR Plot	WDSR Plot
F1	F0 (Control)
F2	F2
F0 (Control)	F1

Figure 2. Field layout of experimental design

2.3 Sampling and measurement

Collected soil, plant, and gas samples were analyzed at the soil science research section and water utilization research section laboratories from the Department of Agricultural Research (DAR), Yezin, Nay Pyi Taw (ISO No. 90012015) under the Ministry of Agriculture, Livestock and Irrigation (MOALI) in Myanmar. Soil sample collection was made before and during field experimentation. Ten composite soil samples (0-15 cm) which had been randomly collected were taken at the experimental site before tillage preparation and at a depth of plow layer from each treatment one day after fertilizer split application at recovery, tillering, early panicle initiation (EPI), and booting stages to be analyzed for pH, EC, available N, P, K, and soil texture for expressing site characterization and to check for soil property changes. The Tyurin's method was used to determine the organic carbon using these soil samples and the result was expressed as percent.

Regarding grain yield of TPR treatments, rice plants were harvested from areas of 5 m^2 (2.74 m × 1.82 m) by rejecting two border rows and a sampling row to avoid interfering border effects. In WDSR treatments, since rice seeds are direct seeded into 20 cm rows, a 25 m linear row was harvested to be the same as 5 m^2 harvested areas. The rice grains were allowed to dry under sunshine to have restored seed moisture from about 16-17% to 14% which was checked by grain moisture meter. According to the guidance of laboratory of Department of Agricultural Research (DAR) DAR, the rice grain yield and biomass of each treatment was expressed as kg/ha.

Adjusted rice grain weight (kg/5 m^2) at 14% moisture
= (100 – M/86) × W

Where; M=moisture content of grain, W= weight of harvested grain from 5 m^2

For on-site data, soil pH, soil temperature and Oxidation-Reduction Potential (ORP) by portable pH/ORP/ISE (HANNA Model-HI98191), and air temperature, water depth and irrigation frequency were recorded at weekly intervals throughout the experiment. Soil temperature was also recorded at the same time of pH measurement.

2.4 Gas sample and analysis

In this study, a closed chamber was used to collect the gas emitted from the rice field (Yuesi and Yinghong, 2003; Zou et al., 2005). There are two parts, a chamber base with a size of 30 cm width × 40 cm length × 15 cm height made of aluminum, and a 30 cm width × 40 cm length × 60 cm or 120 cm height chamber cover made of acrylic. The chamber base was immersed 7.5 cm into the soil throughout cultivation period and the joints of the chamber were sealed by water. There are two holes on the top surface of chamber cover, one is for gas collection and the other one is used for measuring inside air temperature. Two covers having different heights of 60 and 120 cm, respectively, were used depending on plant height. The 60 cm cover was used for early stage while the 120 cm cover was utilized in the older stage of rice plants.

Fifty four (54) gas samples were collected on a weekly basis throughout the growing period from six treatments in three replications at intervals of 0, 10, and 20 min in the morning from 09.00 am to 12.00 am as adapted from several references (Huang et al., 2017; Liu et al., 2014; Venterea et al., 2011). Gas samples were collected into Aluminum foil multi-layer bag-ABS valve (Cap. 0.5 L) through suction with portable battery driven air pump (SB-980). Air temperature inside the chamber was also measured by thermometer with temperature sensor-tip and recorded at the time of gas collection. Collected gas samples were analyzed for CH_4 and N_2O using gas chromatography-GC (SHIMADZU-Model-2010 Plus). An SH-Rt-Q-BOND column (Serial No. 1357883) was used with a flame ignition detector (FID) for CH_4 and electron captured detector (ECD) for N_2O fluxes analysis. CH_4 and N_2O fluxes were calculated according to the following equation;

$$E = \frac{\text{Slope (ppm/min)} \times VC \times MW \times 60 \times 24}{22.4\ (273 + T/273) \times Ac \times 1{,}000}$$

The emissions as kg CH_4 (or kg N_2O)/ha were derived from the slope of the linear regression curve of gas (CH_4 and N_2O) concentrations against the chamber closing time. The slope was referred to as mass per unit area per unit time (mg/m^2/h) (Gaihre et al., 2013), where VC is the volume of the gas chamber in liters (L), MW is the molecular weight of the respective gas, 60 is minutes per hour and twenty four is hours of the day. The volume of 1 mol of gas in L at standard temperature and pressure is 22.4. T is the temperature inside the chamber (ºC) while 273 is the standard temperature of ºK. AC is the chamber area (m^2) and 1,000 is µg/mg (Islam et al., 2020).

According to the Fifth Assessment Report of the Intergovernmental Panel on Climate Change (AR5) CO_2 equivalents are used as 1 kg N_2O = 265 kg CO_2, and 1 kg CH_4 = 28 kg CO_2 (Myhre et al., 2013). GHG intensity (GHGI) (kg CO_2-equivalent/kg) was computed by dividing GWP of CH_4 and N_2O emissions by rice grain yield (Haque and Biswas, 2021).

$$\text{Total GWP (kg } CO_2 \text{ equivalent/ha)} = (CH_4 \text{ emission} \times 28) + (N_2O \text{ emission} \times 265)$$

$$\text{GHGI} = \text{Total GWP/Grain yield}$$

2.5 Statistical analysis

This is performed to compare seasonal value of CH_4 and N_2O gases emission, grain yield as affected by treatments (two factors: fertilizer factor and crop establishment factor) either individually or its interaction by using two way analysis of variances (F-test; ANOVA). Correlation coefficient (r) is used for indicating the relation between dependent variances; CH_4 and N_2O emission, grain yield and independent variances, such as fertilizer factor and crop establishment factor. Moreover, the statistical analysis was made between environmental factors such as pH, Eh, water depth and soil temperature and their influence on the fluxes of CH_4 and N_2O. The statistical significance was tested at (α=0.05) by statistical software SPSS (Statistical Package for Social Science) V.18.

3. RESULTS

3.1 Methane emission

Regarding weekly flux changes, TPR generally produced more CH_4 emissions as compared to WDSR throughout the rice growing period (Figure 3). CH_4 emissions are found to be relatively lower (2.15-5.03 mg/m^2/h) during the 30-48 days after seeding (DAS)

but gradually increased and maximized (20.23-24.04 mg/m^2/h) at EPI (90 DAS). After that, emissions gently decreased and minimized at maturity stage (132 DAS).

As far as fertilizer effect is concerned, flux change patterns throughout the growing period is observed to have similar trends as crop establishment (Figure 4). The emissions of CH_4 for F0, F1, and F2 are more or less minimum between 30-48 DAS but slowly elevated and peaked at EPI (90 DAS). After that, emissions tended to sharply decline up to maturity stage with minimum fluxes.

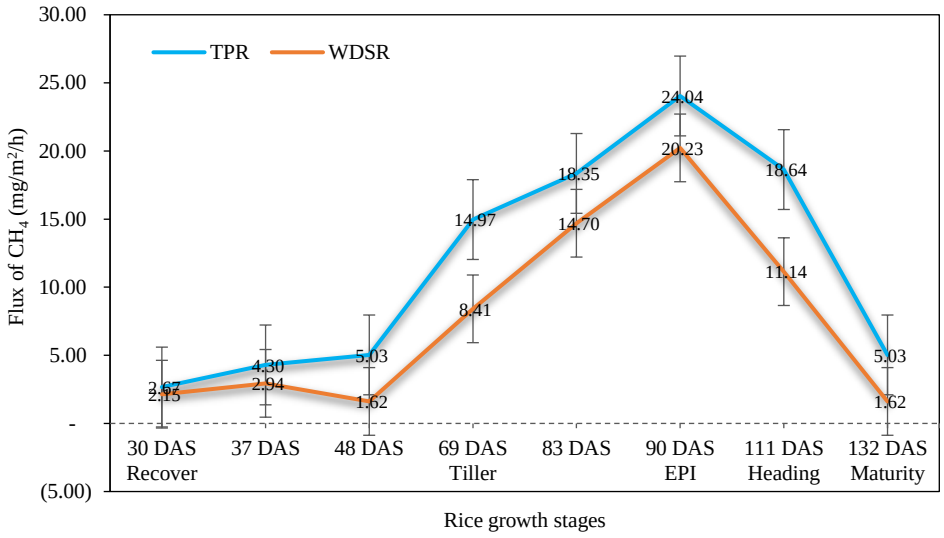

Figure 3. CH_4 fluxes of crop establishment methods (mg/m^2/h) by rice growth stages

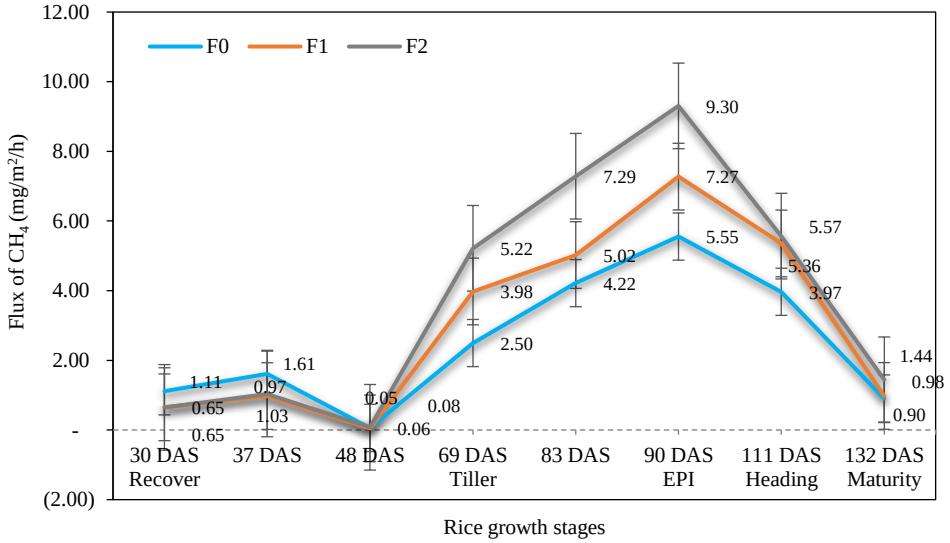

Figure 4. CH_4 fluxes of N fertilizer application methods (mg/m^2/h) by rice growth stages

3.2 Nitrous oxide emission

Regarding weekly N_2O flux changes by rice growth stages as affected by crop establishment, TPR produced slightly more N_2O than that of WDSR throughout the rice growing period, but they are not statistically different (Figure 5). In both TPR and WDSR, N_2O emissions are relatively higher during early stages of 30-37 DAS, unlike CH_4 emission in which fluxes are noticed as minimum during 30-37 DAS (Figure 3 and Figure 4). The N_2O emissions again declined and minimized at the tillering stage (69 DAS). After that, emissions slowly increased and was found to be highest at EPI stage (90 DAS). After EPI stage, N_2O fluxes slightly decreased but remained at levels similar to 30-37 DAS. The trend of all fertilizer treatments were more or less the same throughout the growing period and F2 produce more N_2O than the others (Figure 6). The emissions of N_2O for F0, F1,

and F2 were showed minimum fluxes between 48-83 DAS but slowly elevated and become stable after EPI (90 DAS). According to fluxes of CH_4 and N_2O result, the trade-off effect between CH_4 and N_2O occurred throughout the growth stages of rice cultivation.

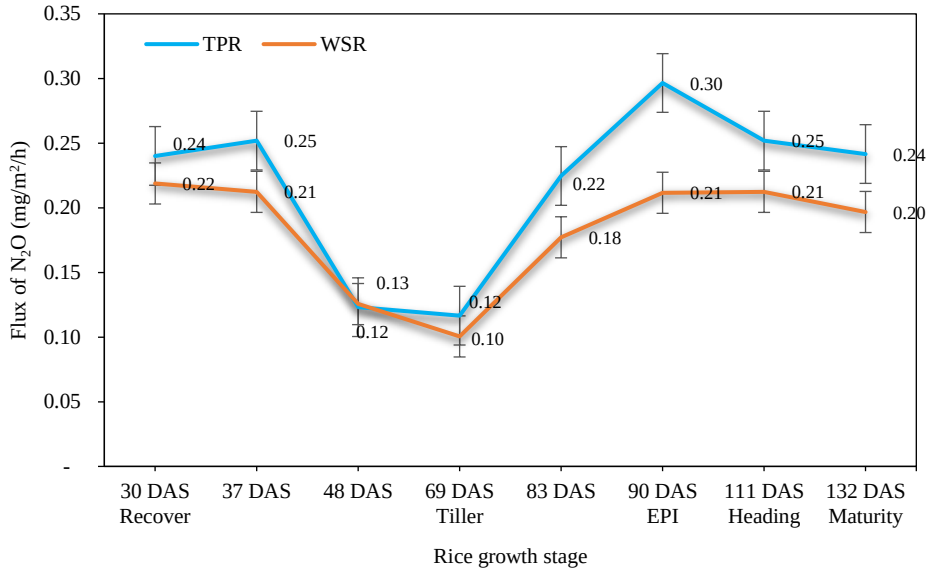

Figure 5. N_2O fluxes of crop establishment methods (mg/m^2/h) by rice growth stage

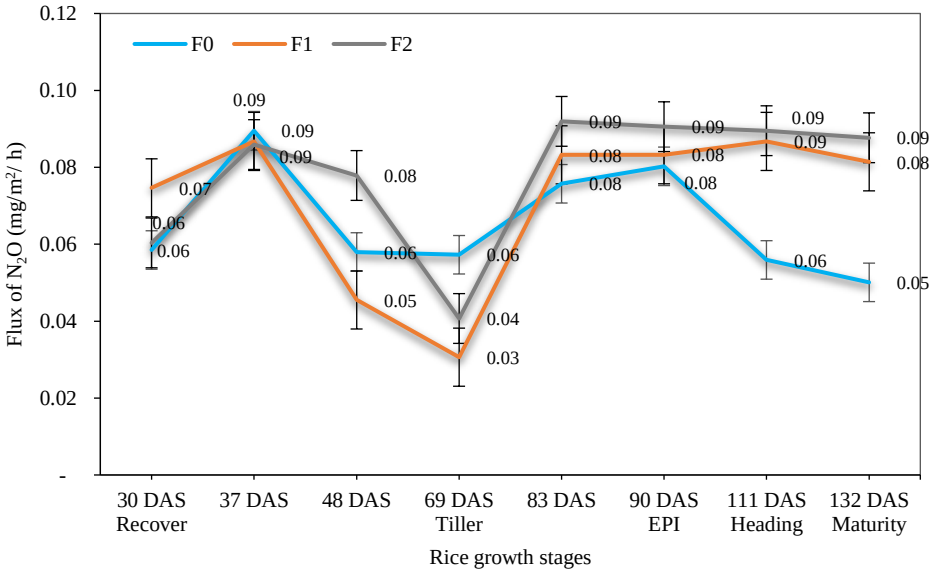

Figure 6. N_2O fluxes of N fertilizer application methods (mg/m^2/h) by rice growth stages

3.3 Rice grain yield

Rice grain yield and fluxes of CH_4 and N_2O as affected by crop establishment and fertilizer are shown in Table 1.

These data revealed that any two combination of crop establishment and fertilizer tested in this experiment (TPR, WDSR, and F1, F2) grain yields are not statistically different from each other (Table 1). Rice grain yields between TPR and WDSR are not significantly different across the fertilizers at the 5% probability level, while among F0, F1, and F2, grain yields are found to be significantly different using F0 (without N), but F1 and F2 were not different from each other.

3.4 Global worming potential (GWP) and greenhouse gas intensity (GHGI)

In Table 2, all fertilizer treatments with TPR contributed more GWP as compared to that of with WDSR indicating again TPR produced more GHG

emissions than WDSR. As for GHGI, GHGI, of TPR with all fertilizer treatments were found to be generally higher than that of WDSR. According to (Song et al., 2021b) WDSR practice indicated 75% lower GHGI than flooded TPR. It is noticeable that WDSR planting method is likely to be acceptable when compared with TRP across the fertilizer treatments owing to lower GHGI. When looking at WF1 (WDSR with urea) and WF2 (WDSR with compound fertilizer), GHGI is similar but WF1 had a 7% higher yield compared to WF2. Thus, based on GWP and GHGI analysis, WF1 (WDR with urea) is noticed to be suitable for cost efficient GHGs mitigation strategy.

Table 1. Rice grain yield (kg/ha) and fluxes of CH_4 and N_2O as affected by crop establishment and fertilizer

No	Treatment		Grain yield (kg/ha)	Average flux (mg/m^2/h)	
	Crop establish	Fertilizer		CH_4	N_2O
1	TPR	F0	5,370.39	3.27198	0.1348830
2	TPR	F1	6,846.36	3.58669	0.0976081
3	TPR	F2	6,868.53	4.68619	0.0683357
4	WDSR	F0	5,283.60	1.83577	0.0738248
5	WDSR	F1	6,527.40	2.71568	0.0844403
6	WDSR	F2	6,100.08	3.29895	0.0778937
5% LSD			**8,91.276**	**1.65580**	**0.1003500**
1	TPR		6,361.76	3.84828	0.1002760
2	WDSR		5,970.36	2.61680	0.0787196
5% LSD			783.367 NS	0.95597*	0.0579372 NS
1		F0	5,327.00	2.55378	0.1043540
2		F1	6,686.88	3.15119	0.0910242
3		F2	6,484.30	3.99257	0.0731147
5% LSD			640.357*	1.17083 NS	0.0709582 NS
C,V%			12.90	28.20	61.60

TPR=transplanted rice, WDSR=wet direct seeded rice, F0=no N, F1=urea, F2=compound fertilizer, LSD=the least significant difference, NS=not significant, *=significant at 5% probability level

Table 2. Average GWP kg CO_2eq/ha and GHGI of six treatments

No	Treatment		Rice grain yield (kg/ha)	CH_4 (kg/ha)	N_2O (kg/ha)	GWP (kg CO_2eq/ha)	GHGI (kg CO_2eq/kg)
	Crop establish	Fertilizer					
1	TPR	F0	5,370.39	109.93	4.53	4,238.48	0.79
2	TPR	F1	**6,846.36**	120.51	3.27	4,213.94	0.62
3	TPR	F2	**6,868.53**	157.45	2.29	4,996.56	0.73
4	WDSR	F0	5,283.60	61.68	2.48	2,362.09	0.45
5	WDSR	F1	**6,527.40**	91.24	2.83	**3,281.23**	**0.50**
6	WDSR	F2	**6,100.08**	110.84	2.61	3,773.66	0.62

TPR=transplanted rice, WDSR=wet direct seeded rice, F0=no N, F1=urea, F2=compound fertilizer

3.5 Environmental factors and GHGs emission correlation

Since the soil is calcareous, the average pH of all experimental units (EU) are kept higher at 8.5-8.6 in early stage during 30-37 DAS but gradually decreased after 37 DAS and maintained 7.05-7.55. The methane emissions in this study are negatively correlated with average soil pH (-0.35*, N=18) (Table 4) as the higher the average soil pH, the lower the CH_4 emission, as found in early growth stages (Table 3). Although soil pH was fairly stable around neutral after 48 DAS, CH_4 emissions are not consistent (Figure 3 and Figure 5). The N_2O emissions in this study did not correlatd with soil pH value (-0.04 ns N=18) (Table 4).

In this study, CH_4 emission are significantly correlated with average soil water depth of all plots (Table 4). The CH_4 emissions are noted as lower when average ORP -110.25 mV to -125.75 mV during 30-48 DAS under the water depth of 1.0-1.5 cm but gradually increased and peaked at -184.84 mV

(90DAS-EPI stage) under the average water depth of 5.8-6.0 cm, after that it sharply decreased when water depth was 0.0-0.5 cm and ORP was -123.64 mV to -125.25 mV at heading and maturity stages. In relation with N_2O emissions, it is relatively higher when ORP was -110.25 mV to -121.6 mV under the presence of water depth 1.0 cm during 30-37 DAS whereas CH_4 emissions are lower at that time. The ORP are noted to be lower (-189.74 mV to -189.84 mV) when water depths were under 5.6-6.0 cm during 69-90 DAS. However, correlation coefficient (r) of ORP between CH_4 and N_2O are 0.08 ns, N=18 and 0.05 ns, N=18, respectively. Thus, it implies that GHG emission (CH_4 and N_2O) is not correlated with ORP in this study.

At the time of 30 DAS, the average soil temperature was 27ºC and gently increased with growth stages, thereby CH_4 emissions are lower at early stages, but it slowly increased with increasing soil temperature. Average CH_4 emission peaked at 90 DAS, EPI when soil temperature reached its highest temperature at 34.84ºC. The correlation coefficient (r) between CH_4 emission and soil temperature is 0.48*, N=18 (Table 4). However, correlation between N_2O emission and soil temperature was not observed during this field experiment.

Table 3. Average soil pH, soil temperature, oxidation reduction potential (ORP), and water depth by rice growth stages

No	Growth stages	Soil pH	Soil temperature (ºC)	ORP (mV)	Water depth (cm)
1	30 DAS	8.60	27.00	-110.25	1.5
2	37 DAS	8.50	27.31	-121.60	1.5
3	48 DAS	7.55	29.30	-125.75	1.0
4	69 DAS Tiller	7.05	29.72	-189.74	5.8
5	83 DAS	7.73	29.91	-187.60	6.5
6	90 DAS EPI	7.50	34.87	-189.84	6.0
7	111 DAS Heading	7.52	29.76	-123.64	0.5
8	132 Maturity	7.52	27.00	-125.23	0.0

DAS=days after seeding

Table 4. Correlation coefficient (r) of GHGs emissions (CH_4 and N_2O) against the environmental factors

GHG ($mg/m^2/h$)	Environmental factors			
	pH	ORP (mV)	Water depth (cm)	Soil temperature (°C)
CH_4	-0.36*	0.08 NS	0.45*	0.48*
N_2O	-0.04 NS	0.05 NS	-0.14 NS	0.07 NS

NS=not significant, *=significant at 5% probability level

4. DISCUSSION

4.1 Emissions pattern of CH_4 and N_2O

Although the measurement of GHGs emissions from rice cultivation have been systemically researched by a number of regional countries in South East Asia, there is no reliable information available from Myanmar, especially CH_4 and N_2O emissions, from existing farmers' adopted fertilizer application under different rice establishment methods (Win et al., 2021). Further, the insight upon the consequences of the local farmers' adopted agricultural practices on CH_4 and N_2O emissions from rice cultivation was gained from this study. In this study, the trade-off effect between CH_4 and N_2O occurred which agreed with other research findings (Janz et al., 2016; Kong et al., 2021; Song et al., 2021b).

Along with the rice growth throughout the season, CH_4 fluxes increase continuously until 90 DAS (EPI stage) and after that descended rapidly, which were similar with the results of the previous studies (Gaihre et al., 2013). This may be due to crop residue accumulation which favors the emission of CH_4 (Janz et al., 2019). Moreover, the period between 83 DAS and 90 DAS (EPI stage) had the highest water depth (Table 3 and Figure 7). The effect of continuously flooded rice fields on CH_4 emission in assisting CH_4 production through creating anaerobic situation has been well documented (Gupta et al., 2016; Song et al., 2021a; Vo et al., 2018; Zhou et al., 2018). The anaerobic situation of soil aids the methanogenic bacteria which are the major source of CH_4 in the atmosphere (Haque and Biswas, 2021; Islam et al., 2020; Kong et al., 2021).

On the other hand, the trends of N_2O emission were not similar with CH_4 trend. The N_2O flux was higher at the 30 DAS and gradually reduced to the minimum rate at the 69 DAS or the tiller stage. Furthermore, the curve of N_2O emissions increased again until the EPI stage which was the highest stage of N_2O, while CH_4 fluxes decreased again from its highest point. According to the data of N_2O emission, the rate of N_2O positively responded to low water depth situation and N fertilizer application. The dry situation and N fertilizer are perfect boosters to generate the nitrification and denitrification process in the soil and that knowledge clearly explains the reason why N_2O emission becomes higher during low water depth and N fertilizer application (Granli, 1994; Janz et al., 2016; Kong et al., 2021).

4.2 Effect of environmental factors on CH_4 and N_2O emission

Over all rice growing stages of this study, TPR always emitted higher CH_4 and N_2O than WDSR. This matches the report that mentioned WDSR could reduce CH_4 emissions significantly over conventional transplanting method (Sandhu et al., 2021) and it showed WDSR can reduce at least 8% GHG emission as compared to TPR. There were numerous causes for higher CH_4 emissions in TPR. Mainly, the water depth of rice field is one of the main influencing factors on CH_4 emission. The minimum irrigation of WDSR produced an aerobic soil environment which depresses emission of CH_4 (Islam et al., 2020; Kumar and Ladha, 2011; Liu et al., 2014) while the TPR always maintains at least 1 cm of water depth (Figure 7).

There was a negative correlation between CH_4 emission and average soil pH (Table 4). Higher average soil pH was recorded while the CH_4 emission reached the lowest rate in early growth stages (Figure 3). This result corresponds with previous research that the impact of pH on the soil organic matter decomposition and the activity of microorganism sometimes retards the growth of methanogens (Tang et al., 2016). The continuous flooding for appropriate amounts of time normally causes the soil pH to approach a neutral level (around 7) which enhances the CH_4 production. Most of the methanogens are neutrophilic and usually active in neutral pH level, thus CH_4 production is most efficient in the pH range between 6.5 and 7.5 under neutral or slightly alkaline conditions (Wang et al., 2018). The N_2O emissions in this study did not statistically correlate with soil pH values in this study since the relationship between pH and N_2O emissions are complex (Smith, 2010; Tang et al., 2016). Although (Wang et al., 2015) mentioned that increasing soil pH inhibits N_2O production, both average soil pH and N_2O emissions were simultaneously higher at the early stage of rice growth (30-48 DAS).

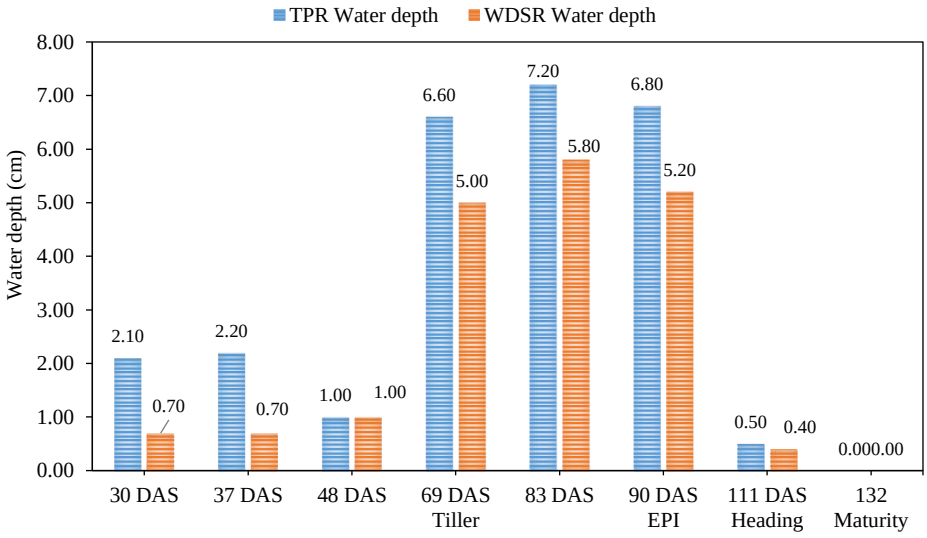

Figure 7. Water depth of TPR and WDSR by rice growing stages

Although no correlation of the soil temperature with N_2O fluxes was observed, there was a positive correlation between soil temperature and average CH_4 emission. Average CH_4 emission peaked at 90 DAS, EPI when soil temperature was highest (34.84ºC). In addition, the differences in CH_4 and N_2O emission between two crop establishment methods and N fertilizer application relatively depends on abiotic factors, precipitation, and soil properties (including soil temperature) that can affect activities of

microorganisms such as oxidation and reduction (Liu et al., 2014; Sandhu et al., 2021; Venterea et al., 2011; Vo et al., 2018)

4.3 Cost efficient GHGs mitigation strategy for Myanmar

In this study, several of the results explain how crop establishments and nitrogen fertilizer influence GHG emissions and also global warming potential (GWP), and greenhouse gases intensity (GHGI). The overall findings of this study indicate the pair of wet bed direct seeded rice and urea fertilizer application (WDSR+F1) is the most appropriate agricultural practice for GHG mitigation technique in sustainable rice production profile, which gives relatively less methane and nitrous oxide emissions in term of lower GWP and GHGI with acceptable rice yield.

According to the statistical analysis, the grain yield of TF1, WF1, TF2 (TPR with compound fertilizer), and WF2 (WDSR with compound fertilizer) are not statistically different to each other at 5% probability level in this study (Table 1). This makes sense because the local farmers obviously select the agricultural practices which ensure productivity and profit. The rice grain yield of TPR and WDSR were more or less the same and this finding was supported by (Liu et al., 2014; Sandhu et al., 2021). As rice plants can be either transplanted or direct seeded, depending on locality, labor availability and initial investment, the yield potential is often the same. The methane flux was 47% higher in TPR compared to WDSR, while there are no significant difference among F0, F1, and F2 in the average flux of CH_4. With regard to average nitrous oxide fluxes, neither crop establishment (TPR, WDSR) nor fertilizers (F0, F1, and F2) were found to be significantly different. In addition, TPR produced more CH_4 and N_2O than WDSR across fertilizers in almost each growth stage throughout the growing period.

Regarding Global Warming potential (Table 2), GWP of both TF1 and TF2 were higher than the WF1 and WF2 as the result of producing more GHG emissions than WDSR. Furthermore, GHGI of WDSR with all fertilizer treatments were found to be generally lower than that of TPR. It is noticeable that WDSR planting method is likely to be acceptable when compared with TRP across the fertilizer treatments owing to lower GHGI. Thus, based on GWP and GHGI analysis, the pair of wet bed direct seeded rice and urea fertilizer application (WDSR+F_1) practices is noted to be suitable for GHG mitigation.

5. CONCLUSION

Currently, several studies highlighted that changing the cultivation practice from TPR to WDSR makes sense to resolve the high cost of farming inputs, water, and labor scarcity. This change has been adapted by farmers themselves based on their experiences and indigenous knowledge (Janz et al., 2016; Pathak et al., 2013). This study indicates a pair of practices (WDSR+F_1) has great potential in mitigating GHGs emission from the agricultural sector since it creates lower GWP and GHGI with acceptable productivity. However, the finding of this study may not be used to generalize the feature of all small farmers in the central dry zone of Myanmar, since it was a pioneer field experiment in Myanmar with limited equipment, facilities, budget and time. Further studies should be done to identify the flexibility (wiggle room) in practices to fulfil the cost efficient GHGs mitigation strategy for Myanmar.

ACKNOWLEDGEMENTS

The authors would like to thank my supervisors and the reviewers for their valuable comments on the paper. Moreover, the authors express their gratitude to Mahidol University Central Institutional Review Board which they allowed this study with Certificate of Approval (CoA) 2020/470.2812. The staffs from Kyaukse, DAR and local farmers are highly acknowledged for their cooperation and contribution along the field data collection.

REFERENCES

Bandumula N. Rice production in Asia: Key to global food security. Proceedings of the National Academy of Sciences, India Section B: Biological Sciences 2018;88(4):1323-8.

Chauhan BS, Jabran K, Mahajan G. Rice Production Worldwide (Volume 247). Switzerland: Springer; 2017.

Conrad R. Control of microbial methane production in wetland rice fields. Nutrient Cycling in Agroecosystems 2002;64(1): 59-69.

Gaihre YK, Wassmann R, Villegas-Pangga G. Impact of elevated temperatures on greenhouse gas emissions in rice systems: Interaction with straw incorporation studied in a growth chamber experiment. Plant and Soil 2013;373(1):857-75.

Granli T. Nitrous oxide from agriculture. Norwegian Journal of Agricultural Sciences 1994;12:Article No. 94128.

Gupta DK, Bhatia A, Kumar A, Das T, Jain N, Tomer R, et al. Mitigation of greenhouse gas emission from rice-wheat system of the Indo-Gangetic plains: Through tillage, irrigation and fertilizer management. Agriculture, Ecosystems and Environment 2016;230:1-9.

Haque MM, Biswas JC. Emission factors and global warming potential as influenced by fertilizer management for the cultivation of rice under varied growing seasons. Environmental Research 2021;197:Article No. 111156.

Huang X, Chen C, Qian H, Chen M, Deng A, Zhang J, et al. Quantification for carbon footprint of agricultural inputs of grains cultivation in China since 1978. Journal of Cleaner Production 2017;142:1629-37.

Islam SM, Gaihre YK, Islam MR, Akter M, Al Mahmud A, Singh U, et al. Effects of water management on greenhouse gas emissions from farmers' rice fields in Bangladesh. Science of the Total Environment 2020;734:Article No. 139382.

Janz B, Weller S, Kraus D, Racela HS, Wassmann R, Butterbach-Bahl K, et al. Greenhouse gas footprint of diversifying rice cropping systems: Impacts of water regime and organic amendments. Agriculture, Ecosystems and Environment 2019;270:41-54.

Janz B, Weller S, Kraus D, Wassmann R, Butterbach-Bahl K, Kiese R. Greenhouse gas emissions and global warming potential of traditional and diversified tropical rice rotation systems including impacts of upland crop management practices ie mulching and inter-crop cultivation. Proceedings of the EGU General Assembly Conference; 2017 Apr 23-28; Vienna: Austria; 2016.

Kong D, Jin Y, Chen J, Yu K, Zheng Y, Wu S, et al. Nitrogen use efficiency exhibits a trade-off relationship with soil N_2O and NO emissions from wheat-rice rotations receiving manure substitution. Geoderma 2021;403:Article No. 115374.

Kumar V, Ladha JK. Direct seeding of rice: Recent developments and future research needs. Advances in Agronomy 2011;111:297-413.

Lam SK, Suter H, Mosier AR, Chen D. Using nitrification inhibitors to mitigate agricultural N_2O emission: A double-edged sword? Global Change Biology 2017;23(2):485-9.

Linquist BA, Adviento-Borbe MA, Pittelkow CM, van Kessel C, van Groenigen KJ. Fertilizer management practices and greenhouse gas emissions from rice systems: A quantitative review and analysis. Field Crops Research 2012;135:10-21.

Liu S, Zhang Y, Lin F, Zhang L, Zou J. Methane and nitrous oxide emissions from direct-seeded and seedling-transplanted rice paddies in southeast China. Plant and Soil 2014;374(1):285-97.

Ministry of Agriculture, Livestock and Irrigation (MoALI). Myanmar Agriculture Sector in Brief. Nay Pyi Taw, Myanmar: MoALI; 2019.

Mosier A, Duxbury J, Freney J, Heinemeyer O, Minami K. Assessing and mitigating N_2O emissions from agricultural soils. Climatic Change 1998;40(1):7-38.

Myhre G, Shindell D, Bréon F, Collins W, Fuglestvedt J, Huang J, et al. Anthropogenic and Natural Radiative Forcing, Climate Change 2013: The Physical Science Basis. Contribution of Working Group I to the Fifth Assessment Report of the Intergovernmental Panel on Climate Change. Cambridge: Cambridge University Press; 2013. p. 659-740.

Pachauri RK, Allen MR, Barros VR, Broome J, Cramer W, Christ R, et al. Climate Change 2014: Synthesis Report. Contribution of Working Groups I, II and III to the Fifth Assessment Report of the Intergovernmental Panel on Climate Change. USA: IPCC; 2014.

Pathak H, Sankhyan S, Dubey D, Bhatia A, Jain N. Dry direct-seeding of rice for mitigating greenhouse gas emission: Field experimentation and simulation. Paddy and Water Environment 2013;11(1):593-601.

Sandhu N, Yadav S, Singh KV, Kumar A. Effective crop management and modern breeding strategies to ensure higher crop productivity under direct seeded Rice cultivation system: A review. Agronomy 2021;11(7):Article No. 1264.

Sass RL, Andrews JA, Ding A, Fisher FM. Spatial and temporal variability in methane emissions from rice paddies: Implications for assessing regional methane budgets. Nutrient Cycling in Agroecosystems 2002;64(1):3-7.

Shukla PR, Skeg J, Buendia EC, Masson-Delmotte V, Pörtner H-O, Roberts D, et al. Climate Change and Land: An IPCC Special Report on Climate Change, Desertification, Land Degradation, Sustainable Land Management, Food Security, and Greenhouse Gas Fluxes in Terrestrial Ecosystems. USA: IPCC; 2019.

Smith KA. Nitrous Oxide and Climate Change. UK and USA: Routledge; 2010.

Song K, Zhang G, Yu H, Huang Q, Zhu X, Wang T, et al. Evaluation of methane and nitrous oxide emissions in a three-year case study on single rice and ratoon rice paddy fields. Journal of Cleaner Production 2021a;297:Article No.126650.

Song K, Zhang G, Yu H, Xu H, Lv S, Ma J. Methane and nitrous oxide emissions from a ratoon paddy field in Sichuan Province, China. European Journal of Soil Science 2021b; 72(3):1478-91.

Sun L, Song C, Miao Y, Qiao T, Gong C. Temporal and spatial variability of methane emissions in a northern temperate marsh. Atmospheric Environment 2013;81:356-63.

Tang J, Liang S, Li Z, Zhang H, Wang S, Zhang N. Emission laws and influence factors of greenhouse gases in saline-alkali paddy fields. Sustainability 2016;8(2):Article No. 163.

Timilsina A, Bizimana F, Pandey B, Yadav RKP, Dong W, Hu C. Nitrous oxide emissions from paddies: Understanding the role of rice plants. Plants 2020;9(2):Article No. 180.

Tubiello FN, Salvatore M, Rossi S, Ferrara A, Fitton N, Smith P. The FAOSTAT database of greenhouse gas emissions from agriculture. Environmental Research Letters 2013;8(1):Article No. 015009.

Venterea RT, Maharjan B, Dolan MS. Fertilizer source and tillage effects on yield-scaled nitrous oxide emissions in a corn cropping system. Journal of Environmental Quality 2011; 40(5):1521-31.

Vo TBT, Wassmann R, Tirol-Padre A, Cao VP, MacDonald B, Espaldon MVO, et al. Methane emission from rice cultivation in different agro-ecological zones of the Mekong river delta: Seasonal patterns and emission factors for baseline water management. Soil Science and Plant Nutrition 2018;64(1): 47-58.

Wang B, Lee X, Theng BK, Cheng J, Yang F. Diurnal and spatial variations of soil NO_x fluxes in the northern steppe of China. Journal of Environmental Sciences 2015;32:54-61.

Wang J, Akiyama H, Yagi K, Yan X. Controlling variables and emission factors of methane from global rice fields. Atmospheric Chemistry and Physics 2018;18(14):10419-31.

Wassmann R, Neue H, Ladha J, Aulakh M. Mitigating greenhouse gas emissions from rice-wheat cropping systems in Asia. In: Wassmann R, Vlek PLG, editors. Tropical Agriculture in Transition: Opportunities for Mitigating Greenhouse Gas Emissions? 4th ed. Springer; 2004. p. 65-90.

Win EP, Win KK, Bellingrath-Kimura SD, Oo AZ. Influence of rice varieties, organic manure and water management on greenhouse gas emissions from paddy rice soils. PloS One 2021;16(6):e0253755.

Yan X, Yagi K, Akiyama H, Akimoto H. Statistical analysis of the major variables controlling methane emission from rice fields. Global Change Biology 2005;11(7):1131-41.

Yuesi W, Yinghong W. Quick measurement of CH_4, CO_2 and N_2O emissions from a short-plant ecosystem. Advances in Atmospheric Sciences 2003;20(5):842-4.

Zhang G, Xiao X, Dong J, Xin F, Zhang Y, Qin Y, et al. Fingerprint of rice paddies in spatial-temporal dynamics of atmospheric methane concentration in monsoon Asia. Nature Communications 2020;11(1):1-11.

Zhou M, Wang X, Wang Y, Zhu B. A three-year experiment of annual methane and nitrous oxide emissions from the subtropical permanently flooded rice paddy fields of China: Emission factor, temperature sensitivity and fertilizer nitrogen effect. Agricultural and Forest Meteorology 2018;250:299-307.

Zou J, Huang Y, Jiang J, Zheng X, Sass RL. A 3-year field measurement of methane and nitrous oxide emissions from rice paddies in China: Effects of water regime, crop residue, and fertilizer application. Global Biogeochemical Cycles 2005;19(2):1-9.

Selectivity of Malachite Green on Cationic Dye Mixtures Toward Adsorption on Magnetite Humic Acid

Nur Ahmad[1,3], Fitri Suryani Arsyad[2], Idha Royani[2], and Aldes Lesbani[2,3*]

[1]Magister Program in Environment Management, Sriwijaya University, Jl. Padang Salasa No. 524 Ilir Barat 1, Palembang 30139, South Sumatera, Indonesia
[2]Graduate School, Faculty of Mathematics and Natural Sciences, Sriwijaya University, Jl. Palembang-Prabumulih, Km.90-32, Ogan Ilir, South Sumatera, Indonesia
[3]Research Center of Inorganic Center of Inorganic Materials and Complexes, Faculty of Mathematics and Natural Sciences, Sriwijaya University, Jl. Padang Salasa No. 524 Ilir Barat 1, Palembang 30139, South Sumatera, Indonesia

ARTICLE INFO

Received: 29 Jun 2022
Received in revised: 31 Jul 2022
Accepted: 8 Aug 2022
Published online: 7 Sep 2022
DOI: 10.32526/ennrj/20/202200142

Keywords:
Magnetite/ Humic acid/ Selectivity/ Malachite green/ Adsorption

*** Corresponding author:**
E-mail:
aldeslesbani@pps.unsri.ac.id

ABSTRACT

Magnetite humic acid (MHA) was successfully synthesized by the coprecipitation method followed by hydrothermal process, as evidenced by the XRD, FTIR, VSM, and SEM analysis characterization results. XRD diffraction shows diffraction peaks at 2θ=21.53º, 35.95º, and 57.93º. The FTIR spectra have a typical absorption at 3,410, 1,589, 1,396, 1,026, 910, 794, and 540 cm^{-1}. Magnetite humic acid was paramagnetic with magnetization (Ms) 17.04 emu/g. Humic acid and magnetite humic acid have an irregular structure; the morphology of magnetite humic acid is smoother than humic acid. Malachite green was more selective than methylene blue and rhodamine B on magnetite humic acid. The adsorption of malachite green on humic acid and magnetite humic acid was carried out at pH_{pzc} 8.06 and 6.08. The adsorption capacity (Q_{max}) of humic acid (77.519 mg/g) and magnetite humic acid (169.492 mg/g) were found with pseudo-second-order kinetic and Langmuir isotherm models. After five regeneration cycles, the adsorption percentages of malachite green with humic acid and magnetite humic acid ranged from 94.67-61.37% and 62.03-21.11%, respectively. Magnetite humic acid has high stability and reusability. The good regeneration of MHA was supported by the XRD diffractogram. Magnetic properties in the material simplify the adsorption process and minimize the potential for damage to the surface of the material.

1. INTRODUCTION

Textile wastewater is a severe problem for the environment. Textile wastewater pollutes water, which is a basic human need. The industrial sector uses 100,000 dyes to generate textile wastewater (Fazal et al., 2018; Khalaf, 2008). However, only 8% of Textile wastewater is treated before being discharged into waters (Roohi et al., 2016). Wastewater is dangerous for the environment and human health because of the carcinogenic effects caused by these dyes. Malachite green (MG) dye is used in textile and paper industries, and even in food coloring additives (Srivastava et al., 2004). Malachite green can cause disturbances in the immune and reproductive systems (Das and Dhar, 2020) and even cause kidney failure (Eltaweil et al., 2020).

There are different technologies for removing dyes from textile wastewater, such as membrane (Januário et al., 2022), electrocoagulation (Signorelli et al., 2021), photocatalytic (You et al., 2022), and adsorption (Sachdev et al., 2022; Zhang et al., 2020). The adsorption process is suitable for its simplicity, effectivness, efficiency, and low cost. Several adsorbents have been reported, including kaolin (Angerasa et al., 2021), bentonite (Wang et al., 2021a), layer double hydroxide (Lesbani et al., 2020; Wijaya et al., 2021), and humic acid (Yang and Antonietti, 2020).

Humic acid (HA) is extracted from peat soil with -COOH and -OH groups (Stevenson, 1994). Humic acid is one of the fractions of humic compounds that are naturally occurring in soil organic matter. Humic acid (HA) has the potential for

Citation: Ahmad N, Arsyad FS, Royani I, Lesbani A. Selectivity of malachite green on cationic dye mixtures toward adsorption on magnetite humic acid. Environ. Nat. Resour. J. 2022;20(6):634-643. (https://doi.org/10.32526/ennrj/20/202200142)

adsorption because of its high adsorption capacity, and use in organic and inorganic pollutants (Shao et al., 2021). However, the structure of humic acid is easily damaged and difficult to separate from aqueous solution. Magnetite (Fe_3O_4) is an iron oxide of the spinel mineral group (She et al., 2021). Magnetite has been applied to adsorption for water treatment (Abdullah et al., 2022; Paz et al., 2022), catalysts (Liu et al., 2018), membrane processes (Vu et al., 2020), and biodegradation (Shen et al., 2021). Magnetite, in adsorption, imparts its magnetic properties to HA, and it can separate the adsorbent from the solution using an external magnet (Lee and Kim, 2022). Composite magnetite with humic acid (MHA) has been reported for removing phosphate (Rashid et al., 2017), gold ion adsorption (Santosa et al., 2021a), and removing Pb(II) (Lu et al., 2019). Selectivity and adsorption of MHA for malachite green has not been registered.

In this study, Magnetite Humic Acid (MHA) was synthesized by the conventional coprecipitation method followed by hydrothermal process as evidenced by the characterization results using XRD, FTIR, VSM, and SEM analysis. A selectivity test was performed by mixing cationic dyes to determine the dye used for the adsorption process. Adsorption processes such as kinetic, isotherm, and thermodynamic, and the stability of the adsorbent with regeneration were evaluated.

2. METHODOLOGY

2.1 Materials and instruments

Humic acid (HA) was extracted from the peat soil of South Sumatra, Indonesia. Chemicals (analytical-grade reagent) used in this study, $FeCl_3$ (Merck, 162.2 g/mol), $FeSO_4{\cdot}7H_2O$ (Merck, 278.01 g/mol), HCl (MallinckrodtAR®, 37%), NaOH (40 g/mol), and NH_3 (25%) were purchased from EMSURE® ACS. Distilled water was purchased from PT. Bratachem Indonesia. Analytical instrumentals used included UV-Vis Spectrophotometer type Biobase BK-UV 1800 PC (China), Fourier Transfer Infra-Red (FTIR, Japan) type Shimadzu Prestige-21, X-Ray Diffractometer (XRD, Japan) type Rigaku Miniflex-6000, Vibrating Sample Magnetometer (VSM, England) type OXFORD VSM1.2H, and FEI Quanta 650 Scanning Electron Microscope (SEM, England) OXFORD.

2.2 Synthesis of magnetite humic acid (MHA)

MHA was synthesized by coprecipitation method followed by hydrothermal process (Taher et al., 2021). $FeCl_3$ (0.6488 g) and $FeSO_4{\cdot}7H_2O$ (0.5560 g) was added to 6 mL of distilled water, then stirred until dissolved. The mixture was added to 1 g of humic acid (HA) and stirred for 3 h at room temperature. NH_3 (3 mL) was added to the mixture slowly, then stirred for 30 min at 75ºC. The obtained slurry was transferred to Teflon for hydrothermal treatment for 3 h at 150ºC. The slurry was washed and then dried at 100ºC.

2.3 Determination of functional group of HA and MHA

2.3.1 Total acidity

HA (0.1 g) or MHA (0.1 g) were added to $Ba(OH)_2$ saturated solution (20 mL) under N_2 atmosphere and stirred for 24 h at 25ºC. Afterward, the HA or MHA treated was filtered using Whatman paper and washed with distilled water. The filtrate and wash water were combined and then titrated with HCl (0.5 M) to pH 8.4 (Santosa et al., 2021a). The total acidity of HA and MHA was then calculated by Equation (1):

$$\text{Total acidity (cmol/kg)} = \frac{(V_0 - V_s) \times M \times 10^5}{W} \quad (1)$$

Where; V_0 and V_s are the volume of HCl for titrated blank solution and sample, respectively; M is the molarity of HCl; W is the mass of HA and MHA.

2.3.2 Carboxyl content

HA (0.1 g) or MHA (0.1 g) were added to the mixture of $Mg(CH_3COO)_2$ 0.5 M (10 mL) and distilled water (40 mL) under N_2 atmosphere and stirred for 24 h at 25ºC. Afterward, the treated HA or MHA was filtered using Whatman paper and washed with distilled water. The filtrate and wash water were combined then titrated with NaOH (0.1 M) to pH 9.8 (Santosa et al., 2021a). The carboxyl content was determined using Equation (2):

$$\text{Carboxyl content (cmol/kg)} = \frac{(V_0 - V_s) \times M \times 10^5}{W} \quad (2)$$

Where; V_0 and V_s are the volume of NaOH for titrated blank solution and sample, respectively; M is the molarity of NaOH; W is the mass of HA and MHA.

2.3.3 Phenolic hydroxyl content

Phenolic hydroxyl content is the difference between total acidity and carboxyl content. Phenolic hydroxyl content was determined using Equation (3):

$$\text{Phenolic hydroxyl content (cmol/kg)} = \text{Total acidity} - \text{Carboxyl content} \quad (3)$$

2.4 Selectivity of cationic dye mixture

Selectivity was carried out to determine the most adsorbed dye by the adsorbent. Selectivity was performed using a mixture of 25 mg/L of rhodamine B, malachite green, and methylene blue. HA and MHA (20 mg) were added to 20 mL of the cationic dye mixture and shaken for 15, 30, 60, 90, 120, and 150 min. The absorbance was measured at the wavelength scan.

2.5 Determination of pH_{pzc} of MHA

pH_{pzc} of HA and MHA was determined by the conventional pH-drift method. HA and MHA (20 mg) were added to 20 mL of 1 M NaCl at various pH from 2 to 11 (Tombácz and Szekeres, 2004). HCl 0.1 M or NaOH 0.1 M was added to adjust the initial pH of the NaCl. Then, the mixture was shaken for 24 h. The final pH of each NaCl was measured.

2.6 Adsorption of malachite green

2.6.1 Adsorption kinetics

HA and MHA (20 mg) were added into 20 mL of malachite green with 60 mg/L, which had been adjusted at pH_{pzc}. Stirring is done with time variations of 10, 20, 30, 40, 50, 60, 70, 90, 120, 150, and 180 min in each beaker at 303 K. After stirring at 100 rpm, MHA was separated from the malachite green using an external magnet. The dye solution has been separated is then measured its absorbance using a UV-Vis at 617 nm. The adsorption kinetics were analyzed by pseudo-first-order (PFO) and pseudo-second-order (PSO) with the following Equations 4 and 5, respectively.

$$\log(Q_e - Q_t) = \log Q_e - \left(\frac{k_1}{2.303}\right) t \quad (4)$$

$$\frac{1}{Q_t} = \frac{1}{k_2 Q_e^{\,2}} + \frac{1}{Q_e} \quad (5)$$

Where; Q_e and Q_t are adsorption capacity at equilibrium and t, respectively (mg/g); k_1 (min^{-1}) and k_2 (g/mg/min) are the rate constant at PFO and PSO, respectively; t is the adsorption time of malachite green (min).

2.6.2 Adsorption isotherms

HA and MHA (20 mg) were added into 20 mL of malachite green with 50, 75, 100, 150, 175, and 200 mg/L, which had been adjusted at pH_{pzc} - stirring for 2 h with various temperatures (303, 313, 323, 333, and 343 K) in each beaker. After stirring at 100 rpm, MHA was separated from the malachite green using an external magnet. The adsorption isotherms were analyzed by Langmuir and Freundlich isotherms model with the following Equations 6 and 7, respectively.

$$\frac{C_e}{Q_e} = \frac{C_e}{Q_m} + \frac{1}{Q_m K_L} \quad (6)$$

$$\log Q_e = \log K_F - {}^{1}/_{n} \log C_e \quad (7)$$

Where; C_e (mg/L) and Q_e (mg/g) are the concentration of malachite green and adsorption capacity at equilibrium, respectively (mg/g); Q_m (mg/g) is the maximum adsorption capacity; K_L and K_F are the rate constant at Langmuir and Freundlich, respectively.

The thermodynamic equation and the Gibbs free energy were determined using Equations 8 and 9, respectively.

$$\ln \frac{Q_e}{C_e} = \frac{\Delta S}{R} - \frac{\Delta H}{RT} \quad (8)$$

$$\Delta G° = \Delta H - T\Delta S \quad (9)$$

Where; C_e (mg/L) and Q_e (mg/g) are the concentration of malachite green and adsorption capacity at equilibrium, respectively (mg/g); ΔS (J/mol.K) is the entropy; $\Delta G°$ (kJ/mol) is the Gibbs free energy. ΔH (kJ/mol) is the enthalpy; R (J/mol/K) is the gas constant; T (K) is the temperature.

2.6.3 Regeneration of MHA

HA and MHA (20 mg) were added to 20 mL of malachite green with a concentration of 80 mg/L adjusted at pH_{pzc}. Stirring was carried out for 2 h at 303 K. After the stirring process is complete, the adsorbent is separated from the adsorbate. After that, the desorption process (distilled water medium) was carried out to remove the dye from the adsorbent. HA and MHA were reused two to five times in the adsorption and desorption processes.

3. RESULTS AND DISCUSSION

3.1 Characteristics of HA and MHA

XRD diffractogram of HA as shown in Figure 1(a) 21.53º, 25.03º, 35.75º, 55.08º, and 62.31º. XRD diffraction of MHA shows diffraction peaks at 2θ=21.53º, 35.95º, and 57.93º. The diffraction peaks that appear at 2θ=21.53º (002) indicate the presence of high amounts of carbon contained in humic acid

(Zhang et al., 2018). The diffraction peaks at 2θ=35.75º (311) and 57.93º (511) are originally peaks from Magnetite (Santosa et al., 2021b).

The FT-IR spectra of HA and MHA are shown in Figure 1(b). HA has a typical absorption at 3,410 cm^{-1} related to OH group stretching from phenolic hydroxyl content (Ahmad et al., 2022), 1,589 cm^{-1} as C=C stretching, 1,396 and 1,026 cm^{-1} indicated as C-O stretching in COO- (carboxyl content) (Anjum et al., 2019). The peak at 910 cm^{-1} is related to C=C bending and 540 cm^{-1} indicating the presence of metal ions in HA. After HA was modified with magnetite (MHA) at 540 cm^{-1}, the absorption became sharper indicating the presence of Fe-O. A new peak was observed at wavenumber 794 cm^{-1} due to the interaction between C-O and Fe-O.

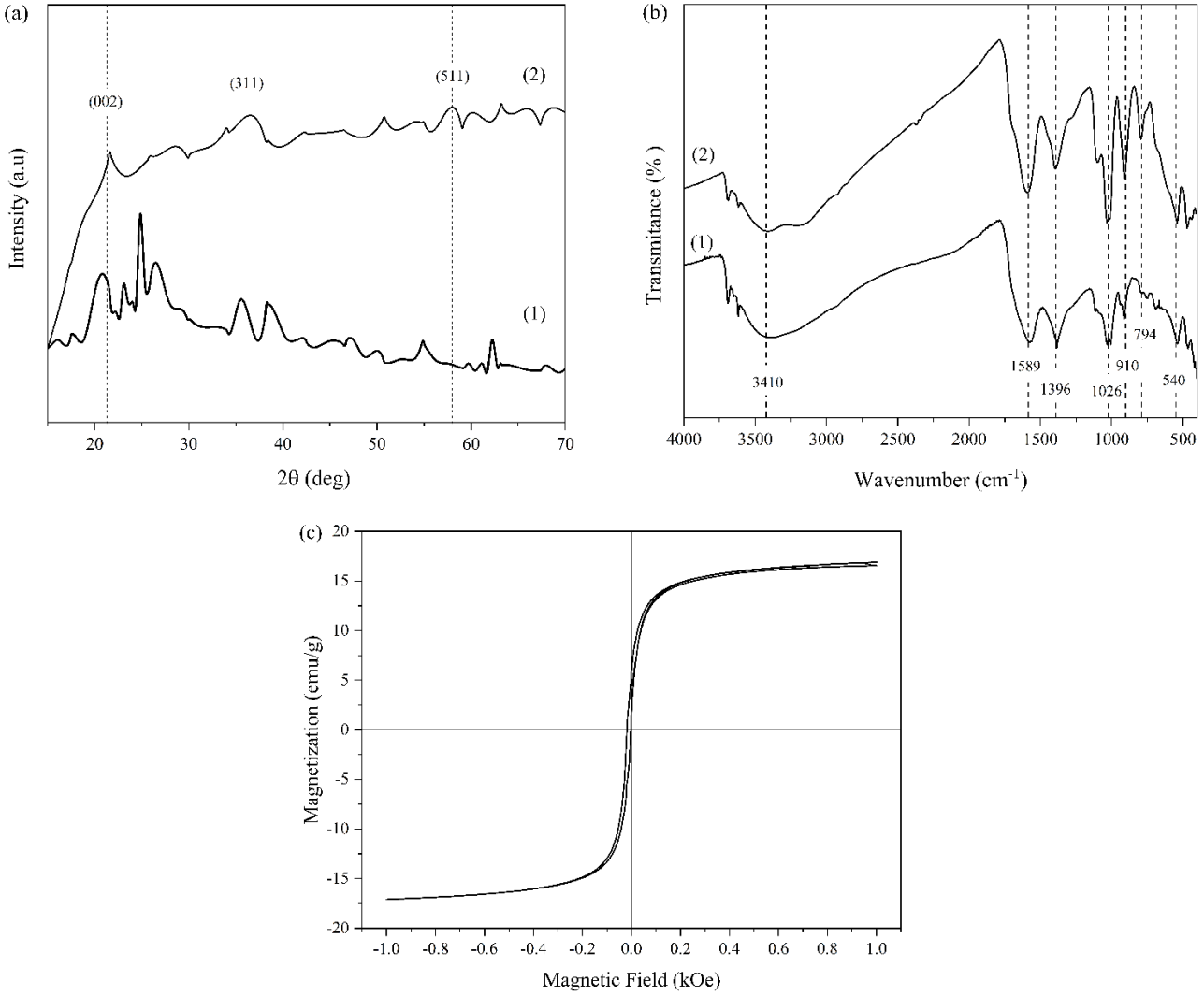

Figure 1. XRD diffractogram (a) and IR spectra (b) of (1) HA, (2) MHA. The measured room temperature magnetization curve of MHA (c)

The magnetic curve of MHA was measured using VSM. Figure 1(c) showed MHA was paramagnetic with magnetization (Ms) 17.04 emu/g. The magnetization (Ms) MHA was lower than Fe_3O_4 (66.3 emu/g) because Fe_3O_4 was classified as superparamagnetic (Santosa et al., 2021b). Figure 2 shows the surface morphology of HA and MHA by SEM images. HA and MHA have irregular structures. The morphology of MHA is smoother than HA. The surface of MHA is smooth because it is synthesized by hydrothermal process.

3.2 Determination of functional group of HA and MHA

Total acidity and carboxylic content were determined by titration using $Ba(OH)_2$ saturated solution and $Mg(CH_3COO)_2$, respectively (Stevenson, 1994). The total acidity, carboxyl content, and Phenolic -OH of HA and MHA are displayed in Table

1. MHA had a drastic decrease in the total acidity and carboxyl content, respectively, from 670 cmol/kg to 317.50 cmol/kg and 296 cmol/kg to 59.33 cmol/kg. This is due to the preparation of MHA carried out under alkaline conditions (addition of NH_3). The carboxyl content and phenolic -OH are iodized and then interact with positively charged Fe^{2+} and Fe^{3+} form Fe_3O_4 (Koesnarpadi et al., 2015). However, the carboxyl group more readily interacts with Fe_3O_4 than the phenolic -OH, so the carboxyl group's reduction is very drastic.

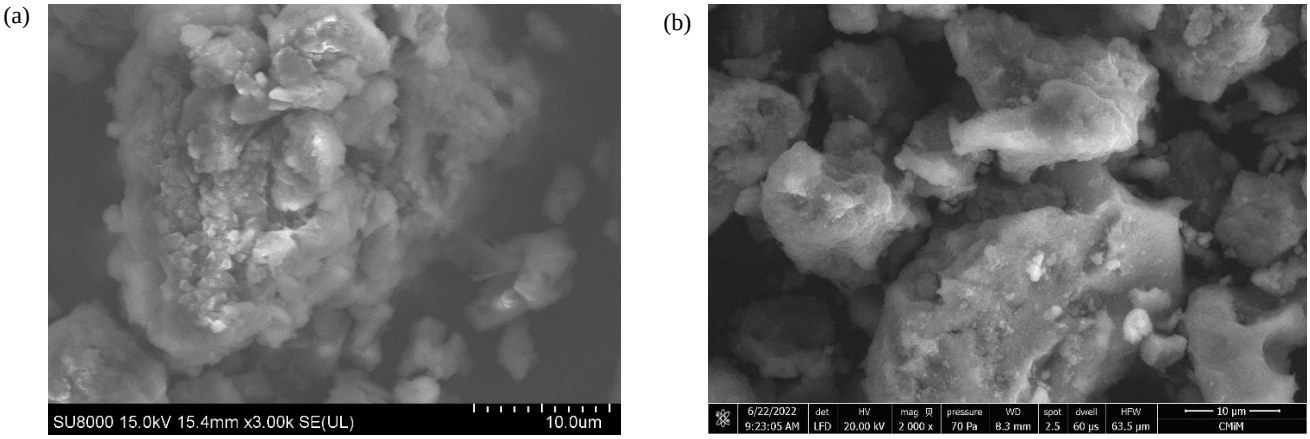

Figure 2. SEM images of HA (a) and MHA (b)

Table 1. Total acidity, carboxyl content, and phenolic -OH of HA and MHA

Functional group	Stevenson (1994) (cmol/kg)	Santosa et al. (2021a) (cmol/kg)		This study (cmol/kg)	
		HA	MHA	HA	MHA
Total acidity	570-890	710.66	320.44	670	317.50
Carboxyl content	150-570	315.79	87.43	296	59.33
Phenolic -OH	150-400	394.87	233.01	374	258.17

3.3 Selectivity adsorbent

Figure 3 shows a wavelength scan for selectivity of malachite green. MHA adsorbed malachite green higher than rhodamine B and methylene blue. The drastic decrease in malachite green concentration indicated that the malachite green structure was smaller than methylene blue and rhodamine B (Mohadi et al., 2021; Palapa et al., 2021). Therefore, malachite green is used for the adsorption process.

3.4 pH_{pzc} of HA and MHA

pH_{pzc} of HA and MHA is the point neither positively nor negatively charged (Derakhshani and Naghizadeh, 2018). Through the movement of H^+ ions from the HA and MHA surface, the pH_{pzc} can be easily measured. Figure 4 shows the movement of H^+ after 24 h in the shaker. At low pH, H^+ moves from the solution to the HA and MHA surface during shaking and increases pH of the solution. At high pH, H^+ moves from the HA and MHA surface to the solution and lowers pH of the solution.

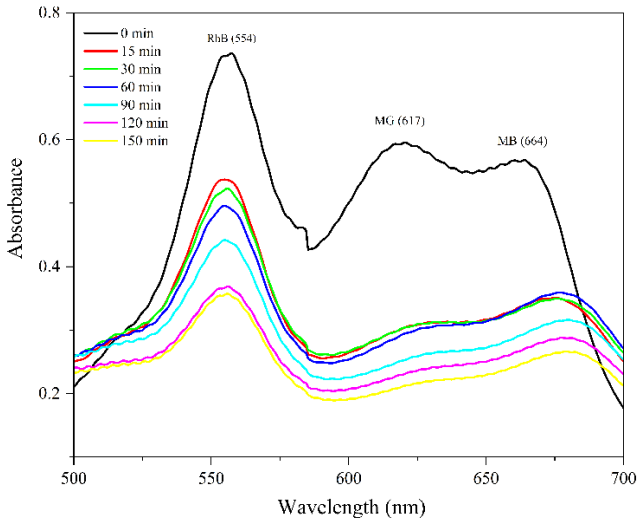

Figure 3. Wavelength scan of adsorption by MHA into a mixture of MG, MB, and RhB

The meeting point between the initial and final pH shows no movement of H^+ ions, which means that this meeting point is that pH_{pzc}. As shown in Figure 4, pH_{pzc} of HA and MHA were at pH 8.08 and 6.08, respectively. In a solution with a pH less than pH_{pzc}, HA, and MHA are positively charged and at pH higher than pH_{pzc}, HA, and MHA are negatively charged.

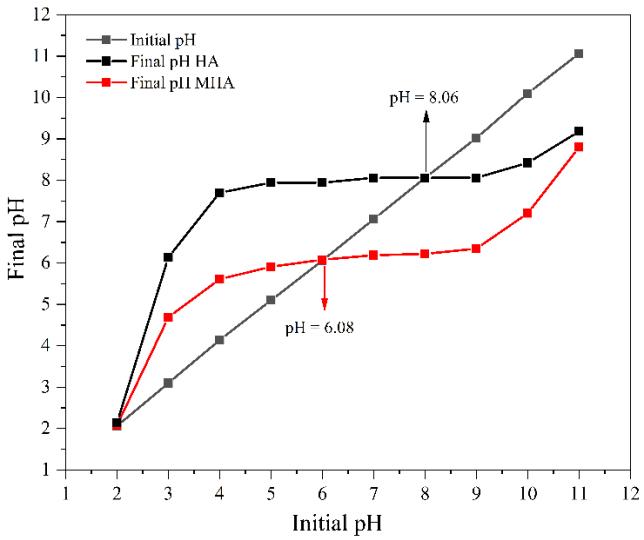

Figure 4. pH_{pzc} of HA and MHA

3.5 Adsorption of malachite green

Figure 5(a) shows that the adsorbed concentration of malachite green increased with time and was constant at 120 min. Pseudo-first-order and pseudo-second-order kinetic adsorption parameters of malachite green are shown in Table 2. The data in Table 2 shows that the value of the coefficient correlation in the adsorption process of malachite green using HA and MHA adsorbent tends to be a pseudo-second-order. The coefficient correlation (R^2) for pseudo-second-order is higher than pseudo-first-order. It means that the greater the concentration of the malachite green, the more adsorbed. Therefore, the adsorption process can be followed by chemisorption (Liu et al., 2020; Siraorarnroj et al., 2022).

Based on Table 2 and Figures 5(b) and 5(c), the coefficient correlation (R^2) of HA and MHA for Langmuir isotherm is higher than Freundlich isotherm at temperature 303 K. The adsorption process tends to follow the Langmuir isotherm. Therefore, the adsorption process can be followed by monolayer adsorption (Wang et al., 2021b). Adsorption capacity (Q_{max}) of HA and MHA was 77.519 and 169.492 mg/g, respectively. Adsorption of malachite green by several adsorbents is shown in Table 3.

Table 2. Kinetic and isotherm model parameter of adsorption on MHA

Kinetic parameter	Parameter	Adsorbent	
		HA	MHA
Pseudo-first-order	Qe_{exp} (mg/g)	41.981	56.075
	Qe_{calc} (mg/g)	52.918	78.289
	k_1 (min^{-1})	0.002	0.002
	R^2	0.980	0.966
Pseudo-second-order	Qe_{exp} (mg/g)	41.981	56.075
	Qe_{calc} (mg/g)	54.945	71.942
	k_2 (g/mg/min)	0.0004	0.0003
	R^2	0.990	0.990
Isotherm parameter	Parameter	Adsorbent	
		HA	MHA
Langmuir	Qmax	77.519	169.492
	kL	0.047	0.042
	R^2	0.968	0.992
Freundlich	N	1.294	2.396
	kF	3.105	21.617
	R^2	0.866	0.935

Table 3. Comparison of HA and MHA with several adsorbents in terms of the adsorption capacity of malachite green

Adsorbent	Q_{max} (mg/g)	Reference
Date stones	98	Hijab et al. (2021)
CuCr-[α-$SiW_{12}O_{40}$]	55.322	Palapa et al. (2020)
ZIF-8@Fe/Ni	151.520	Zhang et al. (2021)

Table 3. Comparison of HA and MHA with several adsorbents in terms of the adsorption capacity of malachite green (cont.)

Adsorbent	Q_{max} (mg/g)	Reference
Chitosan-DES B	17.86	Sadiq et al. (2020)
EPS of *Lysinibacillus* sp. SS1	178.57	Miyar et al. (2021)
GALA	113.5	Chen et al. (2020)
Plasma-based biomass	15.55	Al-Yousef et al. (2021)
S@TP Biochar	30.18	Vigneshwaran et al. (2021)
Chinese fan palm seed biochar	21.4	Giri et al. (2022)
HA	77.519	This study
MHA	169.492	This study

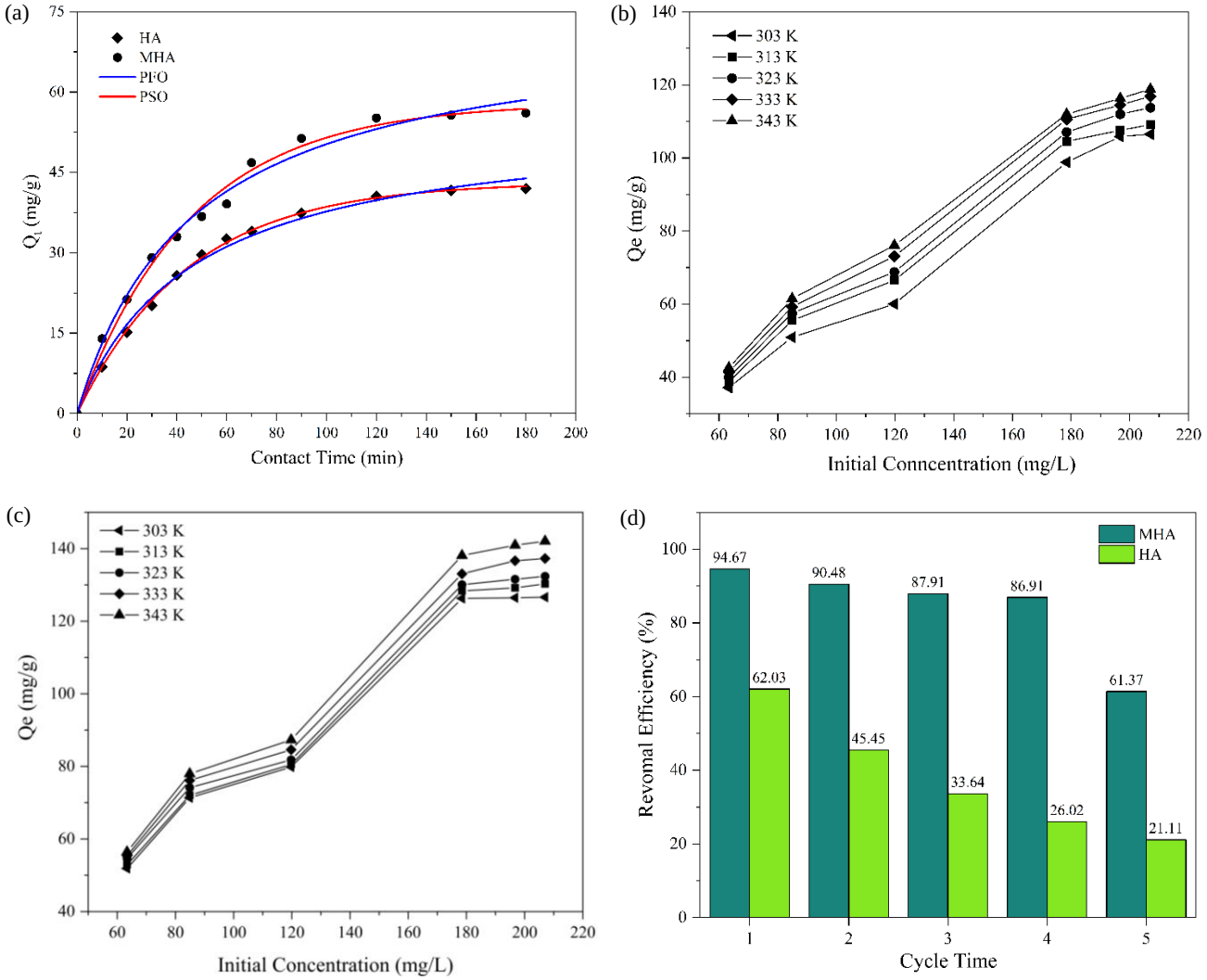

Figure 5. Effect of contact time (a), effect of initial concentration and temperature (b) and (c), regeneration (d) of HA and MHA

Table 4 shows the thermodynamic data of HA and MHA for adsorption of malachite green. The value of ΔG° is negative, meaning that the adsorption takes place spontaneously. ΔH is positive, meaning that the adsorption is endothermic and requires energy for the adsorption process. ΔS is positive, meaning that there is an increase in irregularity on the surface of the adsorbent. Based on Figure 5(d), during five regeneration cycles of HA and MHA, the adsorption percentages of malachite green decreased from 94.6-61.37% and 62.03-21.11%, respectively. Magnetic properties in the material simplify the adsorption process and minimize the potential for damage to the material's surface. MHA has high stability and reusability of adsorbent up to five times. The good regeneration of MHA indicates that MHA has good

Table 4. Adsorption thermodynamic parameter

Adsorbent	ΔH (kJ/mol)	ΔS (kJ/mol)	ΔG (kJ/mol)					R^2
			303 K	313 K	323 K	333 K	343 K	
HA	8.189	0.029	-0.582	-0.871	-1.161	-1.450	-1.740	0.998
MHA	12.940	0.055	-3.764	-4.316	-4.867	-5.418	-5.969	0.988

stability, supported by the XRD diffractogram after adsorption with no significant changes as shown in Figure 6. The diffraction peaks at 2θ=21.53º (002), 35.95º (311), and 57.93º (511) can still be observed. The adsorption mechanism can be studied from electrostatically interacting MHA with the cationic malachite green. In addition, the hydrogen bonding interactions and π-π interactions between the aromatic ring of the malachite green and the MHA can affect the adsorption mechanism.

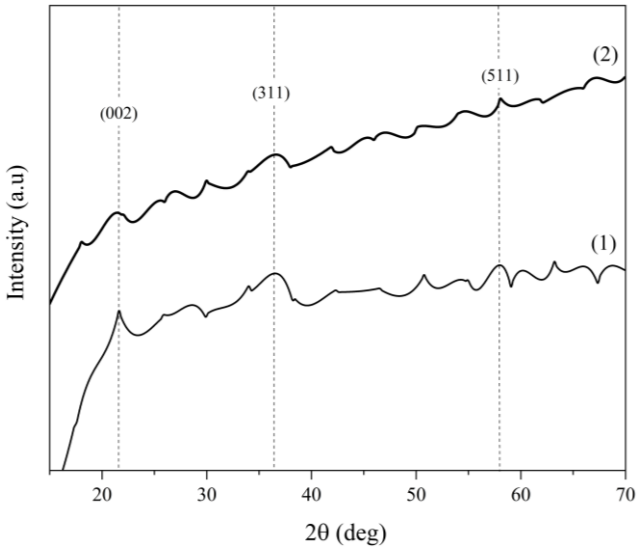

Figure 6. XRD diffractogram of MHA before (1) and after (2) adsorption

4. CONCLUSION

In this study, magnetite humic acid (MHA) was successfully synthesized by the coprecipitation method followed by hydrothermal process. Selectivity of cationic dyes shows that malachite green was more selective than methylene blue and rhodamine B. Malachite green has a smaller structure than methylene blue and rhodamine B. Adsorption capacity (Q_{max}) of HA and MHA was 77.519 and 169.492 mg/g, respectively. After five regeneration cycles, the adsorption percentages of malachite green from HA and MHA ranged from 94.67-61.37% and 62.03-21.11%, respectively. MHA has high stability and reusability as an adsorbent up to five times.

ACKNOWLEDGEMENTS

Authors thank Research Center of Inorganic Materials and Complexes, Faculty of Mathematics and Natural Sciences, Sriwijaya University for instrumental analysis.

REFERENCES

Abdullah TA, Juzsakova T, Mansoor H, Salman AD, Rasheed RT, Hafad SA, et al. Polyethylene over magnetite-multiwalled carbon nanotubes for kerosene removal from water. Chemosphere 2022;287:Article No. 132310.

Ahmad N, Wijaya A, Amri, Fitri ES, Arsyad FS, Mohadi R, et al. Catalytic oxidative desulfurization of dibenzothiophene by composites based Ni/Al-Oxide. Science and Technology Indonesia 2022;7(3):385-91.

Al-Yousef HA, Alotaibi BM, Alanazi MM, Aouaini F, Sellaoui L, Bonilla-Petriciolet A. Theoretical assessment of the adsorption mechanism of ibuprofen, ampicillin, orange G and malachite green on a biomass functionalized with plasma. Journal of Environmental Chemical Engineering 2021;9(1):Article No. 104950.

Angerasa FT, Kalifa MA, Jembere AL, Genet MB. Spent kaolin filter cake as an effective adsorbent for the removal of hexavalent chromium [Cr(VI)] from aqueous solution: Comparative study of wastewater treatment methods. South African Journal of Chemical Engineering 2021;38:90-103.

Anjum H, Johari K, Gnanasundaram N, Appusamy A, Thanabalan M. Investigation of green functionalization of multiwall carbon nanotubes and its application in adsorption of benzene, toluene, and p-xylene from aqueous solution. Journal of Cleaner Production 2019;221:323-38.

Chen H, Liu T, Meng Y, Cheng Y, Lu J, Wang H. Novel graphene oxide/aminated lignin aerogels for enhanced adsorption of malachite green in wastewater. Colloids and Surfaces A: Physicochemical and Engineering Aspects 2020;603:Article No. 125281.

Das KC, Dhar SS. Rapid catalytic degradation of malachite green by $MgFe_2O_4$ nanoparticles in presence of H_2O_2. Journal of Alloys and Compounds 2020;828:Article No. 154462.

Derakhshani E, Naghizadeh A. Optimization of humic acid removal by adsorption onto bentonite and montmorillonite nanoparticles. Journal of Molecular Liquids 2018;259:76-81.

Eltaweil AS, Mohamed HA, El-Monaem EMA, El-Subruiti GM. Mesoporous magnetic biochar composite for enhanced adsorption of malachite green dye: Characterization, adsorption kinetics, thermodynamics and isotherms. Advanced Powder Technology 2020;31(3):1253-63.

Fazal T, Mushtaq A, Rehman F, Khan AU, Rashid N, Farooq W, et al. Bioremediation of textile wastewater and successive biodiesel production using microalgae. Renewable and Sustainable Energy Reviews 2018;82:3107-26.

Giri BS, Sonwani RK, Varjani S, Chaurasia D, Varadavenkatesan T, Chaturvedi P, et al. Highly efficient bio-adsorption of malachite green using Chinese Fan-Palm Biochar (*Livistona chinensis*). Chemosphere 2022;287:Article No. 132282.

Hijab M, Parthasarathy P, Mackey HR, Al-Ansari T, McKay G. Minimizing adsorbent requirements using multi-stage batch adsorption for malachite green removal using microwave date-stone activated carbons. Chemical Engineering and Processing - Process Intensification 2021;167:Article No. 108318.

Januário EFD, Vidovix TB, Calsavara MA, Bergamasco R, Vieira AMS. Membrane surface functionalization by the deposition of polyvinyl alcohol and graphene oxide for dyes removal and treatment of a simulated wastewater. Chemical Engineering and Processing - Process Intensification 2022;170:Article No. 108725.

Khalaf MA. Biosorption of reactive dye from textile wastewater by non-viable biomass of *Aspergillus niger* and *Spirogyra* sp. Bioresource Technology 2008;99(14):6631-4.

Koesnarpadi S, Santosa SJ, Siswanta D, Rusdiarso B. Synthesis and characterizatation of magnetite nanoparticle coated humic acid (Fe_3O_4/HA). Procedia Environmental Sciences 2015; 30:103-8.

Lee WH, Kim JO. Phosphate recovery from anaerobic digestion effluent using synthetic magnetite particles. Journal of Environmental Chemical Engineering 2022;10(1):Article No. 107103.

Lesbani A, Asri F, Palapa NR, Taher T, Rachmat A. Efficient removal of methylene blue by adsorption using composite based Ca/Al layered double hydroxide-biochar. Global Nest Journal 2020;22(2):250-7.

Liu Y, Jia J, Gao T, Wang X, Yu J, Wu D, et al. Rapid, selective adsorption of methylene blue from aqueous solution by durable nanofibrous membranes. Journal of Chemical and Engineering Data 2020;65(8):3998-4008.

Liu Y, Liu Q, Li J, Ngo HH, Guo W, Hu J, et al. Effect of magnetic powder on membrane fouling mitigation and microbial community/composition in membrane bioreactors (MBRs) for municipal wastewater treatment. Bioresource Technology 2018;249:377-85.

Lu M, Zhang Y, Zhou Y, Su Z, Liu B, Li G, et al. Adsorption-desorption characteristics and mechanisms of Pb(II) on natural vanadium, titanium-bearing magnetite-humic acid magnetic adsorbent. Powder Technology 2019;344:947-58.

Miyar HK, Pai A, Goveas LC. Adsorption of malachite green by extracellular polymeric substance of *Lysinibacillus* sp. SS1: Kinetics and isotherms. Heliyon 2021;7(6):e07169.

Mohadi R, Palapa NR, Lesbani A. Preparation of Ca/Al-layered double hydroxides/biochar composite with high adsorption capacity and selectivity toward cationic dyes in aqueous. Bulletin of Chemical Reaction Engineering and Catalysis 2021;16(2):244-52.

Palapa NR, Mohadi R, Rachmat A, Lesbani A. Adsorption study of malachite green removal from aqueous solution using Cu/M^{3+} (M^{3+}=Al, Cr) layered double hydroxide. Mediterranean Journal of Chemistry 2020;10(1):33-45.

Palapa NR, Taher T, Wijaya A, Lesbani A. Modification of Cu/Cr layered double hydroxide by keggin type polyoxometalate as adsorbent of malachite green from aqueous solution. Science and Technology Indonesia 2021;6(3):209-17.

Paz MJ, Vieira T, Enzweiler H, Paulino AT. Chitosan/wood sawdust/magnetite composite membranes for the photo-degradation of agrochemicals in water. Journal of Environmental Chemical Engineering 2022;10(1):Article No. 106967.

Rashid M, Price NT, Pinilla MÁG, O'Shea KE. Effective removal of phosphate from aqueous solution using humic acid coated magnetite nanoparticles. Water Research 2017;123(3):353-60.

Roohi M, Riaz M, Arif MS, Shahzad SM, Yasmeen T, Riaz MA, et al. Varied effects of untreated textile wastewater onto soil carbon mineralization and associated biochemical properties of a dryland agricultural soil. Journal of Environmental Management 2016;183:530-40.

Sachdev D, Shrivastava H, Kajal, Sharma S, Sanjeev, Srivastava S, et al. Potential for hydrothermally separated groundnut shell fibers for removal of methylene blue dye. Materials Today: Proceedings 2022;48:1559-68.

Sadiq AC, Rahim NY, Suah FBM. Adsorption and desorption of malachite green by using chitosan-deep eutectic solvents beads. International Journal of Biological Macromolecules 2020;164:3965-73.

Santosa SJ, Krisbiantoro PA, Ha TTM, Phuong NTT, Gusrizal G. Composite of magnetite and Zn/Al layered double hydroxide as a magnetically separable adsorbent for effective removal of humic acid. Colloids and Surfaces A: Physicochemical and Engineering Aspects 2021b;614:Article No. 126159.

Santosa SJ, Krisbiantoro PA, Yuniarti M, Kustomo, Koesnarpardi S. Magnetically separable humic acid-functionalized magnetite for reductive adsorption of tetrachloroaurate(III) ion in aqueous solution. Environmental Nanotechnology, Monitoring and Management 2021a;15:Article No. 100454.

Shao Y, Bao M, Huo W, Ye R, Liu Y, Lu W. Production of artificial humic acid from biomass residues by a non-catalytic hydrothermal process. Journal of Cleaner Production 2021;335:Article No. 130302.

She HD, Fan HR, Yang KF, Li XC, Wang QW, Zhang LF, et al. In situ trace elements of magnetite in the Bayan Obo REE-Nb-Fe deposit: Implications for the genesis of mesoproterozoic iron mineralization. Ore Geology Reviews 2021;139:Article No. 104574.

Shen X, Dong W, Wan Y, Feng K, Liu Y, Wei Y. Influencing mechanisms of siderite and magnetite, on naphthalene biodegradation: Insights from degradability and mineral surface structure. Journal of Environmental Management 2021;299:Article No. 113648.

Signorelli SCM, Costa JM, Neto AFA. Electrocoagulation-flotation for orange II dye removal: Kinetics, costs, and process variables effects. Journal of Environmental Chemical Engineering 2021;9(5):Article No. 106157.

Siraorarnroj S, Kaewtrakulchai N, Fuji M, Eiad-ua A. High performance nanoporous carbon from mulberry leaves (*Morus alba* L.) residues via microwave treatment assisted hydrothermal-carbonization for methyl orange adsorption: Kinetic, equilibrium and thermodynamic studies. Materialia 2022;21:Article No. 101288.

Srivastava S, Sinha R, Roy D. Toxicological effects of malachite green. Aquatic Toxicology 2004;66(3):319-29.

Stevenson FJ. Humus Chemistry: Genesis, Composition, Reactions. USA: John Wiley and Sons; 1994.

Taher T, Putra R, Palapa NR, Lesbani A. Preparation of magnetite-nanoparticle-decorated NiFe layered double hydroxide and its adsorption performance for congo red dye removal. Chemical Physics Letters 2021;777:Article No. 138712.

Tombácz E, Szekeres M. Colloidal behavior of aqueous montmorillonite suspensions: The specific role of pH in the

presence of indifferent electrolytes. Applied Clay Science 2004;27(1-2):75-94.

Vigneshwaran S, Sirajudheen P, Karthikeyan P, Meenakshi S. Fabrication of sulfur-doped biochar derived from tapioca peel waste with superior adsorption performance for the removal of malachite green and rhodamine B dyes. Surfaces and Interfaces 2021;23:Article No. 100920.

Vu MT, Noori MT, Min B. Conductive magnetite nanoparticles trigger syntrophic methane production in single chamber microbial electrochemical systems. Bioresource Technology 2020;296:Article No. 122265.

Wang M, Li Y, Cui M, Li M, Xu W, Li L, et al. Barium alginate as a skeleton coating graphene oxide and bentonite-derived composites: Excellent adsorbent based on predictive design for the enhanced adsorption of methylene blue. Journal of Colloid and Interface Science 2021a;611:629-43.

Wang Y, Bao S, Liu Y, Yu Y, Yang W, Xu S, et al. CoS_2/GO nanocomposites for highly efficient and ppb level adsorption of Hg(II) from wastewater. Journal of Molecular Liquids 2021b;322:Article No. 114899.

Wijaya A, Siregar PMSBN, Priambodo A, Palapa NR, Taher T, Lesbani A. Innovative modified of Cu-Al/C (C=biochar, graphite) composites for removal of procion red from aqueous solution. Science and Technology Indonesia 2021;6(4):228-34.

Yang F, Antonietti M. Artificial humic acids: Sustainable materials against climate change. Advanced Science 2020;7(5):1-7.

You J, Liu C, Feng X, Lu B, Xia L, Zhuang X. In situ synthesis of ZnS nanoparticles onto cellulose/chitosan sponge for adsorption-photocatalytic removal of congo red. Carbohydrate Polymers 2022;288:Article No. 119332.

Zhang A, Chen W, Gu Z, Li Q, Shi G. Mechanism of adsorption of humic acid by modified aged refuse. RSC Advantages 2018;8:33642-51.

Zhang T, Jin X, Owens G, Chen Z. Remediation of malachite green in wastewater by ZIF-8@Fe/Ni nanoparticles based on adsorption and reduction. Journal of Colloid and Interface Science 2021;594:398-408.

Zhang W, Zhang RZ, Yin Y, Yang JM. Superior selective adsorption of anionic organic dyes by MIL-101 analogs: Regulation of adsorption driving forces by free amino groups in pore channels. Journal of Molecular Liquids 2020; 302:Article No. 112616.

Population Structure and Spatial Distribution of Tree Species in Lower Montane Forest, Doi Suthep-Pui National Park, Northern Thailand

Dokrak Marod[1,2], Prateep Duengkae[1], Sarawood Sangkaew[1], Phruet Racharak[1], Warong Suksavate[1], Suwimon Uthairatsamee[1], Lamthai Asanok[3], Torlarp Kamyo[3], Sathid Thinkampheang[2], Sutheera Heumhuk[4], Panida Kachina[5], Jakkapong Thongsawi[6], Wongsatorn Phumpuang[7], Paanwaris Paansri[2], Wimonmart Nuipakdee[8], Pisut Nakmuenwai[9], and Sura Pattanakiat[9*]

[1]Department of Forest Biology, Faculty of Forestry, Kasetsart University, Bangkok 10900, Thailand
[2]Cooperation Centre of Thai Forest Ecological Research, Kasetsart University, Bangkok 10900, Thailand
[3]Department of Agroforestry, Maejo University Phrae Campus, Phrae 54140, Thailand
[4]Faculty of Agricultural Production, Maejo University, Chiang Mai 50290, Thailand
[5]Faculty of Agriculture, Chiang Mai University, Chiang Mai 50200, Thailand
[6]The Foundation of Mrigadayavan Palace under the Patronage of Her Royal Highness Princess Bejaratana, Phetchaburi 76120, Thailand
[7]Department of National Parks, Wildlife and Plant Conservation, Bangkok 10900, Thailand
[8]Mae Sa-Kog Ma Biosphere Reserve, Chiang Mai 52000, Thailand
[9]Faculty of Environment and Resource Studies, Mahidol University, Nakhon Pathom 73170, Thailand

ARTICLE INFO

Received: 24 Jun 2022
Received in revised: 13 Aug 2022
Accepted: 17 Aug 2022
Published online: 13 Sep 2022
DOI: 10.32526/ennrj/20/202200139

Keywords:
Lower montane forest/ Ecological niche/ Distribution pattern/ Forest dynamics plot

*** Corresponding author:**
E-mail: sura.pat@mahidol.ac.th

ABSTRACT

Plant diversity is important for sustainable development, particularly in watershed areas. This study explored tree population and diversity in a lower montane forest (LMF). A 16-ha permanent plot was established in LMF at Huai Kogma sub-watershed, northern Thailand. All trees with a diameter at breast height ≥ 2 cm were tagged, measured, identified, and their coordinates were mapped. The results showed that 220 species in 139 genera from 63 plant families were found. The dominant families based on species numbers and tree density were Fagaceae, Lauraceae, and Theaceae. The most dominant species were *Castanopsis acuminatissima*, *Schima wallichii*, *Castanopsis armata*, and *Styrax benzoides*. Diameter classes for climax species frequently followed negative exponential distributions, indicating their populations could be maintained into the future. By contrast, pioneer species, such as *Macaranga indica*, *Morus macroura*, and *Rhus javanica*, had discontinuous distribution, and were mostly found in gap areas, indicating successful regeneration may require high light intensity. Spatial distribution patterns based on Morisita's index showed that most of the selected species had clumped patterns, particularly those in the Fagaceae family, which were predominantly distributed along the mountain ridge. Tree distribution patterns can affect ecological dynamics, thus reinforcing patterns dependent on local interactions such as the abundance of and distance to available resources. Our finding can aid evaluations of forest sustainability, and support the biodiversity conservation plans. In particular, the selection of suitable species for LMF restoration programs where mixed plantings of pioneer and climax species are planned.

1. INTRODUCTION

Understanding how species are distributed, and how they assemble to form communities and ecosystems, is an important issue that has attracted considerable scientific interest. Its information is a very useful component of conservation and management decisions, including focused efforts to conserve rare species, habitat management and restoration, anticipation of problematic invasions, and delimit valued habitat types (Franklin, 2010).

Citation: Marod D, Duengkae P, Sangkaew S, Racharak P, Suksavate W, Uthairatsamee S, Asanok L, Kamyo T, Thinkampheang S, Heumhuk S, Kachina P, Thongsawi J, Phumpuang W, Paansri P, Nuipakdee W, Nakmuenwai P, Pattanakiat S. Population structure and spatial distribution of tree species in lower montane forest, Doi Suthep-Pui National Park, Northern Thailand. Environ. Nat. Resour. J. 2022;20(6):644-663. (https://doi.org/10.32526/ennrj/20/202200139)

Vegetation ecologists have engaged in an extended debate on the mechanisms governing species assemblage into complex vegetation communities (Ricklefs, 2008; Brooker et al., 2009). Ongoing global changes, including climate change, deforestation, pollution, and biological invasions, have increased rates of biodiversity loss (Cardinale et al., 2012; Chen et al., 2011; Pereira et al., 2010; Sala et al., 2000). These changes have also heightened the need for knowledge that could help us anticipate and prevent deleterious effects on biodiversity and ecosystem functioning. This is especially important for mountain ecosystems, which are particularly exposed to climate changes (Pepin et al., 2015), and life mainly temperature limited and vulnerable to climatic changes (Amdre et al., 2009).

Mountain ecosystems are mainly defined in terms of their minimum altitude in meters above sea level (m.a.s.l.), which ranges from 300 m at 67°N and 55°S to 1,000 m at the equator. Mountain ecosystems cover about 27% of the Earth's surface (Kapos et al., 2000). They maintain ecological processes and services for both mountain communities and those living in lowlands, wherein demand from population centers, agriculture and industry is high (Regato and Salman, 2008). Mountains are exposed to both natural and anthropogenic drivers of change (Kampmann et al., 2008). In particular, montane plant diversity can be reduced by certain types of land-use, including intensification and land abandonment (Spehn et al., 2006). Mountain biota are adapted to extreme climatic conditions, temperatures, and precipitation (Rashid et al., 2005). Recovery of mountain ecosystems from disturbances is typically slow.

The characteristics of montane forests differ from those of lowland forests due to changes in vegetation composition along the altitudinal gradient (Marod et al., 2014; Richards, 1996). It is now accepted that four forest zones exist for taller tropical mountains up to the tree line, namely lowland, lower montane, upper montane and subalpine forest zones (Ashton, 2003). The transition from lowland to lower montane forest (LMF) seems to be mostly attributable to declining average temperature with elevation. At this threshold, many lowland tree species are displaced by a floristically distinct assemblage of montane species (Kitayama, 1992). Tree species from the Fagaceae and Lauraceae are particularly abundant in massifs, where their abundance in both the canopy and subcanopy has earned these forests the name "oak-laurel forests" (Tagawa, 1995).

Only two mountain forest ecosystems are found in Thailand: the LMF and upper montane forest (UMF). The ecotone between them is located at approximately 1,800 m.a.s.l. based on climatic characteristics and edaphic conditions (Santisuk, 1988). Mount Doi Inthanon, at 2,565 m.a.s.l., is a summit in Thailand with extensive tracts of UMF. Trees are often small in stature and characterized by umbrella-shaped crowns, small leaves, gnarled stems, and branches that are covered by epiphytes such as orchids, ferns, lichens, and mosses (Hara et al., 2002; Khamyong et al., 2004). Several studies have reported that species from the Fagaceae and Lauraceae families are the most abundant, as also seen in tropical mountain forest areas (Kanzaki et al., 2004; Marod et al., 2018; Sri-Ngernyuang et al., 2003).

Intensive studies of species composition, forest structure, and dynamics have been conducted in lowland forests since the 1980s using large-scale research plots (Condit, 1995). Large-scale research plots are not only suitable for studying the distribution patterns of existing trees, but also tree regeneration, which is often expressed in terms of stem-size distributions (Bunyavejchewin et al., 2001; Kanzaki et al., 2004; Yamada et al., 1997). Diameter class distributions (visualized using graphs showing the density of trees in several different classes) can be used to determine whether the density of smaller trees in a forest is sufficient to replace the current population of larger trees (Henle et al., 2004; Rubin et al., 2006; White et al., 2007). Whether a given forest is "sustainable" can be inferred from stand diameter distributions. For example, in the absence of major disturbances, a reversed J-shaped distribution in uneven-aged stands has been regarded as demonstrating dynamic equilibrium in sustainably managed forests (Marod et al., 2020; Nyland, 2002). Unimodal distributions characterized by fewer juveniles relative to adults have been interpreted as evidence of population decline (Condit et al., 1998; Deb and Sundriyal, 2008). The success of regeneration efforts can also be inferred from diameter distribution patterns associated with ecological processes. Distribution patterns (clumped or grouped, and regular or random) can effect ecological changes depending on local interactions among individuals, seed dispersal and germination, abundance, and ecological niche.

Measuring distribution patterns and linking them to ecological processes is an ongoing area of ecological research. The Morisita Index of aggregation (I_δ) can be used to measure and interpret

spatial point patterns (Golay and Kanevski, 2015). This index measures whether a given point pattern is clumped or dispersed relative to a spatially random distribution. The value taken by the index depends on both quadrat size and population density. The Morisita Index has been applied to detect distribution patterns and understand the processes of seed dispersal, seed banking, and tree establishment (De Almeida and Galetti, 2007; Houle, 1994). It has also been used to analyze spatial patterns of regeneration and adult tree distributions (Hubbell, 1979). These data can help us estimate forest sustainability based on population structure and regeneration status. Thus, this study aimed to clarify the population structure and regeneration status of tree species in an area of LMF, and the relative distribution patterns of sapling-, pole-, and adult-stage tree in a 16-ha permanent plot in an LMF.

2. METHODOLOGY

2.1 Study site

The Kog Ma sub-watershed (18°48′N, 98°54′E) is one of the Mae Sa head-watersheds which is located on the east-facing slope of Mount Doi Pui (1,685 m.a.s.l.), 10 km west of Chiang Mai Province in northern Thailand (Figure 1). The sub-watershed area is 0.65 km^2, and covered by primary LMF with canopy heights of 25-40 m. The dominant tree species are predominantly members of the Fagaceae, especially the genera *Castanopsis*, *Lithocarpus*, and *Quercus*, together with a variety of undergrowth, shrub, and epiphytic species (Bhumibhamon and Wasuwanich, 1970). Many hydrological studies were found in several aspects (Kume et al., 2007; Tanaka et al., 2003; Tanaka et al., 2008). However, because less documentation on forest structure and dynamics of LMF has been reported, particularly based on a large permanent plot, an evaluation of LMF was selected for this study. The climate is subtropical, and the wet season (May to October) transitions to a cool dry season (November to January) and subsequent hot dry season (February to April). The mean annual temperature and rainfall are 20°C and 1,700 mm, respectively. The majority of precipitation occurs in the wet season, with only about 8% of the annual total falling during the dry season (Kume et al., 2007; Tangtham, 1974). The soils are classified as reddish-brown laterites (Thailand soil classification) or Ultisols (USDA Soil Taxonomy), with about 50% sand content and 60-74% porosity (Hashimoto, 2005).

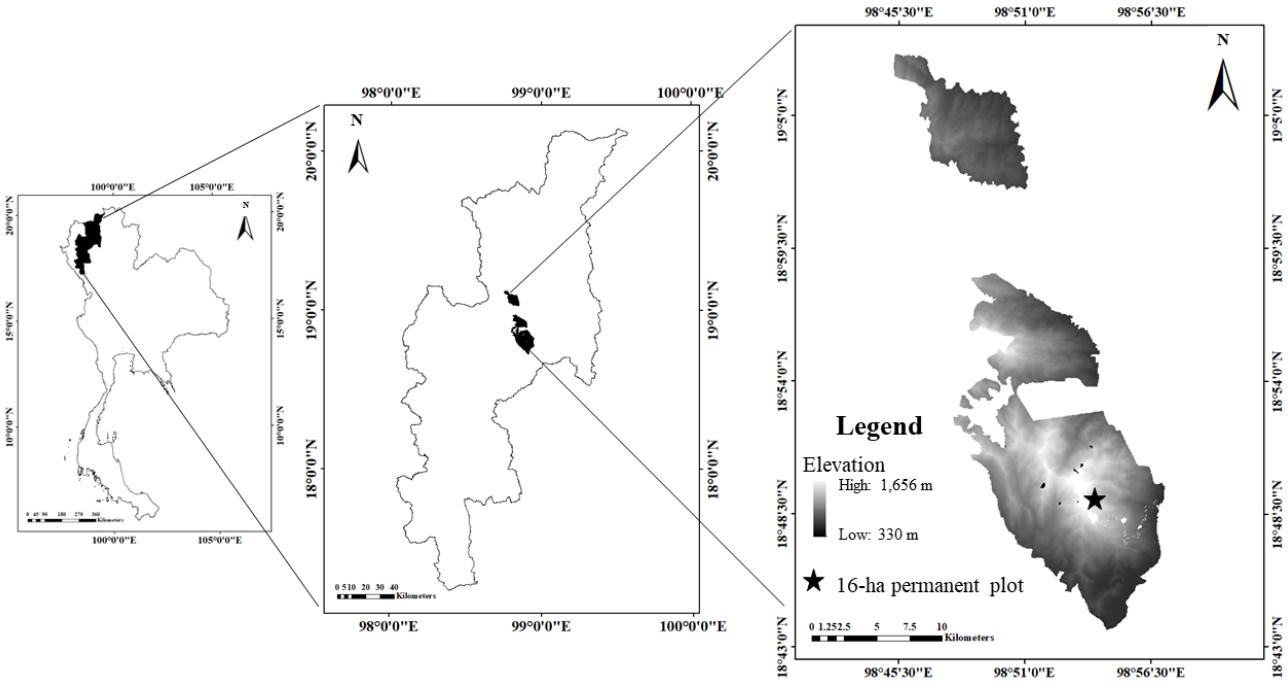

Figure 1. Study area with a 16-ha plot (★) in LMF at Doi Suthep-Pui National Park, northern Thailand

2.2 Data collection

Large permanent plots are widely used to monitor tree spatial distribution and population dynamics relating to the environmental changes (Condit et al., 2000). In 2010, a 16-ha permanent plot was established at an elevation range from 1,300-1,450 m.a.s.l. The plot measured 400 m × 400 m and was subdivided into 1,600 10 m × 10 m subplots to

study forest structure and species composition based on Condit et al. (2014). All trees with a diameter at breast height (DBH, 1.3 m above the soil surface) of ≥2 cm were tagged with a running number, measured, and identified to species. Tree coordinates (x, y) in each subplot were also recorded. Leaf specimens were collected from the enumerated trees and identified by referring to herbarium specimens at the Forest Herbarium of Department of National Parks, Wildlife and Plants Conservation. Species nomenclature was based on Smitinand (2014).

2.3 Data analysis

Plant ecological indices were calculated to clarify the forest structure. For all stems with a DBH ≥ 5.0 cm, the density, dominance and importance value index (IVI) were calculated based on the sum of relative density, dominance and frequency (Krebs, 1994). Basal area (BA), density and diversity were also calculated for each plant family by summing these variables across all species in a given family. The size class distribution for all species with at least 30 individuals in the 16-ha plot were prepared. This analysis included the small size class of saplings (2.0 ≤ DBH < 5.0 cm). The population structure across this size reflects that of larger trees (Mclaren et al., 2005). Size class distribution of each species was defined by families of probability mass functions fitting to the class frequency. In order to specifically select the most suitable family of mass distribution, Anderson-Darling statistic (Anderson and Darling 1952; Liebscher, 2016) and probability-probability plot (Chambers et al., 2017) were then applied to help determine the goodness-of-fit among families of the probability function. Subsequently, the optimal probability function was specified from the set of the distribution function (varied number of parameters) of the selected family using the Likelihood ratio test and Akaike Information criteria (Akaike, 1998). The regeneration status of each tree species was predicted on the basis of its size-class distribution.

To detect the distribution patterns of saplings, pole-stage (5.0 ≤ DBH < 10.0 cm) and mature trees (DBH ≥10.0 cm), all species with >80 individuals were selected (Lan et al., 2009). Morisita's I_δ index was calculated by dividing the plot into quadrats of various sizes. The smallest quadrat size was obtained by dividing the 16-ha plot into square quadrats each with a size of $(0.1)^2$ m × 400 m (i.e., x-axis length) and $(0.10)^2$ × 400 m (i.e., y-axis length), yielding 4 m × 4 m (16 m^2) quadrats. Larger quadrats were obtained by doubling the length of the smaller quadrats, producing quadrats that ranged from 16 m^2 to 6.5 ha. Morisita's I_δ was then calculated using the following equation (Morisita, 1959):

$$I_\delta = q \frac{\sum n_{i-N}^2}{(N^2 - N)}$$

Where; n_i is the number of individuals in each quadrat, N is the total number of individuals in the16 ha plot, and q is the number of quadrats of a given size.

The I_δ value was used to classify distribution patterns as random (I_δ=1), clumped or aggregated (I_δ >1), or regular (I_δ <1). F-tests were used to test for departures from random expectation for each quadrat size. The statistical significance of the F-tests was tested at the 95% confidence limit ($p<0.05$).

3. RESULTS AND DISCUSSION

3.1 Species composition and population structure

A total of 28,078 individuals ≥2 cm DBH were measured and identified. This population was composed of 220 species from 139 genera and 63 families. The average density of all trees ≥5.0 cm DBH was 806.88 stems/ha, and this population included 195 species from 131 genera and 56 families (Table S1). The highest tree density (stems/ha) was found for *Castanopsis acuminatissima* (n=106.56) followed by *Styrax benzoides* (n=38.94), *Vernonia volkameriiolia* (n=36.19), *Castanopsis armata* (n=29.00), *Litsea martabanica* (n=27.31), *Persea gamblei* (n=24.81), *Helicia nilagirica* (n=22.44), *Turpinia pomifera* (n=20.06), and *Schima wallichii* (n=19.13). A number of other temperate tree species were present in low densities, including members of the families Podocarpaceae (*Podocarpus neriifolius* and *Dacrycarpus imbricatus*), Betulaceae (*Betula alnoides* and *Carpinus viminea*), and Juglandaceae (*Engelhardtia spicata* and *E. serrata*). The most dominant tree species, with an average BA of 32.79 m^2/ha and relative basal area (RBA, %) of 14.24, was *Castanopsis acuminatissima*. Other dominant species were *Schima wallichii* (RBA=9.23%), *Manglietia garrettii* (6.41%), *Castanopsis armata* (5.36%), *Castanopsis tribuloides* (4.80%), *Litsea grandis* (3.15%), *Syzygium toddlioides* (2.89%), *Syzygium tetragonum* (2.87%), *Choerospondias axillaris* (2.81%), and *Michelia baillonii* (2.24%). These 10 species accounted for 54.00% of the total BA. To determine the ecological influence of each species, the IVI (%) was calculated. The species with the highest IVI was *Castanopsis acuminatissima* (33.36), followed by *Schima wallichii* (14.61),

Castanopsis armata (12.86), *Styrax benzoides* (9.55), *Castanopsis tribuloides* (8.85), *Litsea martabanica* (8.29), *Manglietia garrettii* (8.23), *Persea gamblei* (8.20), *Vernonia volkameriiolia* (6.21), *Litsea martabanica* (7.45), *Helicia nilagirica* (6.30), and *Syzygium toddlioides* (6.21).

The Euphorbiaceae, Lauraceae, Fagaceae, Moraceae, and Theaceae families had the most species (20, 19, 16, 11, and 8 species, respectively). The Fagaceae family had the highest per hectare tree density (186.31 stems/ha) followed by the Lauraceae (92.69 stems/ha), Euphorbiaceae (71.00 stems/ha), Theaceae (39.69 stems/ha), and Styracaceae (38.94 stems/ha) families. The Fagaceae family also had the highest BA (9.69 m^2/ha), followed by the Lauraceae (4.11 m^2/ha), Theaceae (3.40 m^2/ha), Magnoliaceae (2.76 m^2/ha), and Myrtaceae (2.38 m^2/ha) families (Figure 2).

As also reported for tropical montane forests elsewhere in Southeast Asia (Brambach et al., 2017; Buot and Okitsu, 1998; Maxwell et al., 1997; Ohsawa, 1995; Pendry and Proctor, 1997), the Fagaceae and Lauraceae families were more abundant and more likely to occupy the highest layer of the tree canopy in the LMF in this study. The name "oak-laurel forest" has been used for this vegetation type (Ashton, 2003; Kochummen, 1989). Oak-laurel forests are the dominant vegetation type in the mountains of tropical Asia from the Himalayas to New Guinea (Sri-Ngernyuang et al., 2003), and are closely related to the temperate evergreen oak forests of East Asia (Tagawa 1995; Zhu et al., 2016). However, in Malesia, tropical lower montane forests are often dominated more by Myrtaceae than by Lauraceae (Aiba and Kitayama, 2020; Kochummen, 1982). Ashton (2015) reported that lower-montane oak-laurel forest is rare in Borneo and patchy in Peninsular Malaysia, and he named lower montane forest on Mount Mulu, Borneo, as "lower montane kerangas". A similar name for lower montane forest on old soil with low dominance of Lauraceae at Mount Kinabalu has also been mentioned (Aiba and Kitayama, 2020).

3.2 Regeneration of tree species

The characteristics of regenerating tree populations were explored using DBH-class distributions. In total, 123 tree species with populations comprising >30 individuals were analyzed. The result showed that DBH classes followed two distributions: negative exponential (NE; reverse-J) and polynomial (PO). Size class distributions for 78 species followed an NE distribution. These distributions have the greatest numbers of individuals in the lowest DBH class and progressively fewer individuals in larger DBH classes (Table S1). Considering the dominance of the Fagaceae, only three species from that family - *Castanopsis acuminatissima*, *C. tribuloides*, and *Lithocarpus truncates* - followed NE distributions (Figure 3 (a)-(c)); this indicated that they had a robust capacity to maintain a stable population structure in the future, because smaller trees will grow into larger size classes and thus replace larger trees as they die. In particular, these species would be sustained if mortality were greater among small (suppressed) trees and large trees than among mid-sized co-dominants

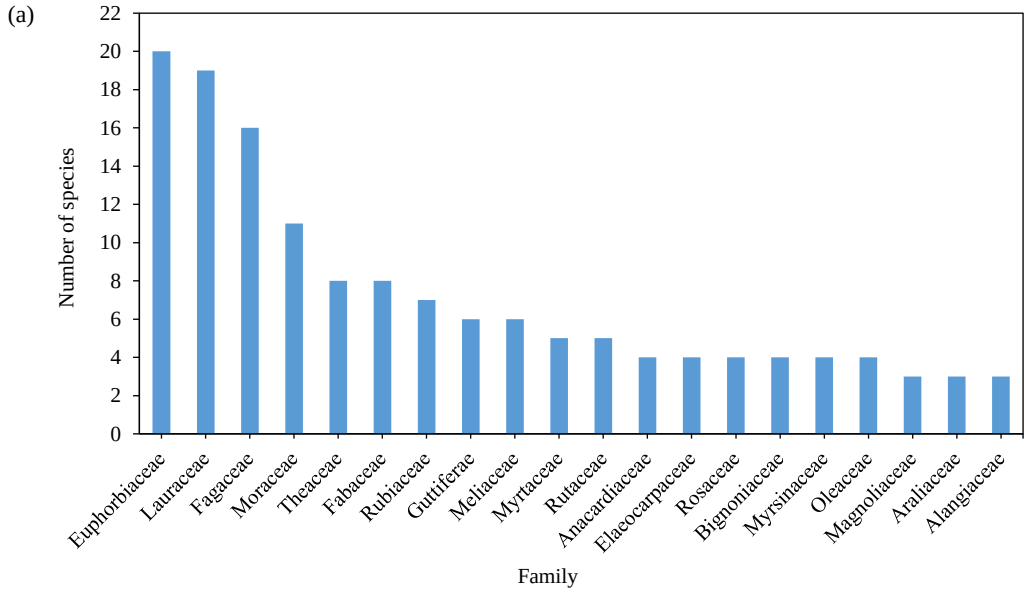

Figure 2. (a) Numbers of species, (b) tree densities, and (c) basal areas of the 20 most dominant families in the LMF for stems ≥ 5.0 cm DBH

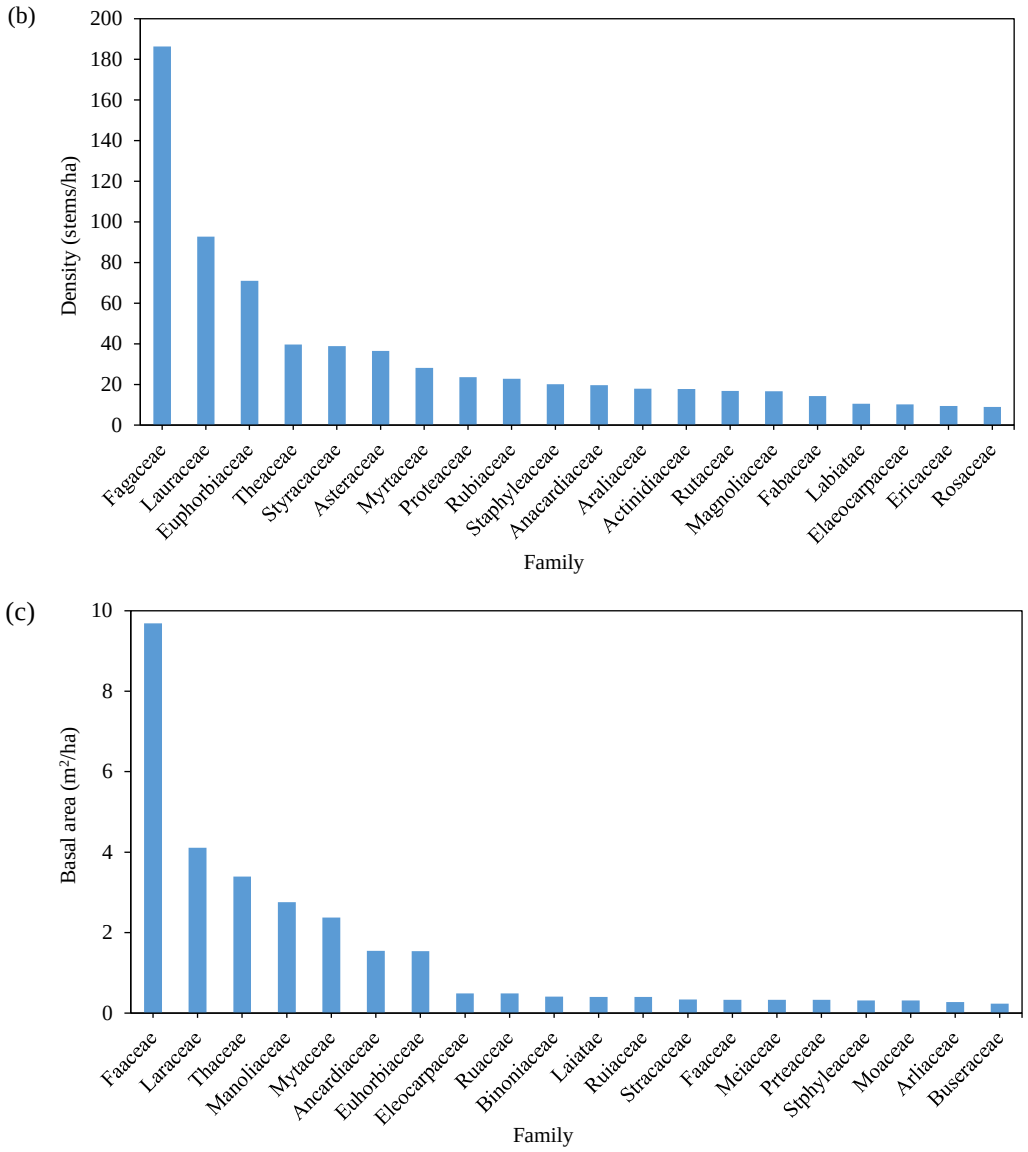

Figure 2. (a) Numbers of species, (b) tree densities, and (c) basal areas of the 20 most dominant families in the LMF for stems ≥5.0 cm DBH (cont.)

(Goff and West, 1975). Other species belonging to the Fagaceae followed PO distributions, in which discontinuous DBH class distributions were detected (Figure 3 (d)-(h)). A lack of successful regeneration could have been caused by the activities of seed predators or frugivores, particularly small rodents that eat the seeds of Fagaceae (Rueangket et al., 2019). The large, edible seeds of *C. diversifolia* and *C. armata* were overexploited by local people, leading to reduced seed germination and discontinuous size-class distributions. Forty-six species followed PO distributions. Most species of Lauraceae, including *Actinodaphne henryi*, *Cinnamomum inner*, and *Litsea pierrei*, had discontinuous size-class distributions expressed through PO curves (Table S1).

Pioneer species, such as *Macaranga indica*, *Morus macroura*, *Erythrina subumbrans*, and *Rhus javanica* (Figure 4 (a)-(d)), also followed PO distributions. The late pioneer species, *Choeros-pondias axillaris*, *Schima wallichii*, and *Betula alnoides*, showed the same patterns (Figure 4 (e)-(g)). Pioneer species were mostly found in canopy gaps, which suggests that bright light conditions in disturbed areas are required for their successful establishment (Goodale et al., 2012; Huth and Wagner, 2006; Miyazawa et al., 2006; Sangsupan et al., 2021; Swinfield et al., 2016).

One of the conifer species, *Podocarpus neriifolius*, had a low population density of eight trees with DBH >10 cm in the whole 16-ha plot. Similarly low densities (2-4 trees/ha of DBH >10 cm) of this

species were found in montane forests in Papua New Guinea (Enright and Jaffré, 2011). Its regeneration may be unable to compete with angiosperms or rainforest tree species that can absorb light as seedlings in a shaded understory, but which rapidly increase their growth rates when light availability increases (Brodribb et al., 2012; Wright et al., 2010). Therefore, we cautiously conclude that diameter distributions can indicate whether the density of smaller trees in a stand is sufficient to replace the current population of larger trees, which may help us to estimate forest sustainability.

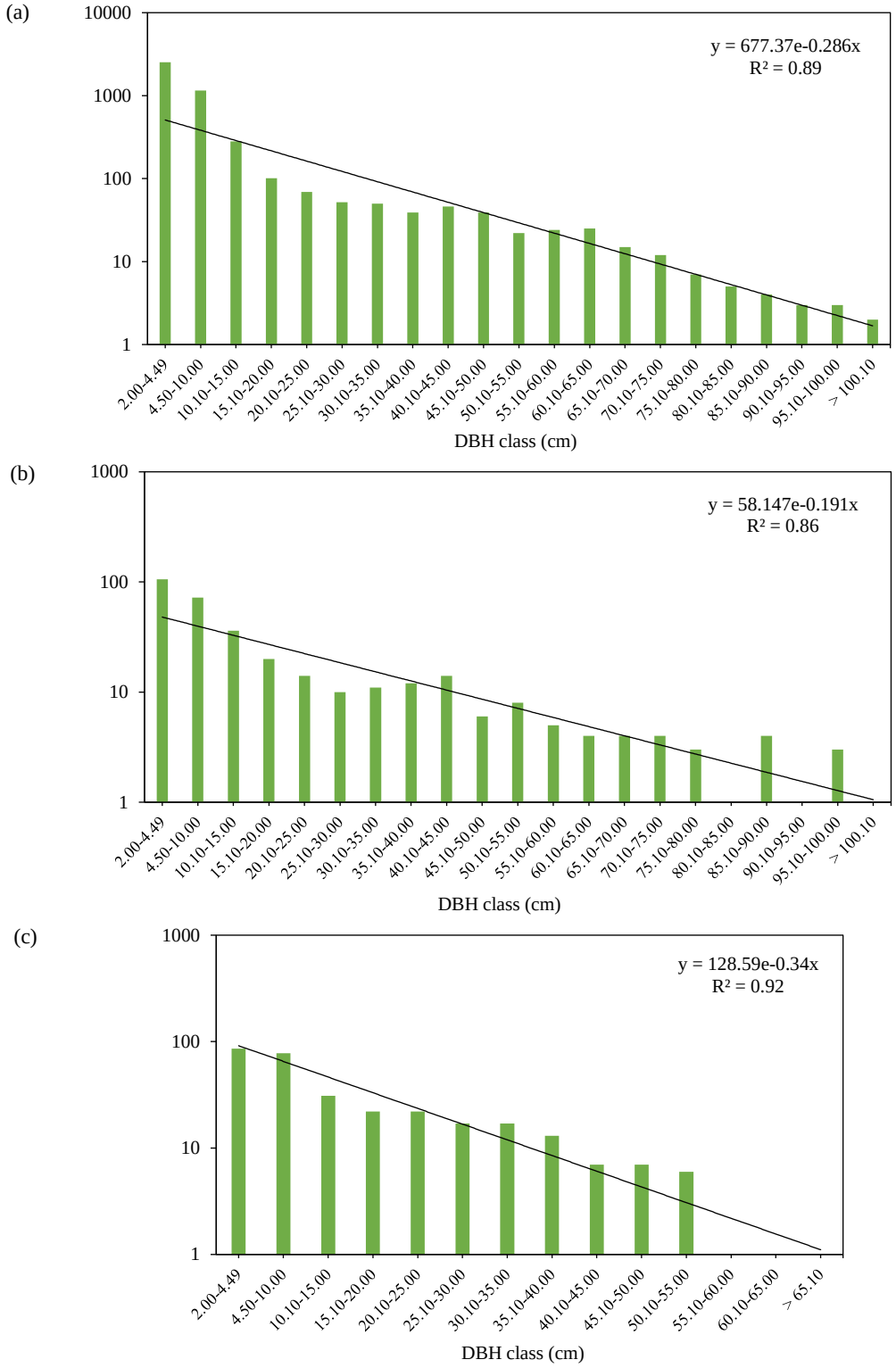

Figure 3. Diameter class distributions plotted on a logarithmic scale for some species of Fagaceae. (a) *Castanopsis accuminatissima*, (b) *Castanopsis tribuloides*, (c) *Lithocarpus truncatus*, (d) *Castanopsis armata*, (e) *Castanopsis diversifolia*, (f) *Castanopsis argyrophylla*, (g) *Lithocarpus mekongensis*, and (h) *Lithocarpus auriculatus*

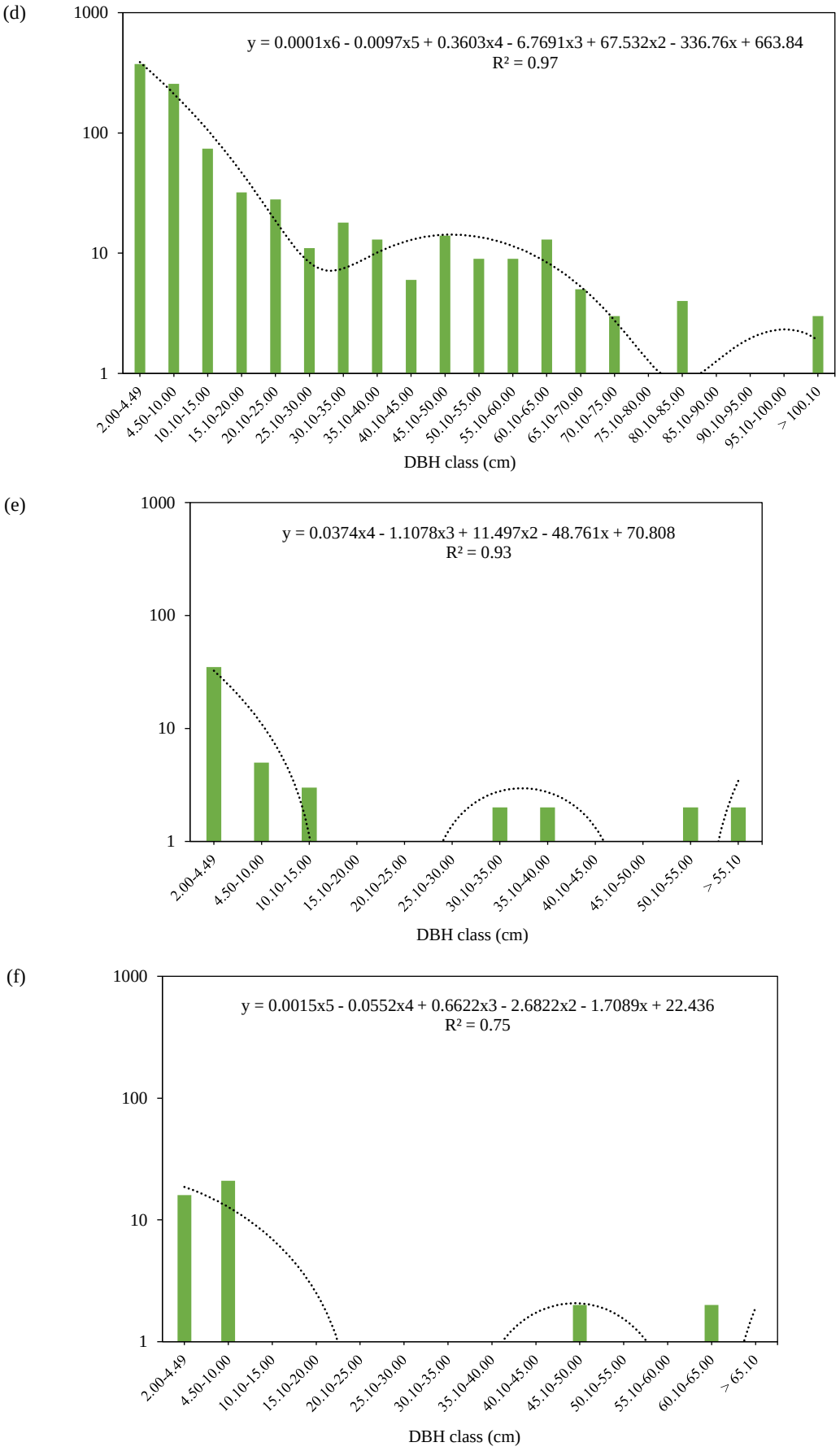

Figure 3. Diameter class distributions plotted on a logarithmic scale for some species of Fagaceae. (a) *Castanopsis accuminatissima*, (b) *Castanopsis tribuloides*, (c) *Lithocarpus truncatus*, (d) *Castanopsis armata*, (e) *Castanopsis diversifolia*, (f) *Castanopsis argyrophylla*, (g) *Lithocarpus mekongensis*, and (h) *Lithocarpus auriculatus* (cont.)

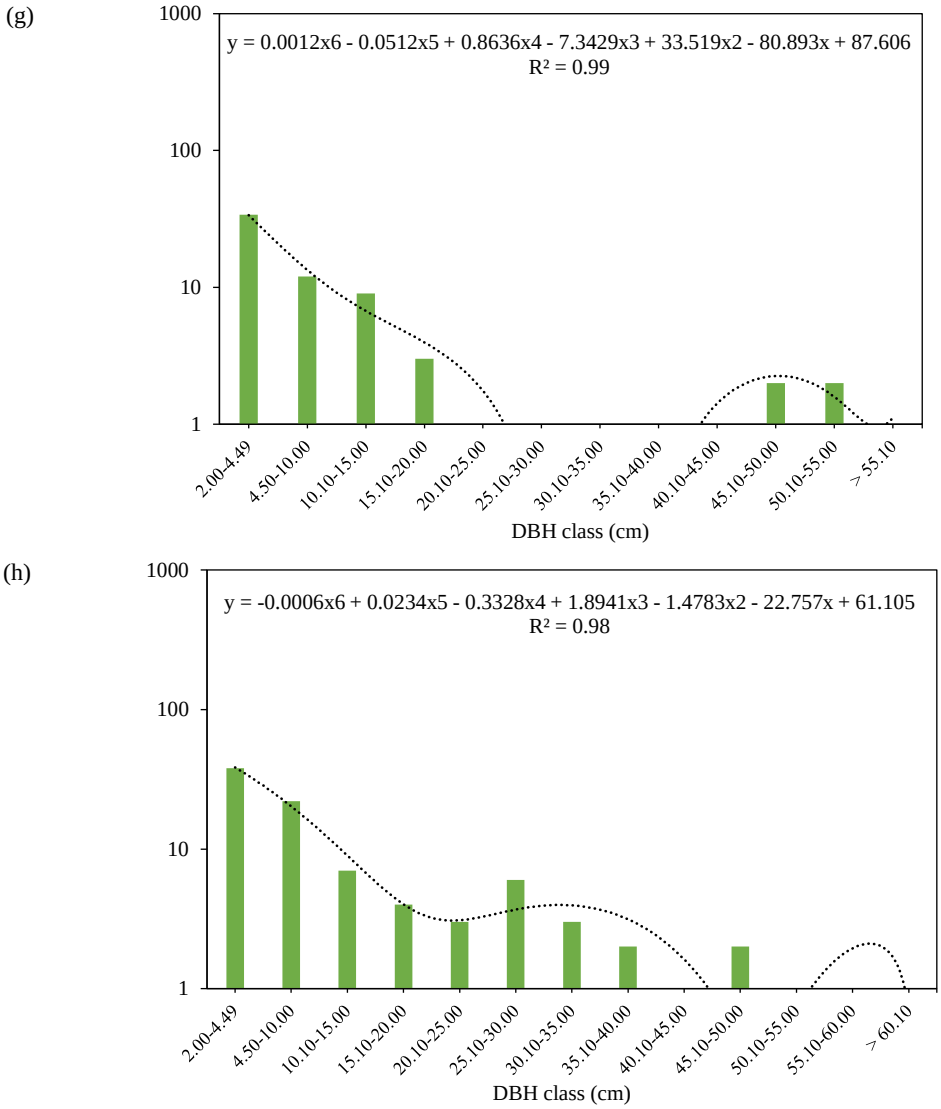

Figure 3. Diameter class distributions plotted on a logarithmic scale for some species of Fagaceae. (a) *Castanopsis accuminatissima*, (b) *Castanopsis tribuloides*, (c) *Lithocarpus truncatus*, (d) *Castanopsis armata*, (e) *Castanopsis diversifolia*, (f) *Castanopsis argyrophylla*, (g) *Lithocarpus mekongensis*, and (h) *Lithocarpus auriculatus* (cont.)

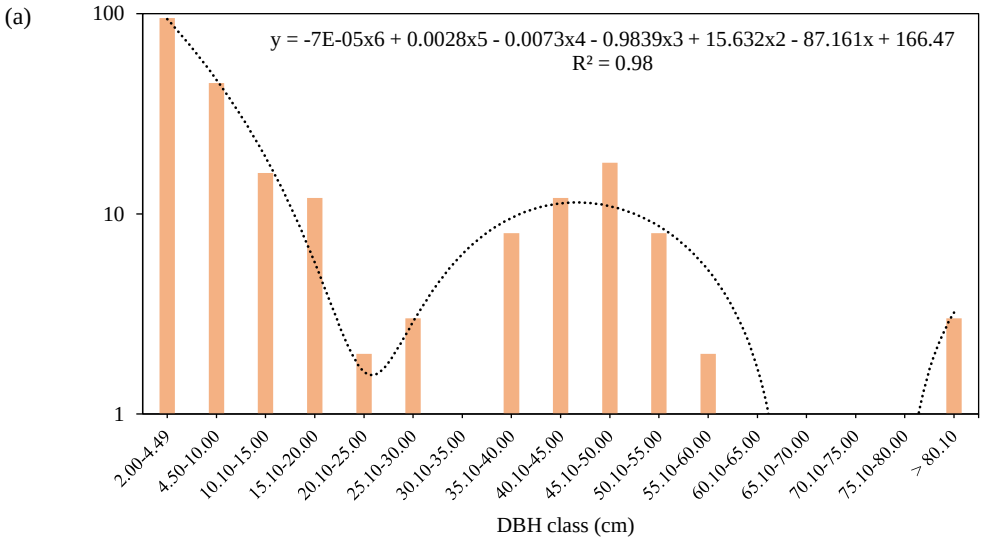

Figure 4. Diameter class distributions plotted on a logarithmic scale for pioneer species: (a) *Macaranga indica*, (b) *Morus macroura*, (c) *Erythrina subumbrans*, (d) *Rhus javanica*, (e) *Choerospondias axillaris*, (f) *Schima wallichii*, (g) *Betula alnoides*, and the shade-tolerant species as (h) *Podocarpus neriifolius*

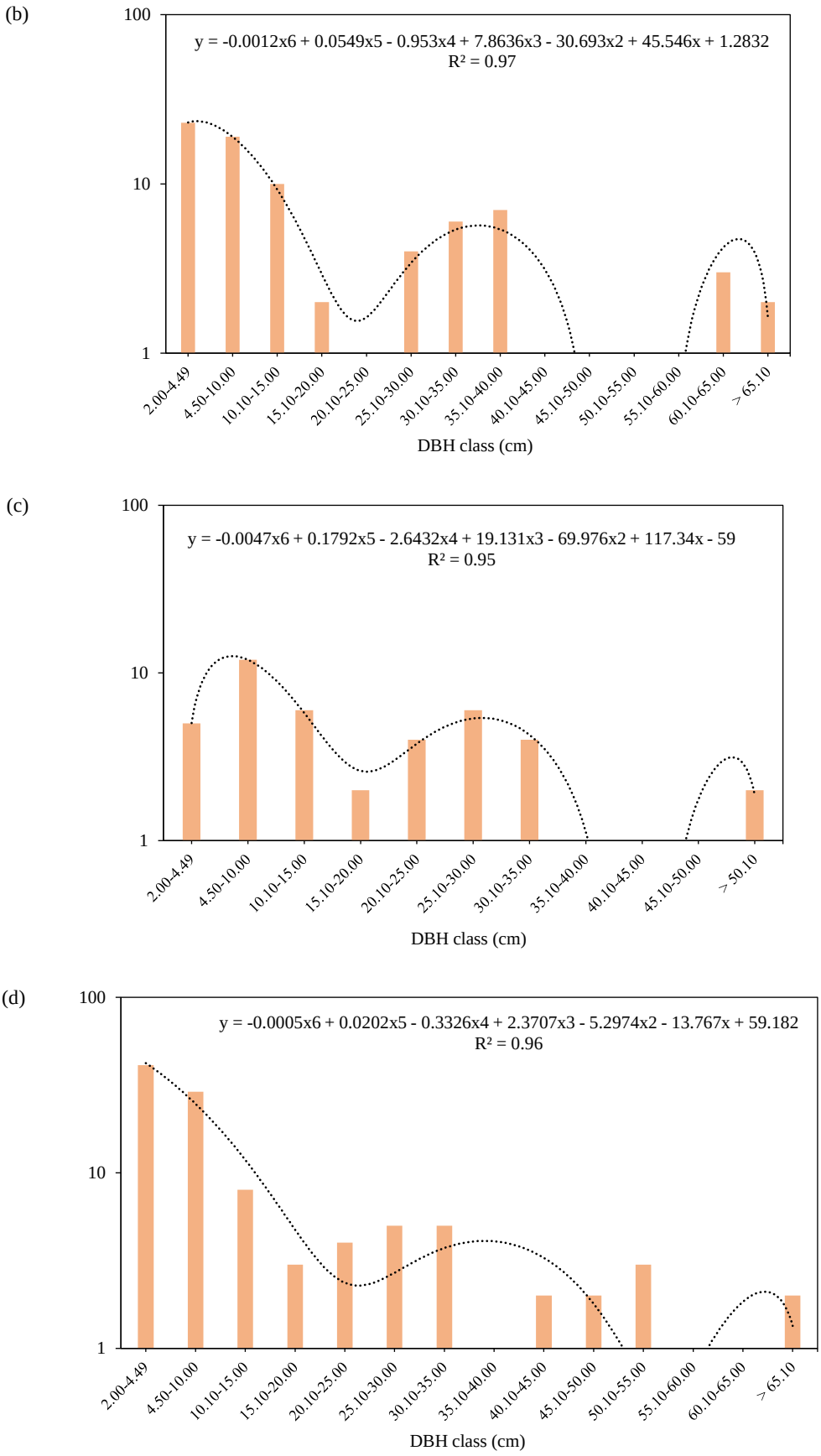

Figure 4. Diameter class distributions plotted on a logarithmic scale for pioneer species: (a) *Macaranga indica*, (b) *Morus macroura*, (c) *Erythrina subumbrans*, (d) *Rhus javanica*, (e) *Choerospondias axillaris*, (f) *Schima wallichii*, (g) *Betula alnoides*, and the shade-tolerant species as (h) *Podocarpus neriifolius* (cont.)

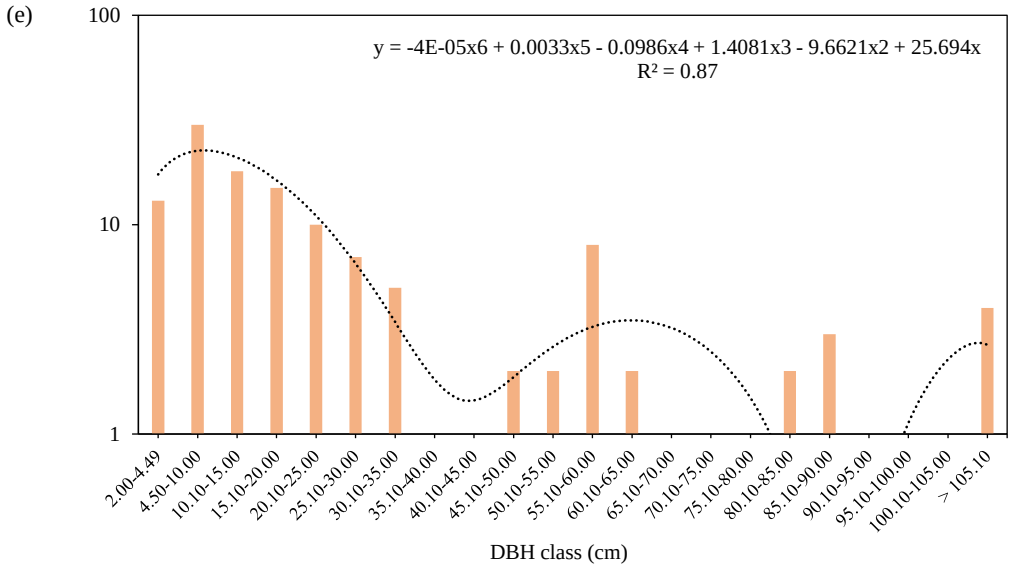

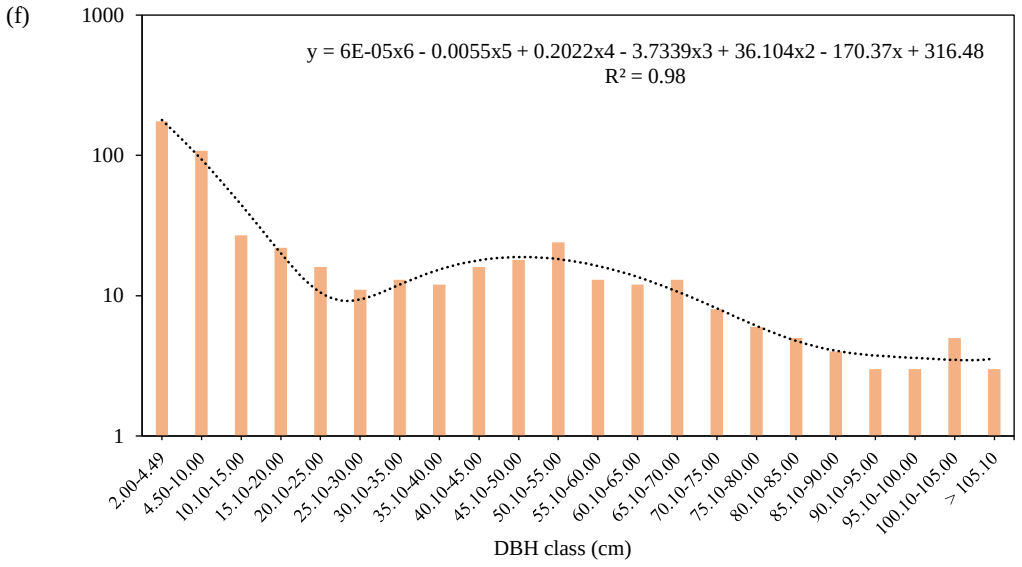

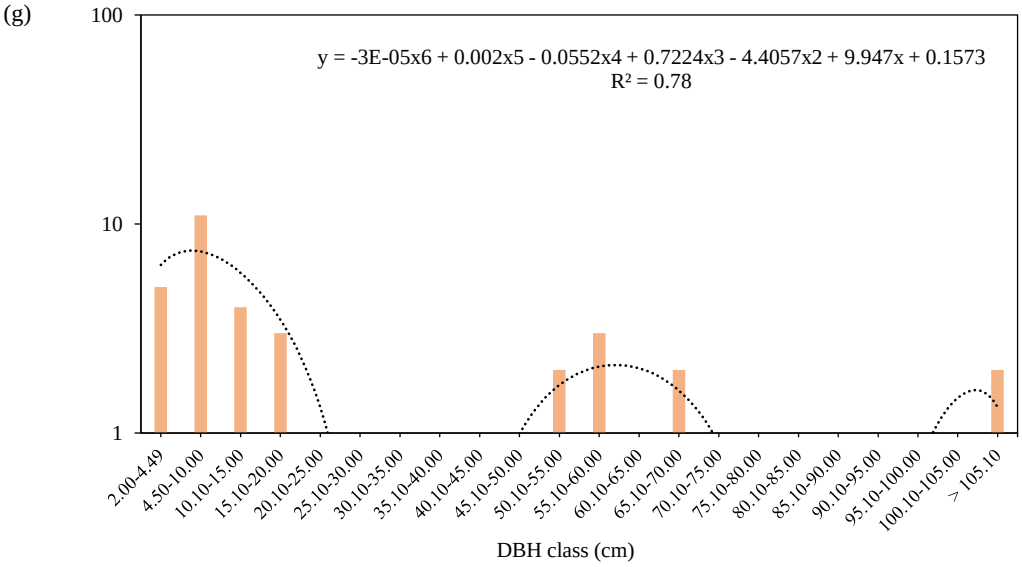

Figure 4. Diameter class distributions plotted on a logarithmic scale for pioneer species: (a) *Macaranga indica*, (b) *Morus macroura*, (c) *Erythrina subumbrans*, (d) *Rhus javanica*, (e) *Choerospondias axillaris*, (f) *Schima wallichii*, (g) *Betula alnoides*, and the shade-tolerant species as (h) *Podocarpus neriifolius* (cont.)

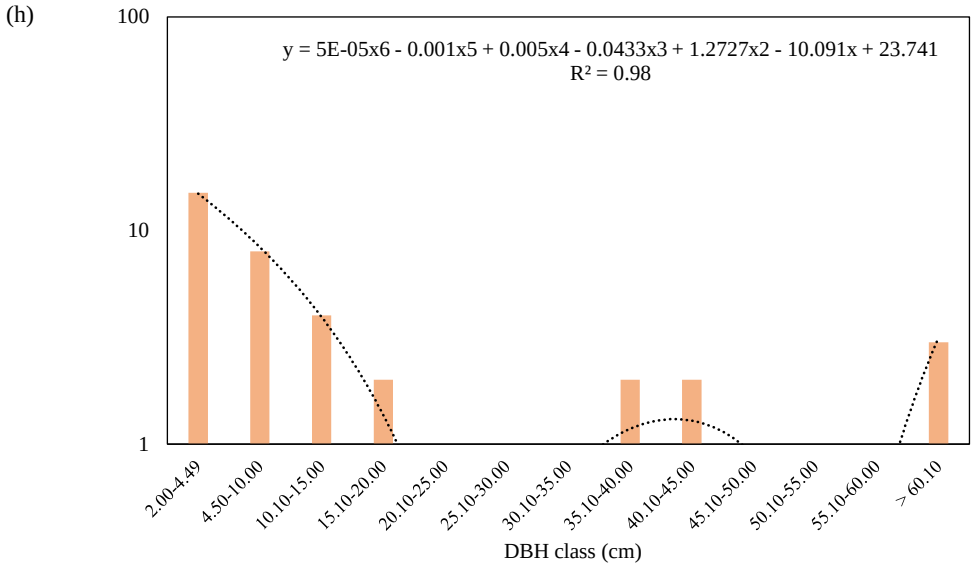

Figure 4. Diameter class distributions plotted on a logarithmic scale for pioneer species: (a) *Macaranga indica*, (b) *Morus macroura*, (c) *Erythrina subumbrans*, (d) *Rhus javanica*, (e) *Choerospondias axillaris*, (f) *Schima wallichii*, (g) *Betula alnoides*, and the shade-tolerant species as (h) *Podocarpus neriifolius* (cont.)

3.3 Tree distribution pattern

Seventy-two species were selected for the analysis of spatial distribution patterns. The Morisita index, I_δ, varied among species, growth stages (sapling, pole stage, and mature tree) and quadrat sizes. As quadrat size increased, the intensity of spatial aggregation decreased. Sixty-two species had clumped patterns ($I_\delta > 1.0$) for all growth stages and quadrat sizes (Table S1). Aggregated spatial patterns were particularly observed in dominant Fagaceae species, such as *Castanopsis acuminatissima*, *C. armata*, and *Lithocarpus truncatus* (Figure 5). *Manglietia garrettii*, *Prunus arborea*, *Bridelia glauca*, *Markhamia stipulate*, and *Lithocarpus dealbatus* followed random patterns as saplings, but were clumped as pole-stage and mature trees (Figure 6). By contrast, *Michelia baillonii*, *Schima wallichii*, *Canarium euphyllum*, and *Elaeocarpus serratus* were clumped as saplings but randomly distributed in other life stages (Figure7). Only one species, *Tarennoidea wallichii*, had a random spatial pattern at every growth stage (Figure 7(d)).

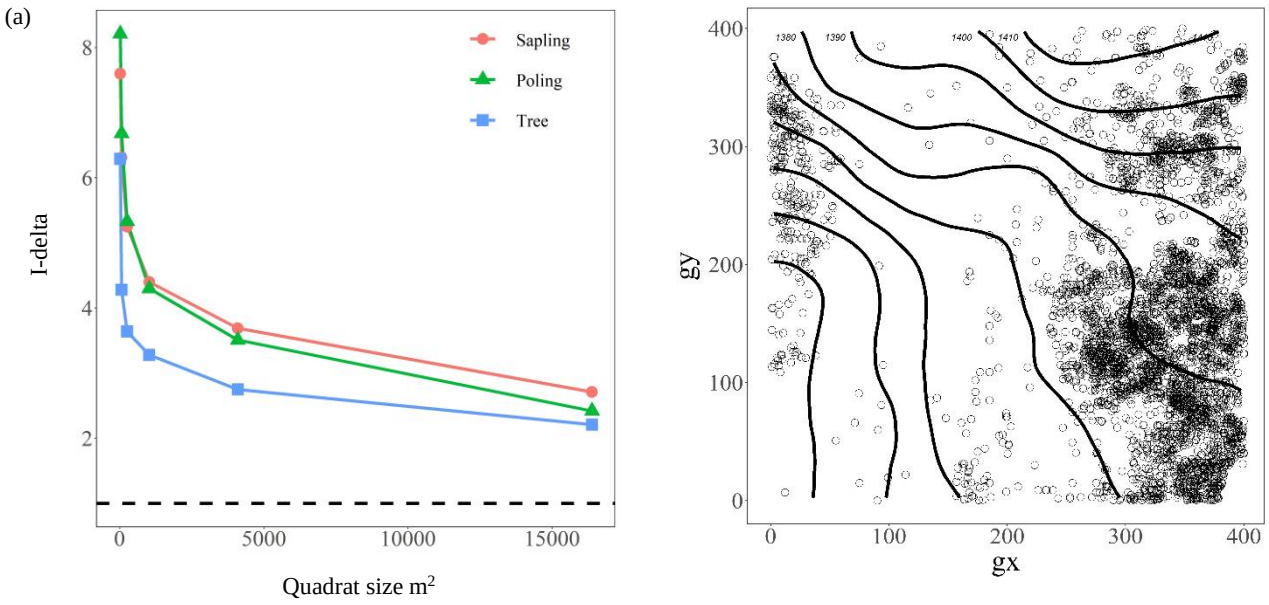

Figure 5. Clumped spatial distribution patterns of dominant Fagaceae at each growth stage in the 16-ha permanent plot at HKM: (a) *Castanopsis accuminatissima*, (b) *C. armata*, (c) *Lithocarpus truncatus*, and (d) *Quercus oidocarpa*

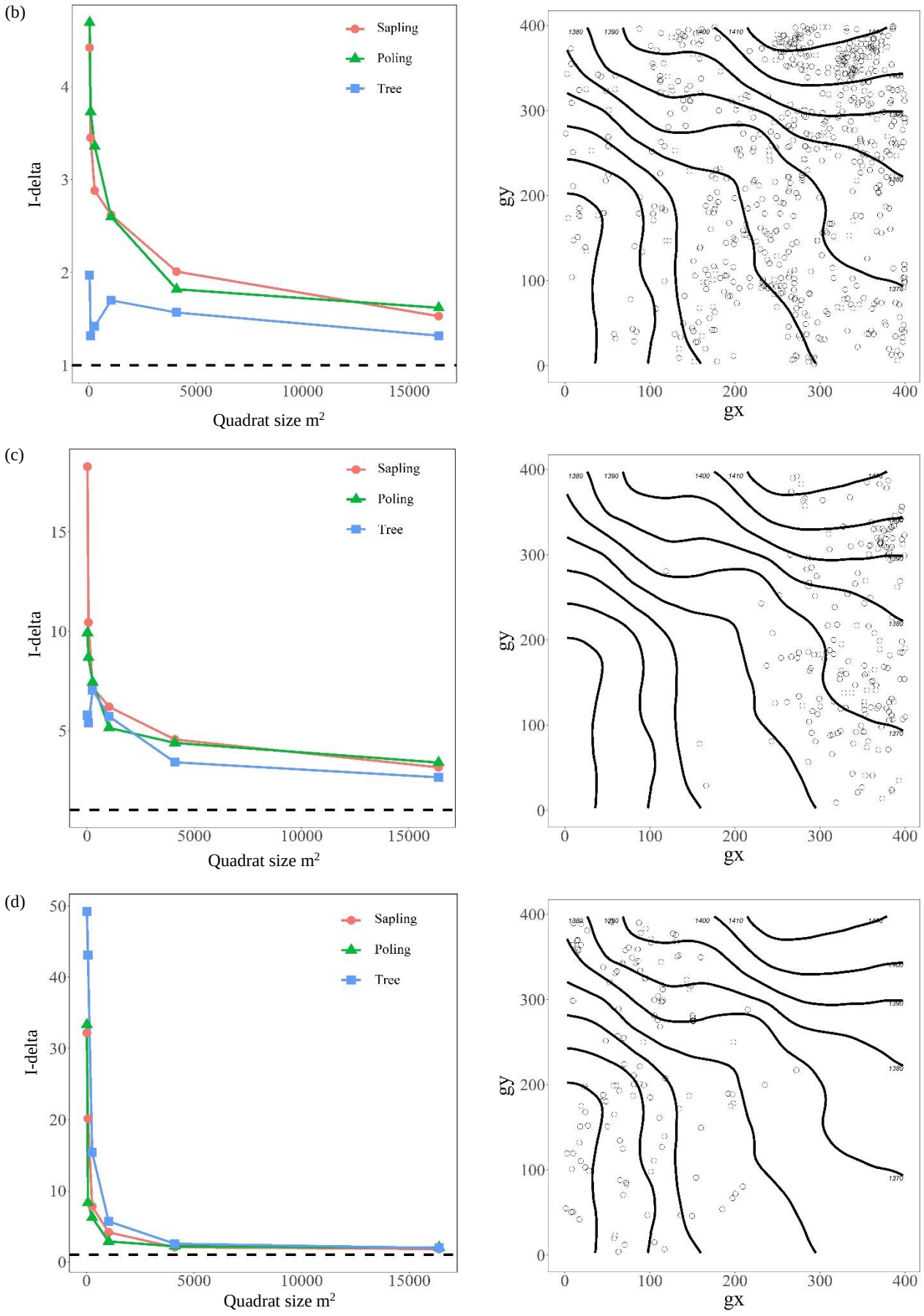

Figure 5. Clumped spatial distribution patterns of dominant Fagaceae at each growth stage in the 16-ha permanent plot at HKM: (a) *Castanopsis accuminatissima*, (b) *C. armata*, (c) *Lithocarpus truncatus*, and (d) *Quercus oidocarpa* (cont.)

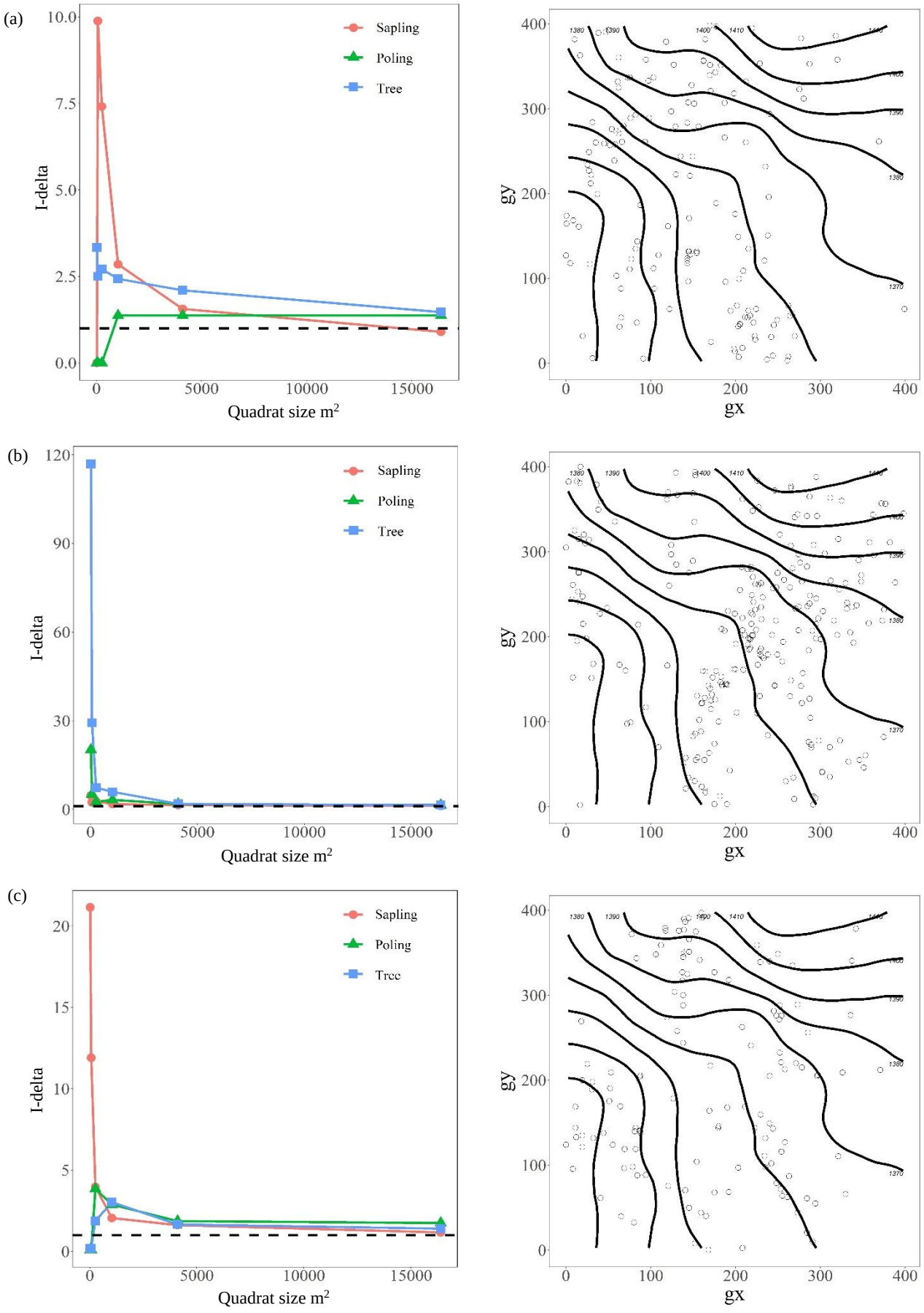

Figure 6. Species with random spatial patterns as saplings and clumped patterns at other stages in the 16-ha plot at HKM: (a) *Mangleitia garetttia*, (b) *Prunus arborea*, (c) *Markhamia stipulata*, and (d) *Bridelia glauca*

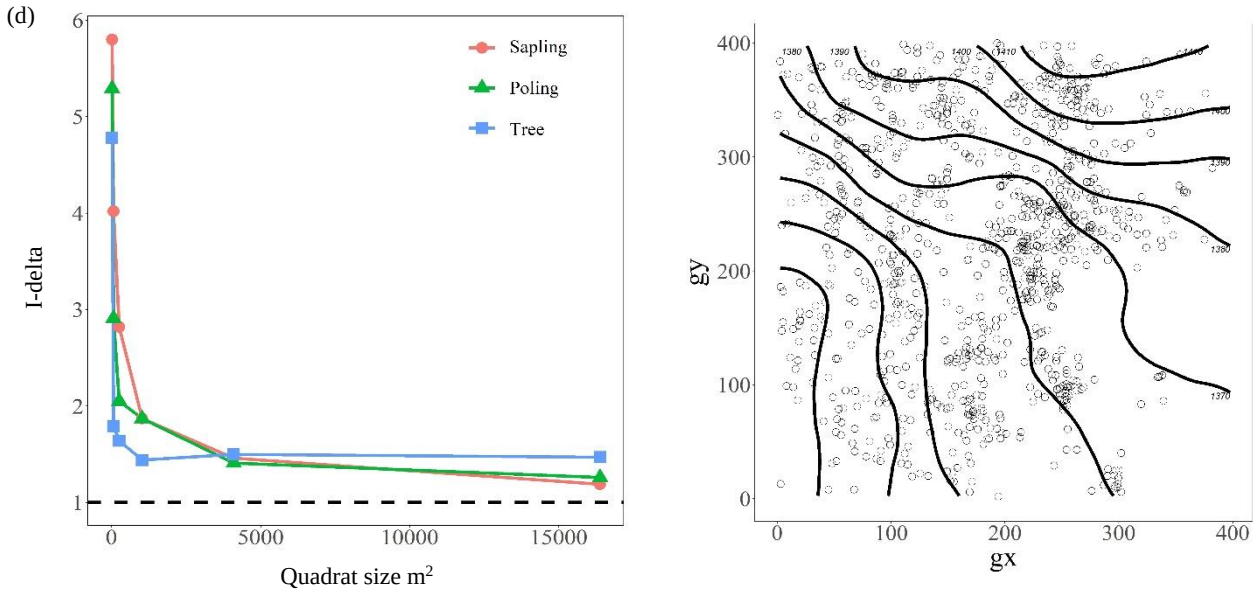

Figure 6. Species with random spatial patterns as saplings and clumped patterns at other stages in the 16-ha plot at HKM: (a) *Mangleitia garetttia*, (b) *Prunus arborea*, (c) *Markhamia stipulata*, and (d) *Bridelia glauca* (cont.)

Clumped spatial patterns are usually observed for tree species in tropical forests. Clumping can be influenced by seed dispersal (Aparajita and Gopal, 2008; Elias et al., 2011). We found that the dominant species of Fagaceae had clumped patterns at every life stage, even though spatial distributions varied among species that preferentially occupied ridge sites (Figure 5). Most species of Fagaceae have acorn or nut fruit types, which fall directly beneath mature trees and generate clumps of saplings around parent trees. Seeds are also eaten by rodents such as squirrels and rats (Rueangket et al., 2019), which are well-known seed predators with strong incisors that enable them to gnaw and consume nuts and other fruits with thick seed coats (Corlett, 2017; Vander Wall, 2001). Some seeds can be distributed by rodents through scatter hoarding. Some seeds may then germinate and become established from forgotten seed caches (Corlett, 2017; Suzuki et al., 2007). By contrast, *Tarenoidea wallichii* (Rubiaceae) has small freshy fruits (Chamchumroon and Puff, 2003; Rueangket et al., 2021), which may facilitate its dispersal by frugivorous birds (Aparajita and Gopal, 2008; Corlett, 2017). Birds not only move seeds away from mature trees, but may also facilitate germination after seeds pass through their digestive system (Murali, 1997). This kind of dispersal typically promotes random rather than clumped patterns, similar to our results.

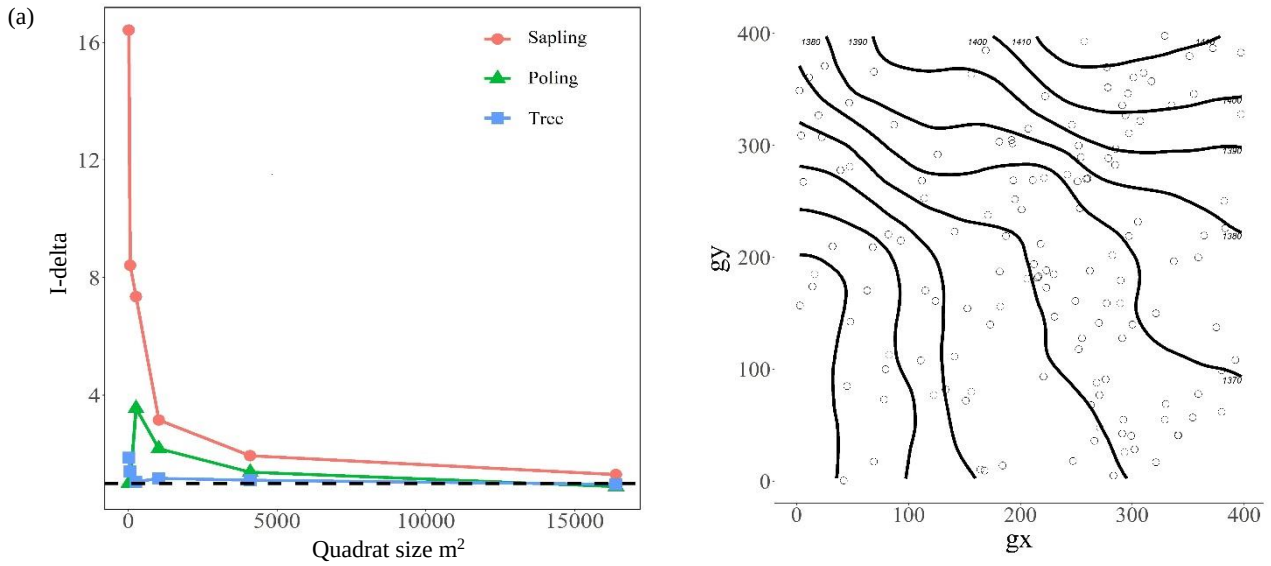

Figure 7. Species with clumped pattern as saplings and random patterns at other life stages in the 16-ha plot at HKM: (a) *Maichelia baillonii*, (b) *Schima wallichii*, and (c) *Canarium euphyllum*, while, and (d) *Tarennoidea wallichii*, which had random spatial patterns at every stage.

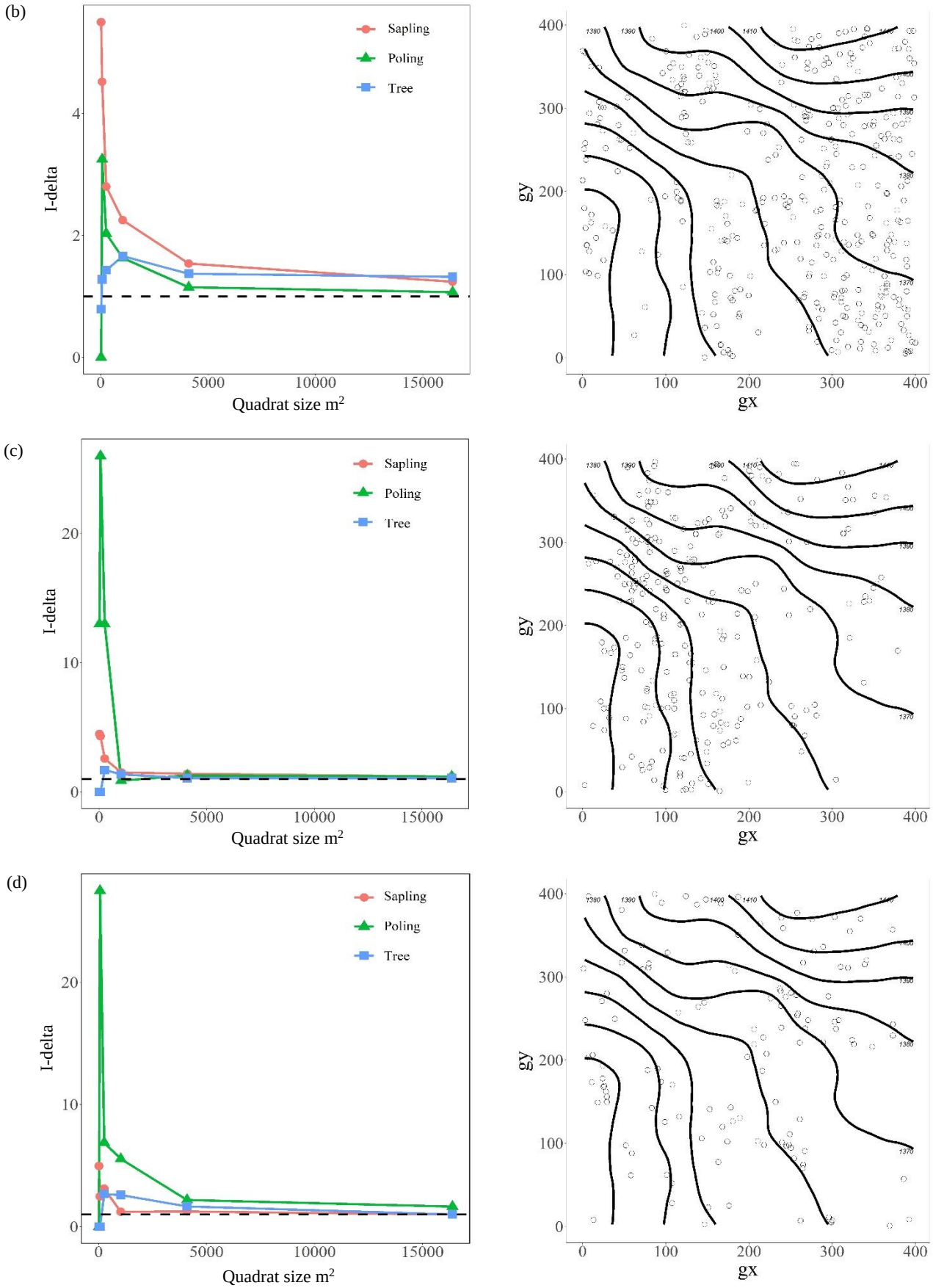

Figure 7. Species with clumped pattern as saplings and random patterns at other life stages in the 16-ha plot at HKM: (a) *Maichelia baillonii*, (b) *Schima wallichii*, and (c) *Canarium euphyllum*, while, and (d) *Tarennoidea wallichii*, which had random spatial patterns at every stage (cont.).

Canarium euphyllum was clumped at the sapling stage but randomly distributed in other stages (Figure 7). Its heavy fruits generally fall close to mature trees (Kitamura et al., 2006), where larger numbers of seedlings and saplings are found than in other places. These dense aggregations of seedlings and saplings experience intense competition and density-dependent mortality, also known as self-thinning (Marod et al., 1999). In this study, survival rates increased with distance from the adult trees, which created a random distribution. Other researchers have reported the effects of natural disturbances on clumped tree species distribution patterns (Bunyavejchewin et al., 2003; Elias et al., 2011; Marod et al., 2021). Environmental changes, particularly the sudden influx of high-intensity light after a big tree falls, can produce clumped tree distributions. Thus, changes in the spatial distributions of trees have implications for all parts of an ecosystem, both biotic and abiotic, and are reflected in different patterns of forest cover and species composition.

4. CONCLUSION

The 16-ha permanent plot in LMF at Doi Suthep-Pui National Park supported high diversity of tree species (220 species in total). The dominant families, based on the numbers of species and population densities, were Fagaceae, Lauraceae, and Theaceae. Tree regeneration based on diameter class distributions suggested that 78 species can maintain their population structure, particularly the dominant species of Fagaceae, *Castanopsis acuminatissima*, *C. tribuloides*, and *Lithocarpus truncata*. Other species had discontinuous unimodal or PO distributions, particularly pioneer species such as *Macaranga indica*, *Morus macroura*, and *Rhus javanica*. These species generally established in canopy gaps, in which the environment was greatly altered and did not support the regeneration of climax species. The establishment of pioneer species may facilitate the development of suitable environments for climax species. Spatial distribution patterns can feed back to affect ecological dynamics, thereby further reinforcing patterns dependent on local interactions. For example, spatial patterns could be affected by the abundance of, and distance to, available resources, as well as by the relationship between seed dispersal and frugivores.

Diameter-class distributions can assist in the evaluation of potential forest sustainability and inform biodiversity conservation plans for species with unimodal or PO distributions. In addition, distributions can inform the selection of species suitable for the LMF restoration program, especially in terms of the appropriate mixtures of pioneer and climax species.

ACKNOWLEDGEMENTS

This research was supported by the Kasetsart University Research and Development Institute (KURDI). We would like to thanks the members of Thai Forest Ecological Research Network and official staffs of Doi Suthep-Pui National Parks who supported field data collection and analysis.

REFERENCES

Aiba S, Kitayama K. Light and nutrient limitations for tree growth on young versus old soils in a Bornean tropical montane forest. Journal of Plant Research 2020;133(5):665-79.

Akaike H. Information theory and an extension of the maximum likelihood principle. In: Parzen E, Tanabe K, Kitagawa G, editors. Selected Papers of Hirotugu Akaike. New York, USA: Springer; 1998. p. 199-213.

Amdre J, Raes F, Menne B. Impacts of Europe's changing climate - 2008 indicator - based assessment. IOP Conference Series: Earth and Environmental Science 2009;6(30):Article No. 292042.

Anderson TW, Darling DA. Asymptotic theory of certain "goodness of fit" criteria based on stochastic processes. The Annals of Mathematical Statistics 1952;23(2):193-212.

Aparajita D, Gopal SR. Dispersal modes and spatial patterns of tree species in a tropical forest in Arunachal Pradesh, northeast India. Tropical Conservation Science 2008;1(3):163-85.

Ashton PS. On the Forests of Tropical Asia, Lest the Memory Fade. Royal Botanic Gardens, Kew, London: Kew Publishing; 2015.

Ashton PS. Floristic zonation of tree communities on wet tropical mountains revisited. Perspectives in Plant Ecology, Evolution and Systematics 2003;6(1-2):87-104.

Bhumibhamon S, Wasuwanich P. The structural characteristics of Huai Kog Ma Forest. Kog Ma Watershed Research Bulletin 1970;4:3-20.

Brambach F, Leuschner C, Tjoa A, Culmsee H. Diversity, endemism, and composition of tropical mountain forest communities in Sulawesi, Indonesia, in relation to elevation and soil properties. Perspectives in Plant Ecology, Evolution and Systematics 2017;27(1):68-79.

Brodribb TJ, Pittermann J, Coomes DA. Elegance versus speed: Examining the competition between conifer and angiosperm trees. International Journal of Plant Sciences 2012;173(6): 673-94.

Brooker RW, Callaway RM, Cavieres L, Kikvidze Z, Lortie CJ, Michalet R, et al. Don't diss integration: A comment on Ricklefs's disintegrating communities. The American Naturalist 2009;174(6):919-27.

Bunyavejchewin S, Baker PJ, LaFrankie JF, Ashton PS. Stand structure of a seasonal dry evergreen forest at Huai Kha Khaeng Wildlife Sanctuary, western Thailand. Natural History Bulletin of the Siam Society 2001;49(1):89-106.

Bunyavejchewin S, LaFrankie JV, Baker PJ, Kanzaki M, Ashton PS, Yamakura T. Spatial distribution patterns of the dominant

canopy dipterocarp species in a seasonal dry evergreen forest in western Thailand. Forest Ecology and Management 2003;175(1-3):87-101.

Buot IE Jr, Okitsu S. Vertical distribution and structure of the tree vegetation in the montane forest of Mt. Pulog, Cordillera mountain range, the highest mountain in Luzon Island, Philippines. Vegetation Science 1998;15(1):19-32.

Cardinale BJ, Duffy JE, Gonzalez A, Hooper DU, Perrings C, Venail P, et al. Biodiversity loss and its impact on humanity. Nature 2012;486(7401):59-67.

Chambers JM, Cleveland WS, Kleiner B, Tukey PA. Graphical methods for data analysis. New York, USA: Chapman and Hall/CRC; 2017.

Chamchumroon V, Puff C. The Rubiaceae of Ko Chang, south-eastern Thailand. Thai Forest Bulletin (Botany) 2003;31(1): 13-26.

Chen IC, Hill JK, Ohlemüller R, Roy DB, Thomas CD. Rapid range shifts of species associated with high levels of climate warming. Science 2011;333(6045):1024-46.

Condit R, Ashton PS, Baker P, Bunyavejchewin S, Gunatilleke S, Gunatilleke N, et al. Spatial patterns in the distribution of tropical trees. Science 2000;288(5470):1414-8.

Condit R, Lao S, Singh A, Esufali S, Dolins S. Data and database standards for permanent forest plots in a global network. Forest Ecology and Management 2014;316(1):21-31.

Condit R. Research in large, long-term tropical forest plots. Trends in Ecology and Evolution 1995;10(1):18-22.

Condit R, Sukumar R, Hubbell SP, Foster RB. Predicting population trends from size distributions: A direct test in a tropical tree community. The American Naturalist 1998; 152(4):495-509.

Corlett RT. Frugivory and seed dispersal by vertebrates in tropical and subtropical Asia: An update. Global Ecology and Conservation 2017;11(3):1-22.

De Almeida LB, Galetti M. Seed dispersal and spatial distribution of *Attalea geraensis* (Arecaceae) in two remnants of Cerrado in Southeastern Brazil. Acta Oecologica 2007;32(2):180-7.

Deb P, Sundriyal RC. Tree regeneration and seedling survival patterns in old-growth lowland tropical rainforest in Namdapha National Park, north-east India. Forest Ecology and Management 2008;225(12):3995-4006.

Elias R, Dias E, Pereira F. Disturbance, regeneration and the spatial pattern of tree species in Azorean mountain forests. Community Ecology 2011;12(1):23-30.

Enright NJ, Jaffré T. Ecology and distribution of the malesian podocarps. In: Turner BL, Cernusak LA, editors. Ecology of the Podocarpaceae in Tropical Forests. Washington DC, USA: Smithsonian Institute Scholarly Press; 2011. p. 57-77.

Franklin J. Mapping Species Distributions: Spatial Inference and Prediction. United Kingdom: Cambridge University Press; 2010.

Goff FG, West D. Canopy-understory interaction effects on forest population structure. Forest Science 1975;21(2):98-108.

Goodale UM, Ashton MS, Berlyn GP, Gregoire TG, Singhakumara BMP, Tennakoon KU. Disturbance and tropical pioneer species: Patterns of association across life history stages. Forest Ecology and Management 2012;277(1):54-66.

Golay J, Kanevski M. A new estimator of intrinsic dimension based on the multipoint Morisita index. Pattern Recognition 2015;48(12):4070-81.

Hara M, Kanzaki M, Mizuno T, Noguchi H, Sri-Ngernyuang K, Teejuntuk S, et al. The floristic composition of tropical montane forest in Doi Inthanon National Park, Northern Thailand, with special reference to its phytogeographical relation with montane forests in tropical Asia. Natural History Research 2002;7(1):1-17.

Hashimoto S. Temperature sensitivity of soil CO_2 production in a tropical hill evergreen forest in northern Thailand. Journal of Forestry Research 2005;10(6):497-503.

Henle K, Lindenmayer DB, Margules CR, Saunders DA, Wissel C. Species survival in fragmented landscapes: Where are we now? Biodiversity and Conservation 2004;13(1):1-8.

Houle G. Spatiotemporal patterns in the components of regeneration of four sympatric tree species - *Acer rubrum*, *A. Saccharum*, *Betula alleghaniensis*, and *Fagus grandifolia*. Journal of Ecology 1994;82(1):39-53.

Hubbell SP. Tree dispersion, abundance, and diversity in a tropical dry forest. Science 1979;203(4387):1299-309.

Huth F, Wagner S. Gap structure and establishment of Silver birch regeneration (*Betula pendula* Roth.) in Norway spruce stands (*Picea abies* L. Karst.). Forest Ecology and Management 2006;229(1-3):314-24.

Kapos V, Rhind J, Edwads M, Price MF, Ravilious C. A State-of knowledge report for 2000, developing a map of the world's mountain forest. In: Price MF, Butt N, editors. Forests in Sustainable Mountain Development. Wallingford, UK: CAB International; 2000. p. 4-9.

Kampmann D, Herzog F, Jeanneret P, Konold W, Peter M, Walter T, et al. Mountain grassland biodiversity: Impact of site conditions versus management type. Journal for Nature Conservation 2008;16(1):12-25.

Kanzaki M, Hara M, Yamakura T, Ohkubo T, Tamura MN, Sri-ngernyuang K, et al. Finding from a large-scale plot network. In: Losos EC, Leigh EG Jr, editors. Tropical Forest Diversity and Dynamics. Chicago, USA: Chicago Press; 2004. p. 474-81.

Khamyong S, Lykke AM, Seramethakun D, Barfod AS. Species composition and vegetation structure of an upper montane forest at the summit of Mt. Doi Inthanon, Thailand. Nordic Journal of Botany 2004;3(1):83-97.

Kitayama K. An altitudinal transect study of the vegetation on Mount Kinabalu, Borneo. Vegetatio 1992;102(2):149-71.

Kitamura S, Suzuki S, Yumoto T, Poonswad P, Chuailua P, Plongmai K, et al. Dispersal of *Canarium euphyllum* (Burseraceae), a large-seeded tree species, in a moist evergreen forest in Thailand. Journal of Tropical Ecology 2006;22(2):137-46.

Kochummen KM. Effects of Elevation on Vegetation on Gunung Jerai, Kedah. Forestry Department, Peninsular Malaysia: Jalan Mahameru; 1982.

Kochummen KM. Tree Flora of Malaya. Volume 4. In: Ng FSP, editor. Malaysia: Longmans, Green and Co; 1989. p. 98-178.

Krebs CJ. Ecology: The Experimental Analysis of Distribution and Abundance. New York, USA: Harper Collins Publishers; 1994.

Kume T, Takizawa H, Yoshifuji N, Tanaka K, Tantasirin C, Tanaka N, et al. Impact of soil drought on sap flow and water status of evergreen trees in a tropical monsoon forest in northern Thailand. Forest Ecology and Management 2007; 238(1):220-30.

Lan G, Zhu H, Cao M, Hu Y, Wang H, Deng X, et al. Spatial dispersion patterns of trees in a tropical rainforest in Xishuangbanna, southwest China. Ecological Research 2009;24(5):1117-24.

Liebscher E. Approximation of distributions by using the Anderson Darling statistic. Communications in Statistics-Theory and Methods 2016;45(22):6732-45.

Marod D, Kutintara U, Tanaka H, Nakashizuka T. Structural dynamics of a natural mixed deciduous forest in western Thailand. Journal of Vegetation Science 1999;10(6):777-86.

Marod D, Sangkaew S, Panmonkol A, Jingjai A. Influences of environmental factors on tree distribution of lower montane evergreen forest at Doi Sutep-Pui National Park, Chiang Mai Province. Thai Journal of Forestry 2014;33(3):23-33.

Marod D, Bootcharee S, Phumphuang W, Asanok L, Kamyo T, Thinkampaeng S, et al. Diversity and spatial distribution of the Fagaceae tree species in the Doi Suthep-Pui National Park, Chiang Mai Province. Journal of Tropical Forest Research 2018;2(2):53-68.

Marod D, Sungkaew S, Mizunaga H, Thinkampheang S, Thongsawi J. Woody plant community and distribution in a tropical coastal sand dune in southern Thailand. Journal of Coastal Conservation 2020;24(4):Article No. 44

Marod D, Phumphuang W, Wachrinrat C. Effect of environmental gradients on tree distribution in lowland dry evergreen forest, northeastern Thailand. Agriculture and Natural Resources 2021;55(5):795-805.

Maxwell JF, Elliott S, Anunsarnsunthorn V. The vegetation of Jae Sawan National Park, Lampang Province, Thailand. Natural History Bulletin of the Siamese Society 1997;45(1):71-97.

McLaren KP, McDonald MA, Hall JB, Healey JR. Predicting Species response to disturbance from size class distributions of adults and saplings in a Jamaican Tropical Dry Forest. Plant Ecology 2005;181(1):69-84.

Miyazawa Y, Tatsuya S, Kikuzawa K, Otsuki K. The light environment, morphology and growth of the early successional tree species *Litsea citriodora*. Forest Ecology and Management 2006;236(2-3):251-8.

Morisita M. Measuring of the dispersion of individuals and analysis of the distributional patterns. Memories of the Faculty of Science, Kyushu University, Series E (Biology) 1959; 2:215-35.

Murali KS. Patterns of seed size, germination and seed viability of tropical tree species in Southern India. Biotropica 1997; 29(3):271-9.

Nyland RD. Silviculture: Concepts and Applications. 2nd ed. London, UK: McGraw-Hill; 2002.

Ohsawa M. The montane cloud forest and its gradational changes in Southeast Asia. In: Hamilton LS, Juvik JO, Scatena FN, editors. Tropical Montane Cloud Forest. New York, USA: Springer; 1995. p. 254-65.

Pepin N, Bradley RS, Diaz HF, Baraer M, Caceres EB, Forsythe N, et al. Elevation-dependent warming in mountain regions of the world. Nature Climate Change 2015;5(5):424-30.

Pendry CA, Proctor J. Altitudinal zonation of rain forest on Bukit Belalong, Brunei: Soils, forest structure and floristics. Journal of Tropical Ecology 1997;13(2):221-41.

Pereira HM, Leadley PW, Proença V, Alkemade R, Scharlemann JPW, Fernandez-Manjarrés JF, et al. Scenarios for global biodiversity in the 21st century. Science 2010;330(6010): 1496-501.

Rashid MH, Robert S, Neville A. Ecosystem and Human Well-Being: Current State and Trends: Findings of the Condition and Trends Working Group. Millennium Ecosystem Assessment (Program): Island Press; 2005.

Regato P, Salman R. Mediterranean Mountains in a Changing World: Guidelines for Developing Action Plans. Switzerland: World Conservation Union Publisher; 2008.

Richards PW. The Tropical Rain Forest: An Ecological Study. 2nd ed. Cambridge, UK: Cambridge University Press; 1996.

Ricklefs RE. Disintegration of the ecological community. The American naturalist 2008;172(6):741-50.

Rueangket A, Duengkae P, Thinkhampang S, Marod D. Utilization of fruit by frugivores in lower montane forest at Doi Suthep-Pui National Park, Chiang Mai Province. Agriculture and Natural Resources 2019;53(5):457-64.

Rueangket A, Duengkae P, Thinkampheang S, Enright NJ, Marod D. Fruit traits of tree species in lower montane rainforest at Doi Suthep-Pui, northern Thailand. Journal of Tropical Ecology 2021;37(5):240-51.

Rubin BD, Manion PD, Faber-Langendoen D. Diameter distributions and structural sustainability in forests. Forest Ecology and Management 2006;222(1-3):427-38.

Spehn EM, Lieberman M, Körner C. Land Use Change and Mountain Biodiversity. Boca Raton: CRC Press; 2006.

Sala OE, Chapin FS, Armesto JJ, Berlow E, Bloomfield J, Dirzo R, et al. Global biodiversity scenarios for the year 2100. Science 2000;287(5459):1770-4.

Sangsupan HA, Hibbs DE, Withrow-Robinson BA, Elliott S. Effect of microsite light on survival and growth of understory natural regeneration during restoration of seasonally dry tropical forest in upland northern Thailand. Forest Ecology and Management 2021;489:Article No. 119061.

Santisuk T. An Account of the Vegetation of Northern Thailand. Franz Steiner, Stuttgart; 1988.

Smitinand T. Thai Plant Name (Revised Edition). Forest Herbarium, Forest and Plant Conservation Research Office, and Department of National Parks, Wildlife, and Plant Conservation: Bangkok; 2014.

Sri-Ngernyuang K, Kanzaki M, Mizuno T, Noguchi H, Teejuntuk S, Sungpalee C, et al. Habitat differentiation of Lauraceae species in a tropical lower montane forest in northern Thailand. Ecological Research 2003;18(1):1-14.

Suzuki S, Kitamura S, Kon M, Poonswad P, Chuailua P, Plongmai K, et al. Fruit visitation patterns of small mammals on the forest floor in a tropical seasonal forest of Thailand. Tropics 2007;16(1):17-29.

Swinfield T, Afriandi R, Antoni F, Harrison RD. Accelerating tropical forest restoration through the selective removal of pioneer species. Forest Ecology and Management 2016;381:209-16.

Tagawa H. Distribution of lucidophyll oak-laurel forest formation in Asia and other areas. Tropics 1995;5(1):1-40.

Tanaka N, Kume T, Yoshifuji N, Tanaka K, Takizawa H, Shiraki K, et al. A review of evapotranspiration estimates from tropical forests in Thailand and adjacent regions. Agricultural and Forest Meteorology 2008;148(5):807-19.

Tanaka K, Takizawa H, Tanaka N, Kosaka I, Yoshifuji N, Tantasirin C, et al. Transpiration peak over a hill evergreen forest in northern Thailand in the late dry season: Assessing the seasonal changes in evapotranspiration using a multilayer model. Journal of Geophysical Research Atmospheres 2003;108(D17):Article No. 4533.

Tangtham N. Preliminary Study of the Ecosystem of Hill Evergreen Forest in Northern Thailand [dissertation]. Pennsylvania, USA: Pennsylvania State University, University Park; 1974.

Vander Wall SB. The evolutionary ecology of nut dispersal. The Botanical Review 2001;67(1):74-117.

White EP, Morgan Ernest SK, Kerkhoff AJ, Enquis BJ. Relationships between body size and abundance in ecology. Trends in Ecology and Evolution 2007;22(6):323-30.

Wright SJ, Kitajima K, Kraft NJB, Reich PB, Wright IJ, Bunker DE, et al. Functional traits and the growth-mortality trade-off in tropical trees. Ecology 2010;91(12):3664-74.

Yamada T, Yamakuara T, Kanzaki M, Itoh A, Ohkubo T, Ogino K, et al. Topography-dependent spatial pattern and habitat segregation of sympatric *Scaphuim* species in a tropical rain forest at Lambir, Sarawak. Tropics 1997;7(1):57-66.

Zhu H, Chai Y, Zhou S, Yan L, Shi J, Yang G. Combined community ecology and floristics, a synthetic study on the upper montane evergreen broad-leaved forests in Yunnan, southwestern China. Plant Diversity 2016;38(6):295-302.

Environment and Natural Resources Journal (EnNRJ)

Volume 20, Number 6, November - December 2022 ISSN: 1686-5456 (Print)
ISSN: 2408-2384 (Online)

LIST OF REVIEWERS IN 2022

Name	Affiliation	Country
Abhijit Maiti, Ph.D.	Indian Institute of Technology (IIT)	India
Abdul Zahir, M.Sc.	National Textile University	Pakistan
Achara Ussawarujikulchai, Ph.D.	Mahidol University	Thailand
Ahmad Zaheer, Ph.D.	The University of Lahore	Pakistan
Aingorn Chaiyes, Ph.D.	Sukhothai Thammathirat Open University	Thailand
Akihida Kasai, Ph.D.	Hokkaido University	Japan
Alin Kadfak, Ph.D.	Swedish University of Agricultural Sciences	Sweden
Amir Sharaai, Ph.D.	Universiti Putra Malaysia	Malaysia
Anak Pattanavibool, Ph.D.	Wildlife Conservation Society	Thailand
Anwar Hussain, Ph.D.	Abdul Wali Khan University Mardan	Pakistan
Athit Phetrak, Ph.D.	Mahidol University	Thailand
Bamidele Iromidayo OLU-OWOLABI, Ph.D.	University Of Ibadan	Nigeria
Bantita Terakulsatit, Ph.D.	Suranaree University of Technology	Thailand
Benhadj Mabrouka, Ph.D.	University of Tebessa	Algeria
Benjaphorn Prapagdee, Ph.D.	Mahidol University	Thailand
Bhanupong Phrommarat, Ph.D.	Silpakorn University	Thailand
Boonlue Kachenchart, Ph.D.	Mahidol University	Thailand
Boontarika Srithai, Ph.D.	Chiang Mai University	Thailand
Boripat Siriaroonrat, DVM, Ph.D.	Mahidol University	Thailand
Chaiwiwat Vansarochana, Ph.D.	Naresuan University	Thailand
Chaowalit Warodomrungsimun, Ph.D.	Mahidol University	Thailand
Chomnutcha Boonmee, Ph.D.	Metal and Materials Technology Center	Thailand
Chuck Chuan Ng, Ph.D.	Xiamen Univ Malaysia	Malaysia
Claude Hammecker, Ph.D.	Ecologie Fonctionnelle et Biogeochimie des Sols et Agrosystemes	France
Daichi Iwase, Ph.D.	Tokyo Zokei University	Japan
Delianis pringgenies, Ph.D.	Diponegoro University	Indonesia
Doan Van Hong Thien, Ph.D.	Can Tho University	Vietnam
Donatus Hendra Amijaya, Ph.D.	Universitas Gadjah Mada	Indonesia
Emma Asnachinda, Ph.D.	Burapha University	Thailand
Ekachai Chukeatirote, Ph.D.	Mae Fah Luang University	Thailand
Eko Hanudin, Ph.D.	Universitas Gadjah Mada	Indonesia
Farshid Ghanbari, Ph.D.	Abadan University of Medical sciences	Iran
Fernando Garrido	Swiss Federal Institute of Aquatic Science and Technology	Spain
Foad Buazar, Ph.D.	Khorramshahr University of Marine Science and Technology	Iran
Fumiaki Takakai	Akita Prefectural University	Japan
Gomathi Thandapani, Ph.D.	Thiruvalluvar University	TamilNadu
Hadi Shayesteh, Ph.D.	Iran University of Science and Technology	Iran
Hazlina Ahamad Zakeri, Ph.D.	Universiti Malaysia Terengganu	Malaysia
Jarupat Kanjanarong, Ph.D.	Rajamangala University of Technology Rattanakosin	Thailand
Jasmina Sinzar-Sekulic, Ph.D.	University of Belgrade	Serbia

Name	Affiliation	Country
Jessie Samaniego, Ph.D.	Philippine Nuclear Research Institute	Philippine
Jindarat Ekprasert, Ph.D.	Khon Kaen University	Thailand
Jogendra Singh, Ph.D.	Gurukula Kangri University	India
Kamalaporn Kanongdate, Ph.D.	Mahidol University	Thailand
Kamonwat Nakason, Ph.D.	Mahidol University	Thailand
Kaveh Ostad-Ali-Askari, Ph.D.	Isfahan University of Technology	Iran
Lamthai Asanok, Ph.D.	Maejo University	Thailand
Lingfeng Huang, Ph.D.	Xiamen University	China
Marcela C. Pagano, Ph.D.	Universidade Federal de Minas Gerais	Brazil
Marcelo C. Andrade, Ph.D.	Universidade Federal do Para	Brazil
Marzuki Ismail, Ph.D.	University Malaysia Terengganu	Malaysia
Md. Saiful Islam, M.Sc.	EQMS Consulting Limited	Bangladesh
M. Oliveira	Universidade de Aveiro	Portugal
Mohamed Elhag, Ph.D.	King Abdulaziz University	Saudi Arabia
Mohamed H. H. Ali, Ph.D.	National Institute of Oceanography and Fisheries (NIOF)	Egypt
Mohammad Mahfuzur Rahman, Ph.D.	Jashore University of Science and Technology	Bangladesh
Mohammad Rajib, Ph.D.	Institute of Nuclear Minerals	Bangladesh
Mohammed Syedul Islam, Ph.D.	International Islamic University	Bangladesh
Mujiyo Mujiyo, Ph.D.	Universitas Sebelas Maret	Indonesia
Myra Tansengco, Ph.D.	Industrial Technology Development Insitute	Philippine
Natchimuthu Karmegam, Ph.D.	Government Arts College Autonomous	India
Natdhera Sanmanee, Ph.D.	Silapakorn University	Thailand
Navaporn Karnjanasiranon, Ph.D.	Mahidol University	Thailand
Nevin Yagci, Ph.D.	Istanbul Technical University	Turkey
Nguyen Minh Ky, Ph.D.	Nong Lam University	Vietnam
Nguyen Thanh Giao, Ph.D.	Can Tho University	Vietnam
Nguyen Thị Thu Ha, Ph.D.	VNU University of Science	Vietnam
Nirjhar Bar, Ph.D.	St James' School	India
Nirmala Chockalingam, Ph.D.	Vinayaka Mission's Kirupananda Variyar Engineering College	India
Nisa Leksungnoen, Ph.D.	Kasetsart University	Thailand
Niyaz Mohammad Mahmoodi, Ph.D.	Institute for Color Science and Technology	Iran
N. K. Srivastava, Ph.D.	Dr BR Ambedkar National Institute of Technology	India
Norberto Asensio, Ph.D.	University of the Basque Country	Spain
Nukoon Tawinteung, Ph.D.	KIngmongktu's Institute of Technology, Bangkok	Thailand
Nuntavun Riddech, Ph.D.	Khon Kaen University	Thailand
O. S. Ajayi, Ph.D.	Obafemi Awolowo University	Nigeria
Pantip Klomjek, Ph.D.	Naresuan University	Thailand
Patcharee Pripdeevech, Ph.D.	Mae Fah Luang University	Thailand
Pathmalal Manage, Ph.D.	University of Sri Jayewardenepura	Sri Lanka
Patricia Krecl, Ph.D.	Universidade Tecnologica Federal do Parana	Brazil
Paul Hua Ming Lau, M.Sc.	Universiti Putra Malaysia Fakulti Perhutanan	Malaysia
Phonekeo Vivarad, Ph.D.	Asian Institute of Technology	Thailand
Piangjai Peerakiatkhajohn, Ph.D.	Mahidol University	Thailand
Pijit Jiemvarangkul, Ph.D.	King Mongkut's University of Technology North Bangkok	Thailand
Preeyaporn Koedrith, Ph.D.	Mahidol University	Thailand
Priyom Roy, Ph.D.	National Remote Sensing Centre	India
Ranjna Jindal, Ph.D.	Mahidol University	Thailand

Name	Affiliation	Country
Rattapon Onchang, Ph.D.	Silpakorn University	Thailand
Ray Joseph George, Ph.D.	Mahatma Gandhi University	India
Ravindran Balasubramani, Ph.D.	Kyonggi University	Korea
Rouholah Zare Dorabei, Ph.D.	Iran University of Science and Technology	Iran
Sagar Kafle, Ph.D.	Tribhuvan University	Nepal
Selvaraj Vasantha Kumar, Ph.D.	Vellore Institute of Technology	India
Shan-Li Wang, Ph.D.	National Taiwan University	Taiwan
Shin-Ichiro Aiba, Ph.D.	Hokkaido University	Japan
Silvester B. Pratasik, Ph.D.	Sam Ratulangi University Hospitalsia	Indonesia
S. M. Mofijul Islam, Ph.D.	Bangladesh Rice Research Institute (BRRI)	Bangladesh
Somboon Tanasupawat, Ph.D.	Chulalongkorn University	Thailand
Subhash Babu, Ph.D.	Indian Agricultural Research Institute	India
Subodh K. Upadhyaya, Ph.D.	Leiden University	Netherlands
Sucheela Polruang, Ph.D.	Kasetsart University	Thailand
Suphachai Amkha, Ph.D.	Kasetsart University	Thailand
Susana Pastor, Ph.D.	Universitat Autonoma de Barcelona	Spain
Sutheera Hermhuk, Ph.D.	Maejo University	Thailand
Suwimon Uthairatsamee, Ph.D.	Kasetsart University	Thailand
Suwit Ongsomwang, Ph.D.	Suranaree University of Technology	Thailand
Tawfik A. Saleh, Ph.D.	King Fahd University of Petroleum and Minerals	Saudi Arabia
Terefe Tolessa, Ph.D.	Ambo University	Ethiopia
Thangavelu Muthukumar, Ph.D.	Bharathiar University	India
Thanomsak Boonphakdee, Ph.D.	Burapha University	Thailand
Thomas Gray, Ph.D.	World Wildlife Fund	United Kingdom
Thongchai Kanabkaew, Ph.D.	Thammasat University	Thailand
Tuanthong Jutagate, Ph.D.	Ubon Ratchathani University	Thailand
Uwe Strotmann, Ph.D.	University of Applied Sciences	Germany
Vasant M. Wagh, Ph.D.	Swami Ramanand Teerth Marathwada University	India
Vasco C. Mota, Ph.D.	NOFIMA Norwegian Institute of Food	Norway
Vo Quang MINH, Ph.D.	Can Tho University	Vietnam
V. Mohanraj, Ph.D.	Sir Theagaraya College Chennai	India
Vorapot Kanokkantapong, Ph.D.	Chulalongkorn University	Thailand
Wanwisa Pansak, Ph.D.	Mahidol University	Thailand
Weerah Wongkham, Ph.D.	Chiangmai University	Thailand
Wei Wu, Ph.D.	Nanjing Agricultural University	China
Witchaya Rongsayamanont, Ph.D.	Mahidol University	Thailand
Yosio Edemir Shimabukuro	Instituto Nacional de Pesquisas Espaciais (INPE)	Brazil
Yuzhuang Sun, Ph.D.	Hebei University of Engineering	China

INSTRUCTION FOR AUTHORS

Publication and Peer-reviewing processes of Environment and Natural Resources Journal

Environment and Natural Resources Journal is a peer reviewed and open access journal that is published twice a year (January-June and July-December). Manuscripts should be submitted online at https://ph02.tci-thaijo.org/index.php/ennrj/about/submissions by registering and logging into this website. Submitted manuscripts should not have been published previously, nor be under consideration for publication elsewhere (except conference proceedings papers). A guide for authors and relevant information for the submission of manuscripts are provided in this section and also online at: https://ph02.tci-thaijo.org/index.php/ennrj/author. All manuscripts are refereed through a **double-blind peer-review** process.

Submitted manuscripts are reviewed by outside experts or editorial board members of **Environment and Natural Resources Journal**. This journal uses double-blind review, which means that both the reviewer and author identities are concealed from the reviewers, and vice versa, throughout the review process. Steps in the process are as follows:

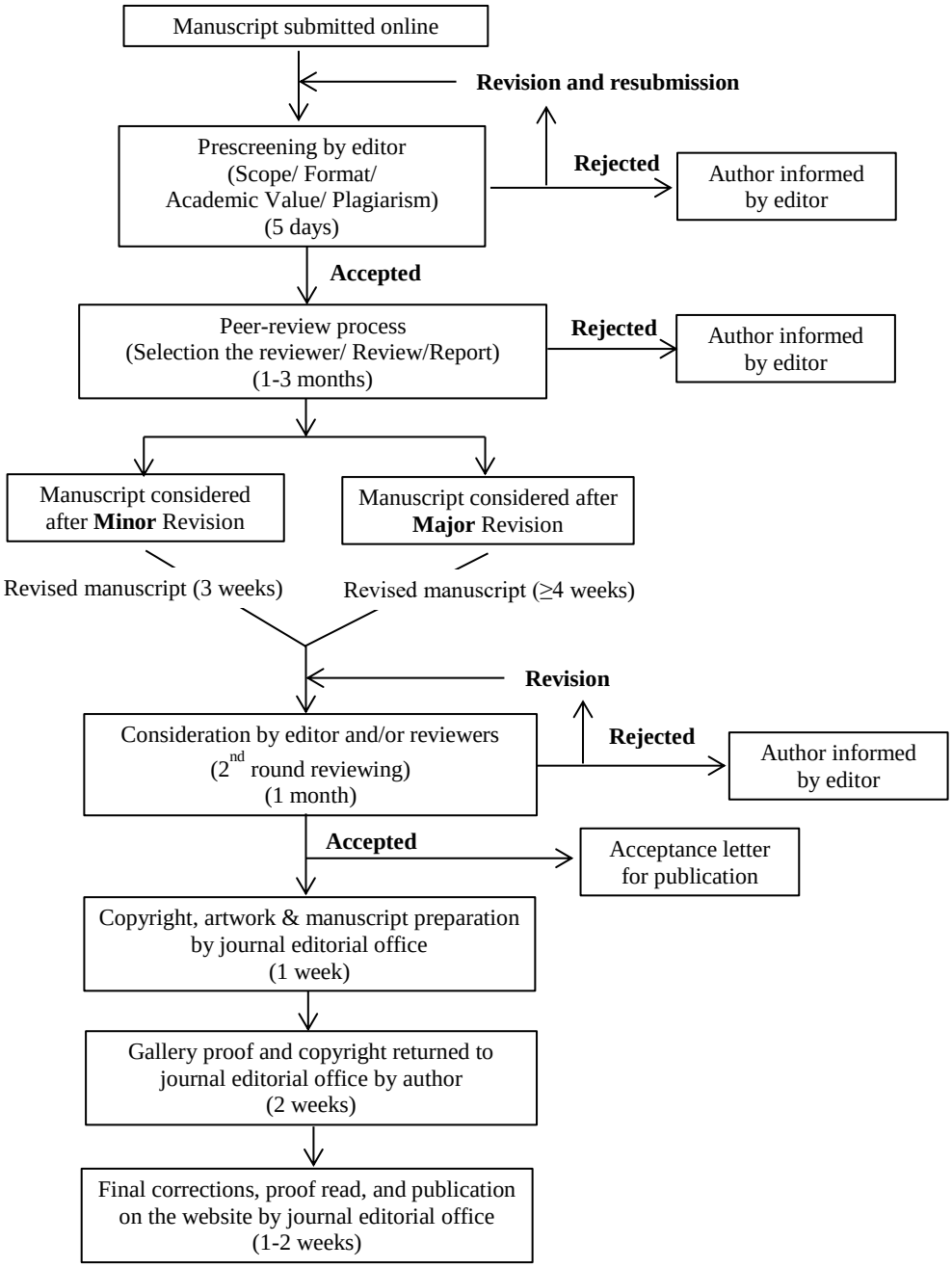

The Environment and Natural Resources Journal (EnNRJ) accepts 2 types of articles for consideration of publication as follows:

- *Original Research Article:* Manuscripts should not exceed 3,500 words (excluding references).
- *Review Article (by invitation):* This type of article focuses on the in-depth critical review of a special aspect in the environment and also provides a synthesis and critical evaluation of the state of the knowledge of the subject. Manuscripts should not exceed 6,000 words (excluding references).

Submission of Manuscript

Cover letter: Key points to include:

- Statement that your paper has not been previously published and is not currently under consideration by another journal
- Brief description of the research you are reporting in your paper, why it is important, and why you think the readers of the journal would be interested in it
- Contact information for you and any co-authors
- Confirmation that you have no competing interests to disclose

Manuscript-full: Manuscript (A4) must be submitted in Microsoft Word Files (.doc or .docx). Please make any identifying information of name(s) of the author(s), affiliation(s) of the author(s). Each affiliation should be indicated with superscripted Arabic numerals immediately after an author's name and before the appropriate address. Specify the Department/School/Faculty, University, Province/State, and Country of each affiliation.

Manuscript-anonymized: Manuscript (A4) must be submitted in Microsoft Word Files (.doc or .docx). Please remove any identifying information, such as authors' names or affiliations, from your manuscript before submission and give all information about authors at title page section.

Reviewers suggestion *(mandatory)*: Please provide the names of 3 potential reviewers with the information about their affiliations and email addresses. *The recommended reviewers should not have any conflict of interest with the authors. Each of the reviewers must come from a different affiliation and must not have the same nationality as the authors.* Please note that the editorial board retains the sole right to decide whether or not the recommended potential reviewers will be selected.

Preparation of Manuscript

Manuscript should be prepared strictly as per guidelines given below. The manuscript (A4 size page) must be submitted in Microsoft Word (.doc or .docx) with Times New Roman 12 point font and a line spacing of 1.5. *The manuscript that is not in the correct format will be returned and the corresponding author may have to resubmit*. The submitted manuscript must have the following parts:

Title should be concise and no longer than necessary. Capitalize first letters of all important words, in Times New Roman 12 point bold.

Author(s) name and affiliation must be given, especially the first and last names of all authors, in Times New Roman 11 point bold.

Affiliation of all author(s) must be given in Times New Roman 11 point italic.

Abstract should indicate the significant findings with data. A good abstract should have only one paragraph and be limited to 250 words. Do not include a table, figure or reference.

Keywords should adequately index the subject matter and up to six keywords are allowed.

Text body normally includes the following sections: 1. Introduction 2. Methodology 3. Results and Discussion 4. Conclusions 5. Acknowledgements 6. References

Reference style must be given in Vancouver style. Please follow the format of the sample references and citations as shown in this Guide below.

Unit: The use of abbreviation must be in accordance with the SI Unit.

Format and Style

Paper Margins must be 2.54 cm on the left and the right. The bottom and the top margin of each page must be 1.9 cm.

Introduction is critically important. It should include precisely the aims of the study. It should be as concise as possible with no sub headings. The significance of problem and the essential background should be given.

Methodology should be sufficiently detailed to enable the experiments to be reproduced. The techniques and methodology adopted should be supported with standard references.

Headings in Methodology section and Results and Discussion section, no more than three levels of headings should be used. Main headings should be typed (in bold letters) and secondary headings (in bold and italic letters). Third level headings should be typed in normal and no bold, for example;

2. Methodology
2.1 Sub-heading
2.1.1 Sub-sub-heading

Results and Discussion can be either combined or separated. This section is simply to present the key points of your findings in figures and tables, and explain additional findings in the text; no interpretation of findings is required. The results section is purely descriptive.
Tables Tables look best if all the cells are not bordered; place horizontal borders only under the legend, the column headings and the bottom.
Figures should be submitted in color; make sure that they are clear and understandable. Please adjust the font size to 9-10, no bold letters needed, and the border width of the graphs must be 0.75 pt. *(Do not directly cut and paste them from MS Excel.)* Regardless of the application used, when your electronic artwork is finalized, please 'save as' or convert the images to TIFF (or JPG) and separately send them to EnNRJ. The images require a resolution of at least 300 dpi (dots per inch). If a label needed in a figure, its font must be "Times New Roman" and its size needs to be adjusted to fit the figure without borderlines.

All Figure(s) and Table(s) should be embedded in the text file.

Conclusions should include the summary of the key findings, and key take-home message. This should not be too long or repetitive, but is worth having so that your argument is not left unfinished. Importantly, don't start any new thoughts in your conclusion.

Acknowledgements should include the names of those who contributed substantially to the work described in the manuscript but do not fulfill the requirements for authorship. It should also include any sponsor or funding agency that supported the work.

References should be cited in the text by the surname of the author(s), and the year. This journal uses the author-date method of citation: the last name of the author and date of publication are inserted in the text in the appropriate place. If there are more than two authors, "et al." after the first author' name must be added. Examples: (Frits, 1976; Pandey and Shukla, 2003; Kungsuwas et al., 1996). If the author's name is part of the sentence, only the date is placed in parentheses: "Frits (1976) argued that . . ."

Please be ensured that every reference cited in the text is also present in the reference list (and vice versa).

In the list of references at the end of the manuscript, full and complete references must be given in the following style and punctuation, arranged alphabetically by first author's surname. Examples of references as listed in the References section are given below.

Book
Tyree MT, Zimmermann MH. Xylem Structure and the Ascent of Sap. Heidelberg, Germany: Springer; 2002.

Chapter in a book
Kungsuwan A, Ittipong B, Chandrkrachang S. Preservative effect of chitosan on fish products. In: Steven WF, Rao MS, Chandrkachang S, editors. Chitin and Chitosan: Environmental and Friendly and Versatile Biomaterials. Bangkok: Asian Institute of Technology; 1996. p. 193-9.

Journal article
Muenmee S, Chiemchaisri W, Chiemchaisri C. Microbial consortium involving biological methane oxidation in relation to the biodegradation of waste plastics in a solid waste disposal open dump site. International Biodeterioration and Biodegradation 2015;102:172-81.

Published in conference proceedings
Wiwattanakantang P, To-im J. Tourist satisfaction on sustainable tourism development, amphawa floating marketSamut songkhram, Thailand. Proceedings of the 1st Environment and Natural Resources International Conference; 2014 Nov 6-7; The Sukosol hotel, Bangkok: Thailand; 2014.

Ph.D./Master thesis

Shrestha MK. Relative Ungulate Abundance in a Fragmented Landscape: Implications for Tiger Conservation [dissertation]. Saint Paul, University of Minnesota; 2004.

Website

Orzel C. Wind and temperature: why doesn't windy equal hot? [Internet]. 2010 [cited 2016 Jun 20]. Available from: http://scienceblogs.com/principles/2010/08/17/wind-and-temperature-why-doesn/.

Report organization:

Intergovernmental Panel on Climate Change (IPCC). IPCC Guidelines for National Greenhouse Gas Inventories: Volume 1-5. Hayama, Japan: Institute for Global Environmental Strategies; 2006.

Remark

** Please be note that manuscripts should usually contain at least 15 references and some of them must be up-to-date research articles.*

** Please strictly check all references cited in text, they should be added in the list of references. Our Journal does not publish papers with incomplete citations.*

Changes to Authorship

This policy of journal concerns the addition, removal, or rearrangement of author names in the authorship of accepted manuscripts:

Before the accepted manuscript

For all submissions, that request of authorship change during review process should be made to the form below and sent to the Editorial Office of EnNRJ. Approval of the change during revision is at the discretion of the Editor-in-Chief. The form that the corresponding author must fill out includes: (a) the reason for the change in author list and (b) written confirmation from all authors who have been added, removed, or reordered need to confirm that they agree to the change by signing the form. Requests form submitted must be consented by corresponding author only.

After the accepted manuscript

The journal does not accept the change request in all of the addition, removal, or rearrangement of author names in the authorship. Only in exceptional circumstances will the Editor consider the addition, deletion or rearrangement of authors after the manuscript has been accepted.

Copyright transfer

The copyright to the published article is transferred to Environment and Natural Resources Journal (EnNRJ) which is organized by Faculty of Environment and Resource Studies, Mahidol University. The accepted article cannot be published until the Journal Editorial Officer has received the appropriate signed copyright transfer.

Online First Articles

The article will be published online after receipt of the corrected proofs. This is the official first publication citable with the Digital Object Identifier (DOI). After release of the printed version, the paper can also be cited by issue and page numbers. DOI may be used to cite and link to electronic documents. The DOI consists of a unique alpha-numeric character string which is assigned to a document by the publisher upon the initial electronic publication. The assigned DOI never changes.

Mahidol University

Wisdom of the Land

Research and Academic Service Section, Faculty of Environment and Resource Studies, Mahidol University
999 Phutthamonthon 4 Rd, Salaya, Nakhon Pathom 73170, Phone +662 441-5000 ext. 2108 Fax. +662 441 9509-10
E-mail: ennrjournal@gmail.com Website: https://www.tci-thaijo.org/index.php/ennrj